

Title	The analysis of Bcr-Abl—Nox signalling in chronic myeloid leukaemia
Authors	Landry, William D.
Publication date	2013
Original Citation	Landry, W.D. 2013. The analysis of Bcr-Abl—Nox signalling in chronic myeloid leukaemia. PhD Thesis, University College Cork.
Type of publication	Doctoral thesis
Rights	© 2013, William D. Landry - http://creativecommons.org/licenses/by-nc-nd/3.0/
Download date	2024-04-18 22:40:04
Item downloaded from	https://hdl.handle.net/10468/1503

The Analysis of Bcr-Abl—Nox Signalling in Chronic Myeloid Leukaemia

A thesis submitted to the National University of Ireland, Cork, in
fulfilment of the requirement for the degree of

Doctor of Philosophy

by

William D. Landry BSc.

**Department of Biochemistry,
University College Cork**

December 2013

**Supervisor: Professor Thomas G. Cotter
Head of Department: Professor David Sheehan**

Declaration

This thesis has not been submitted in whole or in part to this or any other university for any degree and is, unless otherwise stated, the original work of the author.

Signed: _____

William D. Landry

Acknowledgments

I started my PhD just under three and a half years ago, in this time I've faced many highs but also my fair share of lows. Luckily I didn't face any of the good times or the countless hurdles alone and for that there are a couple of people I could do with thanking. Firstly, I'd like to thank my supervisor Prof. Tom Cotter. I'm very grateful for this opportunity, as well as all the help, guidance and advice you've given me.

Since I've started I've seen a lot of faces come and go. To everyone I've worked with since starting (Alice, Anjali, Aoife, Brendan, Carolyn, Dave, Eileen, Fran, Gillian, Joanna, John, Kate, Lavina, Maryanne, Niamh, Peter, Ruth, Saul, Sara... I hope I haven't forgotten anyone) thank you all so much for the help, advice and welcome distractions between experiments! This is for those in "The Cancer Group" which need a special mention. To Ruth, whether you realise it or not I owe you a lot. You trained me in and showed me how this thing called research worked! I hold a lot of how I work and what I know down to those first few months you trained me, I'll be forever grateful. John, although Ruth did the grunt work in making me a researcher you definitely got me thinking like one, thanks. Have to say I miss the banter when we all went out for the odd pint! Aoife thanks for listening every time I complained about my experiments not working (which was a lot!) and for all the friendly advice. Eileen thanks, your friendly positive attitude was always welcome, plus it was always nice knowing I had someone I could rely on if things needed to be done when I was finishing up my project. To the MD's, Brendan, Dave and Peter ye were good craic in the lab, which was always welcome even if the perpetual need to take my stuff and not put it back wasn't! To the "Eye Group", particularly

Maryanne, Fran and Gillian, thanks for answering the hundreds of questions I asked over the years, it was always appreciated!

To my family, thanks for your support over the past few years and I guess over my entire life, without it I wouldn't be who I am today. To my close friends (ye know who ye are!), although it's fairly doubtful ye will ever read this, thanks for helping me wash my PhD-induced stress away on our countless nights in the pub, which always happened on the weekend and never on a "school night", of course.

Finally and most importantly to Catherine, we begun this crazy thing together, you were there before I began encouraging me and there during doing the same. You were always an ear I could confide in, as was I for you. Words can't describe how grateful I am for your support. I have to say it was funny working together at first but I really do miss it now, but who knows it could happen again. In so many respects if it wasn't for you I truly wouldn't be here today finishing this crazy thing! Thank you so much my love, I will be forever grateful and will try my best to return the favour in the many years to come.

Table of Contents

Abstract	viii
Abbreviations	x
Chapter 1	
General Introduction	1
1. Chronic Myeloid Leukaemia	
1.1 Classification of leukaemia	2
1.2 CML: A brief history	2
1.3 CML: A clinical perspective	3
<i>Phases of Disease</i>	4
1.4 Bcr-Abl	6
<i>Bcr-Abl Isoforms</i>	6
<i>ABL1 and BCR genes: Independent and combined properties</i>	7
1.5 Mechanisms of Bcr-Abl oncogenesis	9
<i>Ras Signalling</i>	11
<i>PI3K/AKT Signalling</i>	12
<i>JAK/STAT Signalling</i>	13
1.6 CML treatment and the problems faced	14
<i>Drug Resistance</i>	15
<i>Residual disease: The leukaemic stem cell</i>	17

2. Reactive Oxygen Species (ROS) and Cellular Signalling	
2.1 Classification of ROS	20
2.2 Maintenance of ROS homeostasis	22
<i>Cellular Antioxidants</i>	22
2.3 ROS Signalling	24
3. NADPH Oxidases (Nox)	
3.1 Introduction to the Nox family	27
3.2 Nox Activation and Signalling	28
<i>Nox1, Nox2 and Nox3</i>	30
<i>Nox4</i>	31
<i>Nox5, Duox1 and Duox2</i>	32
<i>Nox signalling and disease</i>	33
4. Objectives	35
Chapter 2	
Materials and methods	36
Chapter 3	
Imatinib and Nilotinib inhibit Bcr-Abl-induced ROS through targeted degradation of NADPH oxidase subunit p22phox.	53
Landry, W. D., Woolley J. F. and Cotter T. G. (2013) Leukemia Research 37, 183-189.	
Supplementary material	61
Chapter 4	
The role of the Nox subunit p22phox in CML disease phenotype	79

Chapter 5

Examining the therapeutic potential of Nox Inhibition	116
--	-----

Chapter 6

General Discussion	178
---------------------------	-----

Bibliography	188
---------------------	-----

Appendix

1. Inhibition of protein-tyrosine phosphatase 1B (PTP1B) mediates ubiquitination and degradation of Bcr-Abl protein.	214
---	-----

Alvira, D., Naughton, R., Bhatt, L., Tedesco, S., Landry, W.D., Cotter, T.G. (2011). *J. Biol. Chem.* 286, 32313–23.

2. Redox-regulated growth factor survival signaling.	226
---	-----

Woolley, J.F., Corcoran, A., Groeger, G., Landry, W.D., Cotter, T.G. (2013). *Antioxid. Redox. Signal.* 19, 1815-27.

Abstract

Chronic Myeloid Leukaemia (CML) is a myeloproliferative disorder characterised by increased proliferation of haematopoietic stem cells in the bone marrow. CML results as a consequence of a reciprocal translocation between chromosomes 9 and 22, producing what is known as the Philadelphia chromosome (Ph). This translocation generates the chimeric protein Bcr-Abl, a constitutively active tyrosine kinase which induces oncogenesis in part by promoting increased cell survival and proliferation. Since the development of Bcr-Abl-specific tyrosine kinase inhibitors (TKIs) there has been a substantial improvement in the clinical treatment of CML. Unfortunately, residual disease and the development of TKI resistance has become an ever growing concern, resulting in the need for a greater understanding of the disease in order to develop new treatment strategies. Interestingly, constitutive expression of the Bcr-Abl in CML is known to produce elevated levels of Reactive Oxygen Species (ROS) which are known to influence a variety of cellular processes. Previous studies have demonstrated that NADPH oxidase (Nox) activity contributes to intracellular-ROS levels in Bcr-Abl-positive cells, having a positive effect on survival signalling. The objective of this study was to elucidate how Nox protein activity was influenced downstream of Bcr-Abl. It was also of interest to examine further how Nox-derived ROS influence CML disease phenotype and identify if there was a potential in targeting these proteins to improve CML treatment.

In the first part of this study, it was shown that inhibition of Bcr-Abl signalling, by either Imatinib or Nilotinib, led to a significant reduction in ROS levels which was concurrent with the Glycogen synthase kinase-3 β (GSK-3 β) dependent, post-translational down-regulation of the small membrane-bound protein p22phox, an essential component of the Nox complex. Furthermore, siRNA

knockdown of p22phox in these cells established its importance in ROS production providing a link between Bcr-Abl signalling and ROS production through Nox activity.

Following on from this work, p22phox function and mediated ROS production was examined to establish how it affected cellular activity and influenced CML disease phenotype. This study identified p22phox to have a significant role in cellular proliferation, demonstrating its importance in G1/S phase cell cycle transition through a pRb-Cyclin E-dependant mechanism. Removal of p22phox expression was also demonstrated to significantly decrease cell viability while producing a minor effect on cell survival. Taken together this work identified the importance of p22phox-mediated Nox protein activity in CML disease phenotype. Furthermore, p22phox removal was demonstrated to make cells significantly more susceptible to Bcr-Abl-specific TKI treatment, while pharmacological silencing of Nox activity in combination with TKIs was demonstrated to produce substantial, synergistic increases in cell death through augmentation of apoptosis, demonstrating a significant improvement on TKI treatment alone.

In summary, this work identified p22phox protein maintenance as a possible mechanism by which Bcr-Abl signalling influences the production of Nox-derived ROS. Furthermore, this work also established the importance of p22phox function in CML disease phenotype while also demonstrating the potential of targeting Nox proteins in combination with Bcr-Abl inhibition.

Abbreviations

•OH	Hydroxyl
¹ O ₂	Singlet oxygen
ABL	Abelson murine leukaemia viral oncogene
ActD	Actinomycin D
ADP	Adenosine diphosphate
AEBSF	4-(2-Aminoethyl) benzenesulfonyl fluoride hydrochloride
ALL	Acute Lymphocytic Leukaemia
AML	Acute Myeloid Leukaemia
AMN-107	Nilotinib
ATP	Adenosine triphosphate
Baf3	Murine bone marrow-derived pro-B-cell line
BCR	Breakpoint Cluster Region
BMP-2	Bone morphogenetic protein-2
BrdU	Bromodeoxyuridine
BSA	Bovine serum albumin
Ca ²⁺	Intracellular calcium
CCyR	Cytogenetic response
CDK	Cyclin dependent kinases
CFDA-SE	Carboxyfluorescein Diacetate Succinimidyl Ester
CFSE	Carboxyfluorescein Succinimidyl Ester
CHR	Complete haematological response
CI	Combination index
Cis	Cisplatin

CML	Chronic Myeloid Leukaemia
CML-BP	Blast phase of CML
CML-CP	Chronic phase of CML
CMR	Complete molecular response
Co-IP	Co-Immunoprecipitation
DCF	Dichlorofluorescein
DMSO	Dimethyl sulfoxide
dNTP	Deoxyribonucleotide triphosphate
Doc	Docetaxel
Dox	Doxycycline
Dox	Doxycycline Hyclate
DPI	Diphenyleneiodonium chloride
DSS	Disuccinimidyl suberate
DTT	Dithiothreitol
DUOX	Dual oxidase
Elect Ctrl	Electroporated control
ERK	Extracellular Regulated Kinase
Etop	Etoposide
F _a	Fraction affected
FACS	Fluorescence Activated Cell Sorting
FACS	Fluorescence assisted flow cytometry
FAD	Flavin adenine dinucleotide
FBS	Fetal Bovine Serum
FBS	Fetal Bovine Serum
FOXO	Forkhead transcription factor

GAPDH	Glyceraldehyde 3-phosphate dehydrogenase
GDP	Guanidine diphosphate
GEF	Guanine exchange factors
GF	Growth factor
GM-CSF	Granulocyte-macrophage colony-stimulation factor
GRB2	Growth factor Receptor-Bound protein 2
Grx	Glutharedoxins
GSH	Reduced glutathione
GSK-3 β	Glycogen synthase kinase 3 beta
GSSG	Oxidized glutathione
GTP	Guanidine triphosphate
H ₂ DCFDA	Dichlorodihydrofluorescein diacetate
H ₂ O ₂	Hydrogen peroxide
HCl	Hydrochloric Acid
HOCl	Hypochlorous acid
HSC	Haematopoietic stem cells
IFN α	Interferon- α
IGF-I	Insulin-like growth factor I
IgG	Immunoglobulin G
IL-3	Interleukin-3
IL-3R	Interleukin-3 Receptor
IL-6	Interleukin-6
IP	Immunoprecipitation
JAK	Janus Kinase
Lact	Lactocystin

LSC	Leukaemic stem cells
LSC	Leukaemic Stem Cell
LY	LY294002
M	Mitosis
MAPK	Mitogen-activated protein kinase
M-bcr	First major breakpoint cluster region
m-bcr	Minor breakpoint cluster region (m-bcr)
MEK	MAPK/ERK kinase
Met	Methotrexate
M-MLV RT	Moloney Murine Leukaemia Virus Reverse Transcriptase
mRNA	Messenger RNA
MsrA/B	Methionine sulfoxide reductases
mTOR	Mammalian target of rapamycin
MTS	3-(4,5-dimethylthiazol-2-yl)-5-(3-carboxymethoxyphenyl)-2-(4-sulfophenyl)-2H-tetrazolium, inner salt
MYC	Myelocytomatosis viral oncogene
NAD	Nicotinamide adenine dinucleotide
NADP	Nicotinamide adenine dinucleotide phosphate
NADPH	Reduced nicotinamide adenine dinucleotide phosphate
Negative	Silencer Select siRNA Negative Control #1 transfected cells
NEM	N-Ethylmaleimide
Nox	NADPH Oxidase
NoxA1	Nox activator 1
NoxO1	Nox organiser 1
NP-40	Nonyl phenoxyethoxyethanol-40

NRT	No reverse transcriptase control
$O_2^{\bullet -}$	Superoxide
O_3	Ozone
PARP	Poly (ADP-ribose) polymerase
PBS	Phosphate-buffered saline
PCR	Polymerase Chain Reaction
PDGF	Platelet-derived growth factor
PDK1	3-phosphoinositide-dependent protein kinase-1
Ph	Philadelphia Chromosome
PI	Propidium iodide
PIP2	Phosolipid phosphatidylinositol biphosphate
PIP3	Phosolipid phosphatidylinositol 3,4,5-triphosphate
PI3K	Phosphatidylinositol 3-kinase
Pim-1	Proviral integration site 1 oncogene
PKC	Protein kinase C
PKC412	Midostaurin
PMA	Phorbol 12-myristate 13-acetate
PMS	Phenazine methosulfate
Poldip2	Polymerase delta-interacting protein
PP1	Protein phosphatase-1
PP1 α	Protein phosphatase-1 α
PP2A	Protein phosphatase-2A
pRb	Retinoblastoma protein
Prx	Peroxiredoxins
PS	Phosphatidylserine

PTEN	Phosphatase and tensin homolog
PTP	Protein tyrosine phosphatase
qRT-PCR	Quantitative Real-Time Polymerase Chain Reaction
RAC1/2	Ras-related C3 botulinum toxin substrate ½
RAS	Rat sarcoma protein kinase
RIPA	Radio immunoprecipitation assay
RNA	Ribonucleic acid
RO•	Alkoxy
RO ₂ •	Peroxy
ROS	Reactive oxygen species
RPMI	Roswell Park Memorial Institute
RT	Room temperature
S	DNA synthesis phase
SB	SB216763
SCF	Stem cell factor
SDS	Sodium dodecyl sulfate
SDS-PAGE	SDS-polyacrylamide gel electrophoresis
SFM	Serum free medium
SH	Src-homology domain
siRNA	Small Interfering RNA
siRNA(i)	p22phox siRNA ID-s3786 transfected cells
siRNA(ii)	p22phox siRNA ID-s194372 transfected cells
SOD	Superoxide dismutase
SOS	Son of Sevenless
Srx	Sulfiredoxins

STAT	Signal Transducers and Activators of Transcription
STI-571	Imatinib Mesylate
STIM	Stop Imatinib trial
TBS/T	Tris-buffered saline/0.1% Tween-20
TGF β	Transforming growth factor- β
TKI	Tyrosine kinase inhibitor
Tks4	Tyrosine kinase substrate with four SH3 domains
TLR4	Toll-like receptor 4
TNF- α	Tumour Necrosis factor- α
TPO	Thrombopoietin
Trx	Thioredoxin
UO	UO126
VAS2870	3-benzyl-7-(2-benzoxazolyl)thio-1,2,3-triazolo[4,5- d]pyrimidine
VHL	von Hippel-Lindau tumour suppressor gene
WEHI-CM	WEHI-conditioned medium

Chapter 1

General Introduction

1. Chronic Myeloid Leukaemia

1.1 Classification of leukaemia

The term leukaemia is derived from the combination of the two Greek words, *leukos* (white) and *haima* (blood), referring to a spectrum of haematological neoplasms of the blood and bone marrow which are characterised by an abnormal accumulation of white blood cells. Accounting for approximately 3% of all cancers diagnosed each year, 12.8 out of 100,000 American adults were newly diagnosed with some form of leukaemia in 2013 and an estimated 310,046 people currently live with or are in remission from this disease in the United States alone (LLS, 2013; Howlader *et al.*, 2013). Leukaemia is broadly classified based on two parameters, the lineage of white blood cells affected, which can be either myeloid or lymphoid, as well as whether or not the onset or progression of the disease presents as chronic or acute. Acute leukaemias demonstrate rapid accumulation of immature white blood cells, causing the disease to progress quickly. In contrast, chronic leukaemias are a group of long-term diseases, typically taking months or years to progress and are characterised by the excessive build up of relatively mature, but still abnormal, white blood cells.

1.2 CML: A brief history

In 1845, pathologists Dr James Hughes Bennett of Edinburgh and Dr Rudolf Virchow of Berlin independently described a disease which was to become known as Chronic Myeloid Leukaemia (CML). Later work by two Philadelphia based cytogeneticists linked this disease to a consistent chromosomal abnormality, which is now known as the Philadelphia (Ph) Chromosome (Nowell and Hungerford, 1960). The Ph Chromosome was subsequently recognised as the product of a reciprocal

translocation between chromosomes 9 and 22 (Rowley, 1972), which fused the *ABL1* proto-oncogene from chromosome 9 (Bartram *et al.*, 1983) to the Breakpoint Cluster Region (*BCR*) gene on chromosome 22 (Groffen *et al.*, 1984). This translocation, designated t(9;22)(q34;q11), generates the chimeric *BCR-ABL1* gene thereby producing the Bcr-Abl oncoprotein (Shtivelman *et al.*, 1985). Bcr-Abl is a constitutively active tyrosine kinase and has been identified as one of the key requirements for oncogenesis in CML (McLaughlin *et al.*, 1987; Lugo *et al.*, 1990).

1.3 CML: A clinical perspective

CML has an incidence of 1-2 in 100 000 individuals, with approximately 70,000 people currently living with the disease in the United States alone and a further 4800 newly diagnosed cases each year more commonly observed in adults with a median age of onset between 45-55years (LLS, 2013; Howlader *et al.*, 2013). Interestingly, low levels of the *BCR-ABL1* mRNA transcript can be detected in approximately 30% of healthy individuals, this occurrence increases with age however only a small percentage of these people will ever develop CML (Bierneux *et al.*, 1995; Bose *et al.*, 1998). Therefore, although Bcr-Abl expression is sufficient to transform haematopoietic cells (McLaughlin *et al.*, 1987, Lugo *et al.*, 1990), Bcr-Abl alone may not be sufficient to induce CML in humans. It is suggested that immune response may eliminate Bcr-Abl expressing cells in these individuals (Posthuma *et al.*, 1999) or further genetic abnormality may be required for disease to develop (Deininger *et al.*, 2000; Ren, 2005). Indeed it has previously been predicted using epidemiological data that two further mutations in addition to Bcr-Abl may be necessary for CML to fully develop (Vickers, 1996). How these mutations arise is uncertain however epidemiologic studies have demonstrated that exposure to

ionizing irradiation increases the risk of acquiring CML, in these cases CML developed after a prolonged latent period (4–11 years on depending on the level of exposure) further suggesting that subsequent mutations may be necessary for development (Tanaka *et al.*, 1989; Corso *et al.*, 1995). It is interesting to note that these epidemiology studies in part focused on CML development in survivors of the atomic bomb.

Phases of Disease

Patients usually present in a chronic phase (CML-CP) which is characterised by an accumulation of functionally normal myeloid cells as well as an increased presence of the immature myeloid progenitor cells (also known as blast cells) in bone marrow, peripheral blood and extramedullary sites (Savage *et al.*, 1997).

Symptoms are mild at this stage and generally consist of splenomegaly, fatigue and weight loss. With effective treatment patients can remain in a CML-CP for several years maintaining a relatively good quality of life. Unfortunately, if treatment is or becomes ineffective the disease will progress to an accelerated phase presenting only for 4-6 months, with an increase in the frequency of progenitor cells detected rather than terminally differentiated mature cells (Calabretta and Perrotti, 2004).

Subsequently the disease enters a blastic phase (CML-BP) which is also referred to as “Blast Crisis”. CML-BP is characterised by a considerable accumulation of progenitor cells and is associated with poor prognosis. Progression to CML-BP occurs after CML progenitors lose what is known as their terminal differentiation capacity, signifying that these cells will not differentiate into mature blood cells (Figure 1). Each stage of disease is determined through examination of different numbers of immature progenitors in peripheral blood or bone marrow, with

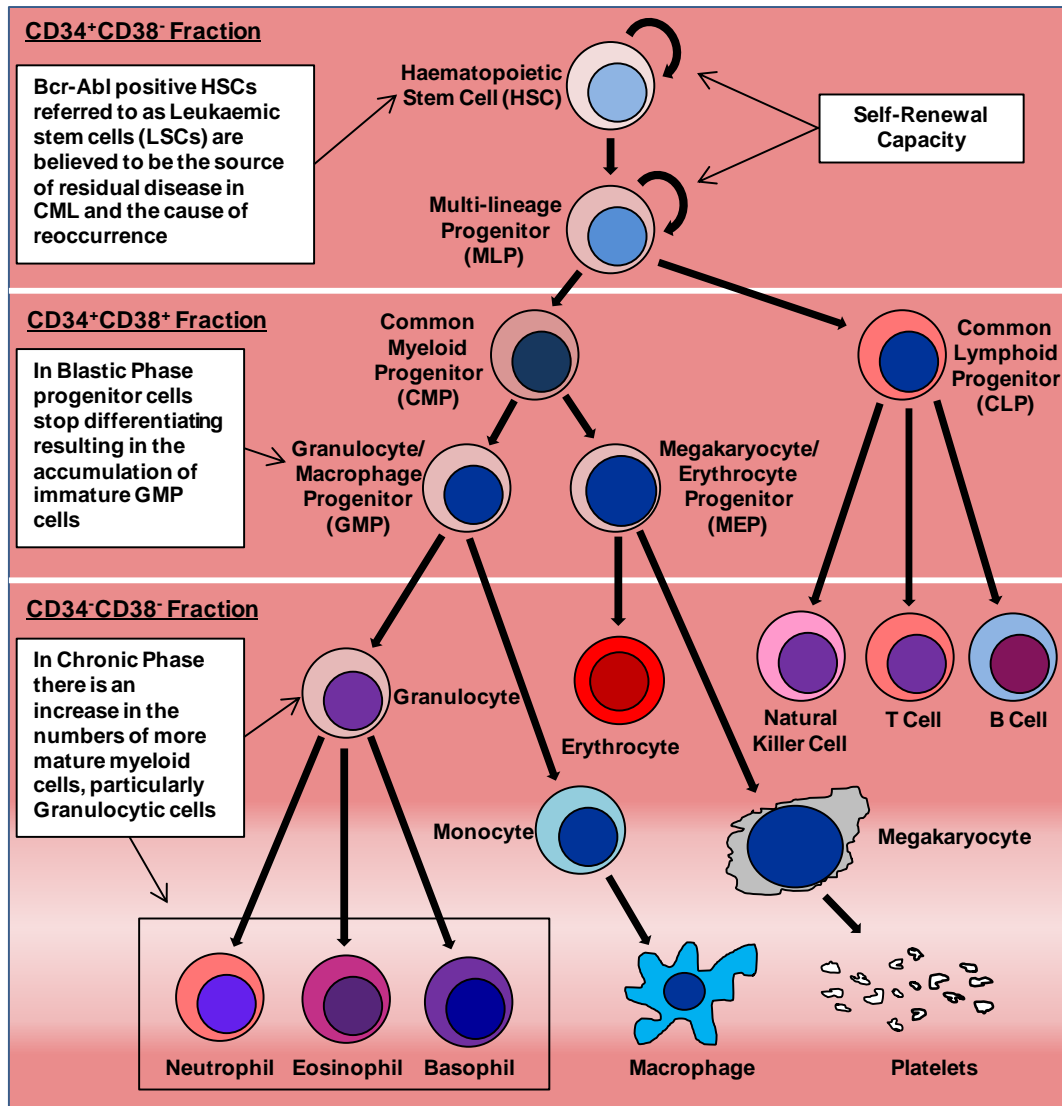


Figure 1. Haematopoiesis and its relationship to CML. Figure illustrates normal cellular haematopoiesis and identifies how it relates to CML. The CD34 and CD38 surface markers are extensively used to define haematopoietic cell hierarchy, with stem cells being CD34⁺ CD38⁻, progenitor cells being CD34⁺ CD38⁺ and matured cells expressing neither (Doulatov *et al.*, 2012). This classification system is also used for CML cell hierarchy, with CD34⁺ CD38⁻ used to identify Leukaemic Stem Cells (LSCs) which will be discussed later.

CML-CP defined by 0-15% blasts, accelerated phase with 16-30% blasts and CML-BP with >30% blasts (Akel *et al.*, 2000).

How progenitors lose their differentiation capacity is not entirely certain however it is known that additional molecular and cytogenetic changes occur in 50-80% of patients that have progressed from chronic to accelerated and blast phases, demonstrating abnormalities in the genes for p53, pRb, c-MYC, p16^{INK4A} and RAS (Faderl *et al.*, 1999). Additionally, Bcr-Abl activity itself may increase significantly as a result of gene amplification, increased promoter activity as well as other methods (Perrotti *et al.*, 2010). Oxidative stress induced as a result of Bcr-Abl kinase activity is a major contributing cause to CML cell genomic instability and the subsequent genetic alterations which result, a factor which is strongly believed to influence disease progression (Nowicki *et al.*, 2004; Rassool *et al.*, 2007; Nieborowska-Skorska *et al.*, 2012). As will be discussed, this increase in genomic instability is also considered to be the main contributing factor for the development of Bcr-Abl resistance to the tyrosine kinase inhibitors (TKI) used to treat CML patients (Koptyra *et al.*, 2006; Sallmyr *et al.*, 2008).

1.4 Bcr-Abl

Bcr-Abl Isoforms

Generation of Ph is not entirely uniform and shows predictable variance and as a result one of three Bcr-Abl isoforms can be formed, each with a different molecular weight which is determined based on the breakpoint position and subsequent number of sequences retained within the *BCR* gene following translocation. Breakpoints within the *BCR* gene during translocation localise to one of three regions, the first major breakpoint cluster region (M-bcr) encodes for a

210kDa protein (p210 Bcr-Abl) which is the hallmark of CML and can also be found in approximately a third of Ph-positive Acute Lymphocytic Leukaemia (ALL) patients (McLaughlin *et al.*, 1987; Maxwell *et al.*, 1987). Further upstream of the M-bcr is the minor breakpoint cluster region (m-bcr) which encodes a 190kDa protein (p190 Bcr-Abl) and is detected in the remaining proportion of Ph-positive ALL cases as well as a minor number of CML cases (Kurzrock *et al.*, 1987; Kantarjian *et al.*, 1991; Suryanarayan *et al.*, 1991). The final breakpoint region, μ -bcr, results in a 230kDa protein (p230 Bcr-Abl) which has been detected in Ph-positive Chronic Neutrophilic Leukaemia (Pane *et al.*, 1996) as well as rare cases of CML (Wilson *et al.*, 1997).

ABL1 and BCR genes: Independent and combined properties

Studies which began more than 40 years ago in the Abelson murine leukaemia virus identified *ABL1* as an oncogene (Abelson and Rabstein, 1970; Goff *et al.*, 1980; Ben-Neriah *et al.*, 1986). This gene and its family members encode for non-receptor tyrosine kinases which have demonstrated importance in linking extracellular stimuli to signalling pathways involved in cell growth, survival, invasion, adhesion and migration (Greuber *et al.*, 2013). *ABL1* and *ABL2* make up the *ABL* gene family however *ABL1* is the gene associated with the translocation, production and oncogenic potential of the *BCR-ABL1* proto-oncogene (Bartram *et al.*, 1983). The 145kDa Abl protein encoded by *ABL1* is ubiquitously expressed and although predominantly nuclear, shuttles between the cytoplasm and nuclei of cells co-localising with F-actin and binding to chromatin respectively (Van Etten *et al.*, 1989; Van Etten *et al.*, 1994). Although heavily implicated in CML, Abl activity has also demonstrated importance in the oncogenesis of solid cancers, particularly breast

cancer (Srinivasan and Plattner, 2006) and lung cancer (Lin *et al.*, 2007) as well as prostate cancer (Drake *et al.*, 2012) and melanoma (Ganguly *et al.*, 2012).

The unique structure of the Abl protein is of great importance for its function. Alternative splicing of the first exon of the *ABL1* gene produces the 1a and 1b isoforms of Abl (Shtivelman *et al.*, 1985). Of the two isoforms, 1b is expressed at a higher level and contains a myristoylated N-terminal glycine, not present in 1a variant, which allows it to attach to the plasma membrane (Daley *et al.*, 1992). Additionally, Abl has three Src-homology (SH) domains in its N-terminal region all of which are very important to mediate interactions with other proteins (Greuber *et al.*, 2013). Intramolecular forces tightly regulate the catalytic activity of the Abl kinase, with the proteins N-terminal "cap", which contains its myristoylated tail and SH3 domain, important for auto-inhibition of function (Pluk *et al.*, 2002). Additionally, in order to stabilise Abl in an active conformation phosphorylation of two tyrosine residues, Y412 and Y245, within a conserved regulatory motif known as its activation loop is required (Tanis *et al.*, 2003).

As discussed, Abl activity is tightly regulated with multiple regulatory mechanisms, most of which are disrupted in the Bcr-Abl fusion protein. Indeed, regulation of Abl activity by its auto-inhibitory N-terminal "cap" is sterically abolished as a result of its fusion to the C-terminus of Bcr sequences, thereby increasing tyrosine kinase activity (Tanis *et al.*, 2003). Bcr is a complex 160kDa protein containing several functional regions and is ubiquitously expressed across human tissues (Collins *et al.*, 1987; Dhut *et al.*, 1988). The independent function of Bcr in cells is still not fully understood however much is known of its function in respect to Bcr-Abl. Indeed, the N-terminus of Bcr contains a novel serine/threonine kinase domain, several important SH2 protein binding domains and an amino

terminal coiled-coil oligomerisation domain, all of which have been demonstrated to be important for Bcr-Abl-mediated transformation (Maru and Witte, 1991; Pendergast *et al.*, 1991; McWhirter *et al.*, 1993a). Activation of Bcr-Abl requires dimerization followed by successive trans- and auto- phosphorylation of the regulatory tyrosines found in the Abl domains activation loop (Smith *et al.*, 2003). Interestingly, the coiled-coil domain of Bcr is essential for dimerisation and therefore activation of Abl tyrosine kinase. Furthermore, this domain of Bcr also promotes Bcr-Abl association with actin, which is essential for proper activation of downstream signalling pathways (McWhirter *et al.*, 1993b; McWhirter and Wang 1993). Finally, Bcr fusion brings new regulatory domains/motifs to Abl kinase inferring the ability for Abl to interact and phosphorylate new substrates. One important example of this involves the phosphorylation of Bcr on tyrosine residue 177, which recruits Growth factor Receptor-Bound protein 2 (GRB2) (Pendergast *et al.*, 1993). GRB2 is an important adaptor molecule and once recruited by Y177 phosphorylation on Bcr, it allows Abl to phosphorylate and initiate the activation of the Ras pathway, which will be discussed later (Ma *et al.*, 1997). This recruitment enhances the oncogenic ability of Abl kinase further contributing to Bcr-Abl pathogenesis.

1.5 Mechanisms of Bcr-Abl oncogenesis

In many ways Bcr-Abl activity mimics growth factor stimulation, activating similar signalling pathways such as the PI3K/Akt, JAK/STAT and Ras-activated Raf/MEK/ERK pathways (Figure 2). Constitutive signalling from these pathways in haematopoietic stem and progenitor cells as a result of Bcr-Abl activity leads to an increase in proliferation which is accompanied by a decrease in apoptosis (Cortez *et*

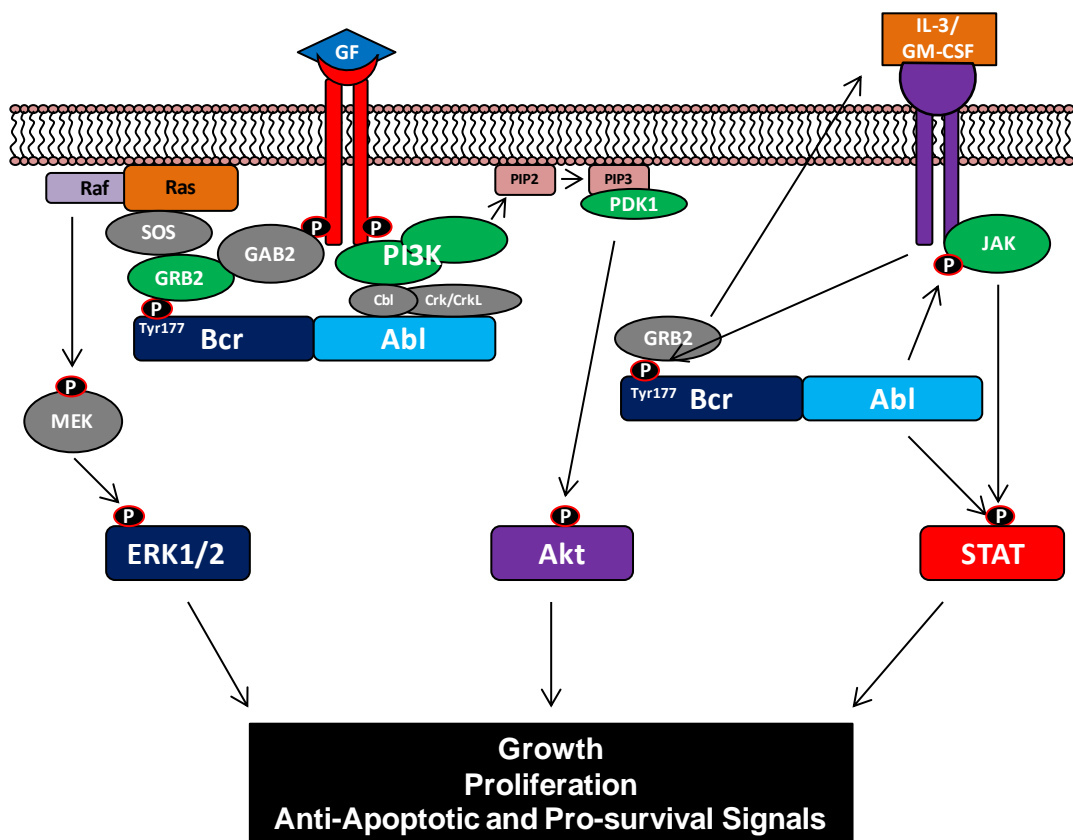


Figure 2. Constitutive tyrosine kinase activity of Bcr-Abl mimics growth factor receptor activation. Growth factors (GF) and cytokines are known to induce signal transduction which activates a host of cellular signalling pathways including the PI3K/Akt, JAK/STAT and Ras activation of Raf/MEK/ERK1/2, all of which are also known to be activated downstream of Bcr-Abl. This figure represents a simplified schematic of the interplay between Bcr-Abl and GF/cytokine receptor signalling, described in detail in text. GF, Growth factor; P, Phosphorylation; MEK, MAPK/ERK kinase; SOS, Son of Sevenless; PIP2, Phosphatidylinositol bisphosphate; PIP3, Phosphatidylinositol 3,4,5-triphosphate; GRB2, Growth factor Receptor-Bound protein 2; ERK, Extracellular Regulated Kinase; IL-3, Interleukin-3; GM-CSF, Granulocyte/Macrophage-Colony stimulating factor; JAK, Janus Kinase; STAT, Signal Transducers and Activators of Transcription; PDK1, 3-phosphoinositide-dependent protein kinase-1.

al., 1995), resulting in the exponential increase in myeloid cell numbers.

Furthermore, these cells demonstrate reduced growth-factor dependence (Daley *et al.*, 1988; Sirard *et al.*, 1994) and increased motility with decreased adhesion to bone marrow stroma and extracellular matrix (Gordon *et al.*, 1987), leading to premature release of immature myeloid cells into circulation. These events coupled with Bcr-Abl induced genomic instability, drive disease progression (Sallmyr *et al.*, 2008).

Ras Signalling

Under normal conditions Ras signalling is involved in the transmission of extracellular signals, usually initiated by epidermal growth factor stimulation, which promote growth, survival and differentiation (Pylayeva-Gupta *et al.*, 2010). This pathway is well studied, with aberrant activation of Ras found in many human cancers (Pylayeva-Gupta *et al.*, 2010). The potential of Bcr-Abl to activate Ras signalling is dependent on the phosphorylation of tyrosine 177 within the Bcr region, which allows for interaction with the adapter molecule GRB2, an important factor in the transformation of human haematopoietic progenitor cells (Pendergast *et al.*, 1993). Bcr-Abl binding to GRB2 enables the formation of complexes between GRB2, the guanine-nucleotide exchange factor Son of Sevenless (SOS) and GAB2 (a scaffolding adaptor protein), thereby activating Ras signaling (Pendergast *et al.*, 1993; Sattler *et al.*, 2002). Ras signalling has been shown to be a key requirement of Bcr-Abl-mediated transformation (Sawyers *et al.*, 1995; Peters *et al.*, 2001), while also being instrumental in the inhibition of apoptosis downstream of Bcr-Abl (Cortez *et al.*, 1996). One of the main groups of proteins activated as a result of Bcr-Abl activity are the Extracellular Regulated Kinase (ERK) family of proteins (Cortez *et al.*, 1997). Ras signalling downstream of Bcr-Abl is crucial in activation of ERK

signalling which is important for the induction of mitogenic and anti-apoptotic effects in CML (Chang *et al.*, 2003).

PI3K/AKT Signalling

The PI3k/Akt pathway is involved in a wide range of cellular functions that include proliferation, differentiation, inhibition of apoptosis and glucose metabolism (Engelman, 2009; Vanhaesebroeck *et al.*, 2012). Activation of this pathway is normally downstream of growth factor receptor tyrosine kinases, with aberrant activity known to play a significant role in oncogenic signaling. Bcr-Abl activates this pathway by recruiting PI3K into a complex with the adapter proteins Crk, CrkL and Cbl, activating PI3K and initiating downstream signalling (Sattler *et al.*, 1996). Furthermore, activation of Ras and recruitment of GAB2 has also been shown as important in PI3K activation (Sattler *et al.*, 2002). Bcr-Abl induces the constitutive activation of PI3K signalling thereby increasing proliferation (Skorski *et al.*, 1995) while also demonstrating the potential to transform haematopoietic cells (Skorski *et al.*, 1997). Akt is a serine/threonine kinase activated downstream of PI3K and is known to activate and inactivate several downstream targets which have important anti-apoptotic and cell survival functions (Vanhaesebroeck *et al.*, 2012). Akt activity downstream of Bcr-Abl signalling is essential in mediating the oncoproteins leukogenic effects by; inhibiting BAD, preventing apoptosis through continual activity of the anti-apoptotic BCL-2 proteins (Salomoni *et al.*, 2000); activating mammalian target of rapamycin (mTOR) which promotes increased cellular growth and division in leukaemic cells (Mohi *et al.*, 2004); up-regulating MDM2, which prevents cell cycle arrest and apoptosis through negative regulation of p53 (Trotta *et al.*, 2003); and inhibiting FOXO transcription factors (FOXO1, FOXO3a, and

FOXO4) through their constitutive phosphorylation and cytoplasmic retention thereby preventing their effects on cell-cycle arrest and apoptosis (Jagani *et al.*, 2008).

JAK/STAT Signalling

The Janus Kinase (JAK) proteins are a group of tyrosine kinases which activate the Signal Transducers and Activators of Transcription (STAT) family of transcription factors which are important in regulating immune response, proliferation, differentiation, cell migration and apoptosis in response to growth factor and cytokine signals, with their aberrant activation implicated in many myeloproliferative disorders including CML (Schindler *et al.*, 2007). Bcr-Abl induces constitutive phosphorylation and activation of STAT1 and STAT5 through JAK2 kinase activity (Chai *et al.*, 1997), which mediates the transcriptional upregulation of several proteins that contribute to Bcr-Abl pathogenesis, including the anti-apoptotic proteins Bcl-x1, Bcl-2, A1 and the serine/threonine kinase pim-1 (Horita *et al.*, 2000; Gesbert and Griffin, 2000; Nieborowska-Skorska *et al.*, 2002). Indeed, STAT5 activation is important in transformation, enhanced growth and viability downstream of Bcr-Abl (de Groot *et al.*, 1999; Sillaber *et al.*, 2000). Studies in mouse models have demonstrated STAT5 to be an indispensable factor for induction and maintenance of Bcr-Abl–positive leukaemia (Ye *et al.*, 2006; Hoelbl *et al.*, 2010). Interestingly, JAK/STAT pathways can be activated through autocrine signalling in early progenitor cells as a result of Bcr-Abl– induced secretion of growth factors such as IL-3 and GM-CSF (Jiang *et al.*, 1999). This is suggested to play a role in promoting cell-cycle entry of primitive leukemic stem cells and progenitors during the CML-CP (Holyoake *et al.*, 2002). Interestingly, similar

extrinsic signalling has also demonstrated involvement in Bcr-Abl-independent TKI resistance (Wang *et al.*, 2007). Indeed, enhanced STAT5 levels have been demonstrated to reduce sensitivity to TKIs thereby inducing resistance (Warsch *et al.*, 2011).

1.6 CML treatment and the problems faced

For a long time allogeneic bone marrow transplantation remained the only curative option for CML, unfortunately this treatment was rarely feasible due to the later age of onset generally observed in CML patients coupled with the difficulty in finding a suitable donor. As such traditional chemotherapeutics such busulfan, hydroxyurea, cytarabine as well as interferon- α (IFN α) were routinely used (Silver *et al.*, 1999). Treatment with IFN α -based regimens remained the standard therapy for many years however the unique presence of Bcr-Abl expression in all CML cells and absence from normal cells made it the central focus in the development of therapeutic treatments (Deininger *et al.*, 2005).

In the 1990s, a targeted rational drug design led to the development of the first clinically significant small-molecule tyrosine kinase inhibitor (TKI) STI571, which subsequently become known as Imatinib. In 1996, Druker *et al.* described the selective effects of this TKI on cells containing Bcr-Abl, resulting in the inhibition of cell growth. This study was the first demonstration of the potential of Imatinib as a treatment for CML. Imatinib works by inhibiting the tyrosine kinase activity of Bcr-Abl through competitive binding of the ATP-binding site, preventing dimerisation, auto-phosphorylation and therefore kinase activation, inhibiting its effects on downstream substrates (Schindler *et al.*, 2000; Nagar *et al.*, 2002). A 5 year follow-up study of newly diagnosed CML-CP patients treated with Imatinib demonstrated it

to extremely successful in the clinic with complete haematological response (CHR: Normalisation of blood counts and spleen size) and cytogenetic response (CCyR: no detection of Ph Chromosome) observed in 97% and 87% of patients respectively without progression to CML-BP in 93% of patients (Druker *et al.*, 2006). The potential of Imatinib treatment for newly diagnosed patients in CMP-CL continued to be demonstrated in further 6 year (Hochhaus *et al.*, 2009) and 8 year (Deininger *et al.*, 2009) follow-up studies. Even more significantly patients who presented with CCyR for at least 2 years were projected to have the same life expectancy as the general population (Gambacorti-Passerini *et al.*, 2011).

Drug Resistance

Imatinib treatment was hailed as major advancement in CML treatment, demonstrating considerable improvements on the previous standard of IFN α treatment (Druker *et al.*, 2006; Hochhaus *et al.*, 2009; Deininger *et al.*, 2009). However, it was evident that Imatinib was not perfect. In the 8 year follow-up study it was demonstrated that 16% of patients had to discontinue treatment with Imatinib as a result of the drug being inadequately effective and a further 6% for adverse effects (Deininger *et al.*, 2009). Furthermore, many patients, although initially demonstrating positive effects to treatment, became resistant to Imatinib treatment which was largely a result of point mutations in the kinase domain of Bcr-Abl disrupting TKI binding (Gorre *et al.*, 2001; Branford *et al.*, 2002; Shah *et al.*, 2002).

As a result, large emphasis was directed to the development of alternative TKIs which circumvent known modes of Imatinib resistance (Quintás-Cardama *et al.*, 2007; Bixby and Talpaz, 2011). Indeed, crystallographical analysis (Schindler *et al.*, 2000; Nagar *et al.*, 2002) which examined the interactions of Imatinib with Bcr-

Abl led to the development of the more potent second generation inhibitors of Bcr-Abl. These were Nilotinib, an Imatinib derivative (Weisberg *et al.*, 2005) and Dasatinib, a dual Src and Abl TKI (Shah *et al.*, 2004), both of which were effective in treating the majority of mutations which conferred resistance to Imatinib and were approved for first-line therapy of CML-CP in 2010. Still these drugs were not without their faults which led to the development of Bosutinib (Puttini *et al.*, 2006), another Src/Abl inhibitor which binds Bcr-Abl in a unique manner, addressing Bcr-Abl mutations which conferred resistance to Nilotinib and Dasatinib treatment (Redaelli *et al.*, 2009; Khoury *et al.* 2012).

Bosutinib is currently being examined as another potential first-line therapy (Cortes *et al.*, 2011a; Khoury *et al.*, 2012) however considering the trends observed in TKI treatment to date there is no doubt that resistance will develop toward this inhibitor requiring the need for more drugs. Indeed, the most problematic point mutation observed to date is the Bcr-Abl^{T315I} “gatekeeper mutation”, which is insensitive to all three of the clinically approved TKIs as well as Bosutinib (O’Hare *et al.*, 2009). As a result there is great anticipation for the clinical approval of third generation Bcr-Abl TKIs, capable of targeting this mutation as a first line therapy and in patients who have relapsed due to this mutation. Two such drugs which are in clinical evaluation are Ponatinib (Huang *et al.*, 2010) and DCC-2036 (Cortes *et al.*, 2011b).

These TKIs were all developed to overcome Bcr-Abl-dependent resistance as a result of point mutation and subsequent structural changes in the protein. Interestingly, it has been also observed that patients can exhibit resistance to TKI treatment without detectable mutations in the *BCR-ABL1* mRNA transcript (Hughes *et al.*, 2009; Garg *et al.*, 2009). Indeed it has been demonstrated that there can be

clinical resistance to TKI treatment despite inhibition of Bcr-Abl activity (Hochhaus *et al.*, 2002). This is referred to as Bcr-Abl-independent resistance and has been linked to the increased activity of various kinases and their associated pathways including PI3K/Akt, Raf/MEK/ERK1/2, Src family of kinases and JAK/STAT (Donato *et al.*, 2003; Burcher *et al.*, 2005; Esposito *et al.*, 2011; Gioia *et al.*, 2011). This has presented a large obstacle for CML treatment, mounting much concern while prompting a reevaluation of therapeutic approach. As a result, much focus has now been placed on the potential of targeting Bcr-Abl activity in combination with these effected pathways and others (Helgason *et al.*, 2011, O'Hare *et al.*, 2012).

Residual disease: The leukaemic stem cell

In addition to the possibility of resistance developing there is also a necessity for continual, lifelong treatment with Imatinib to prevent disease reoccurrence. This was demonstrated in an unusual clinical study, The Stop Imatinib (STIM) trial, which examined the effects of Imatinib discontinuation in 100 patients that had exhibited a complete molecular response (CMR: Undetectable levels of *BCR-ABL1* mRNA transcript) for at least 2 years (Rousselot *et al.*, 2007; Mahon *et al.*, 2010). A 30 month follow-up observed that 61 of these patients experienced molecular reoccurrence of *BCR-ABL1* mRNA transcript with only 56 of these patients sensitive to repeat TKI treatment. Furthermore, a similar study which examined Nilotinib and Dasatinib discontinuation in patients demonstrated equivalent results (Rousselot *et al.*, 2011). Interestingly, this reoccurrence is a result of the clonal expansion of a residual population of Bcr-Abl positive cells, referred to as leukaemic stem cells (LSCs) (Figure 1).

CML LSCs express Bcr-Abl yet are resistant to TKI treatment and are therefore said to lack addiction to Bcr-Abl signalling (Hamilton *et al.*, 2012). LSCs are suggested to be transformed haematopoietic stem cells (HSC) (Takahashi *et al.*, 1998) and as such exhibit self-renewal capacity providing a continual source of disease (Huntly *et al.*, 2004). Furthermore, these cells reside in the bone marrow niche a factor which is believed to in part confer this lack of addiction to Bcr-Abl signalling (Weisberg *et al.*, 2008). This niche presents as a cytokine-rich microenvironment ideal for residual disease to reside, this is due to the fact that high concentrations of stromal cell-derived factors such as granulocyte-macrophage colony-stimulation factor (GM-CSF) and interleukin-6 (IL-6) can provide LSCs cells with extrinsic protection from TKI treatment (Traer *et al.*, 2012; Nair *et al.*, 2012). Interestingly, co-culture of CML LSCs with mesenchymal stromal-cells has also implicated the N-cadherin receptor and WNT- β -catenin signalling in TKI protection (Zhang *et al.*, 2013). In fact, three other major pathways have demonstrated involvement in LSCs survival; Hedgehog (Zhao *et al.*, 2009), TGF β -FOXO3A-BCL-6 (Naka *et al.*, 2010; Hurtz *et al.*, 2011) and JAK2/STAT-PP2A (Neviani *et al.*, 2005; Samanta *et al.*, 2009; Hantschel *et al.*, 2012).

Unfortunately although development of new TKIs can address drug resistance to a degree their use in eradicating residual disease is limited. Treating residual disease remains a challenge as replicating the entire effects of the bone marrow microenvironment in order to design potential therapeutics is difficult, extensively involving murine models which only exhibit CML-like disease. Co-culture studies like those of Zhang *et al.*, (2013) provide an interesting approach to develop further understanding in this area and identify possible targets for treatment.

Targeting essential pathways which infer Bcr-Abl insensitively to LSCs should make these cells susceptible to Bcr-Abl inhibition as a treatment. As such, much interest is now focused on the potential of Bcr-Abl inhibition combined in tandem with simultaneous inhibition of other critical pathways (Helgason *et al.*, 2011; O'Hare *et al.*, 2012). One such study which has demonstrated a substantial increase in LSC death through combination, this treatment utilised the inhibition of autophagy and Bcr-ABL *via* chloroquine and TKI treatment respectively (Bellodi *et al.*, 2009). As a direct result of this study and others, the CHOICES (ChlorOquine and Imatinib Combination to Eliminate Stem cells) clinical trial commenced in the United Kingdom in 2013 to examine the potential of the combined use of chloroquine and Imatinib in treatment of CML patients.

2. Reactive Oxygen Species (ROS) and Cellular Signalling

2.1 Classification of ROS

Reactive Oxygen Species (ROS) are highly reactive oxygen derivatives broadly classified into two groups, radicals which possess unpaired valence shell electrons [e.g. the oxygen ions superoxide ($O_2^{\bullet-}$), peroxy (RO_2^{\bullet}), hydroxyl ($\bullet OH$) and alkoxy ($RO\bullet$)] and non-radicals [e.g. hypochlorous acid (HOCl), ozone (O_3), singlet oxygen (1O_2) and hydrogen peroxide (H_2O_2)] which are easily converted into radicals as a result of their unstable O-O linkage thereby acting as oxidative agents (Bedard and Krause, 2007). Generation of ROS has long been regarded as a by-product of oxygen consumption and cellular metabolism. Indeed, ROS are produced during aerobic respiration as a consequence of electron transport chain activity. During this process electrons are transported between the mitochondrial electron transport chain complexes I, II, III and IV, “leakage” of a single electron at anyone of these complexes has the potential of reducing free oxygen to produce $O_2^{\bullet-}$, which is rapidly neutralised by antioxidant systems such as superoxide dismutase (SOD) and peroxidases present in the mitochondria (Turrens, 2003).

Reduced levels of free radical scavenging enzymes, hypoxic conditions or damage to the mitochondria can result in the escape of ROS from the mitochondria, thereby increasing oxidative stress in the cell. In addition, albeit to a lesser extent systems other than the mitochondria are also known to contribute to endogenous ROS levels as a by-product of their normal function, these include cytochrome P-450 (Gonzalez, 2005), xanthine oxidoreductase (Harrison, 2004), peroxisomes (Schrader and Fahimi, 2004) as well as other cellular elements (Bedard and Krause, 2007). Contrasting to these former sources, ROS can also be generated enzymatically in

response to various stimuli; the NADPH Oxidases (Nox) are an example of a system which produces ROS professionally and not as a by-product of function.

Regardless of the source, ROS can potentially interact with a vast number of biomolecules in the cell such as lipids, proteins, carbohydrates and even nucleic acids, therefore if allowed to accumulate to toxic levels these interactions can have detrimental effects on the function of these biomolecules, leading to induction of apoptosis (Simon *et al.*, 2000). In fact, this unbiased reactivity of ROS has led to their general acceptance as the key factor in the aging process (Beckman and Ames 1998). In addition to these effects, exposure of DNA to ROS can cause double strand breaks or modification of bases through oxidation, both of these effects can disrupt the structure of DNA thereby effecting RNA transcription as well as potentially inducing mutations if not repaired (Cooke *et al.*, 2003). Such effects on DNA can result in the induction of apoptosis in cells however these mutations may also have the potential of initiating oncogenesis. Indeed, many cancer types demonstrate an elevated ROS levels which has been linked to the generation of further genetic alterations thereby contributing to oncogenic phenotype and disease progression (Mitsushita *et al.*, 2004; Wu, 2006; Yamaura *et al.*, 2009; Weinberg and Chandel, 2009; Hole *et al.*, 2011).

Due to their abundance proteins are the most frequent biomolecules to be affected by oxidation and as a result are believed to be the main targets of ROS within cells (Davies, 2005). Fluctuations in ROS levels will therefore influence oxidative-modifications of proteins, the consequence of which being dependent on the concentration of ROS and species involved, while further being influenced by the individual biochemical and structural characteristics of each protein effected. This is down to the secondary and tertiary structures of a protein being affected by oxidative

induced changes in the charge, size, hydrophobicity or polarity of amino acids in its polypeptides, dictating protein stability and therefore activity. This is demonstrated in the fact that oxidation of amino acid side chains can cause inter- and intra-molecular cross-linkages while it is also known that polypeptide backbones are susceptible to $\bullet\text{OH}$ reactivity which can provoke protein fragmentation and degradation (Berlett and Stadtman, 1997). One of the most physiologically important and relevant ROS-mediated oxidative-modifications of proteins is observed in sulphur-containing amino acids such as cysteine and methionine. These amino acids have been demonstrated to be highly susceptible to oxidation (Janssen-Heininger *et al.*, 2008) but more significantly these oxidation events can be reversed by antioxidant mechanisms within the cell (Hoshi and Heinemann, 2001).

2.2 Maintenance of ROS homeostasis

Cellular Antioxidants

Considering the effects of ROS accumulation it comes as no surprise that cells have evolved various mechanisms for ensuring that oxidative stress is prevented or kept to a minimum. One such mechanism is observed within proteins themselves. As discussed, ROS readily react with methionine residues in proteins (Janssen-Heininger *et al.*, 2008). This reaction forms methionine-sulfoxide thereby removing or scavenging the reactive species and preventing its potential to react with other biomolecules. Interestingly, most cells contain methionine sulfoxide reductases (MsrA/B), which catalyze the thioredoxin (Trx)-dependent reduction of methionine sulfoxide back to methionine (Lee and Gladyshev, 2011). It is suggested that this enzymatically-regulated cycling of methionine between oxidised and reduced states has evolved as a buffer against ROS, acting as an endogenous antioxidant in cells

(Luo and Levine, 2009). It is important to note however that methionine sulfoxide can be irreversibly hyperoxidised to form methionine sulfone (Stadtman *et al.*, 2003).

In addition to this system most cell types also express endogenous cellular antioxidant enzymes which prevent oxidative toxicity by scavenging and neutralising accumulated ROS. The glutathione (GSH) system is ubiquitously expressed and among the most active of these systems, important for cellular protection against ROS as well as electrophiles and xenobiotics. Interestingly GSH can act as an important indicator of a cells redox state, a fact which is frequently utilised to examine oxidative stress (Pastore *et al.*, 2001; Piemonte *et al.*, 2001). GSH reduces disulfide bonds formed as a consequence of cysteine oxidation, this process is vital for the recycling of glutaredoxins (Grx) another antioxidant which require GSH as a co-factor (Chen *et al.*, 2009). In order to achieve its function GSH becomes oxidised forming GSSG, before GSH reductases reduce it back to GSH.

Trx is part of another antioxidant system which does not directly remove ROS, but instead supports other important antioxidant proteins by catalysing their reduction through cysteine thiol-disulfide exchange (Nordberg and Arner, 2001). Other important antioxidant mechanisms include the conversion of lipid hydroperoxides to alcohols and H_2O_2 to H_2O by GSH peroxidases (Arthur, 2000), the catalytic conversion of $\text{O}_2^{\bullet-}$ to H_2O_2 achieved by SOD activity (McCord and Fridovich 1988) and the neutralisation of H_2O_2 by catalase activity (Chelikani *et al.*, 2004).

More recently peroxiredoxins (Prx), a family of peroxidases, have been described as another class of cellular redox scavengers, defined by their ability to reduce H_2O_2 . Prx contain highly conserved cysteine residues which are sensitive to

oxidation by H₂O₂. Prx elicit their antioxidant effect through oxidation of these cysteine residues thereby neutralising cellular H₂O₂ (Rhee *et al.*, 2012). Oxidation of these cysteine residues induces the formation of disulfide bonds, which are subsequently reduced by electron donation from cellular thiol thereby reverting Prx back to its reduced state. Uniquely, Prx cysteine residues are able to recover from hyper-oxidation to sulfinic acid. Reduction of this hyper-oxidation is slow requiring the ATP-dependent sulfiredoxins (Srx) but interestingly the presence of this function is believed to be a eukaryotic adaptation to facilitate H₂O₂-dependent signaling (Wood *et al.*, 2003).

2.3 ROS Signalling

Contradictory to the traditional view of ROS being toxic by-products of cellular function there has been a recent emergence of evidence to suggest that ROS actually play significant roles in a diverse range of cellular processes including cell survival (Naughton *et al.*, 2009; Peshavariya *et al.*, 2009), proliferation (Sturrock *et al.*, 2006; Petry *et al.*, 2006; Jeong *et al.*, 2004; Peshavariya *et al.*, 2009), insulin signalling (Mahadev *et al.*, 2004), invasion (Deem and Cook-Mills, 2004), cell senescence (Colavitti and Finkel, 2005), angiogenesis (Ushio-Fukai, 2006), oxygen sensing (Lee *et al.*, 2006), hormone synthesis (Pfarr *et al.*, 2006), cell death (Kim *et al.*, 2007), transformation (Laurent *et al.*, 2008), regulation of transcription factors and gene expression (Li *et al.*, 2010), differentiation (Xiao *et al.*, 2009; Sardina *et al.*, 2010), migration (Meng *et al.*, 2008; Reddy *et al.*, 2011), cytoskeletal remodelling (Lyle *et al.*, 2009), regulation of cellular redox potential (Bedard and Krause, 2007) as well as cross-linking and protein folding (Santos *et al.*, 2009). For all these processes the activity of H₂O₂ is most frequently cited in its involvement,

with many mammalian cell types producing H_2O_2 for the purpose of intracellular signalling in response to various stimuli.

H_2O_2 is distinct in its activity as a messaging molecule in that it does not bind effectors but rather oxidises critical residues. The best understood, and possibly most important method by which ROS such as H_2O_2 achieve regulation of cell function is by acting on redox-sensitive cysteine residues. Cysteine residues within the catalytic domains or active sites of various proteins demonstrate a low pKa value making them very susceptible to oxidation (Rhee and Woo, 2011). Oxidation of these cysteines can be reversed by the antioxidant mechanisms previously discussed thereby circumventing permanent damage to the protein while still inhibiting its activity in the interim. This has been most successfully demonstrated through the inhibition of protein tyrosine phosphatases (PTPs) and the tumour suppressor PTEN as a result of growth factor stimulation (Rhee *et al.*, 2005a; Rhee *et al.*, 2005b; Tonks 2005; Corcoran and Cotter, 2013). Furthermore, some serine/threonine phosphatases such as protein phosphatase-1 and -2A (PP1 and PP2A) also show susceptibility to oxidative inactivation (Rao and Clayton, 2002; O'Loghlen *et al.*, 2003). All of these phosphatases negatively control the phosphorylation state and activity of numerous signal transduction proteins and are therefore influential in the regulation of numerous cellular processes (Tonks, 2005; Corcoran and Cotter 2013). Thus, ROS signalling will decrease phosphatase activity, enhancing protein tyrosine or serine/threonine phosphorylation thereby having the potential to influence signal transduction. Indeed, it is believed that the activation of protein kinase activity alone downstream of some growth factor receptors is not sufficient for complete signal transduction, requiring concurrent inhibition of phosphatases by H_2O_2 (Sundaresan *et al.*, 1995; Bae *et al.*, 1997; Bae *et al.*, 2000; Bokoch *et al.*, 2009).

Until recently it was still unclear how a toxic molecule such as H₂O₂ was able to selectively oxidise effector proteins such as phosphatases without inducing damage to other biomolecules within the cell. One explanation was that ROS production, by dedicated generators such as Nox proteins, was localised. It is now believed that the ability for ROS to regulate and influence signalling pathways and other processes with specificity is dependent on the localisation as well as the compartmentalisation of their production. Indeed, localisation of ROS production to different subcellular compartments of the cell allows for co-localisation with specific ROS targets, reducing the risk of off-target redox signalling (Terada, 2006). In complementation, ROS-scavenging systems are important in the compartmentalisation of the redox signalling, with Prx demonstrating a prominent role in achieving localised, spatial accumulation of H₂O₂ following stimulation. Indeed, Woo *et al.*, (2010) demonstrated that during receptor mediated signalling, production of H₂O₂ is confined to discrete membrane sub-domains which contain Prx. This co-localisation of H₂O₂ and Prx was demonstrated to facilitate the inhibition of PTPs even with low concentrations of H₂O₂. Furthermore, these Prx were spatially restricted thereby insulating the rest of the cell from the potentially detrimental off-target effects of H₂O₂. The study provided an important insight into the potential specificity of ROS signalling.

It does not come as a surprise that such spatially defined, temporal and localised accumulation of ROS production is seldom achieved as a result of ROS generated as a by-product of cellular activity. In fact, of all the cellular processes influenced by redox signalling the Nox family of professional ROS generators are the most frequently cited source of H₂O₂.

3. NADPH Oxidases (Nox)

3.1 Introduction to the Nox family

As discussed ROS generation in eukaryotic cells is a result of oxygen metabolism and can be produced by a variety of sources. However, in contrast to the majority of these sources where ROS are produced as by-products, the NADPH Oxidase (Nox) family of proteins primary function is to generate ROS through specific enzymatic activity. There are seven members of the Nox family. Nox2 (originally named gp91phox) was the first identified member and has been extensively studied in host defence for its role in the ROS-mediated degradation of endocytosed bacterial pathogens in the phagosomes of phagocytic cells (Leto and Geiszt, 2006). Since its identification six additional homologs of Nox2 have been described, these are Nox1, Nox3, Nox4, Nox5, Duox1 and Duox2. Interestingly, the potential for these proteins to function beyond host defence was realised following their description in a variety of different non-phagocytic cell types such as fibroblasts (Meier *et al.*, 1991) vascular smooth muscle cells (Griendling *et al.*, 1994), endothelial cells (Görlach *et al.*, 2000), thyroid cells (De Deken *et al.*, 2000), neurons (Serrano *et al.*, 2003) and hepatocytes (Reinehr *et al.*, 2005) to name but a few. Indeed, Nox protein activity in these cells types has been demonstrated to play important signalling roles in processes including but not limited to cell survival (Naughton *et al.*, 2009; Peshavariya *et al.*, 2009), proliferation (Sturrock *et al.*, 2006; Petry *et al.*, 2006; Jeong *et al.*, 2004; Peshavariya *et al.*, 2009), differentiation (Xiao *et al.*, 2009; Sardina *et al.*, 2010) and migration (Meng *et al.*, 2008; Reddy *et al.*, 2011), with the list continually growing.

The Nox proteins are integral membrane proteins sharing several conserved structural features. The C-terminal tails of all these proteins contain a catalytic

subunit consisting of FAD and NADPH binding sites while the N-terminus is made up of six transmembrane domains and two heme groups which form a channel to allow successive transfer of electrons (Sumimoto, 2008). ROS production is achieved through the removal and transfer of an electron from an NADPH substrate to FAD, then heme, and finally to molecular oxygen, generating $O_2^{\bullet-}$ (Isogai *et al.*, 1995), which is rapidly converted to H_2O_2 by SOD. H_2O_2 is then capable of freely diffusing across membranes due to the activity of aquaporin channel proteins (Bienert *et al.*, 2007). As discussed, once generated H_2O_2 has the potential to affect multiple cellular signalling events.

3.2 Nox Activation and Signalling

Although the Nox proteins are structurally similar, each is activated by specific mechanisms and regulatory subunits (Figure 3). Furthermore, activation of each system is initiated as a response to a variety of stimuli, ranging from LPS and inflammatory mediators, a relic of their original microbicidal role, B and T cell receptor stimulation (Jackson *et al.*, 2004; Richards and Clark 2009), the activity of oncoproteins such as Bcr-Abl (Naughton *et al.*, 2009) as well as stimulation from growth factors such as Platelet-derived growth factor (PDGF), Thrombin, Tumour necrosis factor- α (TNF- α), Angiotensin II (Brown and Griendling, 2009). Indeed, growth factor mediated induction of tyrosine kinase activity has been extensively studied in respect to Nox protein activation and signalling events.

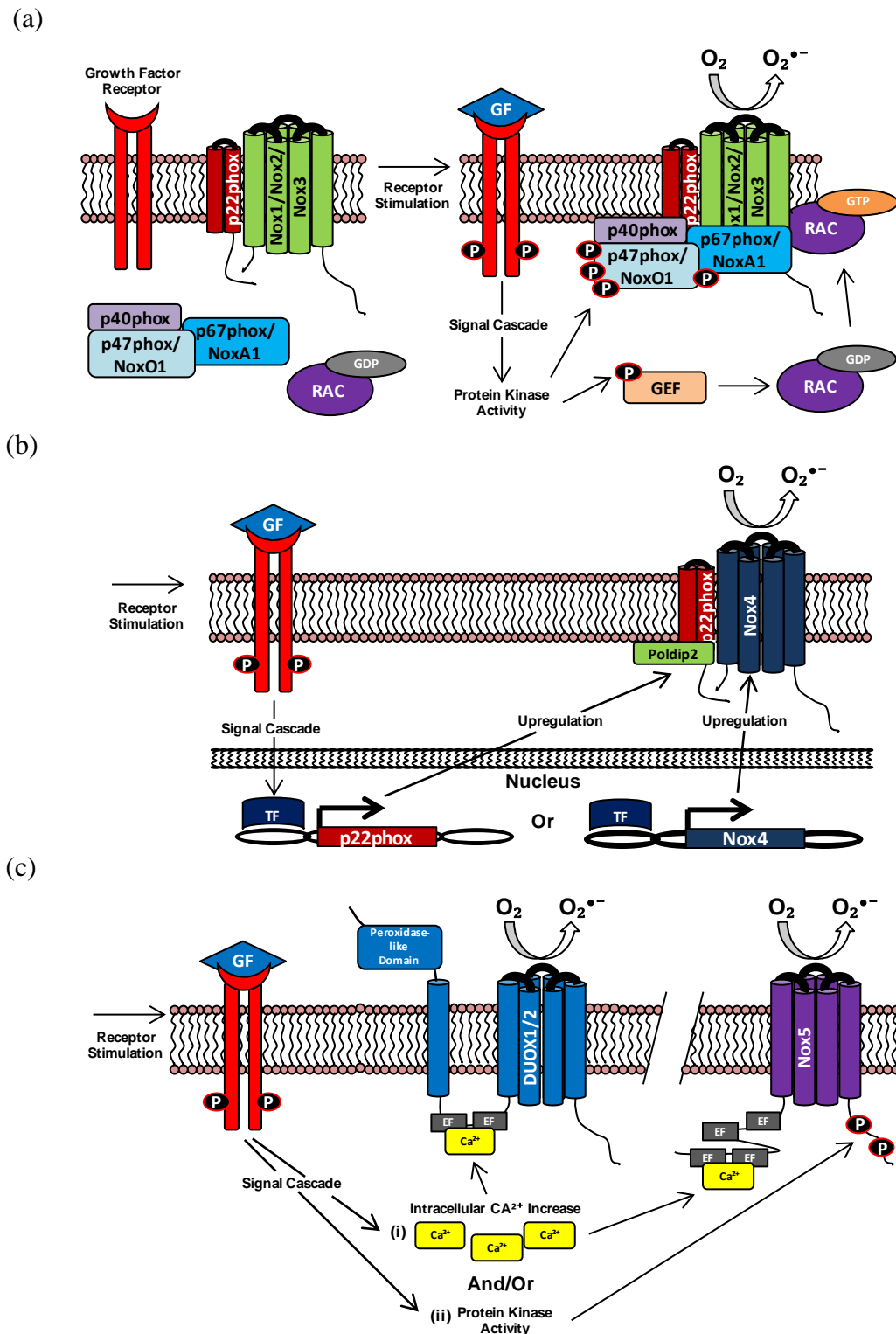


Figure 3. Regulation of Nox activation. Figure illustrates Nox activation downstream of growth factor (GF) receptor stimulation. (a) Activation of Nox1/Nox2/Nox3 requires kinase activity and subsequent phosphorylation (P) to induce the assembly of the Nox complex. (b) Nox4 is constitutively active, regulated transcriptionally or by the presence of p22phox. Poldip2 can also regulate Nox4 activity. (c)(i) Nox5 and DUOX1/2 activation is heavily influenced by the interaction of intracellular calcium (Ca^{2+}) levels with EF-hands on the N-terminal domains of each protein. (ii) In addition, Nox5 activation can be influenced by C-terminal phosphorylation (P). TF, transcription factor.

Nox1, Nox2 and Nox3

There has been extensive study of the regulation of Nox in phagocytes. In this system the enzyme consists of two membrane-bound subunits, the catalytic core Nox2 and p22phox (Figure 3a). The p22phox protein is an integral partner for Nox2 as well as Nox1, Nox3 and Nox4, being essential for activity through stabilising these proteins at the membrane (Ambasta *et al.*, 2004; Ueno *et al.*, 2005). Activity of the enzyme is regulated by three cytosolic proteins; p47phox, p67phox, p40phox, and the small Rho GTPase Rac2 (Lambeth *et al.*, 2007; Groeger *et al.*, 2009). After stimulation, p47phox undergoes a conformational change due to extensive phosphorylation at its autoinhibitory region mediated by the activity of various protein kinases (Akt, PKC, p38 MAPK, ERK and Pak) (Inanami *et al.*, 1998; Bokoch *et al.*, 2009). This in turn facilitates translocation of the p47phox/p67phox/p40phox complex to the membrane where p47phox interacts with p22phox (Lambeth *et al.*, 2007; Groeger *et al.*, 2009). Concurrently activation causes Rac2-GDP to be catalysed to Rac2-GTP by Guanine exchange factors (GEF), Rac2-GTP can now bind p67phox at the membrane resulting in the production of $O_2^{\bullet-}$ which is rapidly dismutated into H_2O_2 . Two homologs exist in the Nox1 system for p47phox and p67phox, these are Nox organiser 1 (NoxO1) and Nox activator 1 (NoxA1) respectively. In addition, Nox1 similarly to Nox2 requires p22phox and small g-protein Rac1 for activity (Cheng *et al.*, 2006). Unlike p47phox, NoxO1 lacks an autoinhibitory region and therefore appears to be constitutively active (Cheng and Lambeth, 2004). Regulation of Nox3 is less well known, ROS generation requires p22phox and is enhanced by p67phox (or NoxA1) and p47phox (or NoxO1) (Ueno *et al.*, 2005).

Regulation of PDGF-dependent H₂O₂ production demonstrated in smooth muscle cells gave one of the first insights into growth factor-receptor induced ROS production (Sundaresan *et al.*, 1995). PDGF induced PKC activity is documented to phosphorylate p47phox facilitating its translocation to the membrane activating Nox2 (Bokoch *et al.*, 2009; Bae *et al.*, 2011). Furthermore, PI3K activation and subsequent production of phospholipid phosphatidylinositol 3,4,5-triphosphate (PIP3) downstream of the PDGF-receptor has been shown to be essential for Nox1 mediated H₂O₂ production in hepatocellular carcinoma cells (Bae *et al.*, 2000). This is achieved through Rac1 activation which results from PIP3 induced phosphorylation and activation of the guanine exchange factor βPix (Park *et al.*, 2004). Furthermore, c-Src substrate proteins Tks4 (tyrosine kinase substrate with four SH3 domains) and Tks5 have been shown to be functional members of a p47phox-related organiser superfamily (Gianni *et al.*, 2009). In this model Src-mediated phosphorylation of Tyr508 on Tks4 and of Tyr110 on NoxA1 induces protein interaction via the SH3 domains of Tks4 and the proline rich region of NoxA1, generating Nox1-dependent ROS (Gianni *et al.*, 2010; Gianni *et al.*, 2011). Interestingly, Tks4 and Tks5 can mediate Nox1 and Nox3 ROS generation but are unable to activate Nox2.

Nox4

Unlike Nox1, Nox 2 or Nox3, Nox4 requires only p22phox for activity (Figure 3b) (Ambasta *et al.*, 2004). In addition to p22phox polymerase delta-interacting protein (Poldip2) has been described as a novel regulator of Nox4 in smooth muscle cells stimulating activation through p22phox interaction (Lyle *et al.*, 2009), the molecular mechanism behind Poldip2 regulation of Nox4 however still remains to be determined. Evidence suggests that Nox4 is regulated at the level of

mRNA as opposed to post-translational protein modifications (Serrander *et al.*, 2007). Furthermore, composition of its C-terminal region is believed to be the cause of its constitutive activity (von Löhneysen *et al.*, 2012). Insulin-like growth factor I (IGF-I), bone morphogenetic protein-2 (BMP-2), transforming growth factor- β (TGF β), and Toll-like receptor 4 (TLR4) are examples of growth factors and receptors which have been shown to activate Nox4 without engaging regulatory subunits (Lee *et al.*, 2007; Maloney *et al.*, 2009; Liu *et al.*, 2010; Mandal *et al.*, 2011; Edderkaoui *et al.*, 2011). To date growth factor mediated activation of Nox4 has only been shown to occur through the transcriptional regulation of either Nox4 or p22phox. IGF-I receptor stimulation has been demonstrated to induce Nox4 dependent ROS production in pancreatic cancer cells, in turn playing an important pro-survival role (Lee *et al.*, 2007). The activation of Nox4 activity in this system is achieved through the transcriptional upregulation of p22phox, this is mediated by NF- κ β downstream of the IGF-I receptor (Edderkaoui *et al.*, 2011). Phosphorylation and activation of Akt after receptor ligand-binding was integral in activating NF- κ β in this system. The role NF- κ β plays in Nox regulation is not limited to p22phox and its activation has also been shown to be involved in the transcriptional upregulation of the Nox4 and Nox1 genes in smooth muscle cells downstream of TNF- α stimulation, indicating a more widespread influence on Nox regulation (Manea *et al.*, 2010).

Nox5, Duox1 and Duox2

Nox5, Duox1 and Duox2 are unlike the other Nox proteins in so far as these proteins do not require p22phox for activity (Figure 3c). Activation is dependent on intracellular calcium levels, which bind EF-hands present in the N-terminal domains

of these proteins inducing a conformational change and subsequent ROS production (Banfi *et al.*, 2001; Ameziane-El-Hassani *et al.*, 2005). Therefore it is possible that any stimulus which increases intracellular calcium concentration could result in increased ROS production. Interestingly, phorbol 12-myristate 13-acetate (PMA) exposure has been shown to increase the sensitivity of Nox5 to calcium, which is mediated through PKC dependent phosphorylation of the Thr494 and Ser498 residues on Nox5 (Jagnandan *et al.*, 2007; Serrander *et al.*, 2007b). This increased sensitivity of Nox5 to calcium circumvents the need for calcium levels to increase and as a result resting levels of this molecule are enough to activate ROS generation. This demonstrated a novel method of Nox5 regulation. Additionally, ERK1/2 signalling has been shown to be important for phosphorylation of Ser498 on Nox5 and preventing this phosphorylation significantly reduces the ability of Nox5 to generate $O_2^{\bullet-}$ (Pandey *et al.*, 2011). PKC can activate Nox5 however it is evident from this study that downstream signalling via the ERK1/2 pathway is also essential.

Nox signalling and disease

In 1995 Sundaresan *et al.*, published one of the first demonstrations where growth factor receptor-mediated signalling generated H_2O_2 which acted as a secondary messenger necessary for signal-transduction. Subsequent studies demonstrated this ROS production to be dependent on Nox and their regulatory proteins (Bae *et al.*, 2000; Park *et al.*, 2004; Bokoch *et al.*, 2009). Since these studies there has been increasing evidence of the influence Nox derived ROS have on signal transduction after the stimulation of a variety of different growth-factor receptors as well as downstream of oncoprotein activity. As discussed, tyrosine kinase activity is capable of initiating signal transduction cascades, which induce downstream effects

including the generation of ROS via activation of the Nox proteins. Therefore the potential for Nox proteins in signalling is evident when you consider the extensive list of growth factors which induce their activity.

ROS production as a result of Nox protein activation downstream of signal transduction is tightly regulated; this coupled with the previously discussed compartmentalisation of ROS production through the activity of antioxidant or ROS-scavenging systems such as peroxiredoxins ensures the specificity of the Nox enzymes in signalling (Ushio-Fukai, 2009; Rhee *et al.*, 2012). Unfortunately, deregulation and aberrant Nox activity does occur, leading to increased ROS production which is implicated in a host of diseases, such as acute renal failure (Nath and Norby, 2000), hypertension (Rey *et al.*, 2002), cardiovascular disease (Heymes *et al.*, 2003), diabetes (Etoh *et al.*, 2003), ischemia leading to cerebral and myocardial infarctions (Hong *et al.*, 2006; Meischl *et al.*, 2006), retinal degeneration (Usui *et al.*, 2009) as well as neurodegenerative disorders such as Alzheimer and Parkinson diseases (Gao *et al.*, 2012).

Furthermore, considering the well established role for Nox proteins downstream of various signalling pathways it is of no surprise that their activity can be subject to de-regulation by aberrant tyrosine kinase activity as a result of oncogenic signalling. An ever growing body of literature has implicated Nox-derived ROS in the cellular transformation and maintenance of a substantial number of common cancer types such as prostate (Brar *et al.*, 2003; Lim *et al.*, 2005; Kumar *et al.*, 2008; Huang *et al.*, 2012a), colon (Fukuyama *et al.*, 2005; Bauer *et al.*, 2012), breast and ovarian (Desouki *et al.*, 2005; Choi *et al.*, 2010), bladder (Shimada *et al.*, 2009; Shimada *et al.*, 2011; Huang *et al.*, 2012b), pancreatic (Vaquero *et al.*, 2004) and thyroid gland cancers (Weyemi *et al.*, 2010) as well as melanoma (Brar *et al.*,

2002; Yamaura *et al.*, 2009), lymphoma (Lan *et al.*, 2007; Hoffmann *et al.*, 2010) and leukaemia (Kamiguti *et al.*, 2005; Prata *et al.*, 2008; Naughton *et al.*, 2009). In these cases Nox proteins have been demonstrated to enhance oncogenesis through induction of increased genomic instability, angiogenesis, invasion, metastasis, cell growth and survival. Interestingly, in the case of CML a role for Nox-derived ROS has also been demonstrated to increase cell survival downstream of Bcr-Abl kinase activity, through augmentation of the PI3K pathway (Naughton *et al.*, 2009).

4. Objectives

ROS generation is now widely accepted as being important for a variety of cellular processes, mediating its effects in part by influencing signal transduction (Bae *et al.*, 2011). One source of ROS which is gaining much attention is the Nox family of professional ROS generators, which have been implicated in the pathogenesis of a many different cancers types (Block and Gorin, 2012). Interestingly, Bcr-Abl signalling has previously been demonstrated to stimulate ROS production by increasing Nox protein activity, which was demonstrated to enhance cell survival by positively influencing the PI3K/Akt survival signalling pathway (Naughton *et al.*, 2009). Although Naughton *et al.* (2009) established a link between Bcr-Abl signalling and Nox-derived ROS, how Bcr-Abl activity influenced the Nox proteins was not certain. In light of this, the objective of this study was to elucidate how the Nox proteins were activated downstream of Bcr-Abl in CML. It was also of interest to examine further how Nox-derived ROS influence CML disease phenotype and identify if there was a potential in targeting these proteins to improve CML treatment.

Chapter 2

Materials and Methods

Chemicals and reagents

Bcr-Abl inhibitors Imatinib Mesylate (STI-571) and Nilotinib (AMN-107) were from Selleck Chemicals (Munich, Germany). The ROS probe DCF (2',7'-dichlorodihydrofluorescein diacetate; H₂DCFDA) was from Molecular Probes (Life Technologies, Dublin, Ireland). The Nox inhibitor VAS2870 (3-benzyl-7-(2-benzoxazolyl)thio-1,2,3-triazolo[4,5-d]pyrimidine) was from Enzo Life Sciences (Lausen, Switzerland). The Mitochondrial complex I inhibitor Rotenone was from Calbiochem (EMD Millipore, MA, USA). Bromodeoxyuridine (BrdU) was from BD Biosciences (Oxford, UK). FITC-conjugated Annexin V used for apoptosis detection was from IQ Products (Groningen, Netherlands). PKC412 and the GSK-3 β inhibitor SB216763 (SB) were from Tocris (Bristol, UK). The PI3K and MEK inhibitors LY294002 (LY) and UO126 (UO) respectively were from Cell Signaling Technology (Boston, MA, USA). Diphenyleneiodonium chloride (DPI), the 20S proteasomal inhibitor Lactacystin (Lact), the chemotherapeutics Etoposide (Etop), Docetaxel (Doc), Cisplatin (Cis), Actinomycin (ActD) and Methotrexate (Met) were all from Sigma-Aldrich and unless otherwise stated all other chemicals and reagents were purchased from Sigma-Aldrich (Dublin, Ireland). In all cases, if not demonstrated, inhibitor concentrations were chosen based on their greatest effect with a negligible decrease in cellular viability

Antibodies

Primary antibodies used for immunoblotting, immunoprecipitation, co-immunoprecipitation or immunofluorescence were; anti-Akt (#9272), anti-phospho-Akt (ser473; #9276), anti-c-Abl (#2862), anti-ERK1/2 (#9102), anti-phospho-ERK1/2 (Thr202/204; #9275), anti-GSK-3 β (Rabbit #9315), anti-phospho-GSK-3 β

(Ser9; #9336S), anti-phospho-CrkL (Tyr207; #3181), anti-pRb (#9309), anti-Ki-67 (#9129), anti-Cyclin E1 (#4129), anti- β -Catenin (#9562), anti-CDK2 (#2546), anti-Cyclin D2 (#3741), anti-p21^{WAF1/CIP1} (#2947), anti-p27^{KIP1} (#3686), anti-Cyclin D3 (#2936), anti-p18^{INK4C} (#2896), anti-Cyclin D1 (#2978), anti-CDK4 (#2906), anti-CDK6 (#3136), anti-Beclin-1 (#3738), anti-LC3B (#3868), anti-phospho-STAT3(tyr 750; #9131) anti-p53 (#2524), anti-STAT3 (#9132), anti-PARP (#9542) and anti-Caspase-3(#9662) all from Cell Signaling Technology (Boston, MA, USA). Anti-p67phox (#sc-15342), anti-DUOX1 (#sc-48858) and anti-p47phox (#sc-14015), anti-p22phox (Rabbit #sc-20781; Mouse sc-130551) and anti-P57^{KIP2} (#sc-1037) all from Santa Cruz Biotechnology (Santa Cruz, CA, USA). Anti-Nox3 (#Ab82708), anti-Nox1 (#Ab55831), anti-DUOX2 (#Ab65813), anti-RAC-2 (#Ab2244), anti-Poldip2 (#Ab84865), anti-BrdU from Abcam (Cambridge, UK). Anti-GAPDH (#RGM2-500) from Advanced Immunochemicals (Long Beach, CA, USA). Anti- β -Actin (#A5441) and anti-Nox5 (#HPA019362) both from Sigma-Aldrich (Dublin, Ireland). Anti-Ubiquitin (#MAB1510), anti-Nox2 (#07-024), anti-phospho-STAT5 (Tyr694/699; #04-886) and anti-p15^{INK4B} (#05-430) all from Millipore/Upstate Biotechnology (MA, USA). Anti-RAC-1 (#ARC03) from Cytoskeleton Inc (Denver, USA). Anti-GSK-3 β (Mouse #610202) and anti-STAT5 (#610191) from BD Biosciences (Oxford, UK). Anti-Nox4 antibody was a kind gift from Dr JD Lambeth (Emory University School of Medicine, Atlanta, GA, USA). Secondary antibodies for western blotting were either peroxidase-conjugated (Dako, Stockport, UK) used for detection with enhanced chemiluminescence (GE Healthcare, Buckinghamshire, UK) or Li-Cor IRDye secondary antibodies (Li-Cor Biosciences, Nebraska, USA) used for detection with the Odyssey System.

Cell lines and culture conditions

All cell lines were maintained in a humidified incubator at 37°C with 5% CO₂ in full medium plus supplements. Full medium is Roswell Park Memorial Institute (RPMI) 1640 (Sigma-Aldrich), 10% Fetal Bovine Serum (FBS) (Sigma-Aldrich), 1% penicillin/streptomycin (Sigma-Aldrich) and 2mM L-glutamine (Gibco, Invitrogen Corporation, Paisley, UK). All cell lines were maintained between 0.1-1.0x10⁶ cells/ml and were subcultured every 2-3 days. Cell counts were obtained using a haemocytometer under a light microscope and viable cells were determined by trypan blue exclusion. K562 and HL-60 cells were purchased from the DMSZ German Collection of Microorganisms and Cell Cultures (Braunschweig, Germany). The TonB.210 cell line was derived from the interleukin-3 (IL-3) dependent murine pro-B cell line BaF3 and contain a Doxycycline (Dox)- responsive promoter whereby Bcr-Abl p210 can be conditionally induced (kindly provided by George Daley, MIT, Cambridge, MA). TonB.210 cells were maintained in full medium plus 1mg/ml G418 sulphate and 10% WEHI-conditioned medium (WEHI-CM) as a source of murine IL-3. For IL-3 starvation experiments, TonB.210 cells were washed twice in serum free medium (SFM) and resuspended in SFM for the indicated times. To induce Bcr-Abl p210 expression cells were incubated with 1µg/ml doxycycline hyclate for the indicated times. In all experiments cells were isolated and washed, unless otherwise stated, by centrifugation at 100 g for 5min.

Measurement of Intracellular Reactive Oxygen Species

As previously described (Naughton *et al.*, 2009), ROS levels were determined using the cell-permeable fluorogenic probe 2,7-dichlorodihydrofluorescein diacetate (H₂DCF-DA, cleaved to DCF intracellularly) (Molecular Probes, Life Technologies.,

Dublin, Ireland). Following treatments, cells were washed in phosphate-buffered saline (PBS) before 50 μ M H₂DCF-DA was then added to cells suspensions and incubated at 37°C in the dark for 15min. Following incubation samples were put on ice. Live cell populations were gated and changes in intracellular ROS levels were determined by recording the geometric mean fluorescent intensity of 10,000 events per sample counted in the FL-1 channel on a FACSCalibur (BD Biosciences Europe, Oxford, UK) flow cytometer using CellQuest Pro software.

Western Blot Analysis

Western Blotting was carried out as previously described (Naughton et al., 2009). Following treatments, whole cell lysates were prepared by washing cells in PBS and centrifuging at 100 g for 5min at 4°C. Cell pellets were then resuspended in RIPA lysis buffer (50mM Tris-HCl pH7.4, 1% NP-40, 0.25% sodium deoxycholate, 150mM sodium chloride, 1mM EGTA, 1mM sodium orthovanadate, 1mM sodium fluoride, 200 μ M 4-(2-Aminoethyl) benzenesulfonyl fluoride hydrochloride (AEBSF) and cocktail protease inhibitors (Roche, Welwyn, Hertfordshire, UK). Samples were incubated for 30min with vortexing at 4°C, followed by centrifugation at 18,000 g for 15min at 4°C to remove cell debris. Protein concentrations were determined by Bio-Rad Protein Assay (Hemel, Hempstead, UK) using bovine serum albumin (BSA) as a protein standard. Equal amounts of protein samples (30-50 μ g per lane) were diluted in 2X sample buffer (10% sodium dodecyl sulfate (SDS), 100mM dithiothreitol (DTT), glycerol, bromophenol blue, Tris-HCl) and resolved by SDS-polyacrylamide gel electrophoresis (SDS-PAGE) and transferred to nitrocellulose membranes (Schleicher & Schuell, Dassel, Germany). Membranes were blocked with 5% (w/v) BSA in Tris-buffered saline/0.1% Tween-20 (TBS/T) or 5% (w/v)

nonfat dry milk in TBS/T for 1hr at room temperature (RT) before being incubated overnight at 4°C with the appropriate antibodies diluted in blocking buffer.

Membranes were washed in TBS/T before being incubated with either peroxidase-conjugated (Dako, Stockport, UK) secondary antibodies and developed using enhanced chemiluminescence (GE Healthcare, Buckinghamshire, UK) or with Li-Cor IRDye secondary antibodies (Li-Cor Biosciences, Nebraska, USA) to be examined with the Odyssey Infrared Imager system and Odyssey software (version 2.1.12, Li-Cor Biosciences, USA). Densitometric analysis was carried out using ImageJ software (<http://rsbweb.nih.gov/ij/>) (version 1.44, NIH, USA) and data are represented in bar charts, calculated as the ratio of the intensity of target bands quantified by densitometry factored by the densitometric measurements of loading control bands.

cDNA Synthesis and Quantitative Real-Time Polymerase Chain Reaction

Following treatments 5×10^6 cells were harvested from each sample. Media was removed and total cellular RNA was isolated using the Isolate RNA mini kit (#BIO-52043; Bioline Ltd, UK), according to the manufacturer's protocol for eukaryotic cells. The concentration of RNA in each sample was determined in triplicate by spectrophotometric analysis using a Biophotometer (Amersham Biosciences). 500 ng of RNA was then run on a 1% agarose gel to check integrity. RNA was treated to remove any contaminating DNA using Amplification Grade DNase I kit (#AMP-D1; Sigma- Aldrich, Dublin, Ireland) as per manufacturer's protocol. cDNA was then synthesised from 2 µg RNA using a cDNA Synthesis Kit (#BIO-65026; Bioline Ltd, UK). The reaction mix consisted of 1x Moloney Murine Leukaemia Virus Reverse Transcriptase (M-MLV RT) buffer, 25mM MgCl₂, 40U/µl RNase inhibitor,

200U/ μ l M-MLV Reverse Transcriptase, 50mM oligo (dT)₁₈ primer mix and 10mM dNTPs or the equivalent volume of RNase-free water for the no reverse transcriptase control (NRT). The reaction was run at 42°C for 1hr, followed by 99°C for 10min, before being stored at 4°C. Quantitative real-time polymerase chain reaction (qRT-PCR) was used to determine the level p22phox expression, with β -Actin as a housekeeping gene for normalisation. Three technical replicates and one NRT control were used per sample for each gene. The qRT-PCR reaction was carried out on a DNA Engine Opticon 2.0 (MJ Research Inc., Waltham, USA), using Quantitect SYBR Green Sensimix kit and Quantitect Primer Assays (Qiagen, West Sussex, UK). Qiagen pre-designed primers were used for human p22phox (CYBA_QT00082481) and β -Actin (β Actin_QT01680476). PCR parameters and data analysis was as described in Woolley *et al.* (2012). Briefly, 50ng cDNA template was combined with 10 μ l of 20x SYBR Green Sensimix and 2 μ l 10X primer in 20 μ l total reaction volume in a 96-well plate (Bio-Rad). The following PCR parameters were used for each primer set: denaturing at 95°C for 15min, followed by 45 cycles of 94°C for 15sec, 56°C for 30sec and extension at 72°C for 30sec. RNA samples were analyzed in triplicate, and p22phox expression relative to β -Actin was obtained using the $\Delta\Delta$ Ct-method. PCR products were then visualised by separation on a 2% agarose gel and staining with SYBR Safe gel stain (Invitrogen).

Ubiquitination assay

Following treatments, approximately 6×10^6 cells were lysed in preboiled 1% SDS lysis buffer (with 10mM N-Ethylmaleimide (NEM; a de-ubiquitinating enzyme inhibitor), 1mM sodium orthovanadate, 200 μ M AEBSF and cocktail protease inhibitors (Roche, Welwyn, Hertfordshire, UK)), vortexed briefly, boiled for 10min

(with intermittent vortexing) and sonicated for 3-6sec to shear DNA. Lysates were clarified by centrifugation at maximum speed (25,000 g) at 4°C for 10min. The supernatants were transferred to a cold eppendorf tube and protein concentration was determined as previously described. 1mg of lysate was immunoprecipitated overnight using Pierce Crosslink Immunoprecipitation Kit (#26147; Thermo Fisher Scientific, Dublin, Ireland) according to the manufacturer's protocol, with 10µg of p22phox antibody crosslinked to Protein A/G agarose using disuccinimidyl suberate (DSS). 10mM NEM was included at all washing steps. The immunoprecipitates were resolved using SDS-PAGE, as described above separated by 10% SDS-PAGE, transferred to nitrocellulose membrane, which was pre-soaked in transfer buffer containing 20% methanol and transferred in the same buffer. Membranes were autoclaved for 15min prior to blocking to expose further ubiquitin moieties for detection, blocked in 5% BSA and probed with anti-ubiquitin and p22phox antibodies.

Electroporation and Small Interfering RNA (siRNA) Transfection

RNA interference in K562 cells was mediated by duplexes of 21-nucleotide RNA (Lonza, Berkshire, UK). Two different Ambion Silencer Select predesigned siRNA (Applied Biosystems, Warrington, UK) were used for silencing p22phox expression, these were siRNA ID-s3786 (siRNA(i)) and ID-s194372 (siRNA(ii)). Transfection with the scrambled siRNA Silencer Select Negative Control #1 (Negative) was used as a control. The transfection of siRNA used the Amaxa Nucleofactor device with the Amaxa cell optimisation kit V (Amaxa, Cologne, Germany) and followed the Amaxa guidelines for K562 cells using the electroporation programme X-001 with 2×10^6 cells and 300nM siRNA used per transfection. Electroporated control (Elect

Ctrl) referred to cells which were electroporated without siRNA.

Live Cell Imaging

Cells were electroporated with either negative siRNA or p22phox siRNA (as described) and plated in poly-d-lysine coated glass bottomed dishes (35 mm Petridishes with 14 mm microwells; MatTek Corporation, Ashland, MA, USA) for 2hr. Cells were incubated in 50 μ M H₂DCF-DA for 1hr at 37°C in the dark.

Following this incubation cells were rinsed and imaged live in growth medium using the Multiphoton Laser scanning microscope Flouview1000 MPE (Mason Technology) with an Infrared mode locked (femtosecond) red Ti:Sapphire Laser as previously described (Woolley *et al.*, 2012). Cells stained with DCF were excited at 488 nm and emissions collected at 530 nm. Images were acquired and visualised with an XLPLN 25xWMP water immersion objective (1.05 numerical aperture: Olympus Optical GmbH, Hamburg, Germany) and stored with an Olympus flouview1000 software (Mason Technology, Dublin, Ireland). Images are represented as a single slice from a Z stack projection. During acquisitions, saturation levels were kept constant for DCF to allow direct comparison of ROS levels between negative siRNA treated cells and p22phox siRNA treated cells.

Cell Death Measurements

Cell death was assessed by propidium iodide (PI) (Sigma-Aldrich) uptake and analysis on a FACSCalibur flow cytometer (BD Biosciences Europe, Oxford, UK). Briefly, following treatments cells were washed and resuspended in PBS. PI (to give 50 μ g/ml) was then added to cells immediately before analysis on the FL-2 channel.

Cell death was indicated by increased fluorescence in the FL-2 channel due to increased membrane permeability and uptake of PI.

Co-Immunoprecipitation

Co-Immunoprecipitation was carried out using the Pierce Crosslink Co-Immunoprecipitation (Co-IP) Kit (#26149; Thermo Fisher Scientific, Dublin, Ireland) according to the manufacturer's protocol. Briefly, 1mg of protein lysate from each sample was prepared and the protein of interest was immunoprecipitated overnight at 4°C using 10µg of the appropriate antibody crosslinked to Protein A/G agarose using DSS. Immunocomplexes were separated by SDS-PAGE as previously described, and transferred to nitrocellulose membrane to be probed with the appropriate antibodies to determine binding partners.

CFSE Cell Proliferation Assay

Carboxyfluorescein Diacetate Succinimidyl Ester (CFDA-SE) is non-fluorescent and highly membrane permeable, once inside a cell its acetate groups are rapidly removed by intercellular esterases producing the highly fluorescent and less permeable molecule Carboxyfluorescein Succinimidyl Ester (CFSE) (Quah *et al.*, 2007). CFSE covalently binds to intracellular molecules, *via* its succinimidyl groups making it highly stable within cells which results in it being retained for long periods of time while being evenly distributed between daughter cells following cell division (Quah *et al.*, 2007). The level of CFSE fluorescence will half every time a cell divides therefore a higher level of fluorescence indicates reduced proliferation while a lower level of fluorescence indicates an increased rate of proliferation. This even distribution of CFSE fluorescence following cell division allows cell proliferation to

be monitored by flow cytometry. To stain with CFSE, the required number of cells were centrifuged at 100 g, resuspended in prewarmed PBS containing 5 μ M CFDA-SE (Sigma-Aldrich) and incubated at 37°C for 15min in the dark. Cells were then centrifuged as before and resuspended in fresh prewarmed full medium. Cells were left to incubate at 37°C for a further 30min in the dark to ensure complete modification of the probe before being washed again and resuspended to 0.2x10⁶ cells/ml in fresh prewarmed full medium. CFSE stained cells were incubated as normal at 37°C and kept in the dark for the duration of the experiment. To determine changes in proliferation rates, K562 cells were stained with CFSE 24hr before transfection to allow CFSE levels to stabilise. 24hr after staining parental population fluorescence was determined by recording the geometric mean fluorescent intensity of 10,000 events counted in the FL-1 channel on a FACSCalibur (BD Biosciences Europe, Oxford, UK) flow cytometer using CellQuest Pro software. Cells were then transfected with siRNA as previously described and CFSE fluorescence was recorded as before 24hr, 48hr and 72hr after transfection. Data was then fit using the Proliferation Wizard on a trial version of ModFit LT 4.0 (Verity Software House).

BrdU Cell Cycle Assay

Bromodeoxyuridine (BrdU) is an analogue of thymidine and is incorporated into DNA during synthesis, substituting thymidine, indicating cells which are actively replicating their DNA and provides accurate distinction of S phase population. As a result cell cycle distribution as determined by BrdU/PI will vary when compared to analysis of the cell cycle using PI alone. 24hr, 48hr and 72hr after each transfection cells were pulsed with 10 μ M BrdU (#550891; BD Biosciences) for 1hr before being centrifuged at 100 g for 5min and media was aspirated. To fix cells, while vortexing

gently, 70% ice cold ethanol was added to cells dropwise to a final concentration of 1×10^6 cells/100 μ l. Cells were then incubated for at least 20min at RT or at -20°C overnight. 100 μ l of each sample was transferred to a FACS tube (#352052; Falcon) and washed twice with 1ml of wash buffer (PBS with 0.5% BSA) and centrifuged at 400 g for 5min. Media was aspirated and cells were resuspended in denaturing solution (2M HCl) for 20min at RT. Cells were washed as before and resuspended in 0.5ml 0.1M sodium borate ($\text{Na}_2\text{B}_4\text{O}_7$, pH 8.5), for 2min at RT to neutralize residual acid. Again cells were washed as before. Anti-BrdU antibody (Abcam) was diluted to 1/100 in dilution buffer (PBS with 0.5% Tween-20 and 0.5% BSA). Each sample was resuspended in 50 μ l of diluted antibody and incubated for 20min at RT before being washed using the dilution buffer as before. FITC-conjugated anti-Rat IgG antibody (# F1763; Sigma-Aldrich) was diluted to 1/200 in dilution buffer. Each sample was resuspended in 50 μ l of diluted secondary antibody and incubated for 20min at RT. Cells were once again washed before all samples were finally resuspended pellet in 0.5ml PI (50 μ g/ml in PBS with 5 μ g RNase A; Sigma-Aldrich) and incubated for 30min at 37°C , protected from light. 20,000 events were analysed by flow cytometry measuring BrdU linked green fluorescence and PI linked red fluoresce from the FL-1 and FL-2 channels respectively of a FACSCalibur (BD Biosciences Europe, Oxford, UK) flow cytometer using CellQuest Pro software. Cell were gated and analysed as described by Crane *et al.* (2011).

Ki-67 Cell Cycle Assay

Ki-67 is a nuclear protein expressed in proliferating cells and is absent in quiescent cells (Gerdes *et al.*, 1983). As a result Ki-67 is only expressed in cells cycling through G1, DNA synthesis (S), G2 or mitosis (M), but not in cells present in the

resting phase G0. Therefore it allows accurate distinction between G0 and G1 phase cells. At the indicated time-points following transfection cells centrifuged at 100 g for 5min and media was aspirated before being fixed by adding 70% ice cold ethanol to cells dropwise to a final concentration of 1×10^6 cells/100 μ l while vortexing gently. Cells were then incubated for at least 20min at RT or at -20°C overnight. 100 μ l of each sample was transferred to a FACS tube (#352052; Falcon) and washed twice with 1ml of wash buffer (PBS with 0.5% BSA) and centrifuged at 400 g for 5min. Anti-Ki-67 antibody (Cell Signaling) was diluted to 1/400 in dilution buffer (PBS with 0.5% Tween-20 and 0.5% BSA). Each sample was resuspended in 50 μ l of diluted antibody and incubated for 20min at RT before being washed using the dilution buffer as before. Alexa Fluor488-conjugated anti-Mouse IgG (#A11001; Life Technologies) was diluted to 1/200 in dilution buffer. Each sample was resuspended in 50 μ l of diluted secondary antibody and incubated for 20min at RT. Cells were once again washed before all samples were resuspended in 0.5ml PI (50 μ g/ml in PBS with 5 μ g RNase A; Sigma-Aldrich) and incubated for 30min at 37°C, protected from light. 20,000 events were analysed by flow cytometry measuring BrdU linked green fluorescence and PI linked red fluorescence from the FL-1 and FL-2 channels respectively of a FACSCalibur (BD Biosciences Europe, Oxford, UK) flow cytometer using CellQuest Pro software. G0 population gating was determined based on secondary antibody only control. All cells with fluorescence above this population were designated as G1 phase cells.

Immunofluorescence

Following treatments, approximately 5×10^4 cells were cytopun onto glass slides for 2min at 500 rpm using a Shandon Cytospin 2 Cyto centrifuge. Cytopins were left to

air dry at RT for 1hr before being fixed with 3% paraformaldehyde. Slides were then washed in PBS twice (all washes were 5min each) before quenching with 50mM NH_4Cl for 10min which was followed by three PBS washes. Cells were then permeabilised in PBS containing 0.2% BSA and 0.05% Saponin for 5min at RT. Following three further PBS washes cells were incubated with anti-Ki-67 antibody (Cell Signaling) at a dilution of 1/400 in 5% FBS/PBS for 2hr at RT, washed in 5% FBS/PBS three times and incubated with the secondary Alexa Fluor488-conjugated anti-rabbit antibody (#A11034; Life Technologies) at 1/200 in 5% FBS/PBS with the nuclear stain Hoescht at 1 $\mu\text{g}/\text{ml}$ (Thermo Fisher Scientific, Dublin, Ireland) for 1hr at RT. Following these washes with PBS, coverslips were mounted onto the glass slides using Mowiol and dried overnight before imaging. Cells were visualised on a Leica DM LB2 fluorescence microscope (Leica, Nussloch, Germany) using a TRITC filter. Images of the cells were acquired by a Nikon Digital Sight DS-Fi1C camera (Nikon, Japan) using NIS-Elements software (version 3.0, Nikon, Japan).

Examining electrophoretic mobility of pRb

In the case of examining the electrophoretic mobility of pRb, western blotting was carried as described previously. Samples were prepared as normal and resolved on a 6% SDS-polyacrylamide gel. As pRb is approximately 110kDa, samples were resolved by SDS-PAGE until just before this molecular weight had run off the gel. This provided enough separation to determine if pRb demonstrated any changes in molecular weight resulting from changes in phosphorylation status.

MTS Conversion-based Cell Viability Assay

Following treatments, cell viability was determined using the CellTiter 96 AQueous Non-Radioactive Cell Proliferation Assay (#G5421; Promega, WI, USA) which

utilised cellular MTS conversion assay. An MTS assay is a quantitative colourmetric assay based on the conversion of the tetrazolium salt 3-(4,5-dimethylthiazol-2-yl)-5-(3-carboxymethoxyphenyl)-2-(4-sulfophenyl)-2H-tetrazolium, inner salt (MTS) to the coloured end product formazan. This conversion is dependent on enzyme activity found in metabolically active cells which directly relates to cell viability (Berridge *et al.*, 2005). Manufacturer's protocol was followed but in brief, 20µl of MTS/phenazine methosulfate (PMS; an electron coupling reagent) solution was added directly to each well of a 96-well plate containing 100µl of cells in full medium and incubated as normal for 1hr at 37°C. For each experiment K562 cells were plated for each treatment in triplicate and at four separate cellular densities (0.005x10⁶, 0.01x10⁶, 0.015x10⁶, and 0.03x10⁶) to ensure accuracy. The absorbance of the resulting formazan solutions was measured using a SpectraMax340 plate reader (Molecular Devices, CA, USA) at 490nm wavelength in SoftMaxPro software.

Analysis of the Levels of Apoptotic Cell Death

To provide a more accurate demonstration of the effects of treatments on cell death levels and induction of cell death Annexin V binding assay was used. Annexin V binds to externalised phosphatidylserine (PS) which is an early indicator of apoptosis. Following treatments, cells were washed in ice cold PBS twice and resuspended in Annexin-binding buffer (10mM HEPES, 140mM NaCl, 2.5mM CaCl₂, pH 7.4), approximately 1x10⁶ cells/100µl, at RT. 5µl of FITC-conjugated Annexin V was added to each 100µl cell suspension and incubated at RT in the dark for 15min. After this incubation a further 350µl of Annexin-binding buffer was added to each sample and samples were then placed on ice until analysis.

Immediately before analysis 50µl of PI (500µg/ml in PBS) was added to each sample. 10,000 events were then analysed per sample by flow cytometry measuring Annexin-V binding and PI uptake in the FL-1 and FL-2 channels respectively of a FACSCalibur (BD Biosciences Europe, Oxford, UK) flow cytometer using CellQuest Pro software. Fluorescence was compensated accordingly and quadrants were positioned based on positive apoptotic control allowing the determination of the percentage of viable cells (lower left quadrant), apoptotic cells (lower right quadrant), necrotic cells (upper left quadrant) and cell death by apoptosis (upper right quadrant). In combination studies cell viability was represented by the percentage of cells in the lower left quadrant. Combination treatments were analysed using CompuSyn Software (CompuSyn Inc. <http://www.combosyn.com/>) with the combined percentages of the upper right and lower right quadrants inputted, as described by Chou, T.C. (2012), for analysis.

Propidium Iodide-based Analysis of the Cell Cycle

PI is a DNA intercalating agent which fluoresces once bound allowing high throughput analysis of cell cycle distribution determined by the intensity of PI fluorescence which directly correlates with the level of DNA content of cells. Following treatments cells were washed twice in PBS before being fixed by adding 70% ice cold ethanol to cells dropwise to a final concentration of 1×10^6 cells/100µl while vortexing gently. Cells were then incubated for at least 1hr at RT or at -20°C overnight. 100 µl of each sample was transferred to a FACS tube (#352052; Falcon) and washed twice with PBS, centrifuged at 400 g for 5min. 1ml of PI (50µg/ml with 5µg RNase A; Sigma-Aldrich) was added to each sample and incubated at 37°C for 1hr in the dark. Geometric mean fluorescent intensity of 20,000 events per sample

was recorded in the FL-2 channel on a FACSCalibur (BD Biosciences Europe, Oxford, UK) flow cytometer using CellQuest Pro software. Cell cycle distribution was then analysed and fit using the Cycle Analyser on a trial version of ModFit LT 4.0 (Verity Software House). Sub G0/G1 and post G2/M (polyploidy) events were omitted from analysis and the final representation of data.

Hematoxylin and Eosin Cell Staining

Following treatment, approximately 5×10^4 cells were cytopspun onto glass slides for 2min at 500rpm using a Shandon Cytospin 2 Cyto centrifuge. Cytospins were left to air dry at RT for 1hr before being fixed with 70% ice cold ethanol for at least 1hr. Slides were then washed in H₂O (each wash consisted of 20 dips into fresh H₂O) before being stained with Hematoxylin Gill No.2 (#GHS-2; Sigma-Aldrich Slide) for 10min and washed again in H₂O twice. For the bluing step, slides were placed in Scotts Tap Water substitute for 2min and washed in H₂O twice. Cells were then counterstained with Eosin Y solution, aqueous (#HT1101; Sigma-Aldrich) for 4min before two further H₂O washes. Cells were then dehydrated by being dipped into increasing percentages of ethanol, cleared with xylene before coverslips were mounted onto the glass slides using DPX mountant and dried overnight before imaging. Cells were visualised on a Leica DM LB2 microscope (Leica, Nussloch, Germany). Images of the cells were acquired by a Nikon Digital Sight DS-Fi1C camera (Nikon, Japan) using NIS-Elements software (version 3.0, Nikon, Japan).

Statistical analysis

Statistical significance between experimental and control groups was evaluated by Student's t-test. P-values of <0.05 were considered significant.

Chapter 3

**Imatinib and Nilotinib inhibit Bcr-Abl-induced ROS
through targeted degradation of NADPH oxidase
subunit p22phox**

Leukemia Research, 2013; 37, 183-189

Supplementary Material

The publication entitled “Imatinib and Nilotinib inhibit Bcr-Abl-induced ROS through targeted degradation of NADPH oxidase subunit p22phox” demonstrated that increased ROS signalling *via* Bcr-Abl in K562 cells is in part Nox-derived and that inhibition of Bcr-Abl signalling leads to GSK-3 β activation which potentially reduces intracellular ROS levels through targeted degradation of p22phox. This work established a link between Bcr-Abl signalling and ROS production through Nox activity. The following section contains supplementary data related to the work presented in that publication.

Figure 1 of Landry *et al.* (2013) demonstrated that inhibition of Bcr-Abl signalling reduces intracellular ROS levels which are in part Nox-derived. In order to establish this several pharmacological agents were used to treat K562 cells. Among these were the Bcr-Abl inhibitors Imatinib and Nilotinib and the Nox inhibitors DPI and VAS2870. To ensure that any effects on ROS levels observed in these experiments did not occur as a result of altered cell viability, cell death was assessed by propidium iodide exclusion following treatments. Figure S1 demonstrates that these treatments did not have any significant effect on cell viability. This indicated that any effects on ROS levels observed were due to the inhibition of signalling pathways in response to treatments and not due to an effect on cell viability.

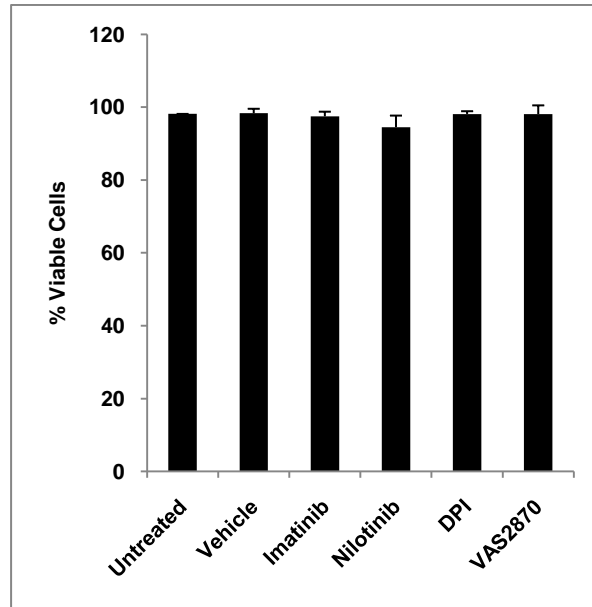


Figure S1. Treatment of K562 cells with various compounds does not affect cell viability. K562 cells were treated with Imatinib (1 μ M, 16hr), Nilotinib (0.1 μ M, 16hr), DPI (10 μ M, 1hr) or VAS2870 (10 μ M, 1hr) and cell viability was analysed by propidium iodide exclusion. Results are expressed as mean \pm SD and are representative of three independent experiments.

Mitochondrial electron transport chain leakage has been previously demonstrated as one possible source of the increased ROS levels associated with Bcr-Abl expression (Sattler *et al.*, 2000). ROS levels related to mitochondrial electron transport chain leakage in K562 cells was examined using Rotenone, a mitochondrial inhibitor which prevents the electron transfer from complex I to ubiquinone (Chance *et al.*, 1963). Rotenone treatment had a significant effect on the level of intracellular ROS in K562 cells and produced an average reduction of approximately 32% (Figure S2). This decrease in intracellular ROS level was comparable to the reductions associated with Nox protein inhibition by either DPI or VAS2870 treatment. These inhibitors produced average decreases of 43% and 35% respectively (Figure 1c). This study demonstrated that mitochondrial electron transport chain leakage contributes in part to the intracellular ROS levels of K562 cells agreeing with the previous study by Sattler *et al.* (2000).

Figure 2 of Landry *et al.* (2013) demonstrated that inhibition of Bcr-Abl signalling by TKI treatment resulted in the post-translational downregulation of p22phox. Interestingly, as demonstrated in Figure S3, the level of reduction in p22phox protein was directly proportional to the level of CrkL dephosphorylation in K562 cells following either Imatinib or Nilotinib treatment. CrkL phosphorylation status is frequently used to demonstrate the decrease in Bcr-Abl kinase activity following TKI treatment. This study further indicated the importance of Bcr-Abl kinase activity in the maintenance of p22phox protein levels.

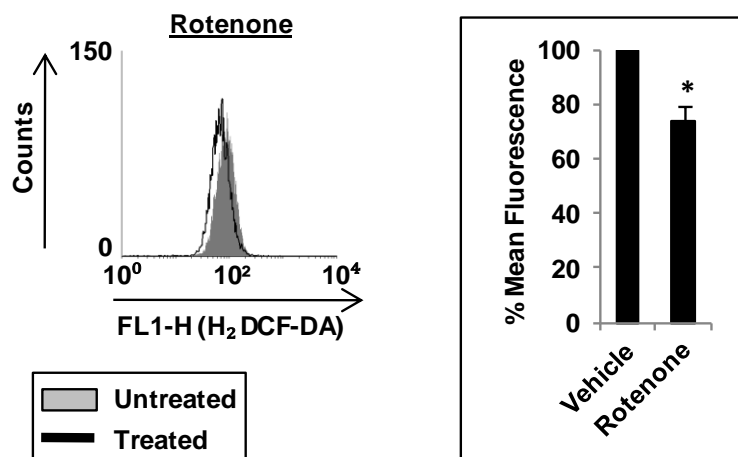


Figure S2. Mitochondrial electron transport chain leakage contributes in part to the intracellular ROS levels of K562 cells. K562 cells were treated with Rotenone (1 μ M, 1hr). Intracellular ROS levels were measured by flow cytometric analysis of relative DCF fluorescence. Bar chart shows the mean relative DCF fluorescence of treated cells expressed as a percentage of the DMSO vehicle control. Results are expressed as mean \pm SD and are representative of three independent experiments. Statistical analysis was carried out using the student t-test (P<0.05 is marked with *).

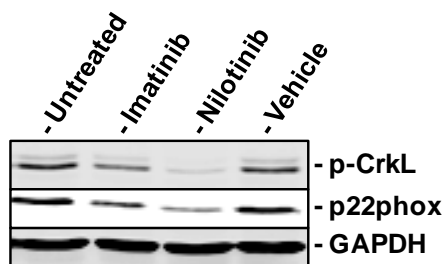
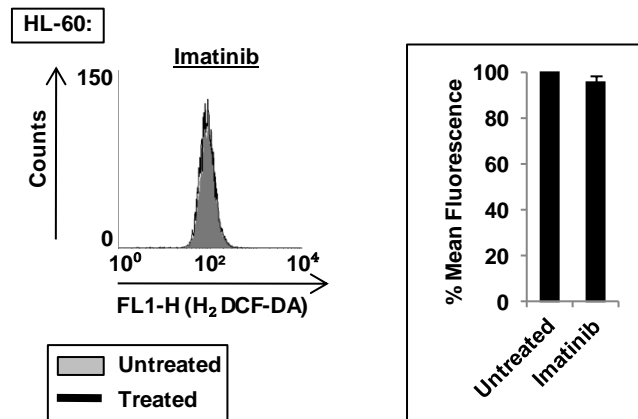


Figure S3. Reduction in p22phox protein level following Bcr-Abl inhibition is proportional to the level of CrkL dephosphorylation. Western blot analysis of p22phox protein levels and phosphorylation status (p-) of CrkL in K562 cells treated with Imatinib (1 μ M, 16hr) and Nilotinib (0.1nM, 16hr). Vehicle is DMSO control. GAPDH is shown as a loading control. Western blot is representative of three independent experiments.

HL-60 cells are an acute promyelocytic human leukaemia cell line and are routinely used as a Bcr-Abl negative control cell line for K562 cell studies. As demonstrated in Figure S4 HL-60 cells were treated with Imatinib to confirm that any effects noted in K562 cells following Imatinib treatment were a direct result of specific Bcr-Abl inhibition. Landry *et al.* (2013) demonstrated that Imatinib treatment significantly decreases ROS levels in K562 cells (Figure 1a). In contrast, Imatinib treated HL-60 cells demonstrated no reduction in ROS levels (Figure S4a). Additionally, Imatinib treatment of K562 cells resulted in a significant decrease in p22phox proteins levels (Figure 2a). No such reduction was noted in HL-60 cells after treatment (Figure S4b). This study demonstrated that both the reductions in ROS levels and p22phox protein levels in K562 cells following Imatinib treatment were due to the specific inhibition of Bcr-Abl signalling.

(a)



(b)

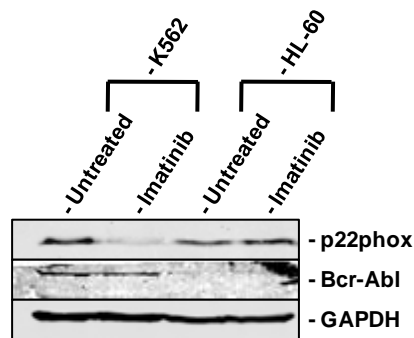


Figure S4. Imatinib treatment has no effect on the intracellular ROS levels or p22phox protein levels of the Bcr-Abl negative HL-60 cell line. (a) HL-60 cells were treated with Imatinib (1 μ M, 16hr). Intracellular ROS levels were measured by flow cytometric analysis of relative DCF fluorescence. Bar chart shows the mean relative DCF fluorescence of treated cells expressed as a percentage of the DMSO vehicle control. Results are expressed as mean \pm SD and are representative of three independent experiments. (b) Western blot analysis of p22phox and Bcr-Abl protein levels in K562 and HL-60 cells treated with Imatinib (1 μ M, 16hr). GAPDH is shown as a loading control.

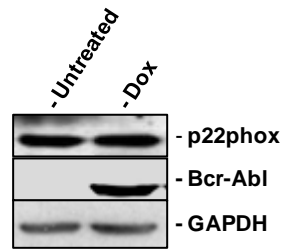
Naughton *et al.* (2009) demonstrated that induction of Bcr-Abl expression increases the level of Nox-derived intracellular-ROS but never established a mechanism for this process. Following on from this work Landry *et al.* (2013) established that inhibition of Bcr-Abl signalling results in the degradation of the NADPH subunit p22phox which coincides with a reduction in intracellular ROS levels. From this work it was concluded that active Bcr-Abl signalling maintains the protein levels of p22phox, which subsequently regulates Nox activity. Furthermore as a result of this study it was hypothesised that induced Bcr-Abl expression may increase the protein levels of p22phox by inhibiting degradation. In order to establish this p22phox protein levels needed to be examined following induction of Bcr-Abl signalling. TonB.210 cells are a derivative of the murine Interleukin-3 (IL-3)-dependent pro-B cell line BaF3 and have inducible Bcr-Abl expression, controlled by a doxycycline (Dox)-dependent promoter. This cell line was utilised to determine if induction of Bcr-Abl expression had any effect on p22phox protein levels (Figure S5). Contradictory to the outlined hypothesis induction of Bcr-Abl expression following 48hr of Dox treatment demonstrated no significant increase in p22phox protein levels (Figure S5a).

The failure of Bcr-Abl induction to increase p22phox protein levels raised multiple questions into the mechanism of p22phox maintenance as outlined in Landry *et al.* (2013). As a result further examination was required in order to achieve a greater understanding of this process. Interestingly, in contrast to K562 cells TonB.210 cells are dependent on supplementation with the cytokine, IL-3. It is well established that signaling through IL-3/IL-3 Receptor (IL-3R) interaction activates a variety of signalling pathways including the Raf/MEK/ERK and PI3K/Akt pathways thereby promoting the survival, growth and differentiation of hematopoietic cells

(Steelman *et al.*, 2004). As discussed previously and demonstrated in Figure 3 of Landry *et al.* (2013) the activity of both the Raf/MEK/ERK and PI3K/Akt pathways were demonstrated to be key in the maintenance of p22phox protein levels downstream of Bcr-Abl signalling in K562 cells. Therefore, IL-3 signalling in TonB.210 cells potentially has both these pathways activated prior to Bcr-Abl induction, preventing p22phox protein degradation. As a result subsequent induction of Bcr-Abl is unlikely to have an effect on p22phox protein levels

To determine if IL-3 signalling was having an effect on p22phox protein levels independent of Bcr-Abl signalling, both untreated and Dox treated TonB.210 cells were starved of IL-3 for 6hr and p22phox protein levels were monitored (Figure S5b). To verify that downstream IL-3R signalling was effected by IL-3 removal, phosphorylation of ERK1/2 was examined. As demonstrated IL-3 removal in untreated cells produced a significant reduction in p22phox protein levels. Furthermore, IL-3 removal in cells expressing Bcr-Abl also demonstrated a decrease in p22phox protein levels however this reduction was less significant than that observed in untreated cells. This suggested that Bcr-Abl signalling was providing a protective effect on p22phox protein levels following IL-3 removal. Taken together this work established that IL-3 signalling has a role similar to Bcr-Abl in the maintenance of p22phox protein levels and thus provided an explanation for the lack of an increase in p22phox proteins levels following Bcr-Abl induction (Figure S5a). Finally it is noteworthy to point out that the prosurvial effect of IL-3 signalling has previously been linked to increased Nox-derived ROS production in the M07e human AML cell line (Maraldi T *et al.*, 2009a; Maraldi T *et al.*, 2009b). This work and the work presented here suggested an important role for p22phox not only in CML but potentially other blood-borne diseases influenced by IL-3 signalling.

(a)



(b)

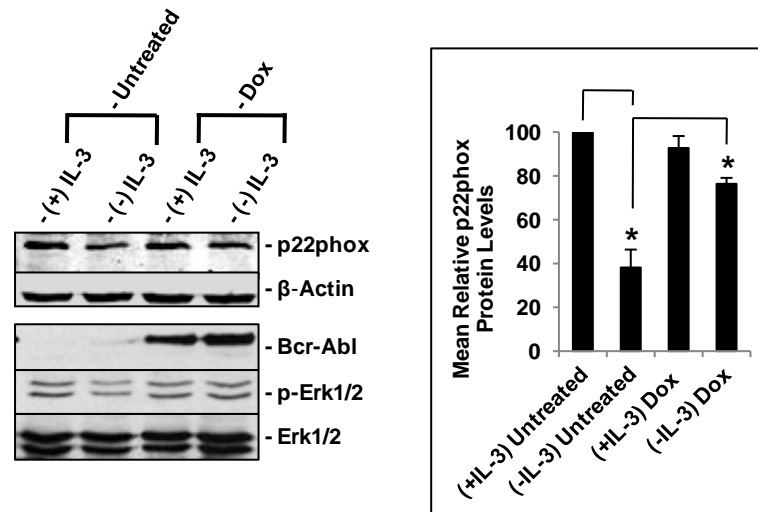
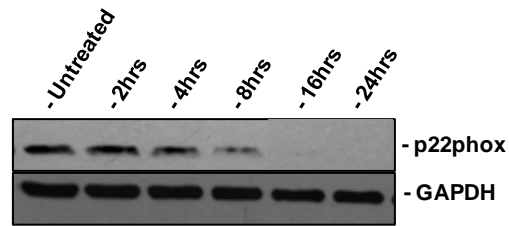


Figure S5. IL-3 receptor signalling maintains p22phox protein levels similarly to Bcr-Abl signalling. (a) Western blot analysis of p22phox and Bcr-Abl protein levels in TonB.210 cells treated with doxycycline (Dox) (1µg/ml, 48hr). GAPDH is shown as a loading control. (b) Western blot analysis of p22phox, Bcr-Abl and phospho-ERK1/2 protein levels in untreated and Dox treated (1µg/ml, 48hr) TonB.210 cells before and after IL-3 starvation (6hr). β-Actin is shown as a loading control. Bar chart shows the mean relative p22phox protein levels of treated cells expressed as a percentage of the Untreated (+IL-3) control as determined by densitometry. Results are expressed as mean ± SD and are representative of three independent experiments. Statistical analysis was carried out using the student t-test (P<0.01 is marked with *).

It was established in Landry *et al.* (2013) that activation of GSK-3 β was required for the degradation of p22phox following Bcr-Abl inhibition (Figure 3). GSK-3 β is highly cited for its role in targeted degradation of proteins. In many cases GSK-3 β kinase activity directly flags proteins for degradation through phosphorylation of serine or threonine residues (Grimes and Jope, 2001; Xu *et al.*, 2009). Once the role had been identified for GSK-3 β in p22phox degradation it needed to be determined if GSK-3 β was directly interacting with p22phox following Bcr-Abl inhibition and targeting it for degradation. To begin this study the earliest time-point at which p22phox protein levels decrease following Imatinib treatment needed to be established. Figure S6a demonstrates that p22phox protein levels start to lower by 4 hours and are still decreasing up to 8 hours after initial Imatinib treatment. 6 hours, a time-point between 4 and 8 hours of Imatinib treatment was identified as ideal for determining an interaction between p22phox and GSK-3 β prior to degradation as a high level of p22phox would still be available to interact with GSK-3 β .

To establish if there was a direct interaction between p22phox and GSK-3 β , GSK-3 β was immunoprecipitated from untreated and Imatinib treated K562 cells (Figure S6b). Once separated and membrane transferred, GSK-3 β immunoprecipitates were immunoblotted to determine if p22phox was co-immunoprecipitated with GSK-3 β . Figure S6b demonstrated that p22phox did not co-immunoprecipitate with GSK-3 β which demonstrated that there was no direct interaction between these two proteins. Co-immunoprecipitation of β -Catenin was checked as a positive control. Furthermore, the reverse immunoprecipitation of p22phox did not demonstrate any co-immunoprecipitation of GSK-3 β . This study suggested that the role GSK-3 β was

(a)



(b)

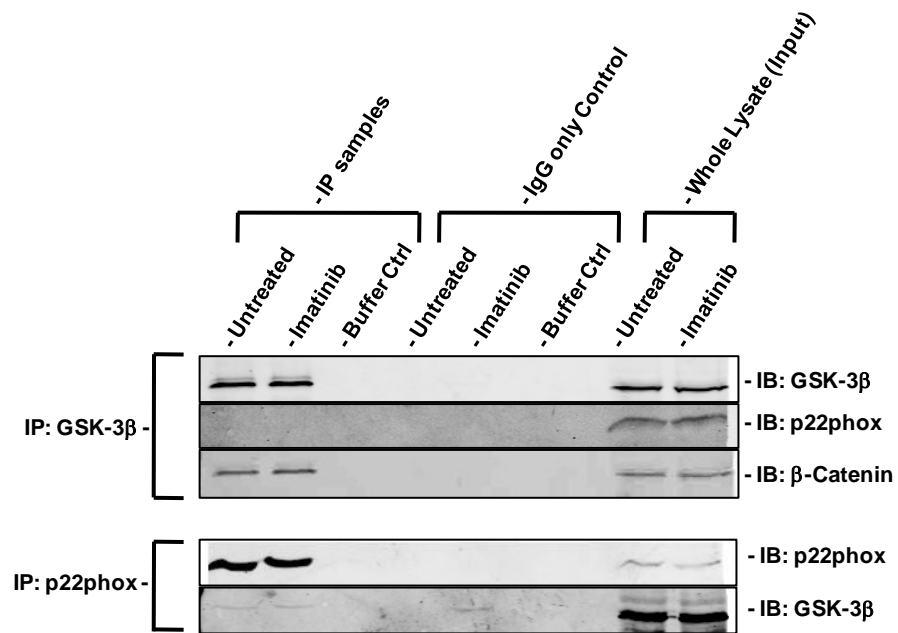


Figure S6. GSK-3β does not directly interact with p22phox prior to degradation.

(a) Western blot analysis of p22phox protein levels in K562 cells treated with Imatinib (1 μM) for the indicated times. GAPDH is shown as a loading control. (b) Immunoprecipitation (IP) of GSK-3β or p22phox from whole-cell lysates of untreated or Imatinib treated (1 μM, 8hr) K562 cells. Nitrocellulose membranes were immunoblotted (IB) for the presence of GSK-3β, p22phox and β-Catenin.

having on p22phox degradation in Figure 3 of Landry *et al.* (2013) maybe due to upstream effects of GSK-3 β activation rather than a direct interaction.

As previously discussed p22phox is necessary for the activity of Nox proteins 1, 2, 3 and 4, as a result p22phox has an essential role in intracellular ROS production (Ambasta *et al.*, 2004; Ueno *et al.*, 2005). Figure 4 of Landry *et al.* (2013) demonstrated this essential role through selective knockdown of p22phox which produced a significant decrease in ROS levels 24hr after transfection. Figure S7 demonstrates the same reduction observed in the intracellular ROS levels of K562 cells 24hr after transfection. In addition to this time-point the ROS levels of K562 cells 48hr and 72hr after transfection are also shown. 24hr after transfection significant reductions in the ROS levels of both the p22phox knockdown samples (siRNA(i) and siRNA(ii)) were observed when compared to cells transfected with negative control siRNA (Negative). However, by 48hr the reduction in ROS levels noted in siRNA(i) transfected cells had halved while siRNA(ii) transfected cells no longer demonstrated any significant reduction in ROS. Neither siRNA(i) or siRNA(ii) transfected cells demonstrated any significant reduction in ROS levels by 72hr.

As demonstrated in Figure 4a and 4e of Landry *et al.* (2013), transfection of K562 cells with siRNA(i) resulted in an almost complete loss of p22phox protein for up to 72hr when compared to cells transfected with negative control siRNA. In contrast, cells transfected with siRNA(ii) were demonstrated at each time-point to have higher expression of p22phox relative to siRNA(i) transfected cells. Protein levels of p22phox siRNA(ii) transfected cells were also demonstrated to increase incrementally at each time-point. The gradual increase of p22phox protein levels in

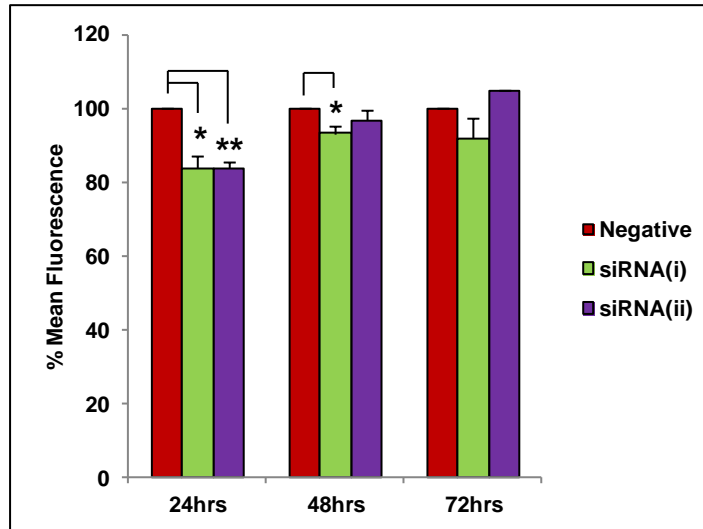


Figure S7. Removal of p22phox expression reduces intracellular ROS from 24hr
 K562 were transfected with siRNA to target p22phox expression. Intracellular ROS levels were then measured by FACS analysis of relative DCF fluorescence 24, 48 and 72hr following p22phox knockdown *via* siRNA. Bar chart shows the mean relative DCF fluorescence of p22phox knockdown cells as expressed as a percentage of the Negative control. Results are expressed as mean \pm SD and are representative of three independent experiments. Statistical analysis was carried out using the student t-test ($P < 0.05$ is marked with *, $P < 0.01$ is marked with **).

siRNA(ii) transfected cells may explain why the ROS decrease lessened between time-points but does not provide an explanation for the return of intracellular ROS back to basal levels by 72hr. Additionally p22phox protein levels in siRNA(i) transfected cells remained reduced for the duration of the study therefore a consistent reduction in ROS levels would have been expected.

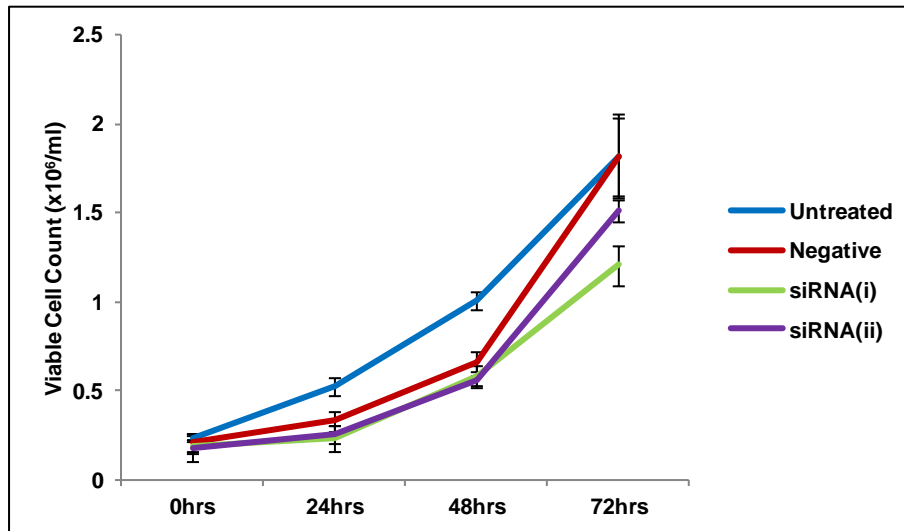
Homeostasis of the redox state in cells is pivotal for the maintenance of normal cell function and survival (D'Autréaux and Toledano, 2007; Circu and Aw, 2010). It is likely that a compensatory mechanism is occurring to return the cells intracellular ROS back to basal levels. This is not unusual with multiple studies demonstrating increases in the activity or expression of alternative Nox proteins or their regulators to compensate for ROS decreases resulting from the targeted inhibition of another Nox protein (Yang *et al.*, 2001; Maytin *et al.*, 2004; Frantz *et al.*, 2006). Additionally it is important to note that p22phox regulation is specific to Nox1, Nox2, Nox3 and Nox4 but has no regulatory role for Nox5, Duox1 or Duox2. The ability of a Nox protein to generate ROS is limited to the availability of the substrate NADPH with activity of Nox5, Duox1 and Duox2 being highly dependent on NADPH levels (Behard and Krause, 2007). Therefore removal of p22phox and subsequent inhibition of Nox proteins 1 to 4 may increase availability of NADPH which could have a positive effect on Nox5, Duox1 or Duox2 activity thus explaining the noted return of intracellular ROS to basal levels.

The final study in Landry *et al.* (2013) examined K562 cells stained with the dye trypan blue to obtain viable cell counts (trypan blue negative) following p22phox knockdown (Figure 4d). This demonstrated that removal of p22phox significantly reduced K562 cell number, which directly correlated with the

expression levels of p22phox following knockdown (Figure 4e). Figure S8a demonstrates all recorded cell counts 0, 24, 48 and 72hr after transfection in the form of a line graph. 24hr after transfection the Negative, siRNA(i) and siRNA(ii) samples all demonstrated a lower cell count than that of the untreated cells. This was likely due to transfection *via* electroporation which can cause minor stress to cells producing short-term cell cycle retardation (Lepik *et al.*, 2003). It is significant to note that at all time-points the Negative transfected cells maintained a higher cell count than either of the p22phox knockdown samples. The difference between cell counts became most noticeable 72hr after transfection with cells transfected with either siRNA(i) or siRNA(ii) showing significant reductions when compared to Untreated or Negative siRNA transfected cells. Cell counts 72hr after transfection are also illustrated as a bar chart in Figure 4d of Landry *et al.* (2013).

In addition to viable cell counts, the number of trypan blue positive cells were also recorded. Figure S8b demonstrates that there was no significant change in cell viability of the Negative, siRNA(i) and siRNA(ii) samples at any time-point. In contrast, untreated cells demonstrated a significant increase in the percentage of trypan blue positive cells by 72hr. This result was most likely due to nutrient depletion and/or overcrowding resulting in suboptimal growth conditions in the culture media by 72hr. As discussed the transfected samples had a lower cell number from 24hr onwards and as a result fewer nutrients would have been utilised providing cells with optimal conditions for a longer period. Figure S8 demonstrates that the number of K562 cells decreased following p22phox knockdown with no significant increase in cell death. This strongly suggested that the decrease in cell number observed was due to a reduction in cell proliferation. This demonstrated a potential role for p22phox in K562 and CML cell proliferation.

(a)



(b)

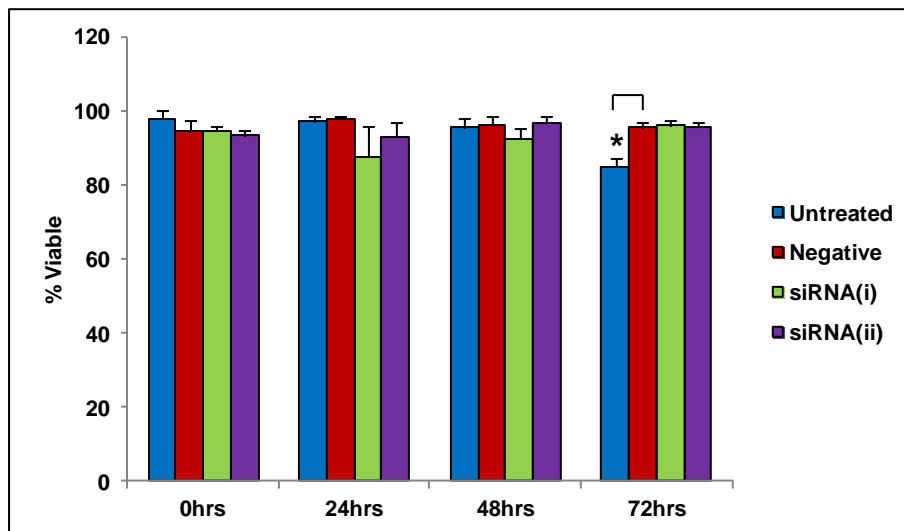


Figure S8. Removal of p22phox reduces cell number while having no effect on the level of cell death. (a) Viable cell counts of K562 cells determined by trypan blue exclusion 0, 24, 48 and 72hr following p22phox knockdown *via* siRNA. (b) Percentage of viable K562 cells determined by trypan blue exclusion 0, 24, 48 and 72hr following p22phox knockdown *via* siRNA. Results are expressed as mean \pm SD and are representative of three independent experiments. Statistical analysis was carried out using the student t-test ($P < 0.05$ is marked with *).

In summary, this work demonstrated that a significant proportion of ROS in K562 cells was derived from Nox proteins and to a lesser extent mitochondrial electron transport chain leakage. Inhibition of Bcr-Abl signalling led to a significant reduction in ROS levels which was concurrent with the post-translational down-regulation of the small membrane-bound protein p22phox, which is an essential subunit of the Nox complex. This down-regulation was dependent on GSK-3 β activity, which is inhibited downstream of the PI3K/Akt and Raf/MEK/ERK1/2 pathways. How GSK-3 β was involved in p22phox degradation was not elucidated, although it was shown that there was no direct interaction between these two proteins. In addition inhibition of p22phox with siRNA significantly affected ROS levels demonstrating the importance of p22phox for ROS generation and suggesting that down-regulation of p22phox protein levels following Bcr-Abl inhibition is in part responsible for the parallel reduction in ROS levels. Given the importance of p22phox for Nox-activity, this study provided a link between Bcr-Abl signalling and Nox-derived ROS. Interestingly, inhibition of p22phox by siRNA also resulted in decreased cell number with no significant increase in cell death suggesting a role for p22phox and therefore Nox activity in cell proliferation.

Chapter 4

The role of the Nox subunit p22phox in CML disease phenotype

Abstract

Nox-derived Reactive Oxygen Species (ROS) production has been implicated in many different cellular processes, while being linked to a variety of diseases including cancer. After establishing a link between Bcr-Abl signalling and the generation of Nox-derived ROS through p22phox, it was of interest to determine how p22phox function and mediated ROS production affected cellular activity and influenced Chronic Myeloid Leukaemia (CML) disease phenotype. This study identified p22phox to have a significant function in cellular proliferation, demonstrating its importance in G1/S phase cell cycle transition through a pRb-Cyclin E-dependent mechanism. Removal of p22phox expression was also demonstrated to significantly decrease cell viability while producing a minor effect on cell survival. Interestingly, p22phox removal was also demonstrated to make cells significantly more susceptible to Bcr-Abl tyrosine kinase inhibition *via* Imatinib. As a result, this work identified the importance of p22phox-mediated Nox protein activity in CML disease phenotype, demonstrating the potential of Nox inhibition as possible treatment for CML.

Introduction

Chronic Myeloid Leukaemia (CML) begins in a chronic phase (CML-CP), which is defined by an increase in the number of mature circulating myeloid cells. Unfortunately without effective therapy patient who present with CML-CP will inevitably progress to blastic phase (CML-BP), also known as blast crisis, where myeloid cells lose their terminal differentiation capacity resulting in a considerable accumulation of immature blasts. This progression is associated with poor prognosis. Bcr-Abl expression is required for the pathogenesis of CML, essential for the initiation, maintenance and progression of the disease and as a result has traditionally been the central focus in the development of therapeutic treatments (Deininger *et al.*, 2005). Indeed, small-molecule tyrosine kinase inhibitors (TKIs), such as Imatinib, which target Bcr-Abl activity have significantly improved CML prognosis (Druker *et al.*, 2005). Unfortunately, even with Imatinib treatment residual disease persists and DNA mutation can lead to drug resistance. In recent years a large emphasis has been directed at the development of alternative TKIs which circumvent known modes of resistance (Quintás-Cardama *et al.*, 2007; Bixby and Talpaz, 2011). This resulted in the development of several new drugs which targeted Bcr-Abl activity with greater efficiency yet they have failed to remove residual disease or the potential for drug resistance to develop. As a consequence the development of alternative strategies to better treat CML are still needed, making it important to identify other essential components which are involved in the pathogenesis of CML.

A number of studies have shown that induced or constitutive expression of Bcr-Abl increases the intracellular levels of Reactive Oxygen Species (ROS) (Sattler *et al.*, 2000; Kim *et al.*, 2005; Naughton *et al.*, 2009). Although traditionally seen as harmful by-products of cellular metabolism, ROS and particularly hydrogen

peroxide (H_2O_2) are now generally recognised as important intracellular signalling molecules (Rhee *et al.*, 2005a; Rhee *et al.*, 2005b; Toledano *et al.*, 2010; Bae *et al.*, 2011). This had lead to studies which have identified the involvement of ROS mediated signalling in multiple factors which define leukaemia disease phenotype including but not limited to cell survival and proliferation (Trachootham *et al.*, 2008; Groeger *et al.*, 2009; Verbon *et al.*, 2012). Additionally Bcr–Abl-induced ROS can contribute to genomic instability, driving the development of drug resistance as well as progression to blast crisis (Nowicki *et al.*, 2004; Rassool *et al.*, 2007; Sallmyr *et al.*, 2008). Indeed a role for ROS production in leukaemia development, progression, and maintenance is becoming more and more evident (Hole *et al.*, 2011).

The NADPH Oxidase (Nox) enzyme family generate ROS as their primary function in cells while mitochondria produce ROS as a by-product of cellular respiration. Both systems are known sources of ROS in CML (Sattler *et al.*, 2000; Kim *et al.*, 2005; Naughton *et al.*, 2009; Landry *et al.*, 2013). In leukaemia Nox-derived ROS have been demonstrated to be involved in a host of cellular activities driving disease phenotype by increasing survival, migration, proliferation and even differentiation (Kim *et al.*, 2005; Naughton *et al.*, 2009; Sardina *et al.*, 2010; Hole *et al.*, 2011; Reddy *et al.*, 2011). The coupling of these processes with genomic instability further contributes to the progression of this myeloproliferative disorder signifying the need to study ROS in order to better understand the pathogenesis of CML.

The work presented in Chapter 3 investigated elevated levels of intracellular-ROS associated with Bcr-Abl signalling in CML. This work established a link between Bcr-Abl signalling and the generation of Nox-derived ROS through the regulation of p22phox protein levels. As discussed ROS signalling can potentially

play a significant role in the disease phenotype of cancers. In light of this the aims of this next study were to investigate p22phox to determine how its expression and influence on ROS levels affect disease phenotype. Particular attention was placed on cell proliferation, after work in Chapter 3 suggested that p22phox had an involvement in this process. In addition Nox-derived ROS has been repeatedly associated with cell proliferation (Jeong *et al.*, 2004; Sturrock *et al.*, 2006; Petry *et al.*, 2006; Reddy *et al.*, 2011). Furthermore, studies by Naughton *et al.* (2009) and others have demonstrated the importance of Nox-derived ROS in CML survival therefore focus was also placed on examining if there was a potential role for p22phox expression and ROS regulation in increased cell viability and survival in CML. As before K562 cells, which constitutively express Bcr-Abl, were used as a model for CML to perform these studies and elucidate a possible role for p22phox regulated ROS in CML disease phenotype.

Results

An examination of the Nox protein subunit p22phox and its effect on cell proliferation

Nox protein activity and ROS production is known to be involved in cell proliferation (Jeong *et al.*, 2004; Sturrock *et al.*, 2006; Petry *et al.*, 2006; Reddy *et al.*, 2011). Studies in Chapter 3 identified the essential subunit for Nox protein activity, p22phox, as having a potential role in K562 cell proliferation. To further investigate and verify if p22phox and therefore Nox-derived ROS have a function in Chronic Myeloid Leukaemia (CML) proliferation, K562 cells were stained with Carboxyfluorescein Succinimidyl Ester (CFSE) and subsequently transfected with siRNA to target p22phox expression using the same method as described in Chapter 3.

CFSE is fluorescent, highly stable within cells and retained for long periods of time while being evenly distributed between daughter cells following cell division (Quah *et al.*, 2007). This even distribution and halving of CFSE fluorescence levels following division allows cell proliferation to be monitored by flow cytometry. Figure 1 demonstrates the level of CFSE fluorescence in K562 cells 24hr, 48hr and 72hr after p22phox knockdown. It was immediately evident that electroporated samples had a higher level of CFSE fluorescence when compared to untreated cells, indicating a reduced rate of proliferation. It is important to note that the difference in fluorescence between untreated and transfected samples showed no significant increase following 24hr. This suggested that any effect electroporation had on proliferation ceased prior to the 24hr time-point. A comparable level of fluorescence was observed between the scrambled siRNA (Negative) transfected control cells and electroporated control (Elect Ctrl) cells. This demonstrated that the changes in CFSE

fluorescence were a result of electroporation rather than siRNA transfection. As discussed in Chapter 3 electroporation can cause minor stress to cells, producing short-term cell cycle retardation. Further comparison of CFSE fluorescence suggested that at each time-point Negative transfected cells proliferated more than the p22phox knockdown samples (siRNA(i) and siRNA(ii)). Furthermore, siRNA(i) transfected cells demonstrated a higher and more significant level of fluorescence than that of cells transfected with siRNA(ii) at the 72hr time-point. It is important to note that no further increase in fluorescence was observed in the siRNA(i) transfected cells from 48hr to 72hr suggesting p22phox knockdown stopped effecting proliferation prior to the 48hr time-point.

Examining CFSE fluorescence of whole cell population is not fully quantitative as cells rarely divide synchronously. As a result this method can only demonstrate whether or not a treatment effects cell proliferation. Using software to analyse CFSE fluorescence it is possible to determine the number of cell divisions following treatment. This method can quantify proliferation providing a more accurate interpretation of the results. As before K562 cells were stained with CFSE and transfected with siRNA. 72hr after transfection CFSE fluorescence was analysed *via* flow cytometry and ModFit LT software was used to fit this data.

This data is represented in Figure 2a which demonstrates the cell generational distribution of each sample 72hr after transfection. On average 85% of Untreated cells were in generation 5, which demonstrated that the majority of cells were in their 4th division cycle. The degree to which electroporation effected proliferation was also demonstrated with the majority of Elect Ctrl or Negative cells having even distribution between generations 4 and 5, approximate averages of 50%/40% and 49%/45% respectively. In addition to this both the p22phox knockdown samples

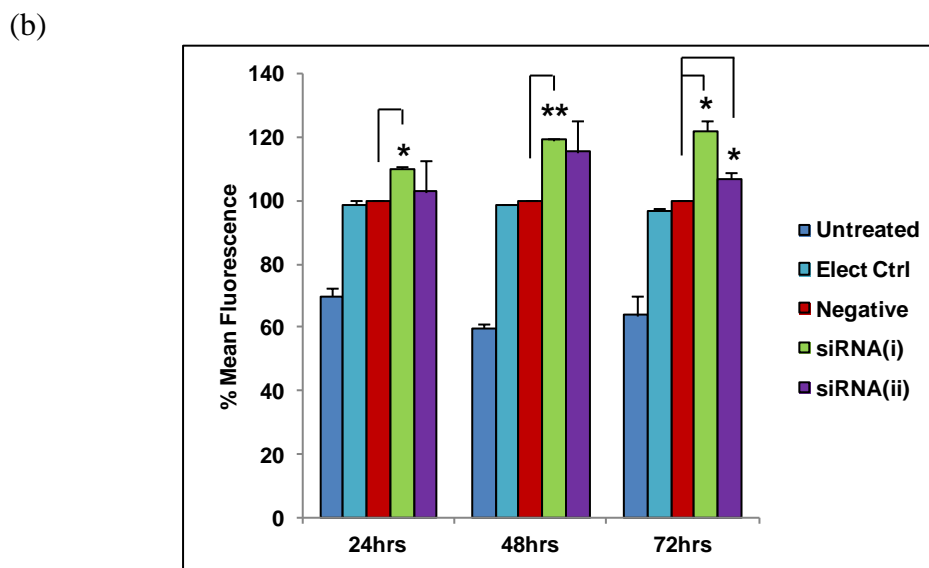
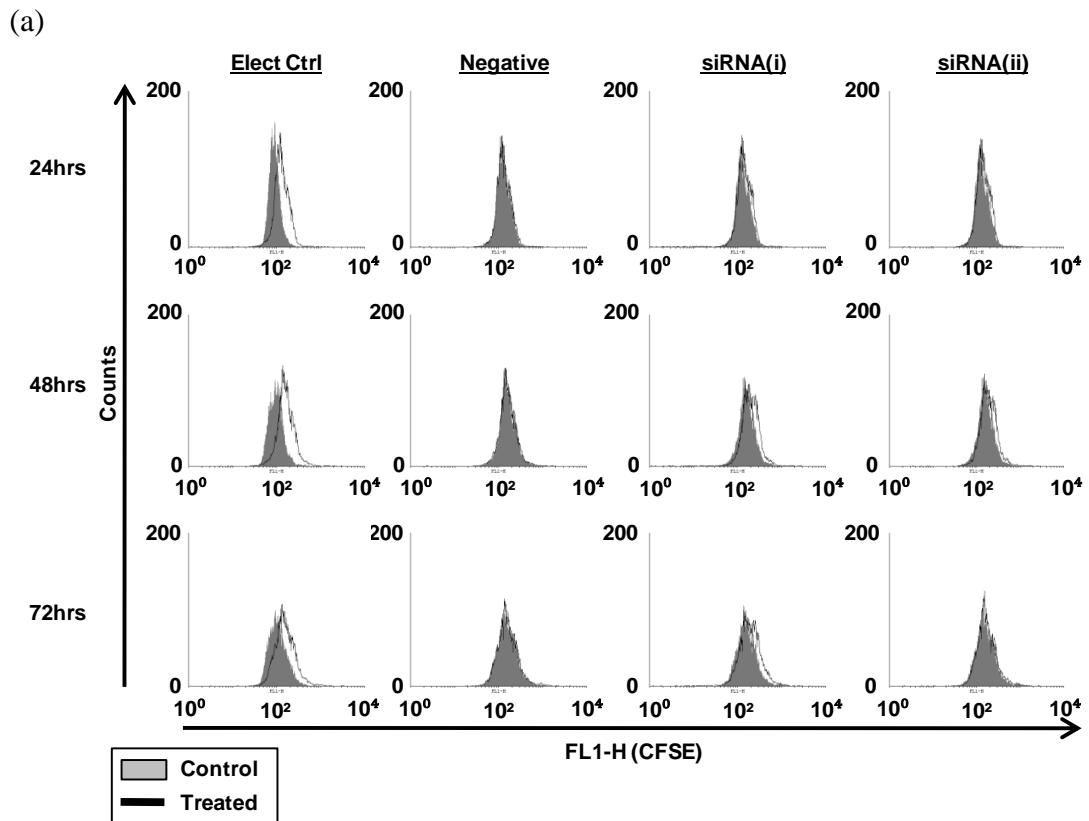


Figure 1. Removal of p22phox expression has a negative effect on K562 cell proliferation. (a) Histograms representing flow cytometric analysis of relative CFSE fluorescence 24, 48 and 72hr after p22phox siRNA transfection. Histograms compare Elect Ctrl to Untreated, Negative to Elect Ctrl and siRNA(i)/siRNA(ii) to Negative. (b) Bar chart shows the mean CFSE fluorescence of cells expressed as a percentage of the Negative siRNA control. Results are expressed as mean \pm SD and are representative of three independent experiments. Statistical analysis was carried out using the student t-test ($P < 0.05$ is marked with *, $P < 0.01$ is marked with **).

siRNA(i) and siRNA(ii), had average distributions of 72%/12% and 55%/33% respectively between generations 4 and 5. Comparing these results to the control samples suggested removal of p22phox expression had an effect on cell proliferation.

In addition to cell generation distribution, the proliferation index of each sample was also determined using Modfit LT and relative proliferation was calculated by normalising each sample to the Negative control (Figure 2b). This data demonstrated that the proliferation rates of K562 cells were significantly reduced following removal of p22phox expression. Furthermore, transfection with siRNA(i) resulted in a greater decrease in proliferation relative to siRNA(ii) transfected cells. Taken together these studies demonstrated the relative effect p22phox expression had on proliferation, implementing Nox-derived ROS in K562 cell proliferation.

Cell cycle distribution following the removal of p22phox expression

Having established a significant role for p22phox expression in K562 cell proliferation further examination was required to elucidate how exactly p22phox function was causing this effect. As before siRNA knockdown was used to target p22phox expression and the cell cycle distribution of K562 cells was determined through Bromodeoxyuridine (BrdU) incorporation and propidium iodide (PI) staining. This study demonstrated that K562 cells transfected with p22phox siRNA demonstrated a small but significant increase in the percentage of cells present in the G0/G1 stage of the cell cycle when compared to negative siRNA transfected control cells 24hr after transfection (Figure 3a). Furthermore, it was demonstrated at the 24hr time-point that knockdown of p22phox expression using siRNA(i) had a more significant effect on cell cycle distribution relative to transfection with siRNA(ii). By 48hr and 72hr however the significant increase in the percentage of G0/G1 cells

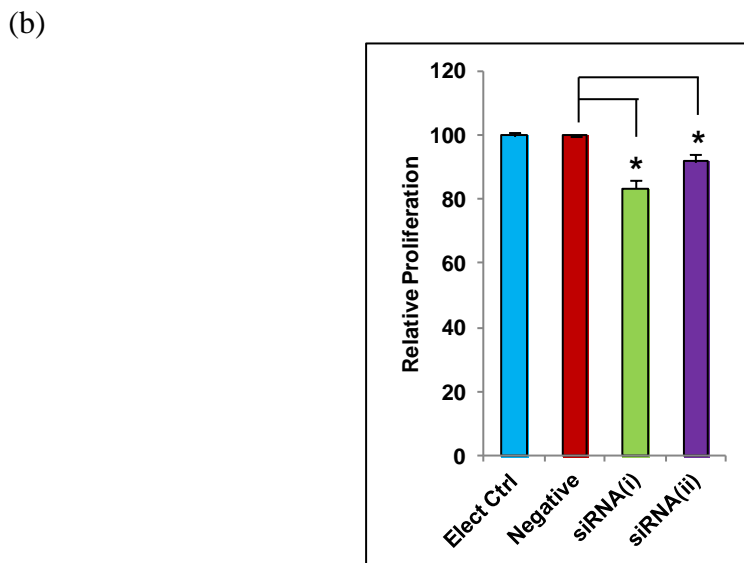
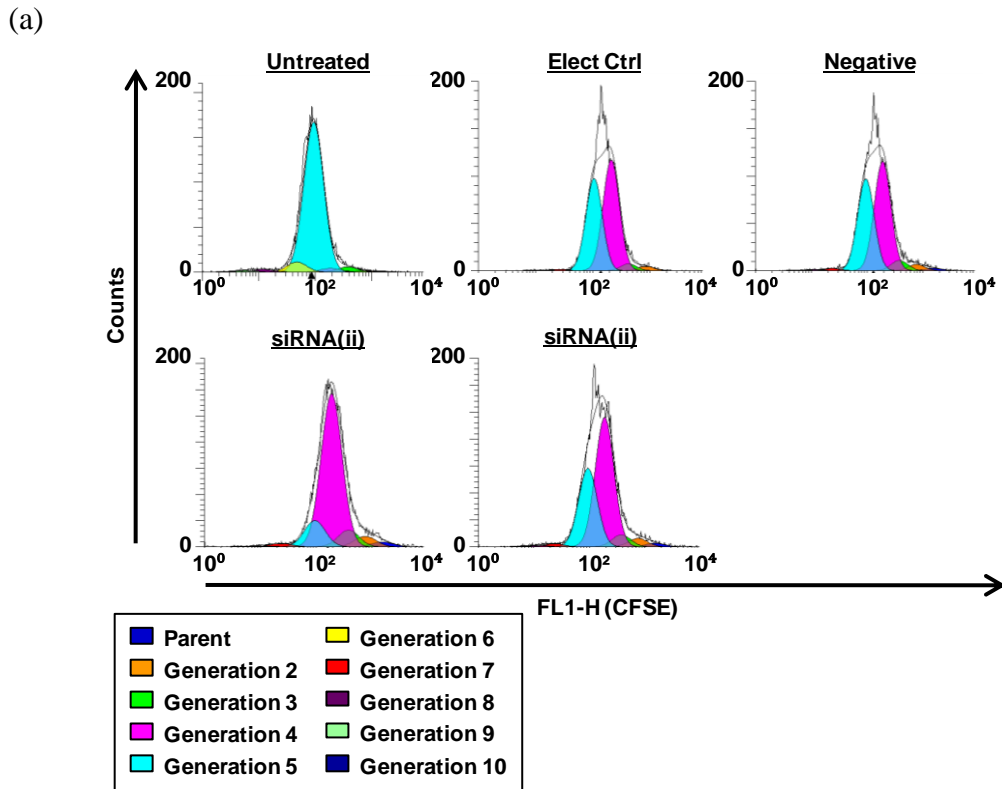


Figure 2. Expression of p22phox is important for the proliferation of K562 cells.

(a) Histograms representing the distribution of cell generations 72hr after p22phox siRNA transfection as determined by ModFit LT. (b) Proliferation index was also determined using ModFit LT software and relative proliferation was calculated by normalising to Negative control. Bar chart shows the relative proliferation of samples 72hr after p22phox siRNA transfection. Results are expressed as mean \pm SD and are representative of three independent experiments. Statistical analysis was carried out using the student t-test ($P < 0.05$ is marked with *).

was no longer observed. The effect noted at 24hr provided a possible explanation for the decreased levels of proliferation noted in K562 cells following p22phox knockdown. K562 cell cycle analysis and percentage distributions at each stage of the cell cycle following p22phox siRNA knockdown are demonstrated and quantified in Figure 3b. It is important to note that BrdU incorporation is more accurate at distinguishing S phase cells; as a result cell cycle distribution determined by BrdU/PI will vary when compared to analysis of the cell cycle using PI alone.

Further analysis of the G0/G1 stage of the cell cycle following p22phox

As demonstrated 24hr after p22phox siRNA transfection of K562 cells there was a small but significant increase in the percentage of cells present in the G0/G1 stages of the cell cycle. To provide a greater understanding of how the cell cycle was effected it first needed to be determined if the observed increase was due to a higher percentage of cells present in the G0 or G1 stages of the cell cycle. To establish this, protein expression of the proliferation marker Ki-67 was examined 24hr after transfection with p22phox siRNA. Ki-67 is a nuclear protein expressed in proliferating cells and is absent in quiescent cells (Gerdes *et al.*, 1983). As a result Ki-67 is only expressed in cells cycling through G1, DNA synthesis (S), G2 or mitosis (M), but not in cells present in the resting phase G0. Examination of Ki-67 expression demonstrated that following removal of p22phox expression there was a significant increase in the percentage of cells in G1 rather than G0 when compared to the Negative siRNA control transfected cells (Figure 4a). As before cells transfected with siRNA(i) demonstrated a greater increase in cells present in G1 when compared to cells transfected with siRNA(ii). Immunofluorescence images detecting Ki-67 protein expression cells further demonstrated no significant change in Ki-67

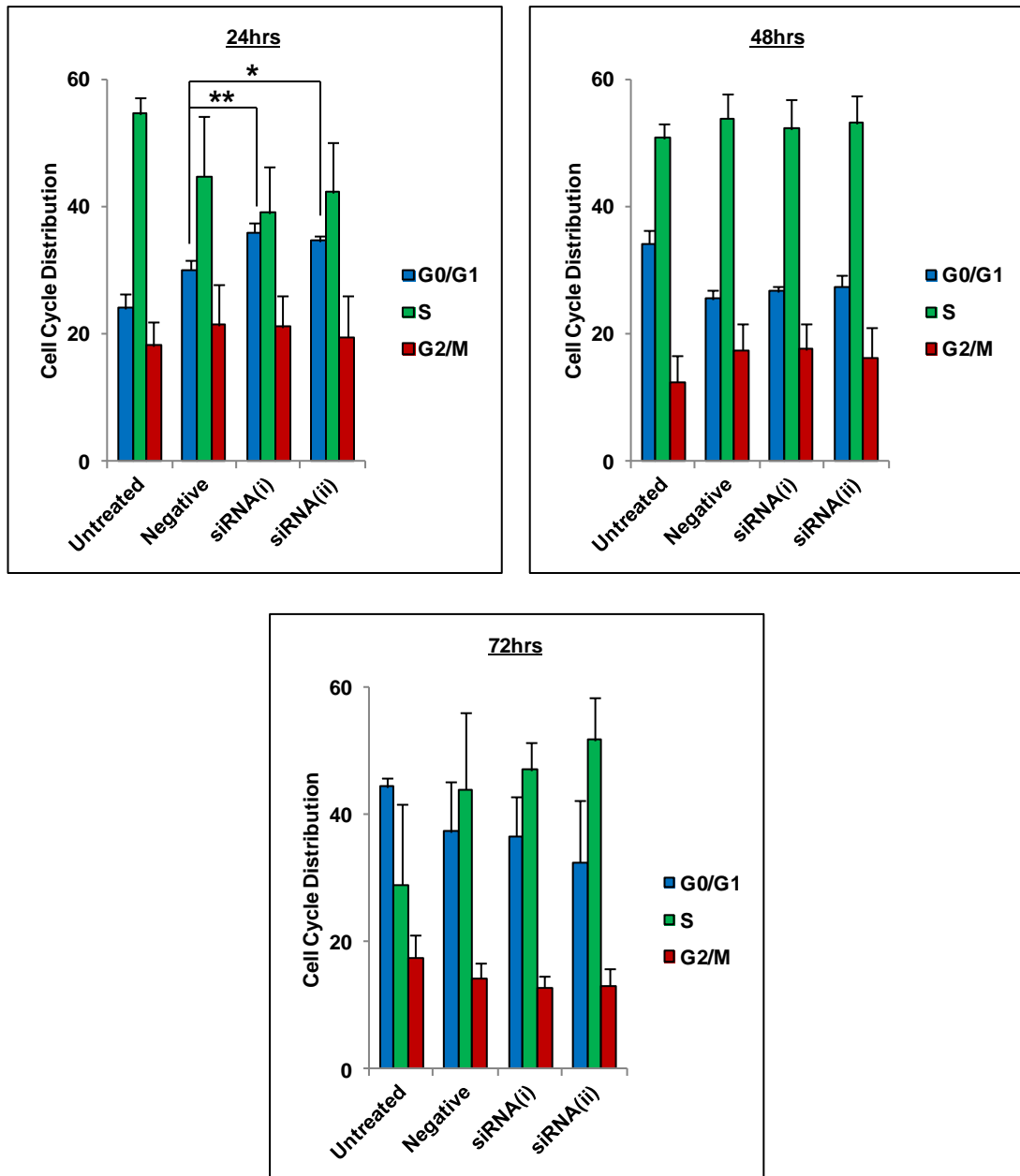
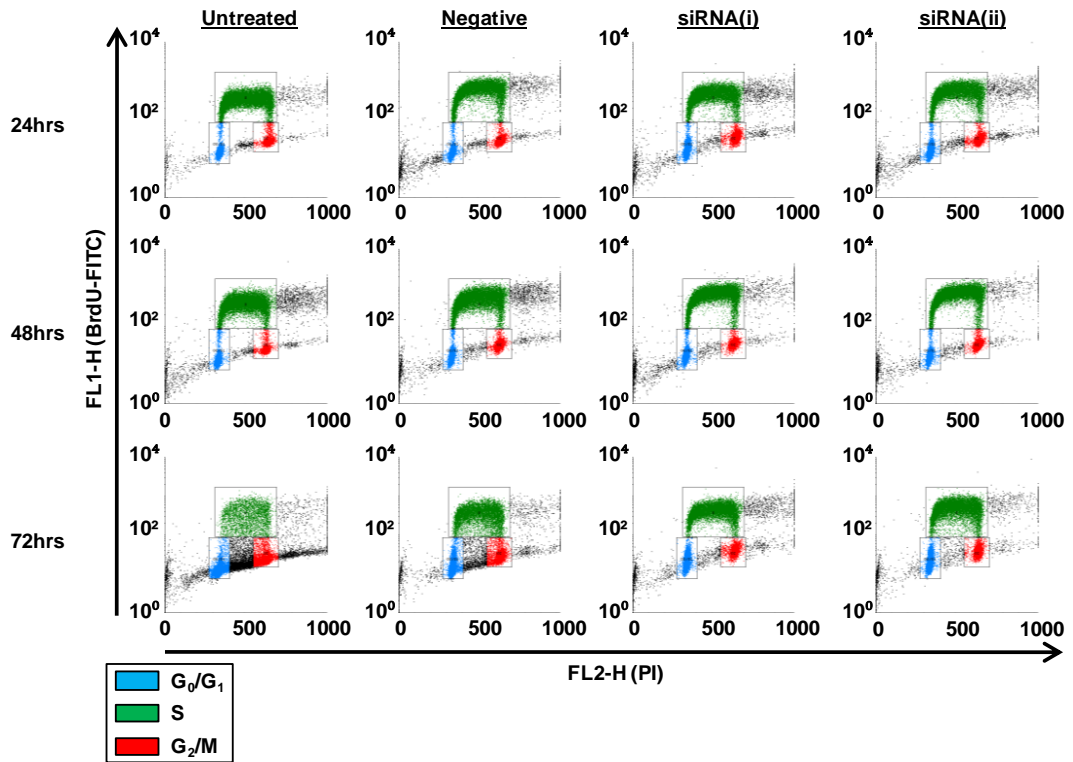


Figure 3a. Removal of p22phox expression significantly effects the cell cycle distribution of K562 cells for 24hr. Bar charts show the cell cycle distribution of K562 cells 24hr, 48hr and 72hr after p22phox siRNA transfection. At each time-point K562 cells were labelled with bromodeoxyuridine (BrdU) for 1hr, cells were fixed then incubated with an anti-BrdU antibody and stained with propidium iodide (PI) before being examined by flow cytometry to determine cell cycle distribution. Results are expressed as mean \pm SD and are representative of three independent experiments. Statistical analysis was carried out using the student t-test ($P < 0.01$ is marked with *, $P < 0.001$ is marked with **).



Sample	Stage	24hrs	48hrs	72hrs
Untreated	G ₀ /G ₁	24.1 ± 2.1	34.2 ± 2.2	44.3 ± 1.4
	S	54.6 ± 2.6	50.8 ± 2.1	28.9 ± 12.7
	G ₂ /M	18.2 ± 3.7	12.5 ± 4.1	17.5 ± 3.7
Negative	G ₀ /G ₁	30.2 ± 1.6	25.6 ± 1.5	37.3 ± 7.9
	S	44.8 ± 9.4	53.8 ± 3.9	43.9 ± 12.0
	G ₂ /M	21.4 ± 6.5	17.5 ± 4.2	14.3 ± 2.3
siRNA(i)	G ₀ /G ₁	36.0 ± 0.9	26.7 ± 0.8	36.6 ± 6.3
	S	39.0 ± 8.0	52.3 ± 4.5	46.9 ± 4.3
	G ₂ /M	21.2 ± 6.4	17.6 ± 3.9	12.9 ± 1.8
siRNA(ii)	G ₀ /G ₁	34.6 ± 1.4	27.4 ± 1.7	32.5 ± 9.7
	S	42.3 ± 7.2	53.1 ± 4.4	51.6 ± 6.7
	G ₂ /M	19.5 ± 5.0	16.2 ± 4.7	13.1 ± 2.6

Figure 3b. Removal of p22phox expression significantly effects the cell cycle distribution of K562 cells for 24hr. Dot plots are representative of the flow cytometric analysis of gated K562 cell populations used to determine cell cycle distribution following Bromodeoxyuridine (BrdU) incorporation and propidium iodide (PI) staining 24hr, 48hr and 72hr after p22phox siRNA transfection. Table contains the mean percentage of cells in each stage of the cell cycle 24hr, 48hr and 72hr after transfection as determined by BrdU incorporation and PI staining. Results are expressed as mean ± SD and are representative of three independent experiments.

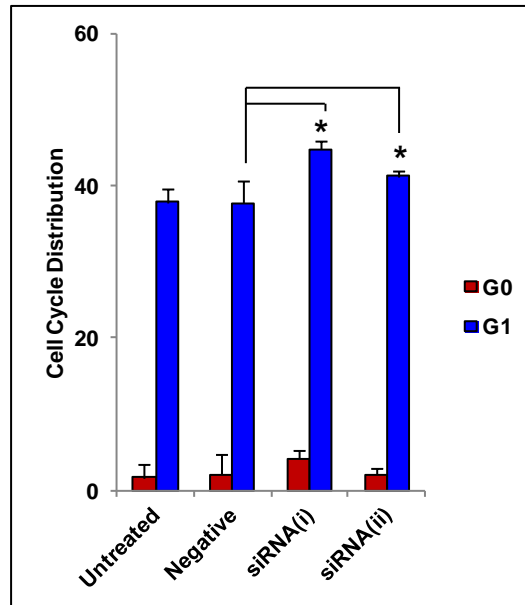


Figure 4a. Percentage of K562 cells in G1 increases following the protein knockdown of p22phox. Bar chart shows the mean percentage of K562 cells present in the G0 and G1 phases of the cell cycle 24hr after p22phox siRNA transfection. At 24hr K562 cells were fixed then incubated with an anti-Ki-67 antibody and stained with propidium iodide (PI) before being examined by flow cytometry to determine G0/G1 distribution. Cells were gated based on 2^o antibody only control for Ki-67. All values are expressed as mean \pm SD and are representative of three independent experiments. Statistical analysis was performed using Student's t-test (*P<0.05).

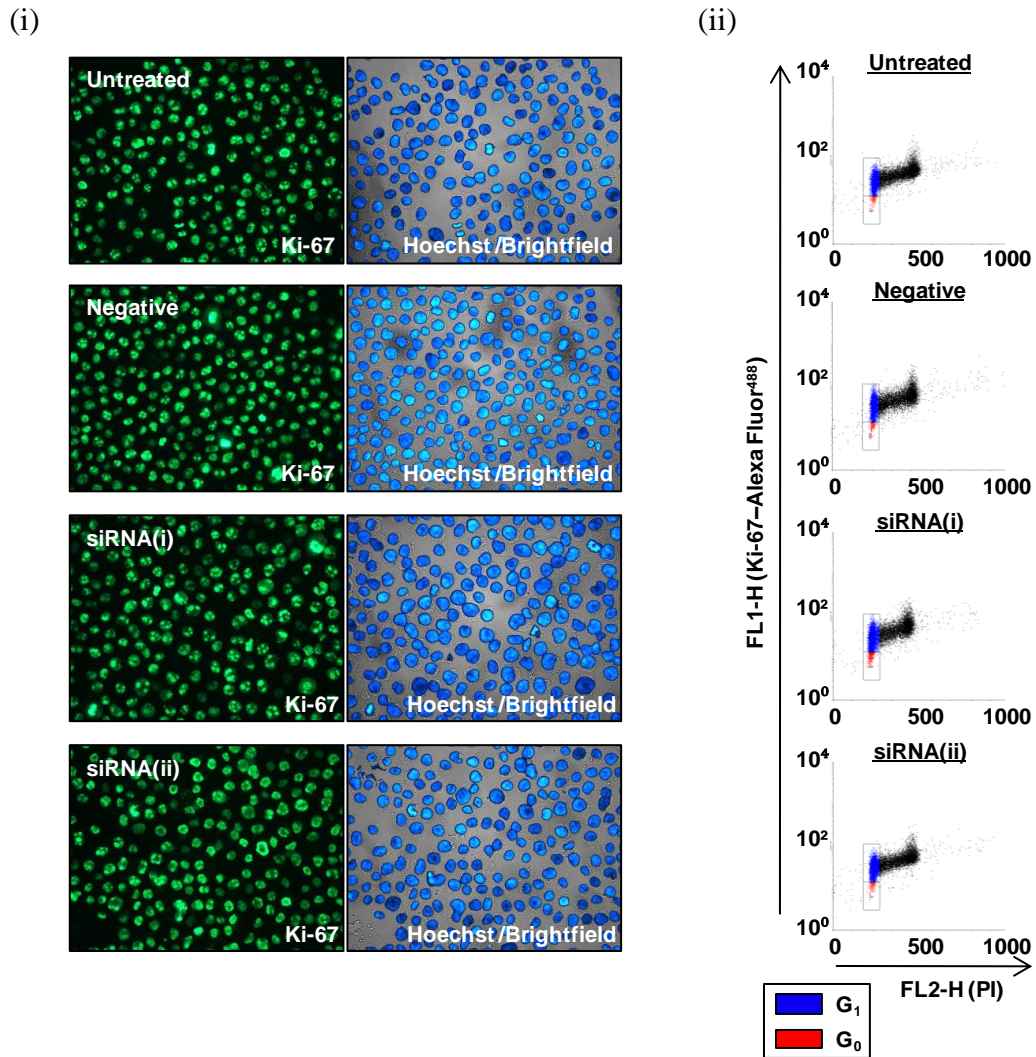


Figure 4b. Percentage of K562 cells in G1 increases following the protein knockdown of p22phox. (i) Immunofluorescence of Ki-67 protein in K562 cells 24hr after p22phox siRNA transfection. (ii) Dot plots are representative of the flow cytometric analysis of gated K562 cell populations used to determine G0/G1 distribution following Ki-67 protein detection and propidium iodide (PI) staining 24hr after p22phox siRNA transfection. Cells were gated based on 2^o antibody only control for Ki-67.

verifying that K562 cells remained proliferating following p22phox knockdown (Figure 4b(i)). Figure 4b(ii) demonstrates the flow cytometric analysis used to determine the distribution of cells between G0 and G1 phases 24hr after transfection with p22phox siRNA. The increase observed in G1 phase cells was comparable to the increase previously determined by BrdU incorporation and PI staining (Figure 3).

The protein levels of CDKs and Cyclins involved in G1 phase progression following targeted knockdown of p22phox

Cyclin dependent kinases (CDKs) are vital for the progression through all stages of the cell cycle and are tightly regulated by the binding of cyclins, proteins which are sequentially synthesized and destroyed in turn driving the cell cycle *via* CDK regulation (Massagué, 2004; Hochegger *et al.*, 2008; Malumbres and Barbacid, 2009). As demonstrated p22phox knockdown suggested an involvement for p22phox and Nox-derived ROS in progression through the G1 phase of the cell cycle. To understand how p22phox function may be involved in this process siRNA was once again used to target p22phox expression in K562 cells. Each transition of the cell cycle is regulated by a specific subset of CDKs and Cyclins, therefore the protein levels of the Cyclins and CDKs known to be active and important during the G1 phase were examined 24hr after transfection. Following this study it was identified that cells with p22phox protein knockdown demonstrated a significant reduction in the protein levels of Cyclin E and CDK2 when compared to the Negative transfected control cells (Figure 5). No significant change was observed in any of the other proteins examined. Interestingly the activity of CDK2, regulated by Cyclin E binding, is essential for G1/S transition (Hochegger *et al.*, 2008). This provided an explanation for the increased percentage of cells in G1 after p22phox knockdown.

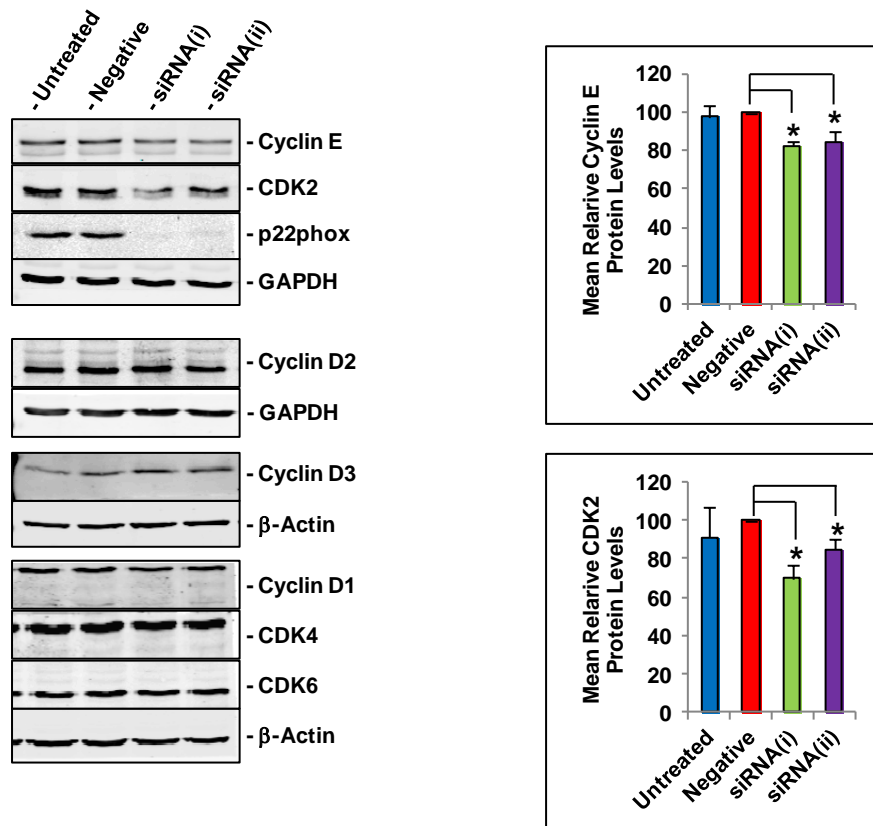


Figure 5. CDK2 and Cyclin E protein levels are significantly decreased following removal of p22phox expression. Western blot analysis of Cyclin E, CDK2, p22phox, Cyclin D2, Cyclin D3, Cyclin D1, CDK4 and CDK6 expression in K562 cells 24hr after p22phox siRNA transfection. GAPDH and β-Actin are shown as loading controls. Bar chart shows the mean relative Cyclin E and CDK2 protein levels of K562 cells 24hr after transfection determined by densitometry and expressed as a percentage of the Negative siRNA transfected control cells. Results are expressed as mean ± SD and are representative of three independent experiments. Statistical analysis was carried out using the student t-test (P<0.05 is marked with *).

An examination of cell cycle inhibitory protein levels following targeted knockdown of p22phox

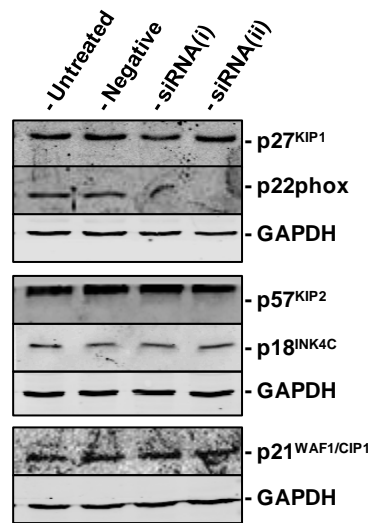
In addition to the CDKs and Cyclins which drive cell cycle progression there is an extensive array of inhibitory proteins which regulate the cell cycle at every stage, inhibiting progression if a problem arises. In normal cells the activity of CDKs is regulated by two families of inhibitors: the INK4 proteins which include p16^{INK4A}, p15^{INK4B}, p18^{INK4C} and p19^{INK4D/Arf} and the Cip/Kip family, consisting of p21^{Cip1/WAF1}, p27^{Kip1} and p57^{Kip2} (Malumbres and Barbacid, 2005). In addition to these proteins, the activity of retinoblastoma protein (pRb) and p53 also have key regulatory roles in the cell cycle (Vousden and Lu, 2002; Giacinti and Giordano, 2006). To continue this study focus was directed towards these inhibitory proteins with the aim of achieving a greater understanding of how p22phox function affects the cell cycle and provides a possible explanation for the reductions observed in Cyclin E and CDK2 protein levels following p22phox knockdown. Interestingly it is well established that K562 cells lack p53, p15^{INK4B}, p16^{INK4A} and p19^{INK4D/Arf} expression (Law *et al.*, 1993; Ogawa *et al.*, 1994; Otsuki *et al.*, 1995; Vonlanthen *et al.*, 1998; Delgado *et al.*, 2000). Indeed p53, p15^{INK4B}, p16^{INK4A} and p19^{INK4D/Arf} were not detected when examined by western blotting in the K562 cells used for these studies. 24hr after transfection with p22phox siRNA there was no significant change observed in the protein levels of any of the INK4 or Cip/Kip family members known to be expressed in K562 cells (Figure 6a). In addition to these proteins pRb was also examined. Interestingly pRb activity is heavily controlled by its phosphorylation state, being active when hypophosphorylated and inhibited if hyperphosphorylated (Giacinti and Giordano, 2006). Changes in K562 cell pRb phosphorylation following transfection with p22phox siRNA was determined by

examining the protein's electrophoretic mobility. As demonstrated in Figure 6b, pRb's electrophoretic mobility increased in p22phox knockdown cells 12hr after transfection which suggested a decrease in pRb phosphorylation and subsequent increase in pRb activity. Furthermore 24hr after transfection pRb protein levels were noted to significantly decrease following dephosphorylation. Active pRb prevents the progression of cells from G1 to S phase by inhibiting Cyclin E transcription, thereby preventing CDK2 activation (Harbour *et al.*, 1999). These results provided an explanation for the effects noted on Cyclin E and CDK2 while furthermore demonstrating the reason for the increased percentage of cells noted in the G1 phase following p22phox knockdown.

The effect of p22phox expression and function on cell viability

Homeostasis of the redox state is pivotal for the maintenance of normal cell function and survival in cells, as a result even small changes in ROS levels can significantly affect cell viability (D'Autréaux and Toledano, 2007; Circu and Aw, 2010). Removal of p22phox by siRNA was demonstrated in Chapter 3 to result in a marked reduction in ROS levels thereby effecting redox levels. To further this study a MTS assay was utilised to determine what effect p22phox function had on cell viability. An MTS assay is dependent on the enzyme activity found in metabolically active cells which directly relates to cell viability (Berridge *et al.*, 2005). Figure 7 demonstrates relative absorbance of cells treated with MTS 24hr, 48hr and 72hr after transfection. This study showed that cells transfected with p22phox siRNA had a significantly reduced viability when compared to Negative control cells 24hr and 48hr after transfection. As with previous experiments siRNA(i) transfection demonstrated the greatest effect. Furthermore, there was no significant effect on

(a)



(b)

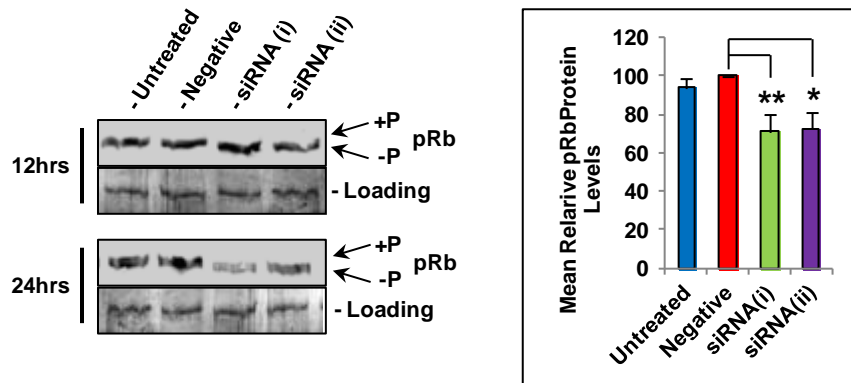


Figure 6. pRb becomes hypophosphorylated and decreases following knockdown of p22phox expression. (a) Western blot analysis of p27^{KIP1}, p22^{phox}, p57^{KIP2}, p18^{INK4C} and p21^{Cip1/WAF1} expression in K562 cells 24hr after p22phox siRNA transfection. GAPDH is shown as a loading control. (b) Western blot analysis of pRb expression in K562 cells 12hr and 24hr after p22phox siRNA transfection. Ponceau is shown as a loading control. Bar chart shows the mean relative pRb protein levels of K562 cells 24hr after transfection determined by densitometry and expressed as a percentage of the Negative siRNA transfected control cells. Results are expressed as mean \pm SD and are representative of three independent experiments. Statistical analysis was carried out using the student t-test (P<0.05 is marked with *, P<0.01 is marked with **).

viability by 72hr in cells transfected with siRNA(i) or siRNA(ii). Regardless the noted effects on viability at 24hr and 48hr still suggested that p22phox and Nox-derived ROS have a significant and important role on K562 cell viability.

Analysis of apoptotic cell death following targeted knockdown of p22phox

Due to the MTS assay results and the known link between ROS signalling and increased cell survival focus was placed on establishing if the decrease noted in K562 cell viability and ROS levels following p22phox knockdown was accompanied by an increase in apoptotic cell death. To determine the percentage of apoptosis and death 24hr, 48hr and 72hr after p22phox siRNA transfection K562 cells were stained with PI/Annexin V and analysed by flow cytometry. Interestingly, 24hr after transfection removal of p22phox expression produced a small but significant increase in the percentage of apoptotic and dead cells when compared to cells transfected with Negative control siRNA (Figure 8a). This increase was noted in both the siRNA(i) and siRNA(ii) transfected samples 24hr after transfection. However, 48hr after transfection only the siRNA(i) transfected cells demonstrated a significant increase in apoptotic cell death and by 72hr no effect was noted. Percentage of viable cells (lower left quadrant), apoptotic cells (lower right quadrant), necrotic cells (upper left quadrant) and cell death by apoptosis (upper right quadrant) following p22phox siRNA knockdown are demonstrated and quantified in Figure 9b.

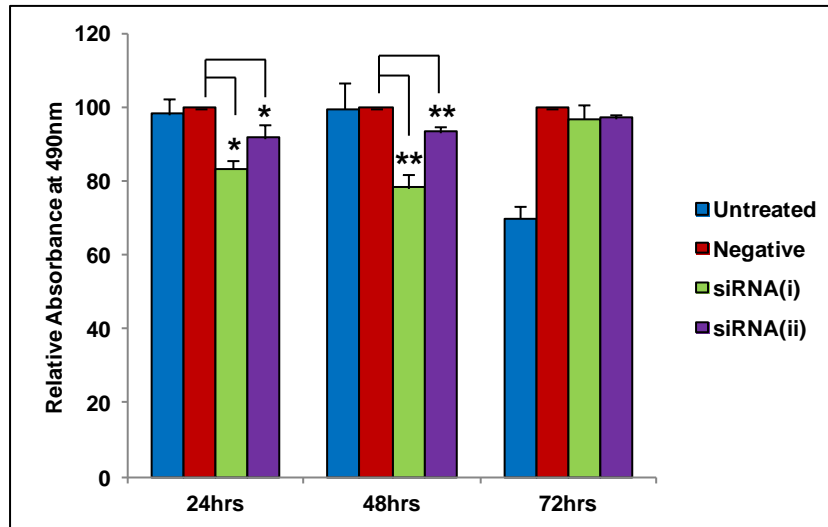
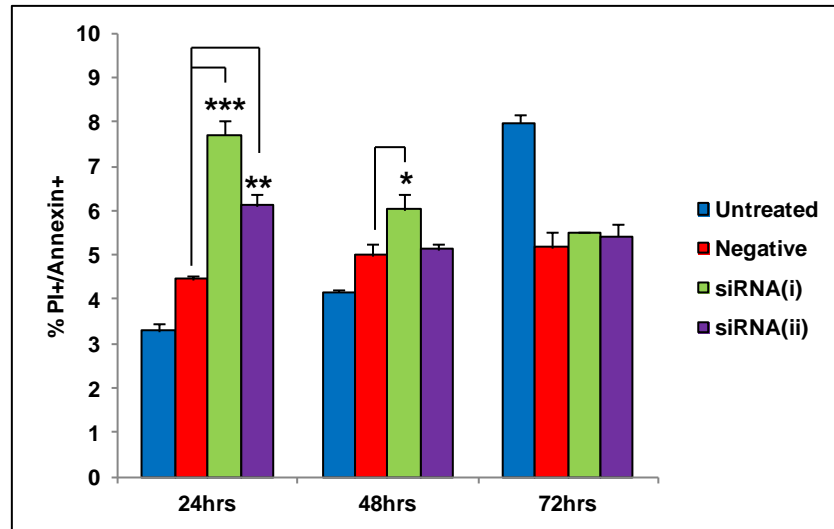


Figure 7. Removal of p22phox significantly reduces cell viability up to 48hr. Bar chart shows the mean Absorbance at 490nm of K562 cells treated with MTS 24hr, 48hr and 72hr after siRNA transfection. Results are expressed as a percentage of the Negative siRNA control. Results are expressed as mean \pm SD and are representative of four independent experiments. Statistical analysis was carried out using the student t-test ($P < 0.05$ is marked with *, $P < 0.005$ is marked with **).

(a)



(b)

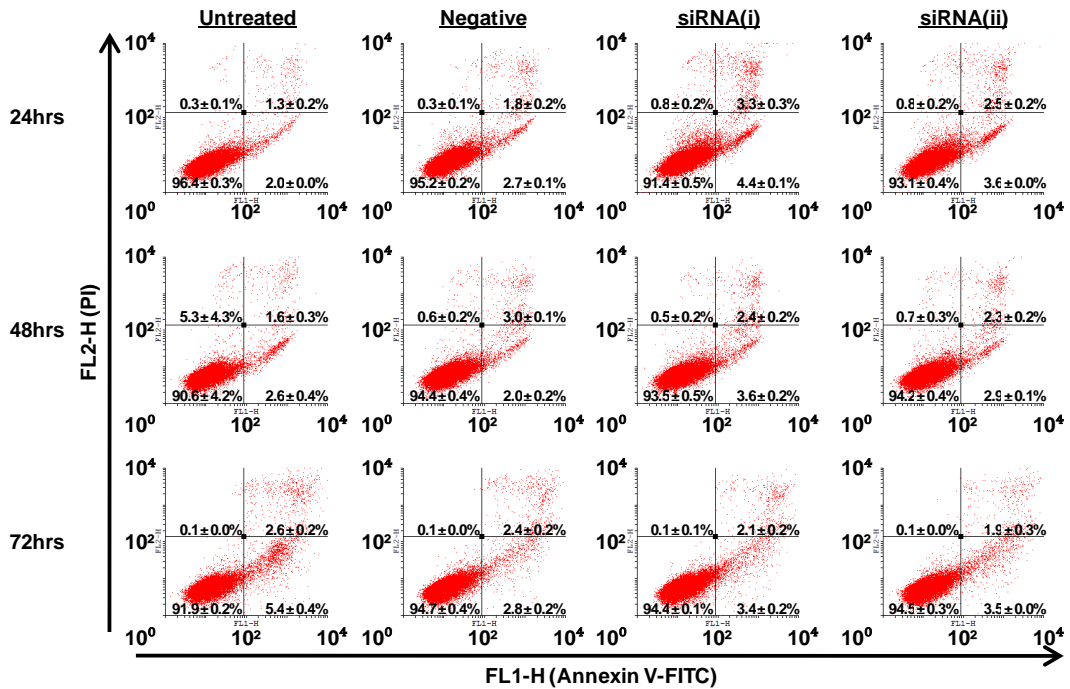


Figure 8. Removal of p22phox expression produces a small but significant increase in apoptotic cell death. (a) Bar chart demonstrates the combined percentages of K562 cells staining positive for Annexin V, propidium iodide (PI) or both 24hr, 48hr and 72hr after siRNA transfection. At each time-point K562 cells were incubated with Annexin V-FITC and then stained with PI immediately before flow cytometric analysis. (b) Dot plots are representative of the flow cytometric analysis of K562 cells following Annexin V and PI staining. Quadrants were positioned based on positive apoptotic control and demonstrate percentage of viable cells (lower left quadrant), apoptotic cells (lower right quadrant), necrotic cells (upper left quadrant) and dead cells by apoptosis (upper right quadrant). All results are expressed as mean \pm SD and are representative of two independent experiments. Statistical analysis was carried out using the student t-test (P < 0.05 is marked with *, P < 0.01 is marked with **, P < 0.005 is marked with ***).

Analysis of autophagic cell death following targeted knockdown of p22phox

Following examination of apoptosis attention was then drawn to autophagy as a mechanism of survival and cell death in CML. Indeed stress to CML cell models through Bcr-Abl inhibition or even treatment with other chemotherapeutics is known to induce autophagy (Crowley *et al.*, 2010). Furthermore ROS signalling and Nox activity have been demonstrated to be integral in autophagy regulation (Scherz-Shouval and Elazar 2011). Therefore it needed to be determined if the noted decrease in ROS levels following p22phox knockdown in K562 cells produced an effect on autophagy levels. To determine if autophagy was affected in K562 cells the autophagic protein markers LC3B and Beclin were examined following p22phox knockdown. Figure 10 demonstrates that no significant change in either LC3B or Beclin was noted 24hr or 48hr after transfection with p22phox siRNA. These results suggested that removal of p22phox expression alone had no effect on autophagy in K562 cells.

Analysis of p22phox mediated ROS levels and their effect on cell survival signalling

ROS are known to act as secondary signalling molecules enhancing cell survival largely through inhibition of phosphatase activity which can negatively regulate survival signalling through dephosphorylation (Trachootham *et al.*, 2008; Groeger *et al.*, 2009; Corcoran and Cotter, 2013). Bcr-Abl signalling increases cell survival mainly through the activation of three major survival pathways, the JAK/STAT, Raf/MEK/ERK and PI3K/AKT pathways (Steelman *et al.*, 2004), all of which can be affected by redox signalling (Sattler *et al.*, 1999; Torres, 2003; Naughton *et al.*, 2009). Work in Chapter 3 demonstrated that removal of p22phox

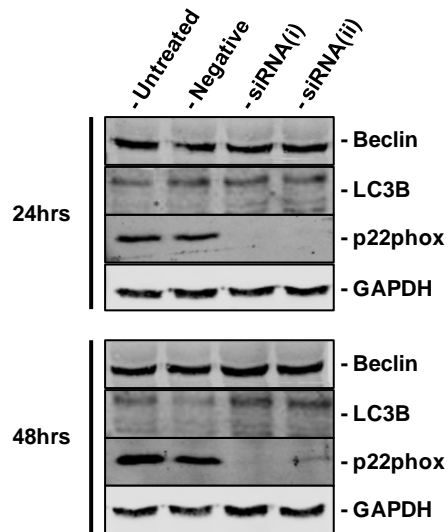


Figure 9. Changes to p22phox expression levels has no effect on autophagy in K562 cells. Western blot analysis of Beclin, LC3B and p22phox expression in K562 cells 24hr and 48hr after p22phox siRNA transfection. GAPDH is shown as a loading control.

expression resulted in a marked decrease in intracellular ROS levels for up to 48hr after transfection. As a result it was questioned if p22phox knockdown would have any effect on K562 cell survival signalling due to decreased ROS levels. To determine this phosphorylation of key proteins in these three survival pathways were examined 24hr and 48hr after transfection (Figure 9). Interestingly although Figure 8 demonstrated an increase in apoptotic cell death and there is a known connection between redox signalling and these pathways, no consistent or significant change was demonstrated in the phosphorylation status of any of the proteins examined. These results suggested that the decrease in ROS levels may not have been large enough to cause a significant effect.

The therapeutic potential of p22phox knockdown combined with Bcr-Abl inhibition.

As discussed small-molecule tyrosine kinase inhibitors (TKIs), such as Imatinib, which target Bcr-Abl activity have fundamentally improved CML prognosis. Unfortunately due to the development of drug resistance and the persistence of residual disease alternative treatment methods still need to be developed to better treat CML. One strategy which is gaining more and more prowess is pharmacological silencing of Bcr-Abl combined with the simultaneous inhibition of other crucial targets (O'Hare *et al.*, 2012). Studies in this chapter have demonstrated the importance of p22phox function and ROS regulation in the proliferation of K562 cells. Additionally removal of p22phox expression significantly decreased K562 cell viability and to a lesser extent increased apoptotic cell death. These results suggested that p22phox expression may be important for disease phenotype in K562 cells and identified it as a potential target for CML

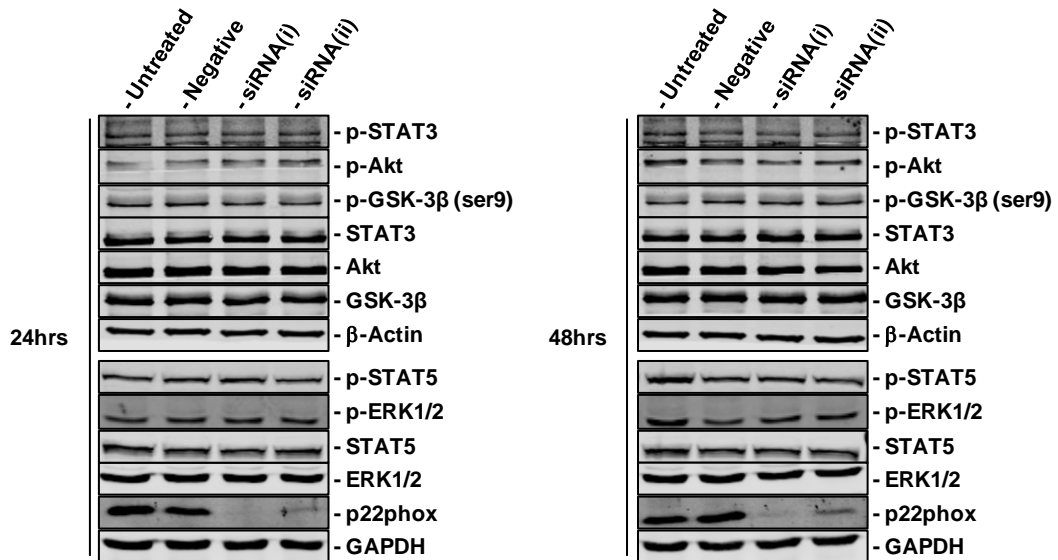
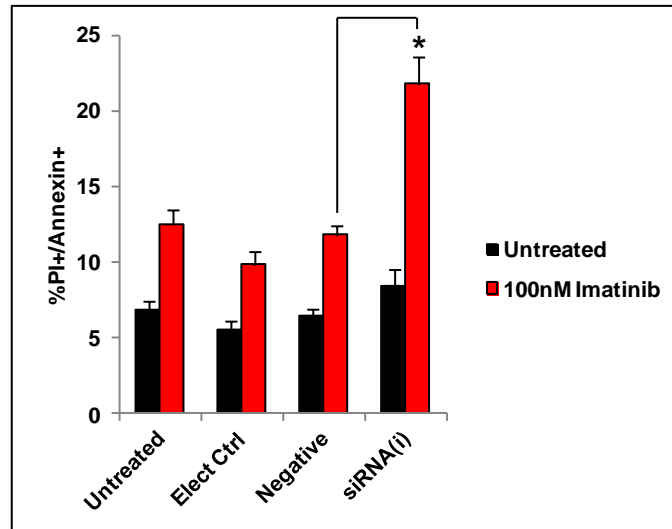


Figure 10. Removal of p22phox expression has no significant effect on the phosphorylation status of important cell survival pathways. Western blot analysis of STAT3, Akt, GSK-3 β , STAT5, ERK1/2 and p22phox expression and/or phosphorylation status (p-) in K562 cells 24hr and 48hr after p22phox siRNA transfection. GAPDH and β -Actin are shown as loading controls.

therapy. However it is also evident from this work that p22phox inhibition alone does not demonstrate a significant enough effect to suggest it as sole treatment for CML. As a result focus was directed towards the potential of targeting p22phox and therefore Nox-activity in combination with Bcr-Abl inhibition. To examine this K562 cells were transfected with p22phox siRNA(i) and 24hr later were treated with Imatinib for 48hr before the level of apoptotic cell death was determined using Annexin V/PI staining. Treatment of p22phox knockdown cells with Imatinib resulted in a significant two-fold increase in apoptotic cell death when compared to Negative transfected cells treated with Imatinib (Figure 11a). Percentage of viable cells (lower left quadrant), apoptotic cells (lower right quadrant), necrotic cells (upper left quadrant) and cell death by apoptosis (upper right quadrant) following p22phox siRNA knockdown and Imatinib treatment are demonstrated and quantified in Figure 11b. This work demonstrated the therapeutic potential of targeting Nox activity in combination with Bcr-Abl inhibition to treat CML.

(a)



(b)

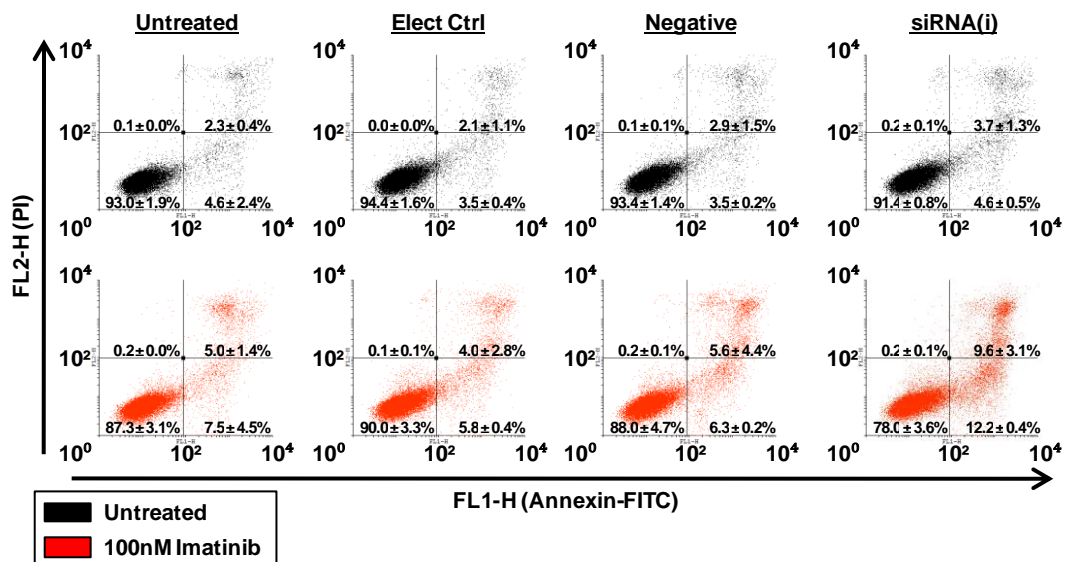


Figure 11. Removal of p22phox expression in combination with Imatinib treatment synergistically increases cell death. 24hr after K562 cells were transfected with p22phox siRNA 100nM of Imatinib was added for 48hr. Following treatment K562 cells were incubated with Annexin V-FITC and then stained with Propidium Iodide (PI) immediately before flow cytometric analysis. (a) Bar chart demonstrates the combined percentages of K562 cells staining positive for Annexin V, propidium iodide (PI) or both. (b) Dot plots are representative of the flow cytometric analysis of K562 cells following Annexin V and PI staining. Quadrants were positioned based on positive apoptotic control and demonstrate percentage of viable cells (lower left quadrant), apoptotic cells (lower right quadrant), necrotic cells (upper left quadrant) and dead cells by apoptosis (upper right quadrant). All results are expressed as mean \pm SD and are representative of three independent experiments. Statistical analysis was carried out using the student t-test ($P < 0.05$ is marked with *).

Discussion

Bcr-Abl expression is the primary cause of pathogenesis in CML and as a result it has been the main target for therapeutic development (Deininger *et al.*, 2005). The development of drugs like Imatinib has greatly improved CML prognosis but unfortunately residual disease persists with a high probability of drug resistance developing (Druker *et al.*, 2006). These obstacles have increased the need to identify other essential components which are involved in the pathogenesis of CML, which will provide a better understanding of the disease facilitating the development of alternative treatment strategies. In Chapter 3 a link was established between Bcr-Abl signalling and Nox-derived ROS through regulation of the protein levels of p22phox, a membrane-bound protein essential for full activity of Nox proteins 1, 2, 3 and 4 (Ambasta *et al.*, 2004; Ueno *et al.*, 2005). Nox protein activity has been linked to a host of cellular activities, from cell survival to proliferation, activities which drive disease phenotype and pathogenesis in leukaemia (Kim *et al.*, 2005; Naughton *et al.*, 2009; Hole *et al.*, 2011; Reddy *et al.*, 2011). As a result of the possible significance of Nox-derived ROS in disease, the aim of this study was directed towards the role p22phox expression may play in CML. In these studies K562 cells, a CML cell line with constitutive Bcr-Abl expression, were used as a model in conjunction with siRNA to study the effects of p22phox expression on disease phenotype. In each case siRNA transfection was used to remove p22phox expression to determine if p22phox regulation of Nox-derived ROS had any effect on the cellular processes examined.

One particular cellular process p22phox function was linked to in Chapter 3 was proliferation. Interestingly numerous studies have demonstrated a role for Nox-derived ROS in cell proliferation with some studies drawing a direct link to an importance in p22phox expression (Jeong *et al.*, 2004; Sturrock *et al.*, 2006; Petry *et*

al., 2006; Reddy *et al.*, 2011). Following on from the preliminary work in Chapter 3, a role for p22phox in proliferation was verified using CFSE, which provided an accurate and detailed representation of the affects of p22phox knockdown on K562 cell proliferation (Figure 1 and Figure 2). It is of interest to note that the effect p22phox knockdown had on cell proliferation ceased prior to 48hr (Figure 1), therefore the reduction noted in proliferation index at 72hr (Figure 2b) was likely a result of decreased proliferation prior to 48hr. Furthermore, although it was demonstrated that p22phox protein levels remain reduced up to 72hr after transfection (Landry *et al.*, 2012 Figure 4a and 4e) the corresponding ROS decrease is no longer observed past the 48hr time-point (Chapter 3, Figure S6). This suggests that the rate of proliferation decreased for the same duration of time as ROS levels were observed to be decreased. Although initially used to examine cell viability in this study, MTS conversion assays are also frequently used to assess cell proliferation (Berridge *et al.*, 2005). Indeed, MTS conversion following p22phox knockdown demonstrated a reduction comparable to that of the decrease observed in proliferation following assessment of CFSE fluorescence (Figure 7). A significant decrease in MTS conversion was not observed past the 48hr time-point which corresponded further with both the CFSE and ROS results. These data coupled with the cited role for Nox-derived ROS in cell proliferation established the importance of p22phox-mediated ROS production on K562 cell and as a result CML proliferation.

Downstream signalling of Bcr-Abl drives CML cell proliferation by positively regulating cell cycle progression (Steelman *et al.*, 2004). Expression of p22phox was demonstrated to affect proliferation therefore determining how the cell cycle status of K562 cells was affected was the next focus. Use of a BrdU incorporation followed by subsequent examination of the Ki-67 proliferation marker

established there was a small but significant increase in the percentage of cells in the G0/G1 stage of the cell cycle 24hr after siRNA transfection (Figure 3 and Figure 4). Furthermore the increase noted in G0/G1 was mostly due to an increase in the percentage of cells in G1 rather than G0 (Figure 4a). For both the BrdU and Ki-67 assays the increase of cells in G1 at 24hr was too minor to suggest a halt in the cell cycle. The high percentage of cells present in S and G2/M phases was indicative that the cell cycle was still progressing therefore a slowdown or delay through this portion of the cell cycle may be a more likely explanation for the significant increase in G1 cells. Interestingly, a delay in G1 phase progression due to the inhibition of Nox activity has been observed previously. A study by Venkatachalam *et al.* (2008) demonstrated that G1 phase progression in fibroblasts was significantly retarded following inhibition of Nox proteins by DPI treatment. The work by Venkatachalam *et al.* (2008) provided validation that G1 to S phase transition can be significantly retarded following Nox inhibition which was achieved here through the removal of p22phox expression.

Progression through each of the four cell cycle stages is dependent on the activation of particular CDKs through the binding of relevant cyclin proteins (Hochegger *et al.*, 2008; Malumbres and Barbacid, 2009). Concentrations of cyclin subunits oscillate, being sequentially synthesized and destroyed at particular points in the cell cycle in turn driving progression *via* CDK regulation (Hochegger *et al.*, 2008; Malumbres and Barbacid, 2009). Each phase of the cell cycle is regulated by a specific CDK bound to the appropriate cyclin. Expression of Cyclin E followed by its binding and activation of CDK2 is pivotal in the progression of cells from G1 into S phase (Massagué, 2004; Hochegger *et al.*, 2008). Rather significantly reductions in the protein levels of both Cyclin E and CDK2 were demonstrated following p22phox

knockdown (Figure 5). Interestingly there is a direct correlation between the level of Cyclin E expression and the length of time it takes a cell to transition through G1/S (Ohtsubo *et al.*, 1995). Here Cyclin E levels were demonstrated to be reduced rather than depleted. A reduction in the presence Cyclin E will therefore decrease the level of active CDK2 present in the cell providing a possible explanation for the slowdown in G1 transition which was demonstrated following p22phox knockdown.

Cyclin E expression is dependent on transcription by the E2F transcription factors which are negatively regulated by active retinoblastoma protein (pRb) (Giacinti and Giordano, 2006). In actively proliferating cancer cells CDKs hyperphosphorylate and deactivate pRb preventing its inhibition of E2F transcription factors thereby ensuring transition of cells out of G1 and into S phase (Giacinti and Giordano, 2006; Malumbres and Barbacid, 2009). Here it was demonstrated that pRb becomes hypophosphorylated 12hr after p22phox siRNA transfection and protein levels are subsequently decreased by 24hr (Figure 6). As stated hypophosphorylation activates pRb, this suggested that the decreases in Cyclin E protein levels could be a result of E2F transcription factor inhibition. Furthermore the reduction of pRb protein levels 24hr after transfection was also interesting. As previously discussed removal of p22phox expression produced a significant increase in the percentage of cells in G1 phase however this increase was only observed at the 24hr time-point. Contradictory to this ROS levels remain significantly reduced up to 48hr after transfection which suggested that this effect on the cell cycle was not directly related to the ROS reduction. However, the noted decrease in pRb protein levels at the 24hr time-point provided a possible explanation for there being no effect on the cell cycle distribution following 24hr, as any decrease in pRb protein levels, regardless of phosphorylation status, would still reduce its cell cycle inhibitory affects. It is

unknown what may have produced the decrease in pRb protein levels however its degradation is linked to the activity of cell cycle inhibitory proteins p21 and p27 (Broude *et al.*, 2007). However, neither of these proteins demonstrated a significant change following removal of p22phox expression.

pRb activity is known to be positively regulated by phosphatase activity, with both the Protein Phosphatase 1 (PP1) and Protein Phosphatase 2A (PP2A) groups of serine/threonine phosphatases implicated in its dephosphorylation (Kolupaeva and Janssens, 2013). PP1 α has been identified as the major pRb cell cycle related phosphatase, capable of inducing cell cycle arrest in G1 by a pRb-dependent manner (Berndt *et al.*, 1997). What is of further interest is that the activity of both PP1 and PP2A is negatively and reversibly regulated by ROS-induced oxidative inactivation (Rao and Clayton, 2002; O’Loughlen *et al.*, 2003). Furthermore work by Naughton *et al.* (2009) has implemented Nox-derived ROS in the inhibition of PP1 α activity downstream of Bcr-Abl signalling. In light of this information it was purposed that the reductions in ROS levels following p22phox knockdown could potentially increase phosphatase activity due to reduced inhibition by ROS-induced oxidation. This increase in phosphatase activity has the potential to hypophosphorylate pRb, resulting in its activation and the inhibition of the E2F transcription factors early in G1 phase which will reduce Cyclin E expression and thereby slow the transition from G1 to S phase. Taken together this provides a possible explanation for the effect noted on cell proliferation following removal of p22phox expression demonstrating the importance of Nox-derived ROS in cell proliferation.

As previously discussed removal of p22phox expression caused a significant decrease in cell viability (Figure 7) which was concurrent with ROS reductions

suggesting the importance of p22phox regulated ROS in cell viability. Further examination of K562 cells following p22phox knockdown demonstrated a small but significant increase in cell death and apoptosis which also remained increased up to and including the 48hr time-point (Figure 8). Further evaluation of cellular survival mechanisms demonstrated that removal of p22phox expression had no significant effect on K562 cell autophagy levels (Figure 9). Furthermore phosphorylation of key proteins involved in the JAK/STAT, Raf/MEK/ERK and PI3K/AKT pathways demonstrated no significant change following removal of p22phox regulated ROS (Figure 10). Even small changes in the level of ROS can alter the redox state of cells thereby affecting many cellular processes, potentially decreasing cell viability (D'Autréaux and Toledano, 2007; Circu and Aw, 2010). In addition, ROS are known to act as secondary signalling molecules with the ability to enhance cell survival (Rhee *et al.*, 2005a; Rhee *et al.*, 2005b; Trachootham *et al.*, 2008; Groeger *et al.*, 2009; Toledano *et al.*, 2010; Bae *et al.*, 2011). As a result it was believed that any effect on ROS levels in K562 cells would significantly affect overall cell survival and viability.

Removal of p22phox expression did reduce cell viability however only a minor increase was observed in the level of cell death and apoptosis. It is important to note that examination of viability was obtained using an MTS assay which is dependent on enzyme activity found in metabolically active cells (Berridge *et al.*, 2005) and as such this assay does not directly correlate with cell death. Levels of cell death are heavily affected by cell survival signalling yet no significant changes were noted in the pathways examined following p22phox knockdown. Interestingly reductions in pRb proteins levels have been linked with increased cell death and apoptosis, which provides a possible explanation for the small but significant

increase noted following p22phox knockdown (Classon and Harlow, 2002; Harbour *et al.*, 2000; Broude *et al.*, 2007). Furthermore, Nox protein activity and ROS signalling is known to be involved in autophagy, however mitochondrial derived ROS are believed to be the more important regulatory source of ROS in this process (Scherz-Shouval and Elazar, 2011). This may explain why no significant effect was noted on autophagy following p22phox knockdown.

Previous studies have demonstrated the importance of redox signalling in the JAK/STAT, Raf/MEK/ERK and PI3K/AKT pathways (Sattler *et al.*, 1999; Torres 2003; Naughton *et al.*, 2009) therefore it was unexpected that there was no significant effect on these pathways following p22phox knockdown. Work by Naughton *et al.* (2009) demonstrated the relevance of Nox-derived ROS in PI3K/AKT pathway activity downstream of Bcr-Abl in CML. As a result it was believe that the reduction in ROS levels noted following p22phox knockdown would have significantly affected activation of this pathway. As there was no significant change in this pathway it may suggest the reductions in ROS levels from p22phox knockdown were not significant enough to cause an effect. Work in Chapter 3 demonstrated that the only expressed Nox proteins dependent on p22phox function in K562 cells are Nox2 and Nox4 (Landry *et al.*, 2013, Figure 3a). In the study by Naughton *et al.* (2009) Nox4 was identified as an important source of ROS downstream of Bcr-Abl. Direct knockdown of Nox4 expression in this study produced a far more significant decrease in ROS levels when compared to the decrease noted in this study following p22phox knockdown. Interestingly, Nox4 demonstrates a reduced basal activity independent of p22phox expression (Ambasta *et al.*, 2004) which may suggest why Nox4 knockdown has a greater effect on ROS levels. Furthermore this basal activity may explain why no significant, consistent

reduction was noted in PI3K/AKT pathway signalling in K562 cells following p22phox knockdown.

Studies in this chapter demonstrated the importance of p22phox-mediated ROS production in the proliferation and viability of K562 cells. These studies in K562 cells suggested that p22phox expression may be important for CML pathogenesis however it was evident that p22phox inhibition alone does not demonstrate a significant enough effect to suggest it as sole treatment for CML. Combining p22phox removal with Imatinib treatment significantly increased the potential of p22phox targeting as a possible therapy for CML treatment (Figure 11). As discussed small-molecule tyrosine kinase inhibitors (TKIs), such as Imatinib, which target Bcr-Abl activity have fundamentally improved CML prognosis yet due to the development of drug resistance and the persistence of residual disease alternative treatment methods still need to be developed to better treat CML. It was concluded from this work that p22phox removal in a way weakens cells, priming Bcr-Abl inhibition to produce a substantially greater effect on cell death. These studies demonstrated the clinical potential of targeting p22phox and therefore inhibiting Nox proteins in combination with Bcr-Abl inhibition.

Chapter 5

Examining the therapeutic potential of Nox Inhibition

Abstract

Since the development of Bcr-Abl specific tyrosine kinase inhibitors (TKIs) there has been a substantial improvement in the clinical treatment of Chronic Myeloid Leukaemia (CML). Unfortunately, residual disease and the development of TKI resistance has become an ever growing concern, resulting in the need for a greater understanding of the disease in order to develop new treatment strategies. Previous work identified p22phox function to have a significant involvement in cellular processes key for CML pathogenesis while identifying the potential of combined Nox and Bcr-Abl inhibition in the improvement of CML treatment. Continuing on from this work pharmacological silencing of Nox activity was examined in combination with Bcr-Abl TKIs. These combinations were synergistic, producing substantial increases in cell death through augmentation of apoptosis, demonstrating a significant improvement on TKI treatment alone. It was concluded from this work that Nox protein inhibition may prime cells for Bcr-Abl inhibition thereby producing a substantially greater effect on cell death. This demonstrated the clinical potential of targeting Nox proteins in combination with Bcr-Abl inhibition, however it was evident that better, more specific inhibitors of Nox protein activity would be required if such a treatment was ever to be implemented.

Introduction

Reactive Oxygen Species (ROS) were once believed to be harmful by-products of cellular activity but now ROS and particularly hydrogen peroxide (H₂O₂) are generally recognised as important intracellular signalling molecules (Rhee *et al.*, 2005a; Rhee *et al.*, 2005b; Toledano *et al.*, 2010; Bae *et al.*, 2011). ROS are produced in eukaryotic cells by several sources, however the mitochondrial electron transport chain and NADPH Oxidases (Nox) are the two major sources implicated in cancer. The Nox proteins primary function is to produce ROS. Therefore unlike mitochondrial electron transport chain leakage, Nox-derived ROS production is not a by-product of its normal function. There are seven members of the Nox family and they are Nox1, Nox2, Nox3, Nox4, Nox5, Duox1 and Duox2. Interestingly, Nox proteins and their regulators have been implicated in most of the common cancer types which includes but are not limited to cancers of the prostate (Brar *et al.*, 2003; Lim *et al.*, 2005; Kumar *et al.*, 2008; Huang *et al.*, 2012a), colon (Fukuyama *et al.*, 2005; Bauer *et al.*, 2012), breast and ovaries (Desouki *et al.*, 2005; Choi *et al.*, 2010), bladder (Shimada *et al.*, 2009; Shimada *et al.*, 2011; Huang *et al.*, 2012b), pancreas (Vaquero *et al.*, 2004) and thyroid gland (Weyemi *et al.*, 2010) as well as melanoma (Brar *et al.*, 2002; Yamaura *et al.*, 2009), lymphoma (Lan *et al.*, 2007; Hoffmann *et al.*, 2010) and of particular interest to these studies leukaemia (Kamiguti *et al.*, 2005; Prata *et al.*, 2008; Naughton *et al.*, 2009). In these cases Nox proteins have been demonstrated to enhance oncogenesis through induction of increased genomic instability, angiogenesis, invasion, metastasis, cell growth and survival. This highlights the importance of Nox proteins and ROS generation in the development and maintenance of many cancers.

The activity of Nox proteins is not limited to oncogenesis, in fact Nox-derived ROS have demonstrated involvement in many other diseases such as Ischemic stroke, Alzheimer's Disease, Parkinson's Disease, Crohn's disease, several cardiovascular diseases and diabetes to name a few (Bedard and Krause, 2007). Interestingly, several clinical studies have examined the potential of antioxidant therapies as a way of inhibiting the effects of increased ROS levels generated from Nox activity (Vivekananthan *et al.*, 2003; Kris-Etherton *et al.*, 2004; Bjelakovic *et al.*, 2007; Altenhöfer *et al.*, 2012). Unfortunately these studies demonstrated minimal success with some treatments even being deleterious. It is believed that a more effective method would be to specifically target Nox proteins to prevent ROS generation which has resulted in extensive interest in the development and characterisation of novel Nox inhibitors as therapeutics (Altenhöfer *et al.*, 2012; Cifuentes-Pagano *et al.*, 2012; Krause *et al.*, 2012).

Previous work investigated elevated levels of intracellular-ROS in CML, establishing a link between Bcr-Abl signalling and the generation of Nox-derived ROS through the regulation of p22phox protein levels (Landry *et al.* 2013). p22phox is a membrane-bound protein essential for the full activity of Nox proteins 1, 2, 3 and 4 (Ambasta *et al.*, 2004; Ueno *et al.*, 2005). Additional studies established an involvement for p22phox in cell proliferation and viability suggesting an importance for this protein in CML pathogenesis. This work identified Nox proteins as a potential therapeutic target which was further emphasised after removal of p22phox expression *via* siRNA was combined with Imatinib treatment, producing a synergistic two-fold increase in cell death (Chapter 4, Figure 11). Small-molecule tyrosine kinase inhibitors (TKIs), such as Imatinib, which target Bcr-Abl activity have fundamentally improved CML prognosis yet due to the development of drug

resistance and the persistence of residual disease alternative treatment methods still need to be developed to better treat this disease. A large amount of research is now focused on the targeting of Bcr-Abl along with simultaneous inhibition of other crucial targets (O'Hare *et al.*, 2012).

Work in previous chapters has demonstrated the potential of Nox proteins as one possible target for combined CML treatment. Unfortunately these previous studies have utilised siRNA to remove p22phox and inhibit Nox activity. Safe and effective ways of delivering siRNA to patients are currently being investigated however these methods are not fully tested or optimised and are therefore not feasible approaches at present (Gavrilova and Saltzman, 2012). As such traditional pharmacological silencing of targets still remains the best approach for therapy. In light of this the aims of this next study were to investigate the potential of Nox protein inhibitors in the treatment of CML when combined with Bcr-Abl inhibition. Furthermore, as discussed Nox activity is implicated in a many cancers therefore the potential of Nox inhibition is not just limited to CML treatment. As a result Nox inhibition as a combined therapy with other chemotherapeutics was investigated to establish its potential as a treatment for a broader spectrum of cancers. As with previous studies K562 cells, which constitutively express Bcr-Abl were used as a model to perform these studies.

Results

DPI, an inhibitor of Nox proteins: Determination of optimal concentrations and characterisation of the effects of treatment

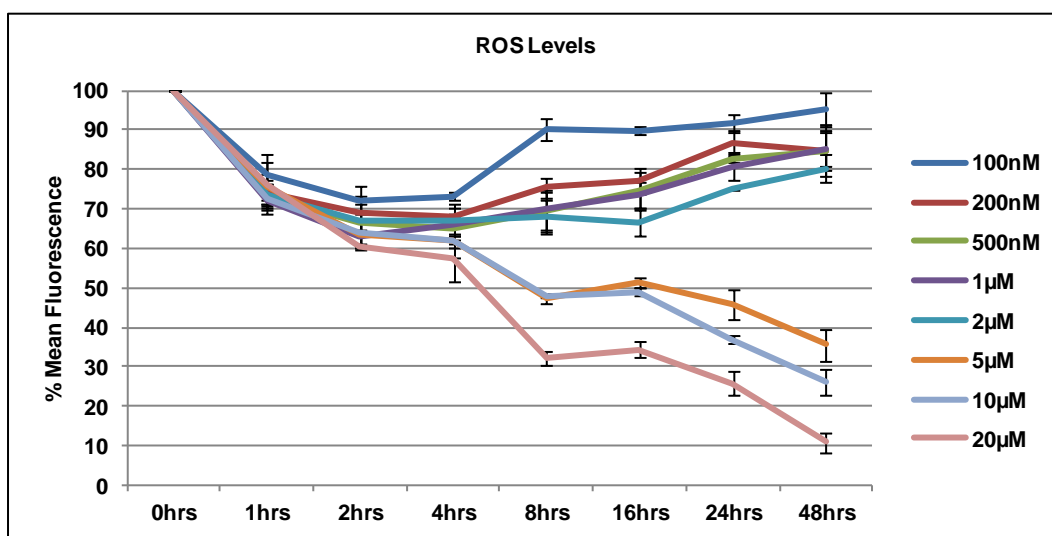
The iodonium-derivative and flavoprotein inhibitor diphenylene iodonium (DPI) is the most commonly used and cited compound utilised to inhibit Nox activity (Bedard and Krause, 2007). DPI inhibits Nox activity by interfering with electron transport thereby preventing ROS generation (O'Donnell *et al.*, 1993). Studies in Chapter 3 utilised DPI along with another Nox inhibitor, VAS2870, to demonstrate that an extensive proportion of endogenous ROS levels in K562 cells were Nox protein derived (Chapter 3, Figure 1). As a result of this work coupled with the highly cited use of DPI to inhibit Nox proteins this next study followed on from the results of Chapter 4 and focused on establishing whether or not the inhibitory activity of DPI could be utilised to increase the effectiveness of Bcr-Abl inhibition when treating CML.

To begin the effects of DPI treatment on K562 cells at varying concentrations was examined over 48hrs. Previous work with DPI did not require cells to be treated for extended periods of time therefore this examination was to characterise how this drug effected cells over long periods and to identify ideal concentrations for subsequent combination studies with other drugs. To do this K562 cells were treated with a low to high range of DPI concentrations and were examined after initial treatment in intervals of 1hrs, 2hrs, 4hrs, 8hrs, 16hrs, 24hrs and 48hrs. As this study was focused on the potential of Nox protein inhibition as a possible therapeutic, it was important to examine how varying concentrations of DPI affected endogenous ROS levels in K562 cells over time. Treatment of K562 cells with DPI at all concentrations resulted in comparative decreases in endogenous ROS levels within

the first hour of treatment (Figure 1a(i)). With the exception of 100nM all other concentrations demonstrated a reduction in ROS levels for the entire duration of the study (up to 48hrs). It is important to note that the decreases observed in ROS levels directly correlated with DPI concentration. K562 cells treated with lower concentrations of DPI (100nM to 1 μ M) demonstrated a minimal increase in cell death while considerable levels of cell death were observed with concentrations of 2 μ M or higher following the 16hrs time-point (Figure 1a(ii)). Furthermore, depending on the concentration of DPI treatment variable effects were noted on cell cycle distribution. Lower concentrations of DPI (100nM to 500nM) were observed to induce an increase in the percentage of cells present in G0/G1 however at higher concentrations of DPI (2 μ M or higher) there was a steady shift with a large increase of cells in both the S and G2/M phases which was observed up to 48hrs (Figure 1b).

Work in Chapter 4 established that p22phox knockdown and subsequent inhibition of Nox-derived ROS produced an increase in the percentage of cells present in G1 due to a slowdown in transition to S phase (Chapter 4, Figure 3 and Figure 4). Furthermore, these studies established that inhibition of p22phox regulated Nox activity had a significant effect on cell viability but did not demonstrate a large increase in cell death (Chapter 4, Figure 7 and Figure 8). As a result concentrations of DPI below 2 μ M were believed to most suitable for subsequent studies with DPI as they induced effects in K562 cells similar to p22phox knockdown, a comparable increase in the percentage of cells in G0/G1 without having a substantial effect on cell death. As 100nM treatment did not decrease ROS levels below basal levels for the entire 48hrs duration 200nM, 500nM and 1 μ M were chosen.

(i)



(ii)

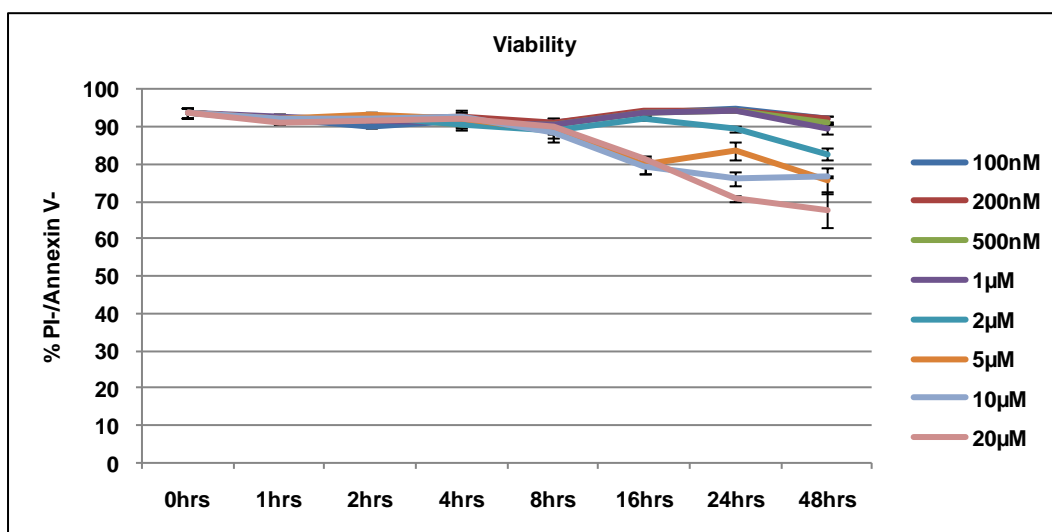


Figure 1a. DPI: Determination of optimal concentrations and characterisation of the effects of treatment. K562 cells were treated with increasing concentrations of DPI (100nM, 200nM, 500nM, 1µM, 2µM, 5µM, 10µM, 20µM) and were examined at the indicated time-points (1hrs, 2hrs, 4hrs, 8hrs, 16hrs, 24hrs and 48hrs). (i) ROS levels: Intracellular ROS levels were measured by flow cytometric analysis of relative DCF fluorescence. The line graph demonstrates the mean relative DCF fluorescence of treated cells expressed as a percentage of the DMSO vehicle control (0hrs). (ii) Viability: At each time-point treated cells were incubated with Annexin V-FITC and then stained with propidium iodide (PI) immediately before flow cytometric analysis. The line graph demonstrates the percentage of K562 cells staining negative for both Annexin V and PI. Viability of DMSO vehicle control cells represents 0hrs. Results are expressed as mean \pm SD and are representative of three independent experiments.

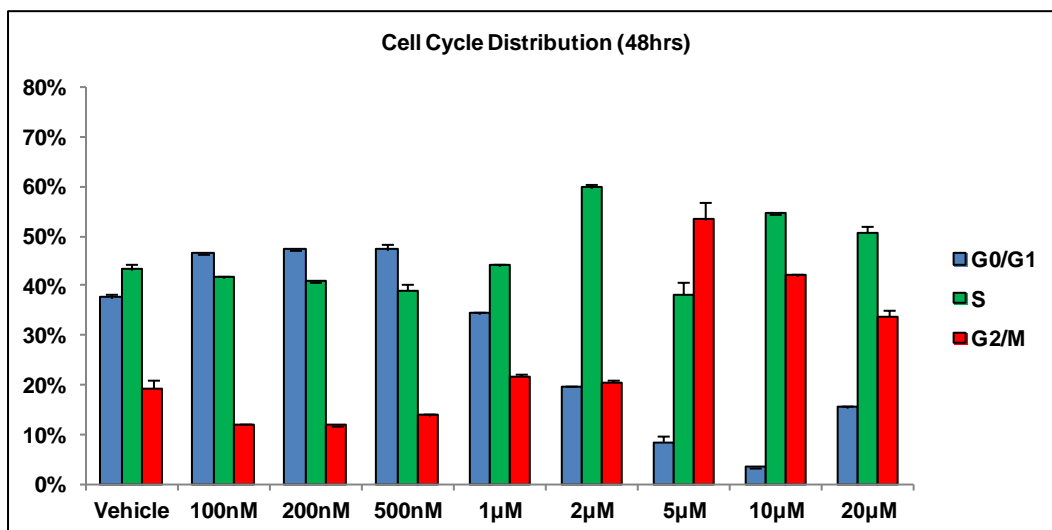


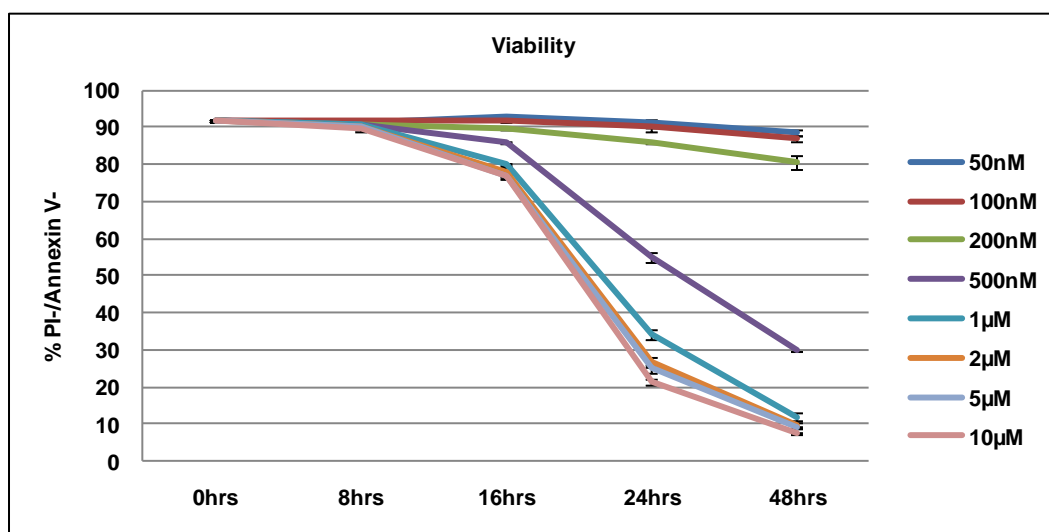
Figure 1b. DPI: Determination of optimal concentrations and characterisation of the effects of treatment. K562 cells were treated with increasing concentrations of DPI (100nM, 200nM, 500nM, 1µM, 2µM, 5µM, 10µM, 20µM) and were examined at the indicated time-points (1hrs, 2hrs, 4hrs, 8hrs, 16hrs, 24hrs and 48hrs). Cell cycle distribution: At each time-point treated cells were fixed then stained with propidium iodide (PI) before being examined by flow cytometric analysis. The bar chart demonstrates the cell cycle distribution of treated K562 cells as determined by ModFit LT software analysis 48hrs after treatment. Vehicle control is DMSO. Cell cycle distribution of treated cells at 48hrs is representative of earlier time-points. Results are expressed as mean \pm SD and are representative of three independent experiments.

Imatinib: Determination of optimal concentrations and characterisation of the effects of treatment

As with DPI, before combination studies could commence the effects of Imatinib treatment on K562 cells at varying concentrations were examined over 48hrs. Imatinib was used in previous chapters to study Bcr-Abl signalling through inhibition therefore these original studies were optimised to have minimal effect on cell death while inducing maximal inhibition. In contrast the aim of this study was to examine how varying concentrations of Imatinib induced cell death and as a result cells needed to be treated for extended periods of time to facilitate the identification of suitable drug concentrations for subsequent combination studies. In addition to cell death, cell cycle distribution was also examined to characterise and better understand the effects of the drug on K562 cells.

K562 cells were treated with a low to high range of Imatinib concentrations and were examined after initial treatment in intervals of 8hrs, 16hrs, 24hrs and 48hrs. All treatments with Imatinib induced some degree of cell death by 48hrs with higher concentrations demonstrating significant increases as early as 16hrs (Figure 2a). The extent of cell death directly correlated with Imatinib concentration. It is important to note that concentrations above 500nM induced a similar level of effect with near complete death of the cell populations. These concentrations were identified as too high to distinguish any additional increase in cell death that may arise if used in combination with another drug. Alternatively both 50nM and 100nM showed minimal effects on cell death and were believed to be too weak to be used for further examination. Examination of cell cycle distribution demonstrated that all concentrations of Imatinib induced an increase in the percentage of cells present in G0/G1 up to 48hrs (Figure 2b). Increases in the percentage of cells in S phase were

(a)



(b)

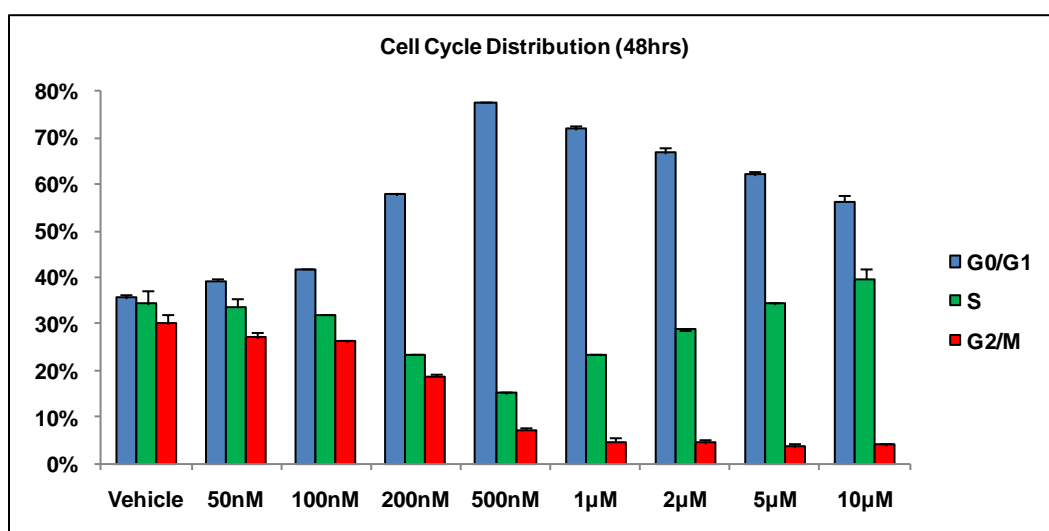


Figure 2. Imatinib: Determination of optimal concentrations and characterisation of the effects of treatment. K562 cells were treated with increasing concentrations of Imatinib (50nM, 100nM, 200nM, 500nM, 1µM, 2µM, 5µM, 10µM) and were examined at the indicated time-points (8hrs, 16hrs, 24hrs and 48hrs). (a) Viability: At each time-point treated cells were incubated with Annexin V-FITC and then stained with propidium iodide (PI) immediately before flow cytometric analysis. The line graph demonstrates the percentage of K562 cells staining negative for both Annexin V and PI. Viability of untreated cells represents 0hrs. (b) Cell cycle distribution: At each time-point treated cells were fixed then stained with propidium iodide (PI) before being examined by flow cytometric analysis. The bar chart demonstrates the cell cycle distribution of treated K562 cells as determined by ModFit LT software analysis 48hrs after each treatment. Vehicle refers to untreated cells. Cell cycle distribution at 48hrs is representative of earlier time-points. Results are expressed as mean \pm SD and are representative of three independent experiments.

not observed prior to 48hrs. Taken together these examinations identified Imatinib at concentrations of 200nM and 500nM to be suitable for combination studies. Both produced distinctive affects on cell death and cell cycle distribution while still producing a large difference in their degree of potency, providing an ideal range.

Imatinib and DPI: A study examining the effects of combined treatment on cell viability

After establishing suitable concentrations for DPI and Imatinib the next step was to treat K562 cells with combinations of these drugs. Each of the three chosen DPI concentrations were used to treat cells in combination with either of the two concentrations of Imatinib (200nM and 500nM). K562 cells were treated with these six separate drug combinations before cell death was examined 8hrs, 16hrs, 24hrs and 48hrs after initial treatment. Figure 3a clearly demonstrates that all three combinations which utilised Imatinib at 200nM induced a greater than two-fold increase in cell death when compared to Imatinib treatment alone. The effectiveness of a drug combination is generally determined based on whether a synergistic, additive or antagonistic effect is observed following treatment. The most accepted and highly cited method of determining whether a drug combination produces one of these three effects is through the calculation of a combination index (CI) a method mathematically defined by Chou and Talalay in 1984 (Chou and Talalay, 1984; Chou 2007). Calculated CI values of < 1 , $= 1$ or > 1 indicate whether treatment with a drug combination is synergistic, additive or antagonistic respectively.

To determine the CI values for these six drug combinations the percentage of cell death observed at 48hrs as a result of individual drug treatments as well as combined drug treatments was analysed using CompuSyn software. Analysis

generated two values for each drug combination, CI and fraction affected (F_a). F_a is an assigned value between 0.01 and 0.99, representative of the level of cell death and the value inputted for analysis. Figure 3b illustrated this analysed data in the form of a F_a -CI plot along with a table containing the F_a and CI values for each combination. Data points below the line illustrated in a F_a -CI plot represent combinations which had a synergistic effect, the closer the point to the X-axis the greater the level of synergy. In this study all drug combinations produced CI values less than 1, with combinations containing higher concentrations of DPI demonstrating the lowest CI values. This work established that the combined treatment of DPI and Imatinib in K562 cells was synergistic. This result was interesting and highlighted the possible benefit of pharmacological Nox inhibition in combination with Imatinib as a potential treatment strategy for CML.

Examination of the apoptotic pathway and cell morphology following combined treatment of cells with Imatinib and DPI

Annexin V is a recombinant protein that interacts strongly and specifically with phosphatidylserine residues which are externalised on the cell surface during early stages of apoptosis (van Engeland *et al.*, 1998; Arur *et al.*, 2003). The use of annexin V when examining cell viability following drug treatments established that the increase in cell death was a result of increased apoptosis. Due to this it was of interest to determine how combined DPI and Imatinib treatment affected the apoptotic process. Following initiation of apoptosis the cleavage and subsequent activation of the cysteine protease Caspase-3 is important for continuing the process of programme cell death (Elmore, 2007). Combined treatment with DPI at 200nM and Imatinib at 200nM demonstrated a distinct synergistic increase in cell death

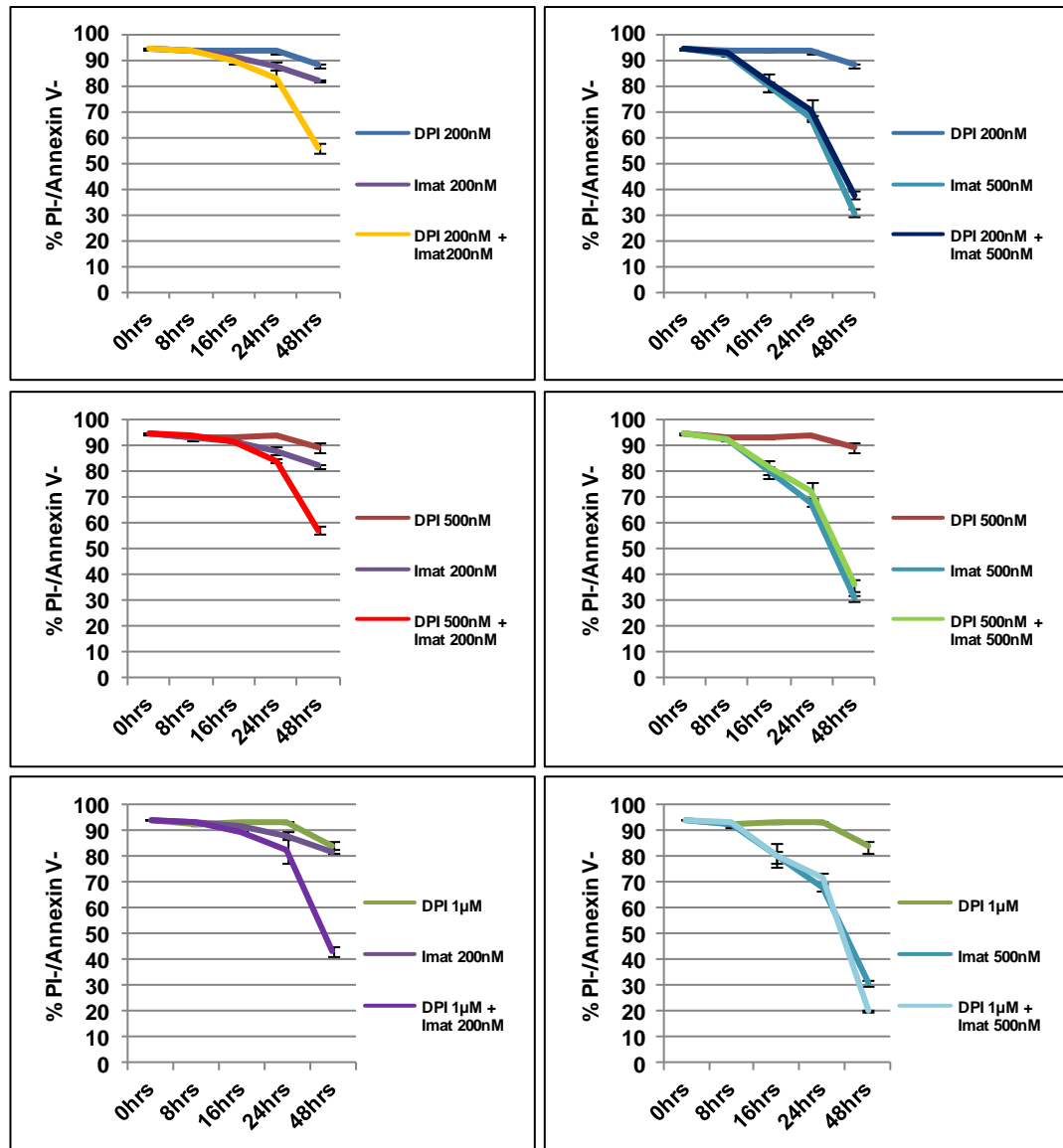
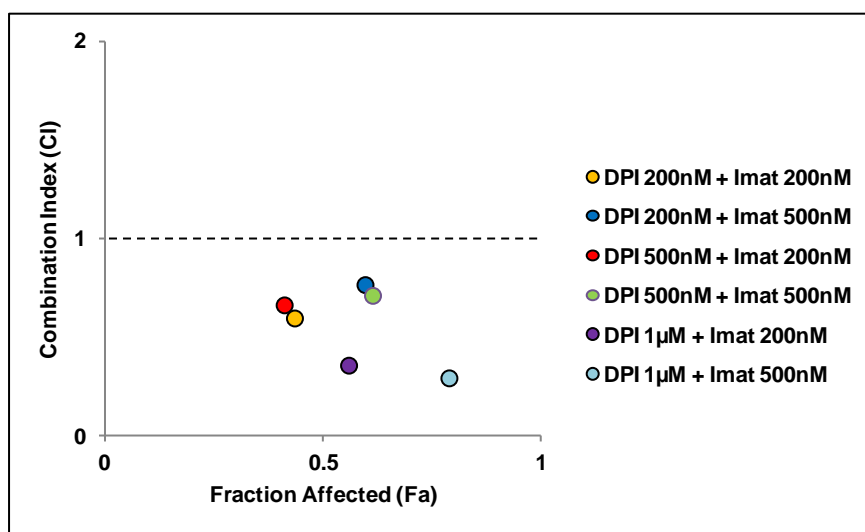


Figure 3a. Combined treatment with both DPI and Imatinib synergistically decreases cell viability. K562 cells were simultaneously treated with both DPI and Imatinib (Imat) at varying concentration combinations (DPI + Imat respectively: 200nM + 200nM, 200nM +500nM, 500nM +200nM, 500nM+500nM, 1μM + 200nM, 1μM + 500nM) and were examined at the indicated time-points (8hrs, 16hrs, 24hrs and 48hrs). At each time-point treated cells were incubated with Annexin V-FITC and then stained with propidium iodide (PI) immediately before flow cytometric analysis. The line graph demonstrates the percentage of K562 cells staining negative for both Annexin V and PI. Viability of DMSO vehicle control cells represents 0hrs. Results are expressed as mean \pm SD and are representative of three independent experiments.

(i)



(ii)

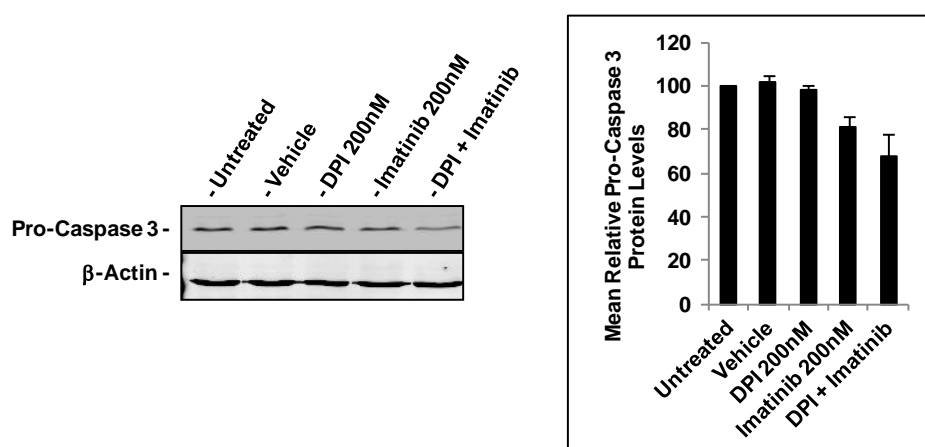
Drug Combinations	Fa Value	CI Value
DPI 200nM + Imat 200nM	0.4357	0.60274
DPI 200nM + Imat 500nM	0.59755	0.77198
DPI 500nM + Imat 200nM	0.4121	0.66922
DPI 500nM + Imat 500nM	0.6148	0.71752
DPI 1µM + Imat 200nM	0.5599	0.36353
DPI 1µM + Imat 500nM	0.7901	0.29927

Figure 3b. Combined treatment with both DPI and Imatinib synergistically decreases cell viability. K562 cells were simultaneously treated with both DPI and Imatinib (Imat) at varying concentration combinations (DPI + Imat respectively: 200nM + 200nM, 200nM +500nM, 500nM +200nM, 500nM+500nM, 1µM + 200nM, 1µM + 500nM). At 48hrs treated K562 cells were incubated with Annexin V-FITC and then stained with propidium iodide (PI) immediately before flow cytometric analysis. Data was analysed using CompuSyn software to determine if the noted changes in K562 cell viability following combined treatment were synergistic (CI < 1), additive (CI = 1) or antagonistic (CI > 1). (i) A F_a -CI plot for all combinations as determined by CompuSyn software analysis at 48hrs. (ii) Table represents F_a and CI values for each combination.

when compared to single drug treatments. Following the treatment of K562 cells with this particular drug combination the levels of Pro-Caspase-3 were examined (Figure 4a). In addition to examining Caspase-3, poly (ADP-ribose) polymerase (PARP) a substrate of active Caspase-3 was also examined (Figure 4b). Following treatment for 48hrs, Pro-Caspase-3 protein levels were demonstrated to decrease in samples treated with Imatinib alone or with combined DPI and Imatinib (Figure 4a). This suggested an increase in cleaved Caspase-3 levels. Interestingly, although the decrease in Pro-Caspase-3 levels following combination treatment was marginally greater the difference was not significant. However, examination of PARP protein levels demonstrated a significantly greater increase in PARP cleavage in the samples treated with the drug combination *versus* Imatinib alone.

Following these studies morphological changes in K562 cells were examined 48hrs after treatment. Various morphological changes such as cell shrinkage, nuclear condensation, plasma membrane blebbing and the formation of apoptotic bodies occur during apoptosis (Häcker, 2000). To allow histological analysis cells were cytopun to slides, fixed and stained with hematoxylin and eosin following combination treatment. This study showed untreated, DMSO vehicle or DPI treated cells to have no noticeable changes in cell morphology (Figure 5). However, samples treated with Imatinib exhibited cells with some degree of morphological change while more significantly samples treated with the drug combination demonstrated a large number of dense purple fragments suggestive of condensed nuclear chromatin or apoptotic bodies as well as an excessive level of blebbing cells (Figure 5). Taken together these results demonstrated that combined treatment with DPI and Imatinib inhibiting both Nox and Bcr-Abl activity significantly increase the apoptotic process, further highlighting the potential for targeted Nox inhibition in CML treatment.

(a)



(b)

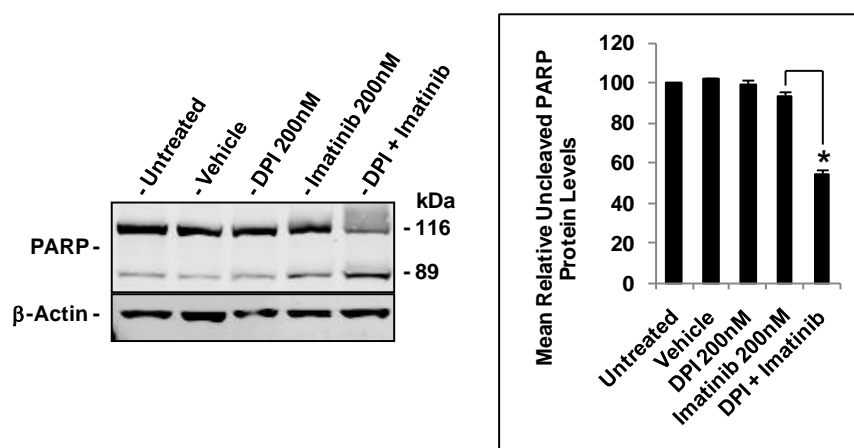


Figure 4. Combined treatment with both DPI and Imatinib results in a significant increase in PARP cleavage. K562 cells simultaneously treated with both Imatinib and DPI (200nM + 200nM respectively) for 48hrs. (a) Western blot analysis of Pro-Caspase 3 protein levels. Bar chart shows the mean relative Pro-Caspase 3 protein levels of K562 cells 48hrs after treatment as determined by densitometry and expressed as a percentage of the untreated control cells. (b) Western blot analysis of PARP protein levels. Bar chart shows the mean relative uncleaved PARP protein levels of K562 cells 48hrs after treatment as determined by densitometry and expressed as a percentage of the untreated control cells. Vehicle refers to DMSO control. β -Actin is shown as a loading control. Results are expressed as mean \pm SD and are representative of three independent experiments. Statistical analysis was carried out using the student t-test ($P < 0.05$ is marked with *).

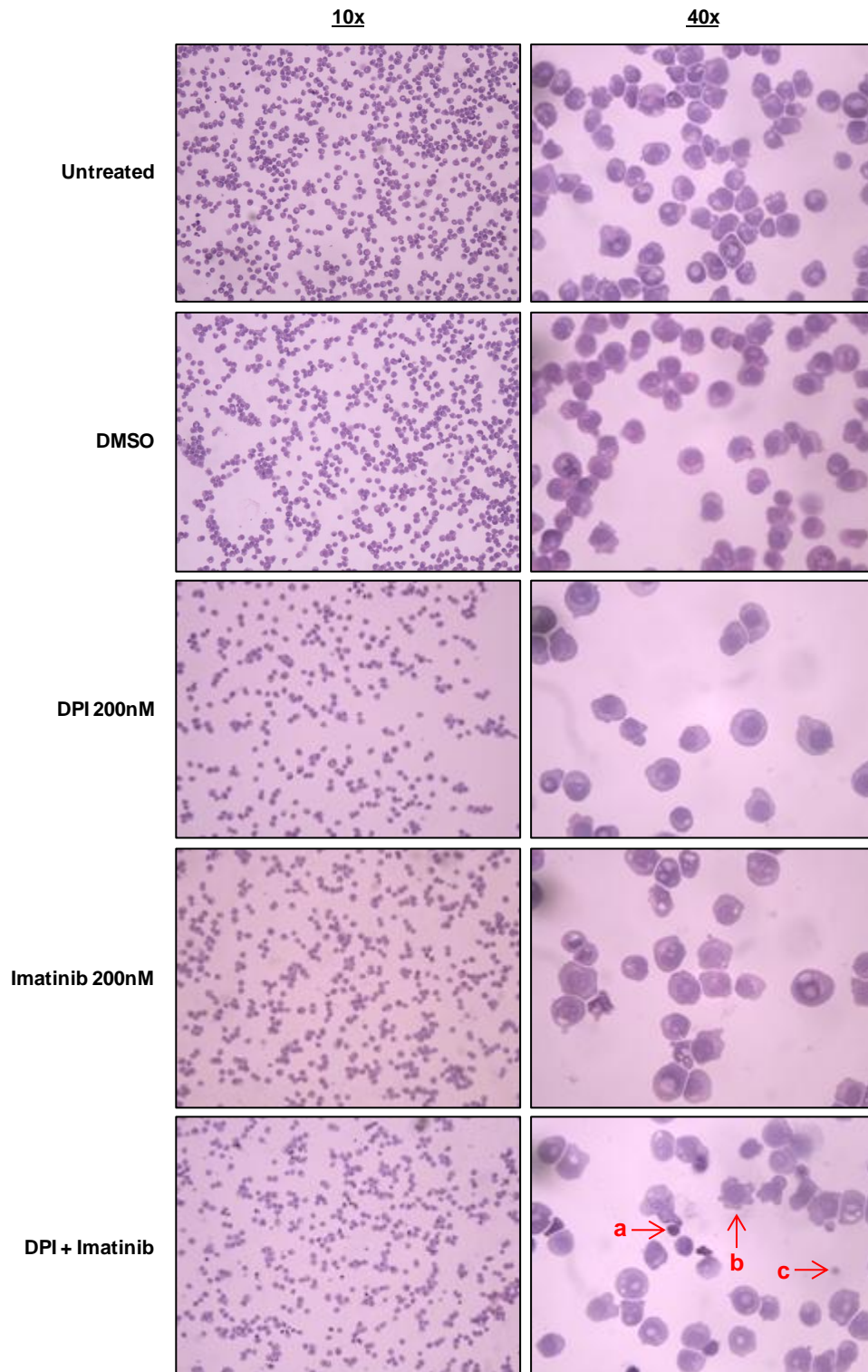


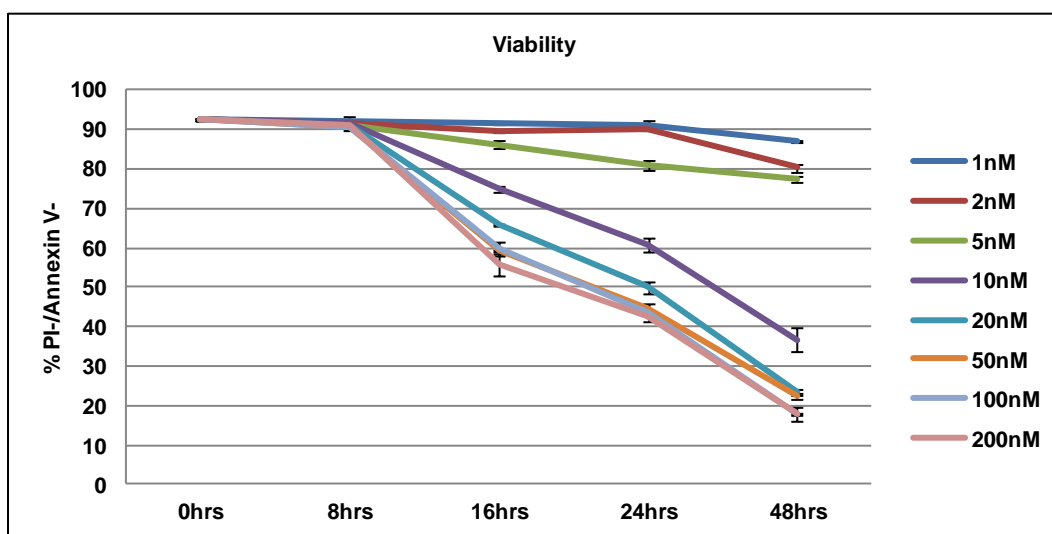
Figure 5. Histological analysis of cells treated with both Imatinib and DPI results in an increase in the number of apoptotic bodies. K562 cells simultaneously treated with both Imatinib and DPI (200nM + 200nM respectively) for 48hrs. Cells were cytospun onto slides, fixed and subsequently stained with haematoxylin and counterstained with eosin before being viewed under a light microscope. Arrows indicate cells with; shrinkage and nuclear condensation (a), plasma membrane blebbing (b) and apoptotic bodies (c). Images are representative of three independent experiments.

Nilotinib: Determination of optimal concentrations and characterisation of the effects of treatment

Nilotinib is a derivative of Imatinib and therefore another small molecule TKI developed to inhibit Bcr-Abl activity (Weisberg *et al.*, 2005). Furthermore, Nilotinib binds Bcr-Abl with a higher affinity than Imatinib making it significantly more potent and giving it a lower IC₅₀ value in comparison. Considering the level of synergy demonstrated following simultaneous Nox and Bcr-Abl inhibition *via* combined DPI and Imatinib treatment the aim of this study was to determine if this synergy would be replicated using a different Bcr-Abl inhibitor. This would confirm that the previous results were due to the specific effects of Bcr-Abl inhibition as opposed to any off target effects of Imatinib treatment. As with the previous drugs and for the same reasons, before combination studies could commence the effects of Nilotinib treatment on K562 cells at varying concentrations needed to be examined.

K562 cells were treated with a low to high range of Nilotinib concentrations and were examined after initial treatment in intervals of 8hrs, 16hrs, 24hrs and 48hrs. The effects of Nilotinib treatment were similar to those demonstrated following Imatinib treatment, albeit with the use of considerably lower concentrations. All treatments with Nilotinib induced some degree of cell death by 48hrs with higher concentrations demonstrating significant increases as early as 16hrs (Figure 6a). Furthermore, the extent of cell death directly correlated with the concentration of Nilotinib. Examination of cell cycle distribution demonstrated a similar pattern of concentration dependent G1 arrest as previously demonstrated with Imatinib treatment (Figure 6b). As with Imatinib increases in the percentage of cells in S phase at higher concentrations were not observed prior to 48hrs. Interestingly when examining cell death all concentrations above 10nM induced substantial levels of

(a)



(b)

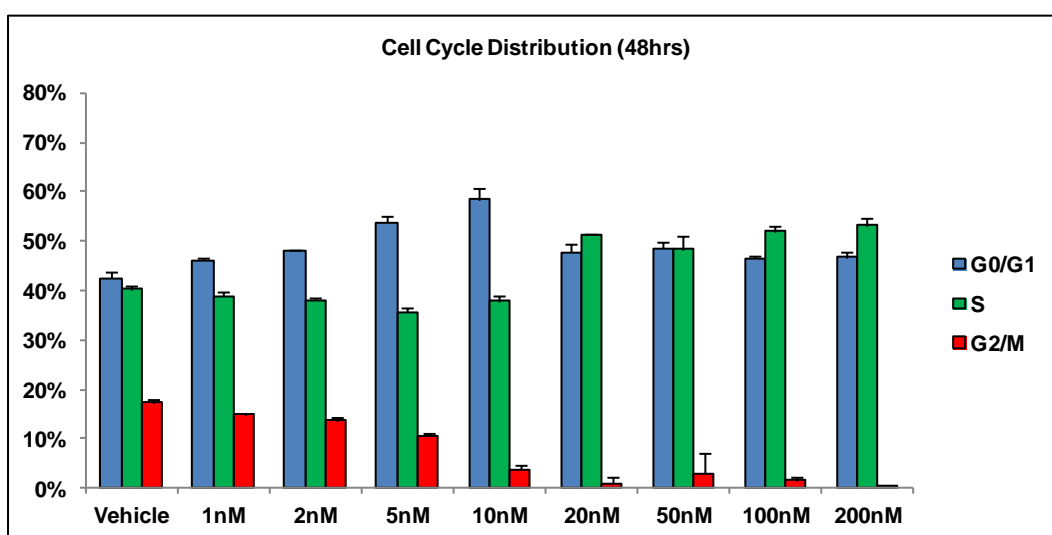


Figure 6. Nilotinib: Determination of optimal concentrations and characterisation of the effects of treatment. K562 cells were treated with increasing concentrations of Nilotinib (1nM, 2nM, 5nM, 10nM, 20nM, 50nM, 100nM, 200nM) and were examined at the indicated time-points (8hrs, 16hrs, 24hrs and 48hrs). (a) Viability: At each time-point treated cells were incubated with Annexin V-FITC and then stained with propidium iodide (PI) immediately before flow cytometric analysis. The line graph demonstrates the percentage of K562 cells staining negative for both Annexin V and PI. Viability of DMSO vehicle control cells represents 0hrs. (b) Cell cycle distribution: At each time-point treated cells were fixed then stained with propidium iodide (PI) before being examined by flow cytometric analysis. The bar chart demonstrates the cell cycle distribution of treated K562 cells as determined by ModFit LT software analysis 48hrs after treatment. Vehicle control is DMSO. Cell cycle distribution of treated cells at 48hrs is representative of earlier time-points. Results are expressed as mean \pm SD and are representative of three independent experiments.

cell death making these concentrations too high to allow further analysis of effects if used in combination with another drug. Alternatively, although 1nM and 2nM treatments showed an effect on cell death, these were believed to be too weak to be used for further examination. As a result concentrations of 5nM and 10nM were chosen as suitable for combination studies. As with the previously examined drugs, these concentrations were chosen as both produced distinctive affects on cell death and cell cycle distribution while still producing a large difference in their degree of potency, providing an ideal range for treatment.

Nilotinib and DPI: A study examining the effects of combined treatment on cell viability

Following the previous study the chosen concentrations of Nilotinib were used to treat K562 cell in combination with DPI. As before each of the three chosen DPI concentrations were used to treat cells in combination with either of the two concentrations of Nilotinib (5nM and 10nM) thereby making six separate drug combinations in total. As before cell death was examined 8hrs, 16hrs, 24hrs and 48hrs after initial treatment followed by calculation of CI values. Figure 7a clearly demonstrates a very similar pattern to that observed following DPI and Imatinib treatment with all three combinations utilising the lower concentration of Nilotinib (5nM) inducing a greater than two-fold increase in cell death when compared to Nilotinib treatment alone.

As before CI values of the drug combinations were determined using CompuSyn software analysis. Again as previously observed with Imatinib, all drug combinations here produced CI values less than 1, with the lowest values being produced from combinations containing the higher DPI concentrations (Figure 7b).

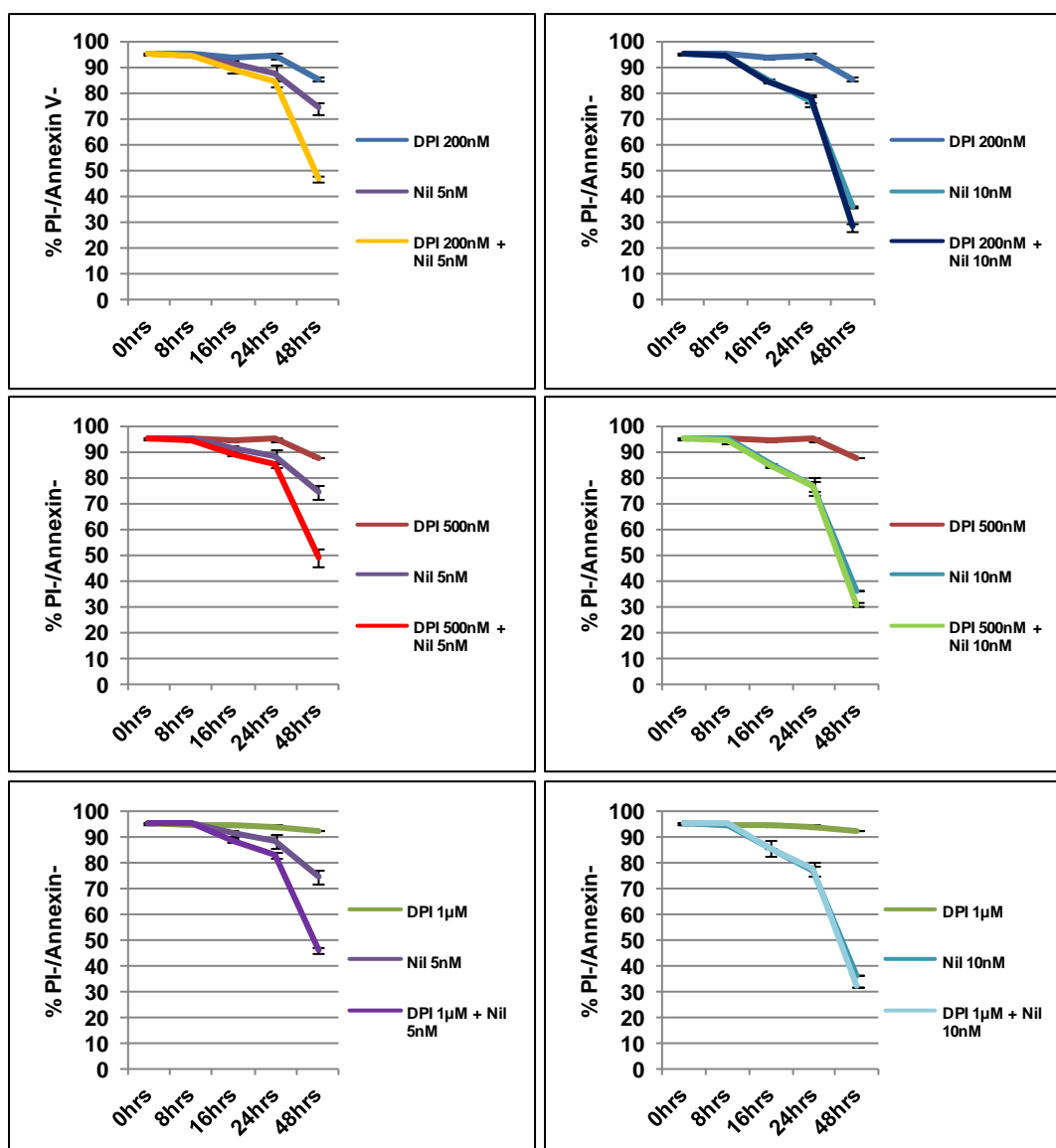
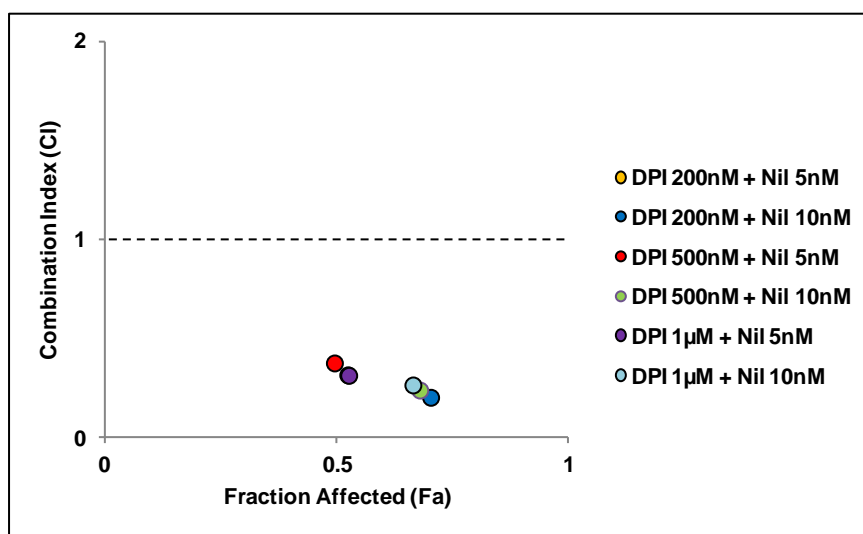


Figure 7a. Combined treatment with both DPI and Nilotinib synergistically decreases cell viability. K562 cells were simultaneously treated with both DPI and Nilotinib (Nil) at varying concentration combinations (DPI + Nil respectively: 200nM + 5nM, 200nM + 10nM, 500nM + 5nM, 500nM + 10nM, 1µM + 5nM, 1µM + 10nM) and were examined at the indicated time-points (8hrs, 16hrs, 24hrs and 48hrs). At each time-point treated cells were incubated with Annexin V-FITC and then stained with propidium iodide (PI) immediately before flow cytometric analysis. The line graph demonstrates the percentage of K562 cells staining negative for both Annexin V and PI. Viability of DMSO vehicle control cells represents 0hrs. Results are expressed as mean \pm SD and are representative of three independent experiments.

(i)



(ii)

Drug Combinations	Fa Value	CI Value
DPI 200nM + Nil 5nM	0.5248	0.32145
DPI 200nM + Nil 10nM	0.7035	0.20807
DPI 500nM + Nil 5nM	0.496	0.38152
DPI 500nM + Nil 10nM	0.6802	0.24451
DPI 1µM + Nil 5nM	0.5268	0.31898
DPI 1µM + Nil 10nM	0.6653	0.27036

Figure 7b. Combined treatment with both DPI and Nilotinib synergistically decreases cell viability. K562 cells were simultaneously treated with both DPI and Nilotinib (Nil) at varying concentration combinations (DPI + Nil respectively: 200nM + 5nM, 200nM + 10nM, 500nM + 5nM, 500nM + 10nM, 1µM + 5nM, 1µM + 10nM) and were examined at the indicated time-points (8hrs, 16hrs, 24hrs and 48hrs). At 48hrs treated K562 cells were incubated with Annexin V-FITC and then stained with propidium iodide (PI) immediately before flow cytometric analysis. Data was analysed using CompuSyn software to determine if the noted changes in K562 cell viability following combined treatment were synergistic (CI < 1), additive (CI = 1) or antagonistic (CI > 1). (i) A F_a -CI plot for all combinations as determined by CompuSyn software analysis at 48hrs. (ii) Table represents F_a and CI values for each combination.

These results established that combined treatment of DPI and Nilotinib in K562 cells was highly synergistic. This confirmed that previous synergy observed with Imatinib treatment were likely due to specific Bcr-Abl inhibition coupled with DPI treatment. Furthermore this emphasised the potential of Bcr-Abl inhibition in conjunction with the use of Nox inhibitors again highlighting the potential of pharmacological Nox inhibition in combination with Bcr-Abl inhibition in CML treatment.

VAS2870, an alternative Nox Inhibitor: Determination of optimal concentrations and characterisation of the effects of treatment

VAS2870 (3-benzyl-7-(2-benzoxazolyl) thio-1,2,3-triazolo[4,5-d]pyrimidine) is described as a novel and specific Nox inhibitor (Tegtmeier *et al.*, 2005). As discussed studies in Chapter 3 utilised DPI along with another Nox inhibitor, VAS2870, to demonstrate that an extensive proportion of endogenous ROS levels in K562 cells were Nox protein derived (Chapter 3, Figure 1). As a result of the previous studies it was of interest to determine if Nox inhibition *via* VAS2870 treatment combined with Bcr-Abl inhibition would produce the same level of synergy as demonstrated with DPI. As before the effects of VAS2870 treatment on K562 cells was examined, however as the IC₅₀ of VAS2870 had previously been established across various cells lines (ten Freyhaus *et al.*, 2006; Stielow *et al.*, 2006; Lange *et al.*, 2009) a narrower range of concentrations was examined.

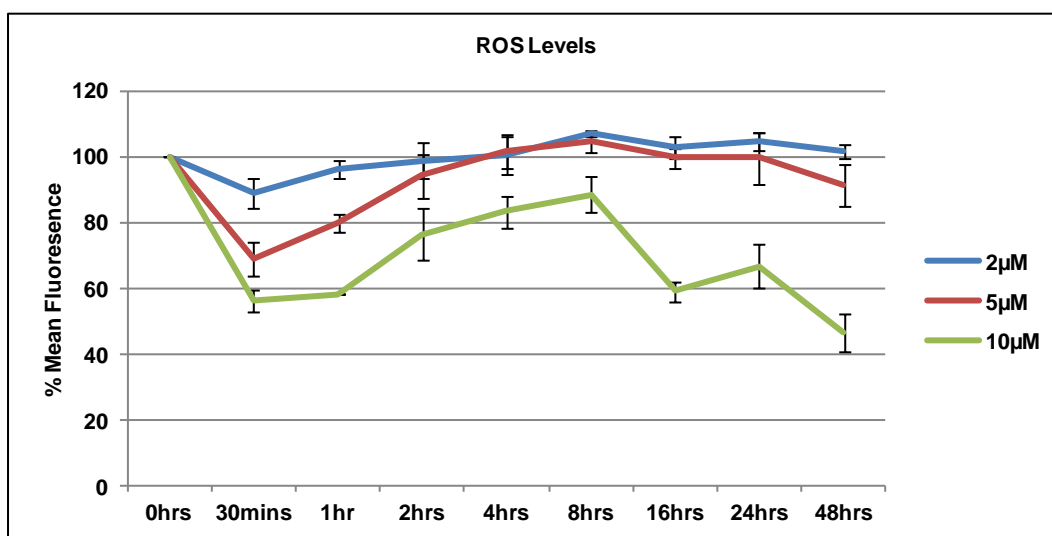
As VAS2870 is a Nox protein inhibitor the endogenous ROS levels of K562 cells needed to be examined following treatment. Interestingly each of the three concentrations of VAS2870 (2µM, 5µM, 10µM) induced a decrease in endogenous ROS levels within 30mins of treatment (Figure 8a(i)). Of the three concentrations only cells treated with 10µM demonstrated a significant reduction in ROS levels for

the entire duration of the study (up to 48hrs). In fact 2 μ M and 5 μ M treated cells showed no significant decrease in ROS following 2hrs. Furthermore, 10 μ M treatment demonstrated a double dip reduction in ROS levels, initially at 30mins and another following 8hrs of treatment. As was the case with DPI, K562 cells treated with VAS2870 demonstrated no significant increase in cell death prior to 8hrs (Figure 8a(ii)). Treatment with VAS2870 at 2 μ M demonstrated no significant effect on cell death at any time point while cells treated with 5 μ M and 10 μ M exhibited substantial concentration dependent increases in cell death. Additionally, unlike DPI VAS2870 treatment at lower concentrations exhibited no significant change in the percentage of cells in G0/G1 but did induce an increase of cells in the G2/M phase following treatment with the higher 10 μ M treatment (Figure 8b). Treatment of K562 cells with VAS2870 produced results which contradicted the work demonstrated in Chapter 4 regarding p22phox knockdown. Although these results were contradictory it was still decided to examine the potential of VAS2870 treatment combined with Bcr-Abl inhibition. As only three concentrations of VAS2870 were examined all three were used for the subsequent combination studies.

Imatinib and VAS2870: A study examining the effects of combined treatment on cell viability

Combined treatment of K562 cells with Imatinib and VAS2870 was carried out as per the protocol used for previous combination studies. Interestingly unlike combinations utilising DPI, there was no clear increase or enhancement of Imatinib potency when used in combination with VAS2870 following examination of cell death levels (Figure 9a). As a result examination of CI values was required to provide a better understanding of these results. After calculating the CI values it was

(i)



(ii)

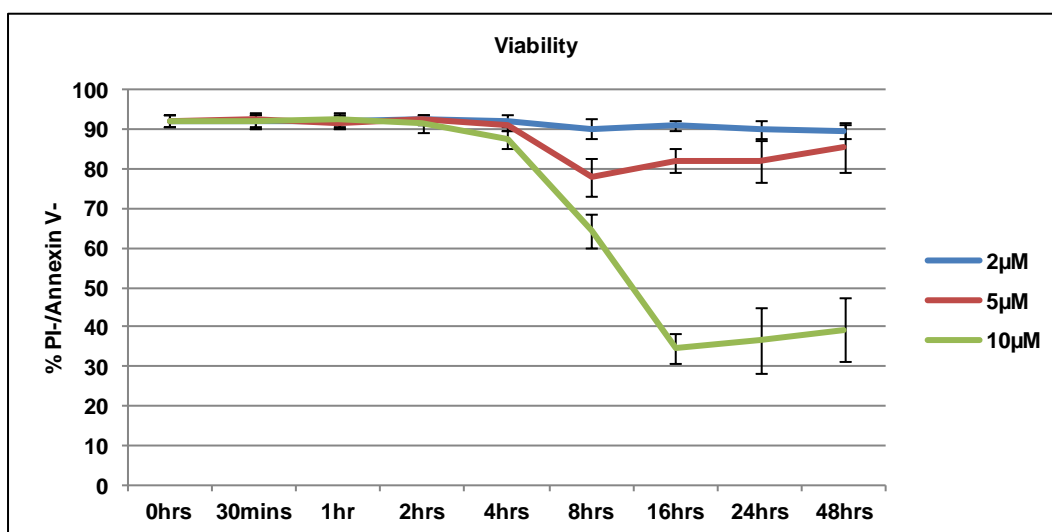


Figure 8a. VAS2870: Determination of optimal concentrations and characterisation of the effects of treatment. K562 cells were treated with increasing concentrations of VAS2870 (2µM, 5µM, 10µM) and were examined at the indicated time-points (30mins, 1hrs, 2hrs, 4hrs, 8hrs, 16hrs, 24hrs and 48hrs). (i) ROS levels: Intracellular ROS levels were measured by flow cytometric analysis of relative DCF fluorescence. The line graph demonstrates the mean relative DCF fluorescence of treated cells expressed as a percentage of the DMSO vehicle control (0hrs). (ii) Viability: At each time-point treated cells were incubated with Annexin V-FITC and then stained with propidium iodide (PI) immediately before flow cytometric analysis. The line graph demonstrates the percentage of K562 cells staining negative for both Annexin V and PI. Viability of DMSO vehicle control cells represents 0hrs. Results are expressed as mean \pm SD and are representative of three independent experiments.

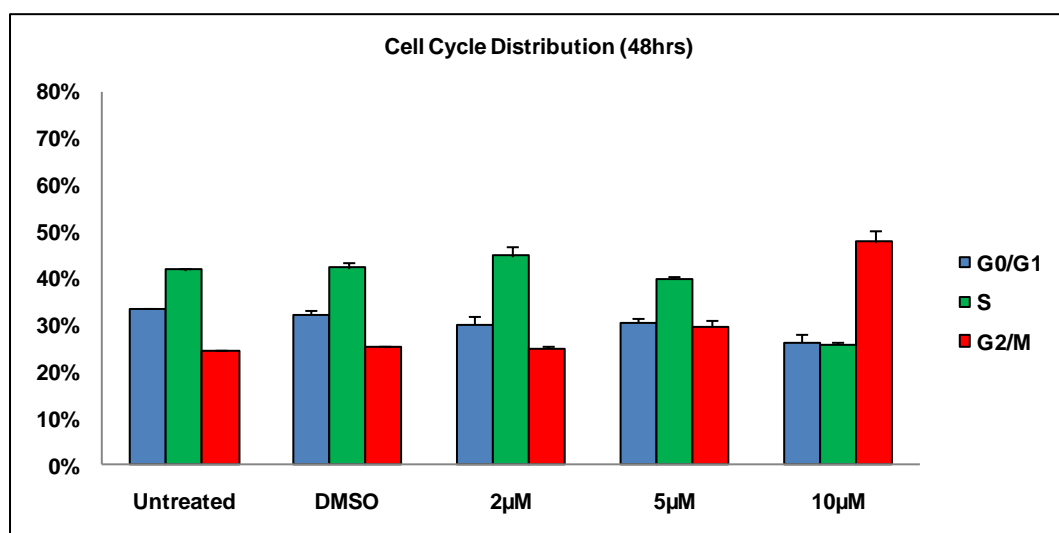


Figure 8b. VAS2870: Determination of optimal concentrations and characterisation of the effects of treatment. K562 cells were treated with increasing concentrations of VAS2870 (2µM, 5µM, 10µM) and were examined at the indicated time-points (30mins, 1hrs, 2hrs, 4hrs, 8hrs, 16hrs, 24hrs and 48hrs). Cell cycle distribution: At each time-point treated cells were fixed then stained with propidium iodide (PI) before being examined by flow cytometric analysis. The bar chart demonstrates the cell cycle distribution of treated K562 cells as determined by ModFit LT software analysis 48hrs after treatment. Vehicle control is DMSO. Cell cycle distribution of treated cells at 48hrs is representative of earlier time-points. Results are expressed as mean \pm SD and are representative of three independent experiments.

evident that out of the six drug combinations used the four utilising lower VAS2870 levels (2 μ M and 5 μ M) induced an antagonistic effect while the two treatments using 10 μ M demonstrated some degree of synergy. Indeed, some combination treatments produced CI values too high to be represented in the F_a -CI plot. This work indicated that the combined treatment of VAS2870 and Imatinib in K562 cells was variable. This was very interesting and highlighted that the use of VAS2870 in combination with Bcr-Abl may not be an ideal drug for these studies.

Nilotinib and VAS2870: A study examining the effects of combined treatment on cell viability

Following the previous study which combined Imatinib and VAS2870 treatment it was of interest to determine whether or not the use of Nilotinib in place of Imatinib would elicit an alternative result. Combined treatment of VAS2870 and Nilotinib was examined on K562 cells in the same manner as with previous combinations. As with combined Imatinib and VAS2870 treatment, there was no clear increase or enhancement of the level of cell death following combined treatment with VAS2870 and Nilotinib (Figure 10a). In fact the effect and pattern of cell death was very similar to the previous combination study with Imatinib. Similarly again, calculation of CI values demonstrated that only two of the six combinations were synergistic. With the exception of the VAS 2 μ M + Nil 10nM combination which demonstrated an additive effect the remaining three treatments were antagonistic. This work confirmed that treatment of VAS2870 in combination with Bcr-Abl inhibition in K562 cells produced variable results; further highlighting that VAS2870 may not be an ideal drug for CML treatment.

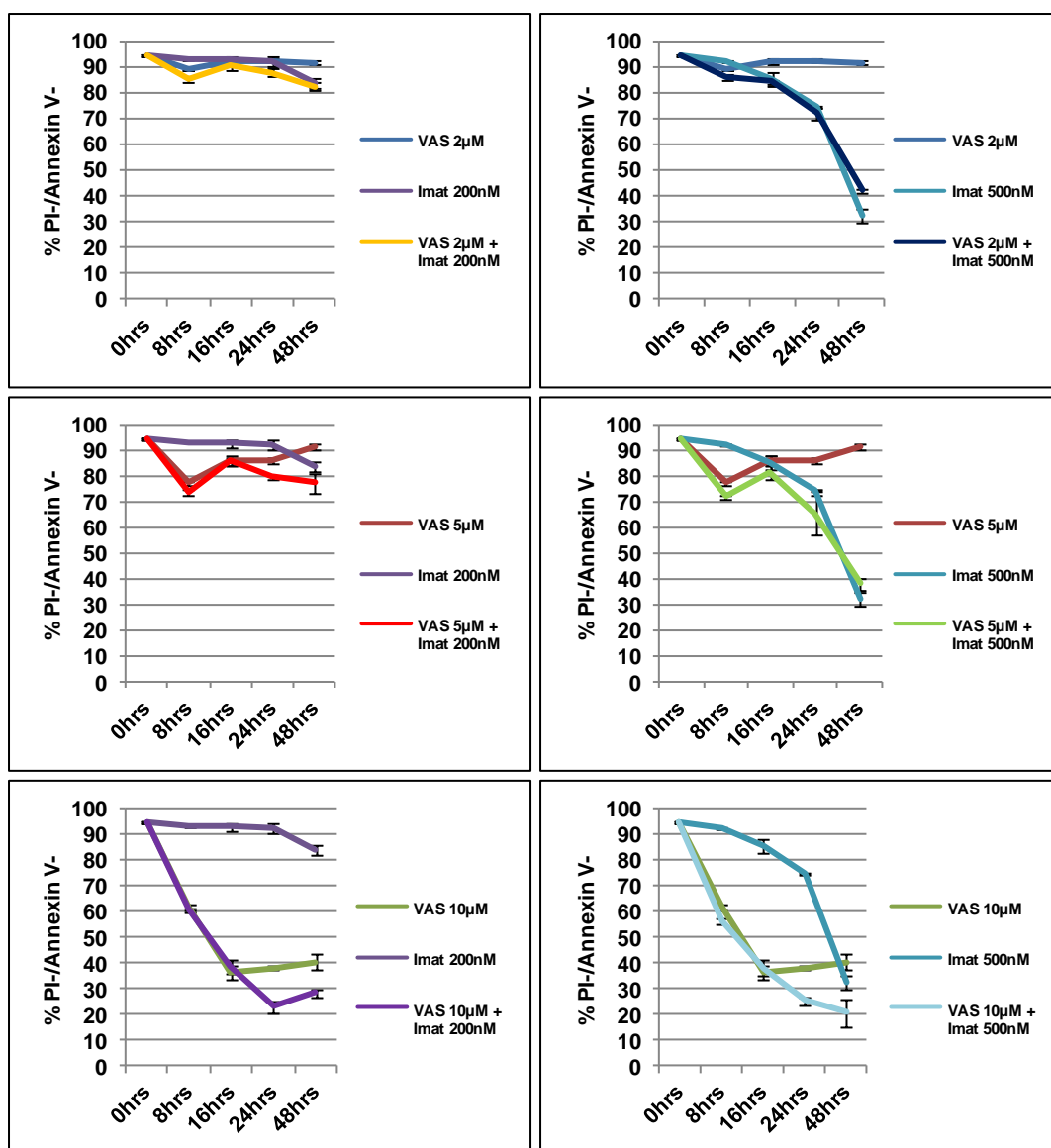
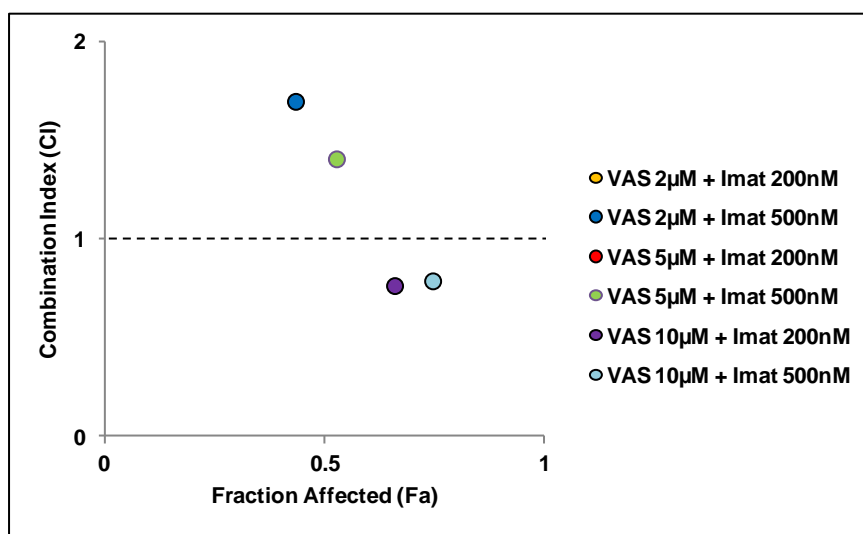


Figure 9a. Combined treatment with both VAS2870 and Imatinib can produce a synergistic or antagonistic effect on cell viability. K562 cells were simultaneously treated with both VAS2870 (VAS) and Imatinib (Imat) at varying concentration combinations (VAS + Imat respectively: 2 μ M + 200nM, 2 μ M + 500nM, 5 μ M + 200nM, 5 μ M + 500nM, 10 μ M + 200nM, 10 μ M + 500nM) and were examined at the indicated time-points (8hrs, 16hrs, 24hrs and 48hrs). At each time-point treated cells were incubated with Annexin V-FITC and then stained with propidium iodide (PI) immediately before flow cytometric analysis. The line graph demonstrates the percentage of K562 cells staining negative for both Annexin V and PI. Viability of DMSO vehicle control cells represents 0hrs. Results are expressed as mean \pm SD and are representative of three independent experiments.

(i)



(ii)

Drug Combinations	Fa Value	CI Value
VAS 2µM + Imat 200nM	0.16685	2.83128
VAS 2µM + Imat 500nM	0.4347	1.70102
VAS 5µM + Imat 200nM	0.2153	2.65515
VAS 5µM + Imat 500nM	0.5278	1.40954
VAS 10µM + Imat 200nM	0.6601	0.76706
VAS 10µM + Imat 500nM	0.74675	0.79103

Figure 9b. Combined treatment with both VAS2870 and Imatinib can produce a synergistic or antagonistic effect on cell viability. K562 cells were simultaneously treated with both VAS2870 (VAS) and Imatinib (Imat) at varying concentration combinations (VAS + Imat respectively: 2µM + 200nM, 2µM + 500nM, 5µM + 200nM, 5µM + 500nM, 10µM + 200nM, 10µM + 500nM) and were examined at the indicated time-points (8hrs, 16hrs, 24hrs and 48hrs). At 48hrs treated K562 cells were incubated with Annexin V-FITC and then stained with propidium iodide (PI) immediately before flow cytometric analysis. Data was analysed using CompuSyn software to determine if the noted changes in K562 cell viability following combined treatment were synergistic (CI < 1), additive (CI = 1) or antagonistic (CI > 1). (i) A F_a -CI plot for all combinations as determined by CompuSyn software analysis at 48hrs. (ii) Table represents F_a and CI values for each combination.

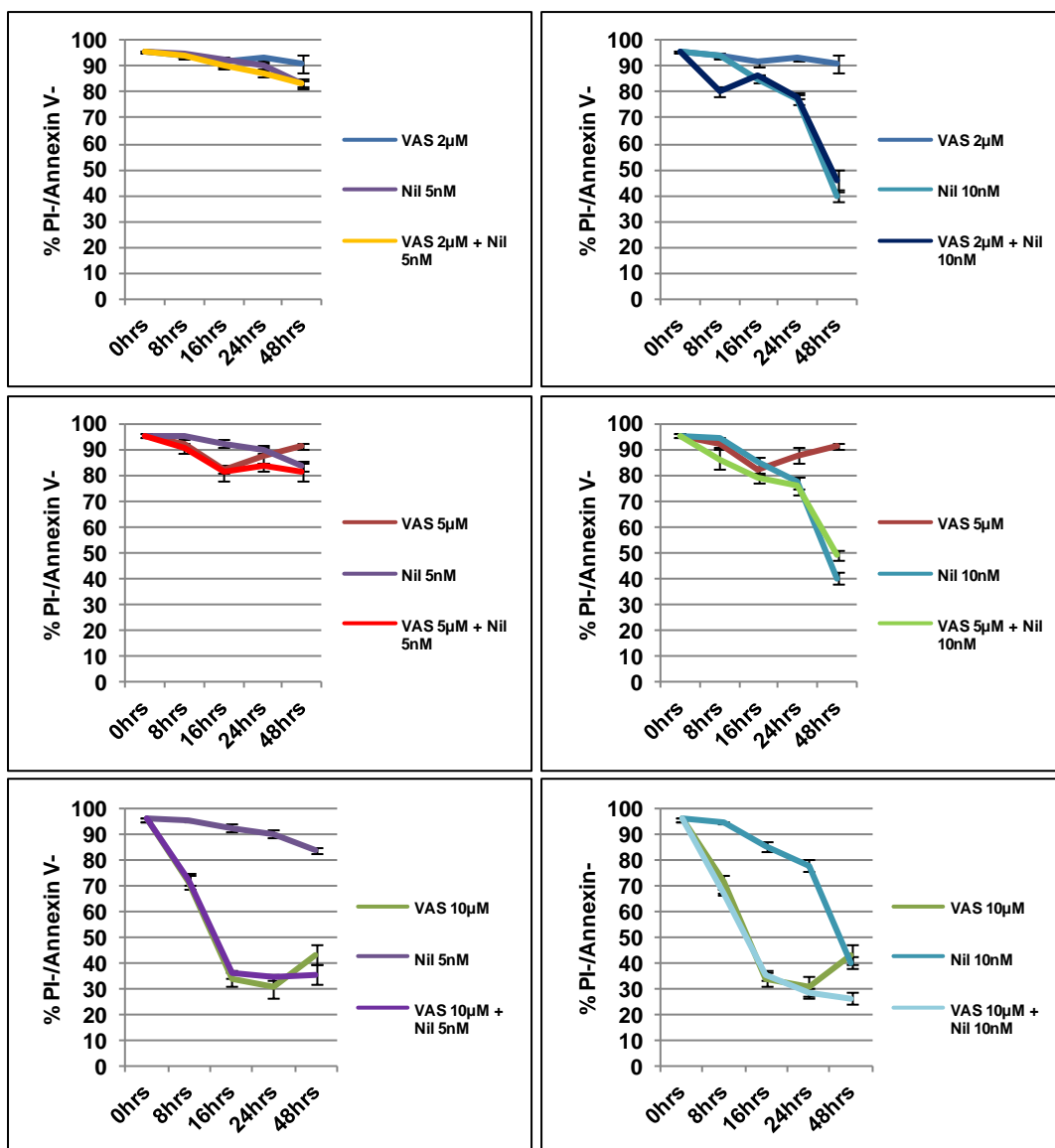
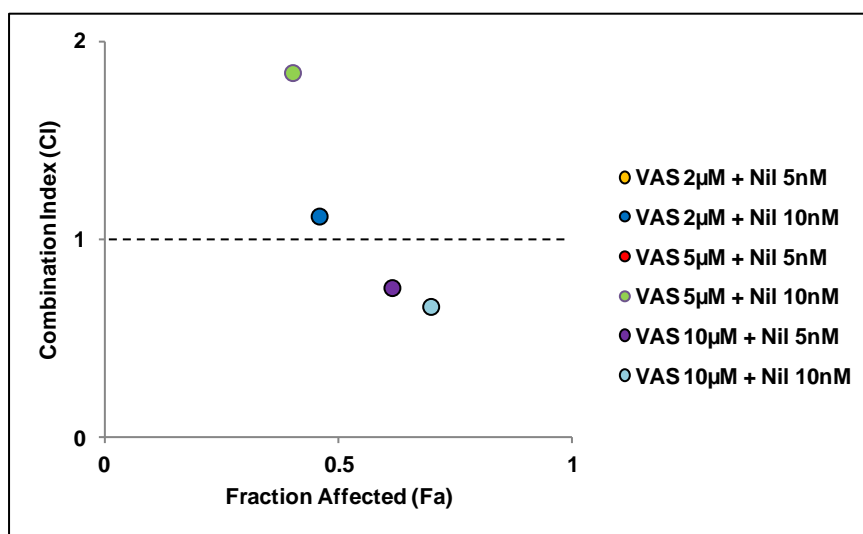


Figure 10a. Combined treatment with both VAS2870 and Nilotinib can produce a synergistic or antagonistic effect on cell viability. K562 cells were simultaneously treated with both VAS2870 (VAS) and Nilotinib (Nil) at varying concentration combinations (VAS + Nil respectively: 2 μ M + 5nM, 2 μ M + 10nM, 5 μ M + 5nM, 5 μ M + 10nM, 10 μ M + 5nM, 10 μ M + 10nM) and were examined at the indicated time-points (8hrs, 16hrs, 24hrs and 48hrs). At each time-point treated cells were incubated with Annexin V-FITC and then stained with propidium iodide (PI) immediately before flow cytometric analysis. The line graph demonstrates the percentage of K562 cells staining negative for both Annexin V and PI. Viability of DMSO vehicle control cells represents 0hrs. Results are expressed as mean \pm SD and are representative of three independent experiments.

(i)



(ii)

Drug Combinations	Fa Value	CI Value
VAS 2µM + Nil 5nM	0.15965	4.77546
VAS 2µM + Nil 10nM	0.45885	1.12332
VAS 5µM + Nil 5nM	0.17585	4.72414
VAS 5µM + Nil 10nM	0.40185	1.84797
VAS 10µM + Nil 5nM	0.61435	0.76209
VAS 10µM + Nil 10nM	0.6972	0.66701

Figure 10b. Combined treatment with both VAS2870 and Nilotinib can produce a synergistic or antagonistic effect on cell viability. K562 cells were simultaneously treated with both VAS2870 (VAS) and Nilotinib (Nil) at varying concentration combinations (VAS + Nil respectively: 2µM + 5nM, 2µM + 10nM, 5µM + 5nM, 5µM + 10nM, 10µM + 5nM, 10µM + 10nM) and were examined at the indicated time-points (8hrs, 16hrs, 24hrs and 48hrs). At 48hrs treated K562 cells were incubated with Annexin V-FITC and then stained with propidium iodide (PI) immediately before flow cytometric analysis. Data was analysed using CompuSyn software to determine if the noted changes in K562 cell viability following combined treatment were synergistic (CI < 1), additive (CI = 1) or antagonistic (CI > 1). (i) A F_a -CI plot for all combinations as determined by CompuSyn software analysis at 48hrs. (ii) Table represents F_a and CI values for each combination.

Examination of the potential of using DPI as a Nox inhibitor in combination with alternative chemotherapeutic drugs

Having established the potential of DPI treatment when used in combination with either Imatinib or Nilotinib, it was of interest to determine if Nox inhibition *via* DPI could be used to increase the effectiveness of chemotherapeutic drugs which do not inhibit Bcr-Abl activity. The aim of this study was to provide a basis for studies which might examine the potential of combined Nox inhibition in the treatment of cancers other than CML. To do this the effects of multiple broad spectrum chemotherapeutic drugs each inducing cell death through a different mechanism of action were examined alone and in combination with DPI treatment.

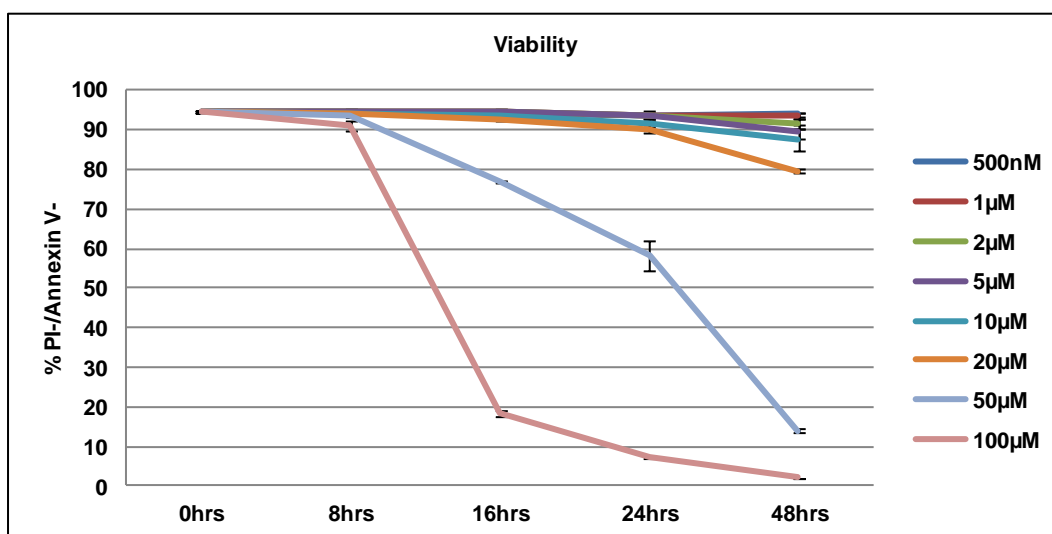
Nox inhibition by VAS2870 was not chosen for this study due to the variable results it produced when used in the previous combination studies. Once again K562 cells were used as a model for these studies. K562 cells express the oncogene Bcr-Abl and are a well established model used in the study of leukaemias, CML in particular. However, Bcr-Abl is the archetypical oncogene and induces its oncogenic effects through mechanisms similarly observed in many other cancers. As a result it was believed that K562 cells could be used as a model to provide an insight into how many other cancers may respond to Nox inhibition *via* DPI treatment in combination with the chosen chemotherapeutics. For each of these chemotherapeutics, the concentrations used in combination with DPI were chosen using the same criteria previously utilised in the Imatinib and Nilotinib studies. Furthermore examination of combined DPI and chemotherapeutic treatment was carried out for each drug using the same methods as before.

Cisplatin

Cisplatin (cis-Diammineplatinum(II) dichloride) is a broad spectrum anti-neoplastic agent containing platinum. This agent elicits its cytotoxic effects by interacting with DNA to form DNA adducts, crosslinking DNA thereby inhibiting DNA repair and synthesis, suppressing RNA transcription, affecting the cell cycle and subsequently inducing apoptosis (Siddik, 2003). Frequently Cisplatin is wrongly designated as an alkylating agent due to its similar mode of action however it does not have an alkyl group.

Treatment of K562 cells with Cisplatin induced significant levels of cell death when used at the higher concentrations (Figure 11a). Furthermore treatment induced a substantial increase in the percentage of cells in S phase as well as a slight increase of cells present in G2/M phase while a reduction in G0/G1 was noted (Figure 11b). Combination studies with Cisplatin and DPI treatment demonstrated interesting results. All treatments containing 20 μ M Cisplatin exhibited an antagonistic effect on cell death yet a considerable degree of synergy was noted in combinations utilising the higher level 50 μ M concentration of Cisplatin (Figure 12a and b). This suggested that higher levels of Cisplatin treatment would be required to induce the desired effect when combined with DPI.

(a)



(b)

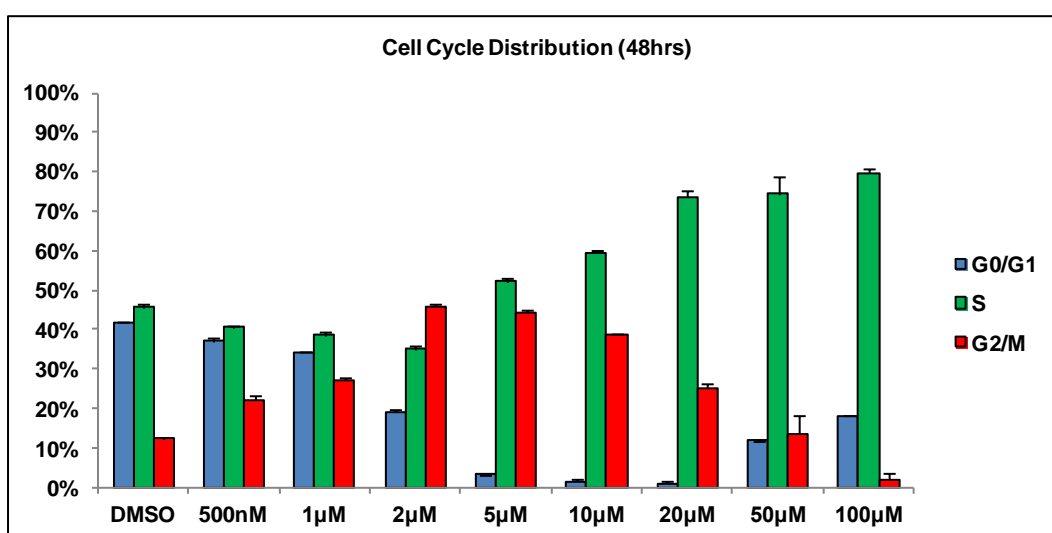


Figure 11. Cisplatin: Determination of optimal concentrations and characterisation of the effects of treatment. K562 cells were treated with increasing concentrations of Cisplatin (500nM, 1µM, 2µM, 5 µM, 10µM, 20µM, 50µM, 100µM) and were examined at the indicated time-points (8hrs, 16hrs, 24hrs and 48hrs). (a) Viability: At each time-point treated cells were incubated with Annexin V-FITC and then stained with propidium iodide (PI) immediately before flow cytometric analysis. The line graph demonstrates the percentage of K562 cells staining negative for both Annexin V and PI. Viability of DMF vehicle control cells represents 0hrs. (b) Cell cycle distribution: At each time-point treated cells were fixed then stained with propidium iodide (PI) before being examined by flow cytometric analysis. The bar chart demonstrates the cell cycle distribution of treated K562 cells as determined by ModFit LT software analysis 48hrs after treatment. Vehicle control is DMF. Cell cycle distribution of treated cells at 48hrs is representative of earlier time-points. Results are expressed as mean \pm SD and are representative of three independent experiments.

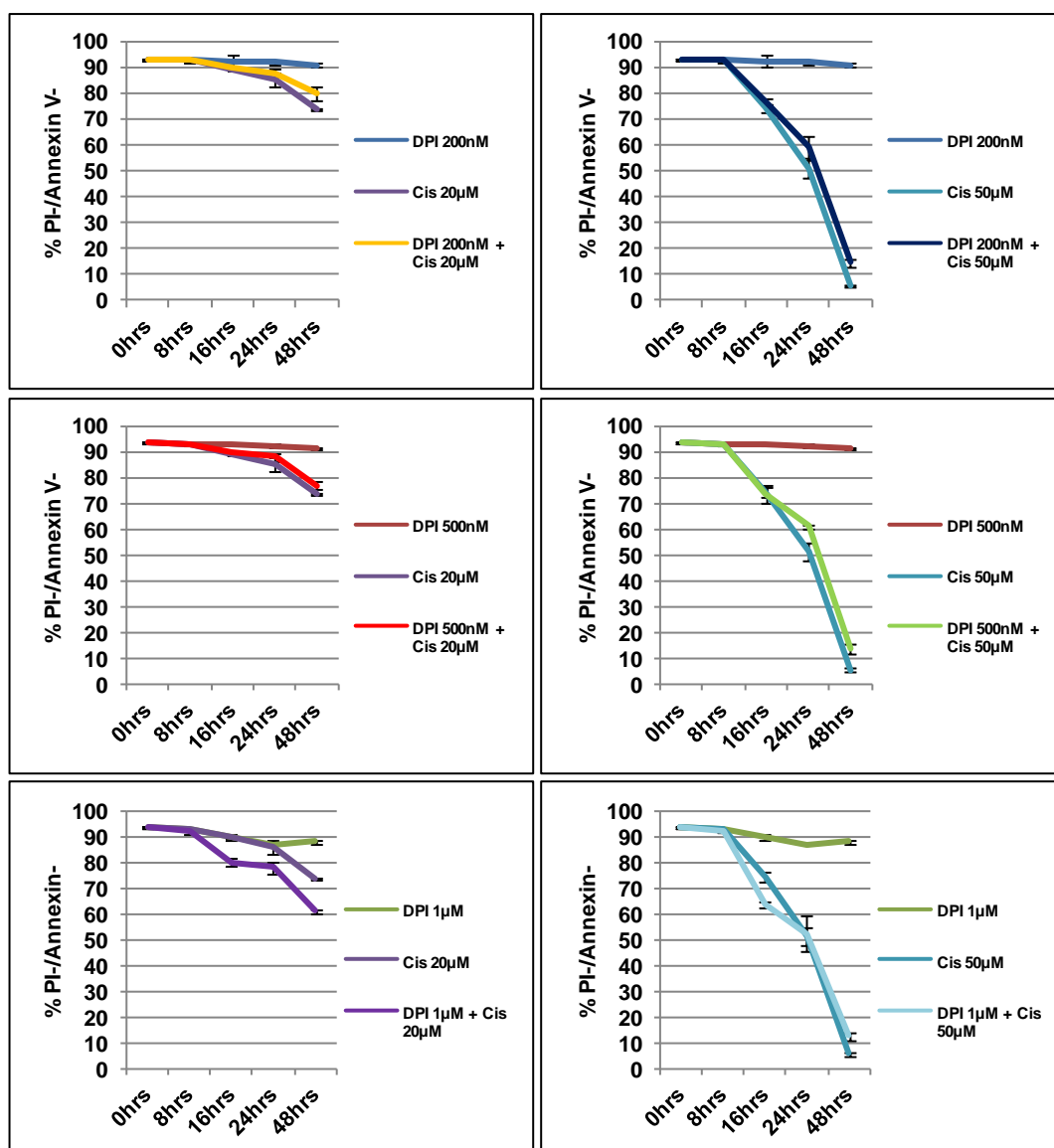
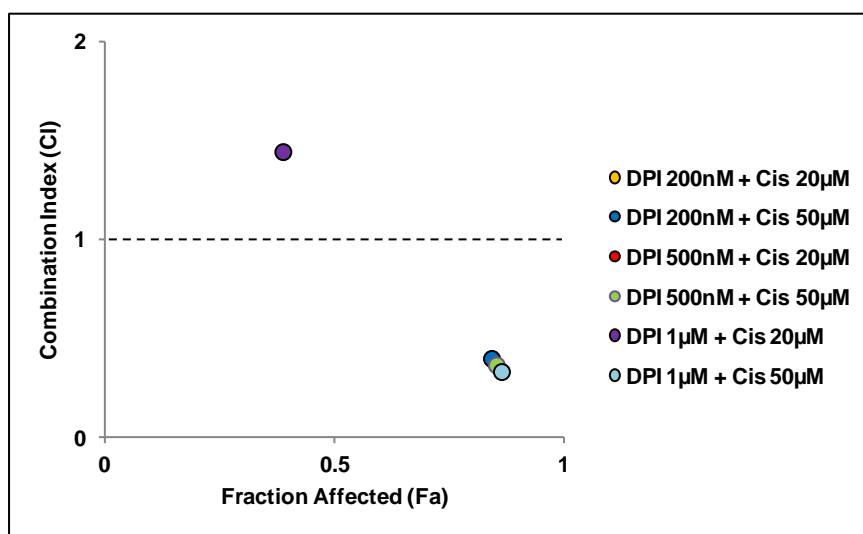


Figure 12a. Combined treatment with both DPI and Cisplatin can produce a synergistic or antagonistic effect on cell viability. K562 cells were simultaneously treated with both DPI and Cisplatin (Cis) at varying concentration combinations (DPI + Cis respectively: 200nM + 20μM, 200nM + 50μM, 500nM + 20μM, 500nM + 50μM, 1μM + 20μM, 1μM + 50μM) and were examined at the indicated time-points (8hrs, 16hrs, 24hrs and 48hrs). At each time-point treated cells were incubated with Annexin V-FITC and then stained with propidium iodide (PI) immediately before flow cytometric analysis. The line graph demonstrates the percentage of K562 cells staining negative for both Annexin V and PI. Viability of DMSO vehicle control cells represents 0hrs. Results are expressed as mean ± SD and are representative of three independent experiments.

(i)



(ii)

Drug Combinations	Fa Value	CI Value
DPI 200nM + Cis 20µM	0.19485	3.89129
DPI 200nM + Cis 50µM	0.8443	0.40434
DPI 500nM + Cis 20µM	0.2282	3.20397
DPI 500nM + Cis 50µM	0.85475	0.37203
DPI 1µM + Cis 20µM	0.38915	1.44875
DPI 1µM + Cis 50µM	0.866	0.3381

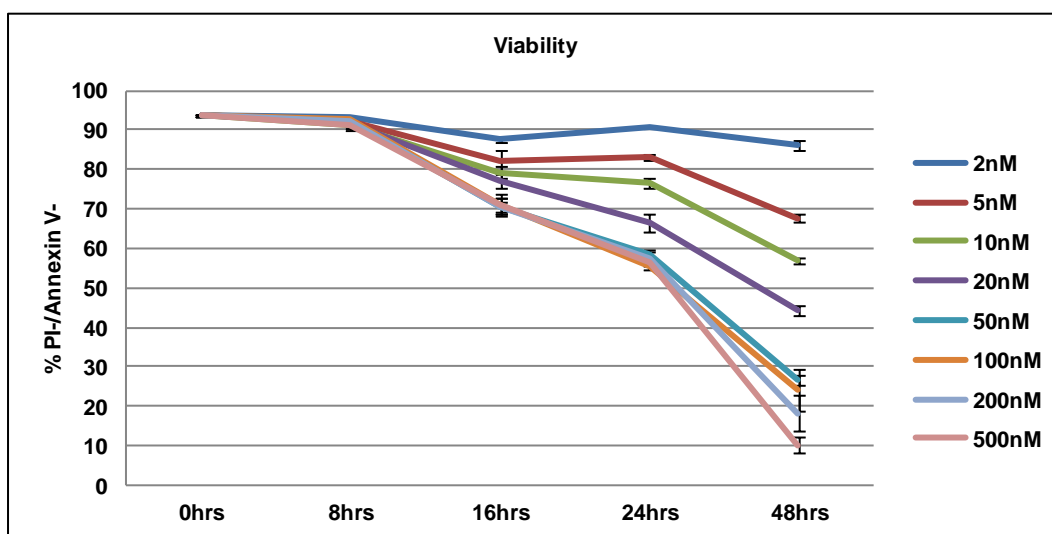
Figure 12b. Combined treatment with both DPI and Cisplatin can produce a synergistic or antagonistic effect on cell viability K562 cells were simultaneously treated with both DPI and Cisplatin (Cis) at varying concentration combinations (DPI + Cis respectively: 200nM + 20µM, 200nM + 50µM, 500nM + 20µM, 500nM + 50µM, 1µM + 20µM, 1µM + 50µM) and were examined at the indicated time-points (8hrs, 16hrs, 24hrs and 48hrs). At 48hrs treated K562 cells were incubated with Annexin V-FITC and then stained with propidium iodide (PI) immediately before flow cytometric analysis. Data was analysed using CompuSyn software to determine if the noted changes in K562 cell viability following combined treatment were synergistic (CI < 1), additive (CI = 1) or antagonistic (CI > 1). (i) A F_a -CI plot for all combinations as determined by CompuSyn software analysis at 48hrs. (ii) Table represents F_a and CI values for each combination.

Docetaxel

Docetaxel is a semi-synthetic analogue of paclitaxel (Taxol), a compound originally isolated from the bark of the rare Pacific yew tree (*Taxus brevifolia*). Both drugs belong to a group of anticancer agents known as taxanes, which bind to and stabilise microtubules, inhibiting mitosis thereby arresting the cell-cycle and subsequently inducing apoptosis (Montero *et al.*, 2005).

Treatment of K562 cells with Docetaxel at each of the concentrations induced significant levels of cell death (Figure 13a). It is interesting to note that the level of cell death directly correlated to the concentration of Docetaxel treatment. Furthermore treatment at all of the concentrations induced a substantial G2 arrest with negligible numbers of cells present in either G0/G1 or S phase (Figure 13b). Combination studies with Docetaxel and DPI treatment gave positive results with all treatments demonstrating a strong additive effect on cell death with one combination (DPI 1 μ M + Doc 2nM) demonstrating synergy (Figure 14a and b).

(a)



(b)

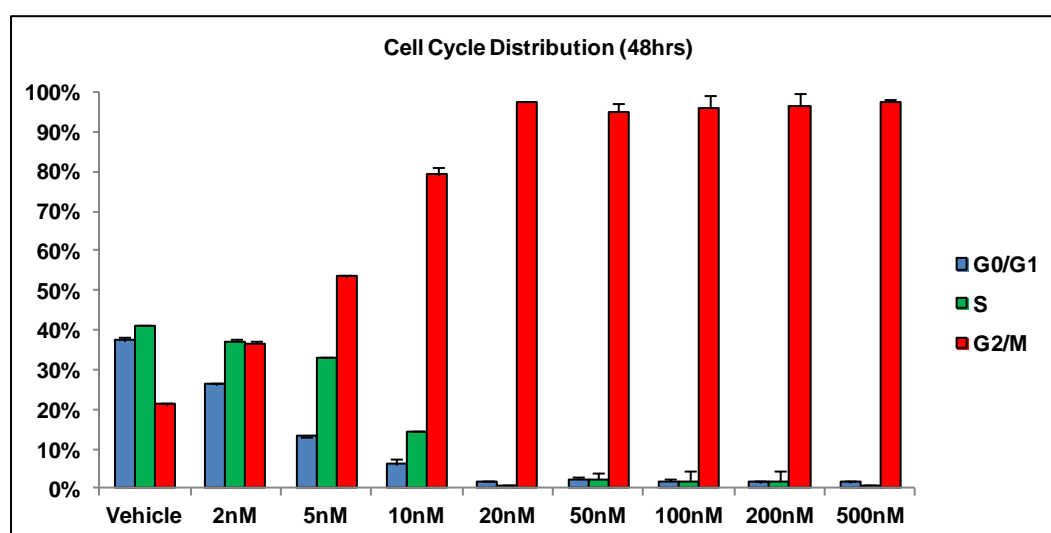


Figure 13. Docetaxel: Determination of optimal concentrations and characterisation of the effects of treatment. K562 cells were treated with increasing concentrations of Docetaxel (2nM, 5nM, 10nM, 20nM, 50nM, 100nM, 200nM, 500nM) and were examined at the indicated time-points (8hrs, 16hrs, 24hrs and 48hrs). (a) Viability: At each time-point treated cells were incubated with Annexin V-FITC and then stained with propidium iodide (PI) immediately before flow cytometric analysis. The line graph demonstrates the percentage of K562 cells staining negative for both Annexin V and PI. Viability of DMSO vehicle control cells represents 0hrs. (b) Cell cycle distribution: At each time-point treated cells were fixed then stained with propidium iodide (PI) before being examined by flow cytometric analysis. The bar chart demonstrates the cell cycle distribution of treated K562 cells as determined by ModFit LT software analysis 48hrs after treatment. Vehicle control is DMSO. Cell cycle distribution of treated cells at 48hrs is representative of earlier time-points. Results are expressed as mean \pm SD and are representative of three independent experiments.

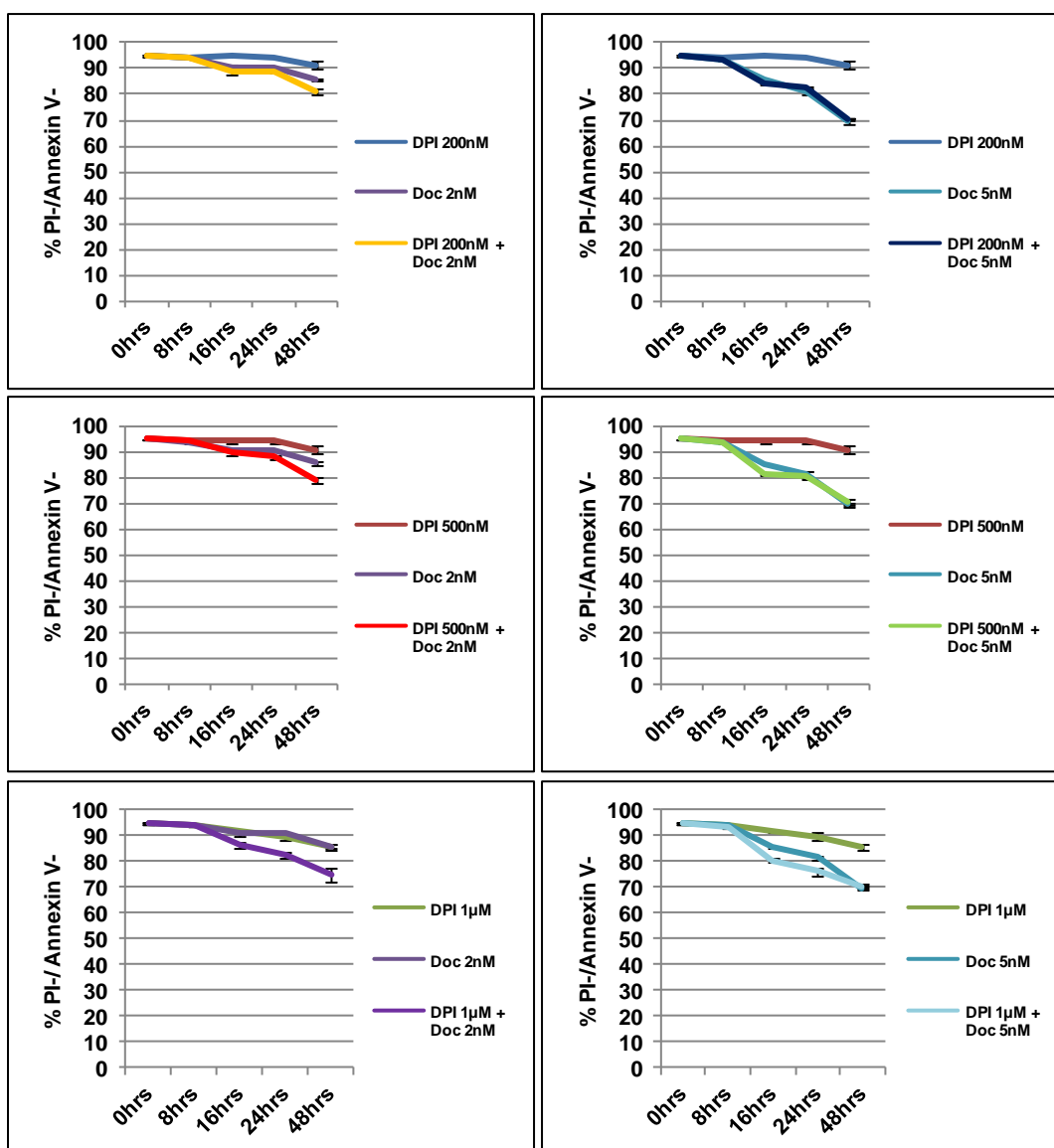
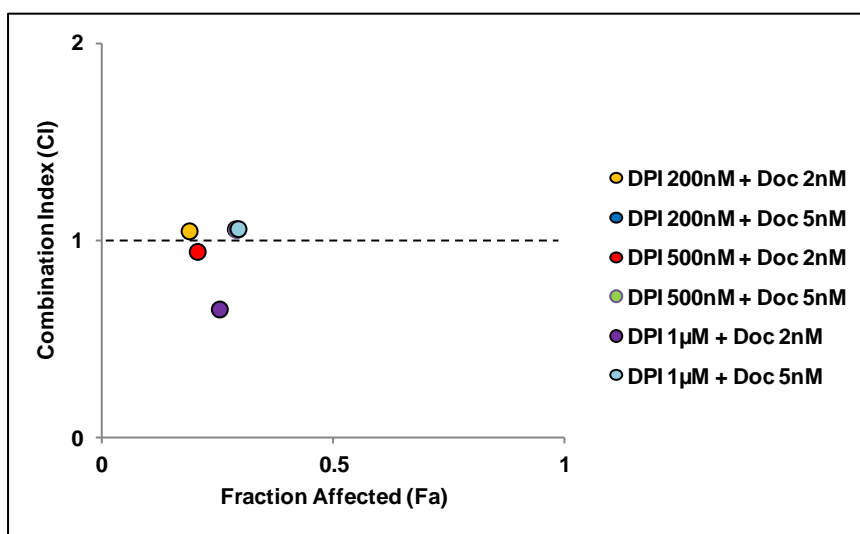


Figure 14a. Combined treatment with both DPI and Docetaxel produces an additive effect on cell viability with some synergy. K562 cells were simultaneously treated with both DPI and Docetaxel (Doc) at varying concentration combinations (DPI + Doc respectively: 200nM + 2nM, 200nM + 5nM, 500nM + 2nM, 500nM + 5nM, 1µM + 2nM, 1µM + 5nM) and were examined at the indicated time-points (8hrs, 16hrs, 24hrs and 48hrs). At each time-point treated cells were incubated with Annexin V-FITC and then stained with propidium iodide (PI) immediately before flow cytometric analysis. The line graph demonstrates the percentage of K562 cells staining negative for both Annexin V and PI. Viability of DMSO vehicle control cells represents 0hrs. Results are expressed as mean \pm SD and are representative of three independent experiments.

(i)



(ii)

Drug Combinations	Fa Value	CI Value
DPI 200nM + Doc 2nM	0.18565	1.04473
DPI 200nM + Doc 5nM	0.2857	1.05462
DPI 500nM + Doc 2nM	0.2032	0.94026
DPI 500nM + Doc 5nM	0.2884	1.05119
DPI 1µM + Doc 2nM	0.251	0.64837
DPI 1µM + Doc 5nM	0.29145	1.05555

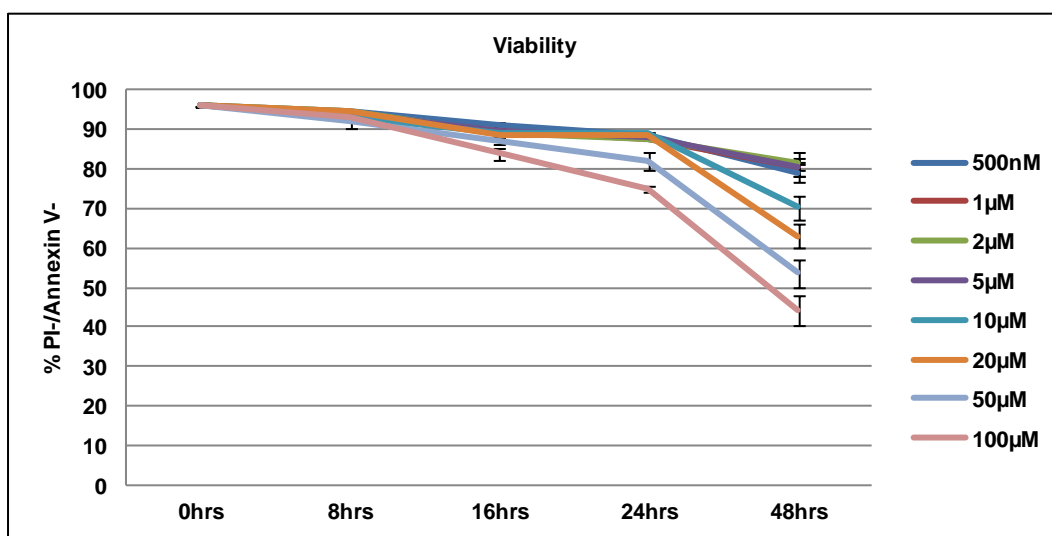
Figure 14b. Combined treatment with both DPI and Docetaxel produces an additive effect on cell viability with some synergy. K562 cells were simultaneously treated with both DPI and Docetaxel (Doc) at varying concentration combinations (DPI + Doc respectively: 200nM + 2nM, 200nM + 5nM, 500nM + 2nM, 500nM + 5nM, 1µM + 2nM, 1µM + 5nM) and were examined at the indicated time-points (8hrs, 16hrs, 24hrs and 48hrs). At 48hrs treated K562 cells were incubated with Annexin V-FITC and then stained with propidium iodide (PI) immediately before flow cytometric analysis. Data was analysed using CompuSyn software to determine if the noted changes in K562 cell viability following combined treatment were synergistic ($CI < 1$), additive ($CI = 1$) or antagonistic ($CI > 1$). (i) A F_a -CI plot for all combinations as determined by CompuSyn software analysis at 48hrs. (ii) Table represents F_a and CI values for each combination.

Etoposide

Etoposide is a semi-synthetic derivative of podophyllotoxin (podofilox), a substance originally extracted from the root of the plant *Podophyllum peltatum*. Etoposide is a potent anti-neoplastic agent eliciting its effects by binding to and inhibiting Topoisomerase II, resulting in the accumulation of DNA single- or double-strand breaks, the inhibition of DNA replication and transcription, followed by eventual apoptotic cell death (Nitiss, 2009).

All concentrations of Etoposide used to treat K562 cells induced significant levels of cell death by 48hrs (Figure 15a). It is interesting to note that the level of cell death induced by all concentrations below 5 μ M demonstrated comparable reductions while treatments of 10 μ M and above induced levels of cell death which directly correlated with Etoposide concentration. Furthermore treatment of K562 cells with lower concentrations of Etoposide (500nM, 1 μ M and 2 μ M) induced substantial increases in the percentage of cells present in G2/M phase while treatment with higher concentrations produced an increase in cells present in S phase (Figure 15b). All treatments induced a considerable reduction in the percentage of cells present in G0/G1. Combination studies with Etoposide and DPI treatment gave varied results with four of the six combinations demonstrating strong antagonism, while the combinations of DPI 200nM + Etop 20 μ M and DPI 1 μ M + Etop 20 μ M both demonstrated synergy (Figure 16a and b).

(a)



(b)

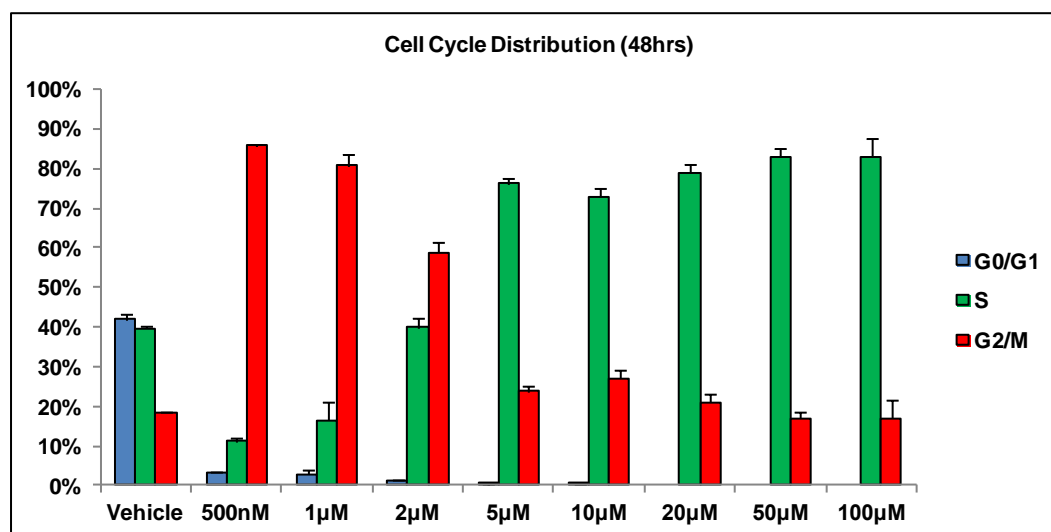


Figure 15. Etoposide: Determination of optimal concentrations and characterisation of the effects of treatment. K562 cells were treated with increasing concentrations of Etoposide (500nM, 1µM, 2µM, 5 µM, 10µM, 20µM, 50µM, 100µM) and were examined at the indicated time-points (8hrs, 16hrs, 24hrs and 48hrs). (a) Viability: At each time-point treated cells were incubated with Annexin V-FITC and then stained with propidium iodide (PI) immediately before flow cytometric analysis. The line graph demonstrates the percentage of K562 cells staining negative for both Annexin V and PI. Viability of DMSO vehicle control cells represents 0hrs. (b) Cell cycle distribution: At each time-point treated cells were fixed then stained with propidium iodide (PI) before being examined by flow cytometric analysis. The bar chart demonstrates the cell cycle distribution of treated K562 cells as determined by ModFit LT software analysis 48hrs after treatment. Vehicle control is DMSO. Cell cycle distribution of treated cells at 48hrs is representative of earlier time-points. Results are expressed as mean \pm SD and are representative of three independent experiments.

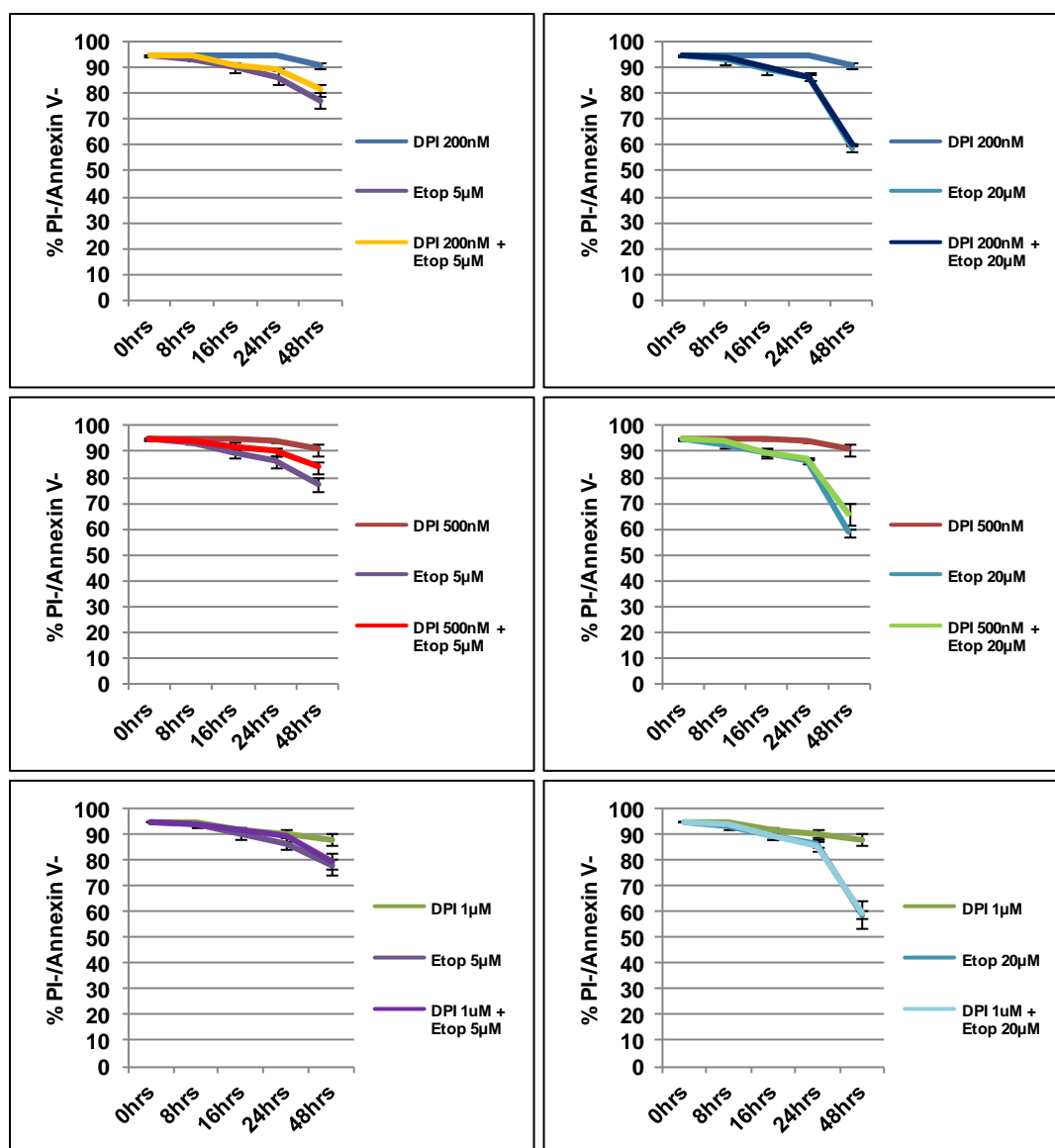
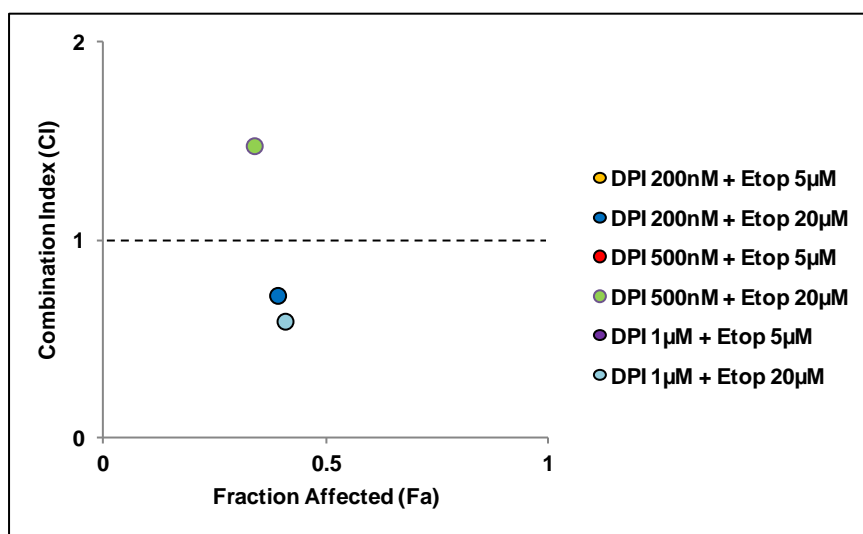


Figure 16a. Combined treatment with both DPI and Etoposide produces a significant antagonistic effect on cell viability with some synergy. K562 cells were simultaneously treated with both DPI and Etoposide (Etop) at varying concentration combinations (DPI + Etop respectively: 200nM + 5µM, 200nM + 20µM, 500nM + 5µM, 500nM + 20µM, 1µM + 5µM, 1µM + 20µM) and were examined at the indicated time-points (8hrs, 16hrs, 24hrs and 48hrs). At each time-point treated cells were incubated with Annexin V-FITC and then stained with propidium iodide (PI) immediately before flow cytometric analysis. The line graph demonstrates the percentage of K562 cells staining negative for both Annexin V and PI. Viability of DMSO vehicle control cells represents 0hrs. Results are expressed as mean \pm SD and are representative of three independent experiments.

(i)



(ii)

Drug Combinations	Fa Value	CI Value
DPI 200nM + Etop 5µM	0.17815	5.40054
DPI 200nM + Etop 20µM	0.38975	0.71743
DPI 500nM + Etop 5µM	0.15825	8.60447
DPI 500nM + Etop 20µM	0.33715	1.47618
DPI 1µM + Etop 5µM	0.1993	3.69068
DPI 1µM + Etop 20µM	0.4065	0.58653

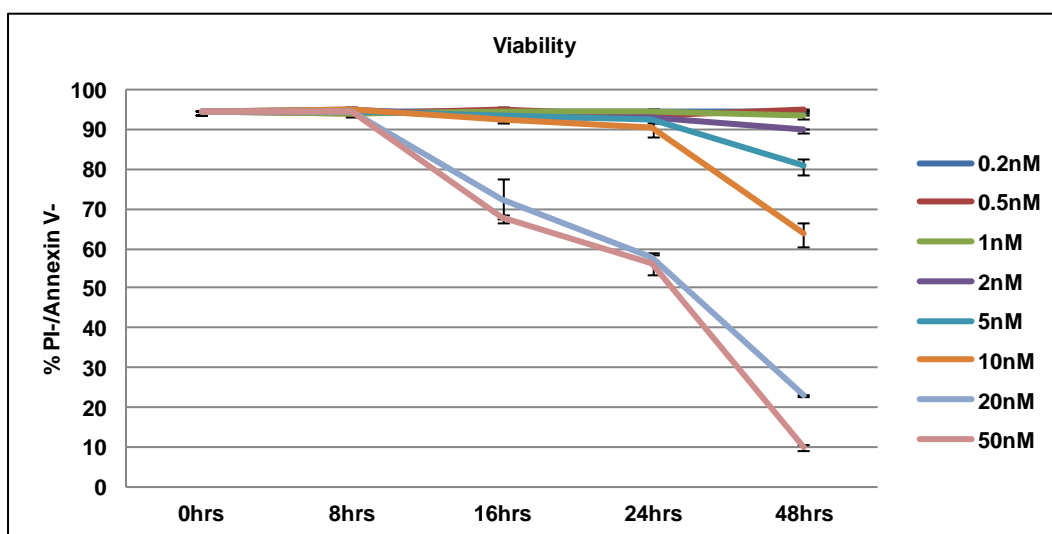
Figure 16b. Combined treatment with both DPI and Etoposide produces a very significant antagonistic effect on cell viability with some synergy. K562 cells were simultaneously treated with both DPI and Etoposide (Etop) at varying concentration combinations (DPI + Etop respectively: 200nM + 5µM, 200nM + 20µM, 500nM + 5µM, 500nM + 20µM, 1µM + 5µM, 1µM + 20µM) and were examined at the indicated time-points (8hrs, 16hrs, 24hrs and 48hrs). At 48hrs treated K562 cells were incubated with Annexin V-FITC and then stained with propidium iodide (PI) immediately before flow cytometric analysis. Data was analysed using CompuSyn software to determine if the noted changes in K562 cell viability following combined treatment were synergistic ($CI < 1$), additive ($CI = 1$) or antagonistic ($CI > 1$). (i) A F_a -CI plot for all combinations as determined by CompuSyn software analysis at 48hrs. (ii) Table represents F_a and CI values for each combination.

Actinomycin D

Actinomycin D is a polypeptide antibiotic isolated from a soil bacterium found in the genus *Streptomyces*. This antibiotic elicits its cytotoxic effects by binding DNA at transcription sites, preventing elongation of the RNA chain by RNA polymerase thereby inhibiting transcription and subsequent protein synthesis (Sobell 1985). Furthermore this antibiotic is also suggested to affect the activity of Topoisomerase I and II (Koba and Konopa, 2005).

Treatment of K562 cells with Actinomycin D at each of the concentrations above 2nM induced significant levels of cell death (Figure 17a). As with the previous chemotherapeutics the level of cell death directly correlated to the concentration of treatment. Interestingly treatment of K562 cells with Actinomycin D produced varying degrees of effect on cell cycle distribution over 48hrs. The highest concentrations of Actinomycin D (20nM and 50nM) induced an increase in the percentage of cells present in G₀/G₁ phase and a decrease in G₂/M, while treatments of 5nM and 10nM demonstrated the complete opposite result (Figure 17b). Concentrations below these values produced no significant change to cell cycle distribution. Furthermore increases in the percentage of cells present in S phase were not observed prior to 48hrs. All six Actinomycin D and DPI combination treatments demonstrated additive effects (Figure 18a and b). While four of these demonstrated a strong additive effect, the DPI 200nM + ActD 5nM and DPI 500nM + ActD 5nM combinations demonstrated a minor level of antagonism.

(a)



(b)

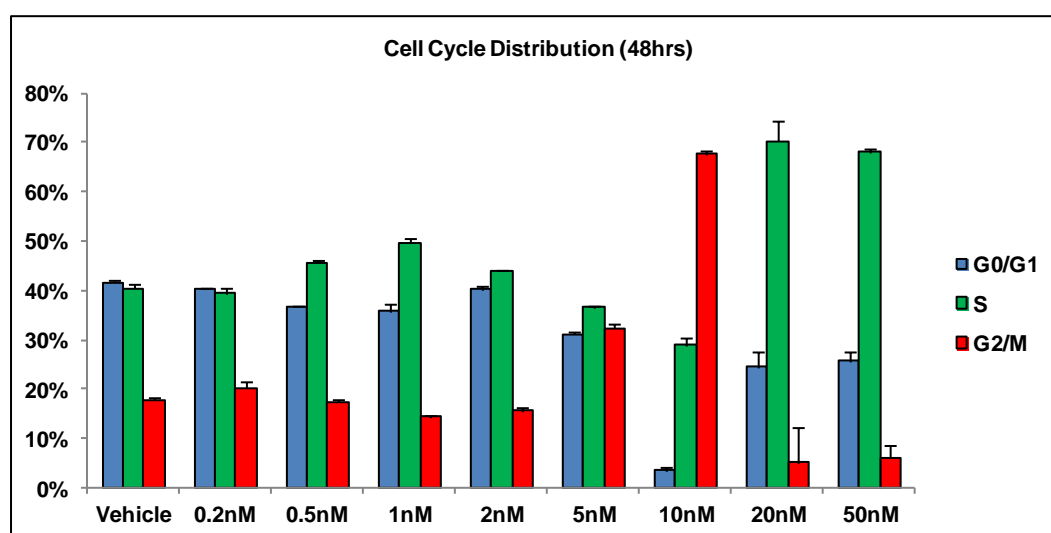


Figure 17. Actinomycin D: Determination of optimal concentrations and characterisation of the effects of treatment. K562 cells were treated with increasing concentrations of Actinomycin D (0.2nM, 0.5nM, 1nM, 2nM, 5nM, 10nM, 20nM, 50nM) and were examined at the indicated time-points (8hrs, 16hrs, 24hrs and 48hrs). (a) Viability: At each time-point treated cells were incubated with Annexin V-FITC and then stained with propidium iodide (PI) immediately before flow cytometric analysis. The line graph demonstrates the percentage of K562 cells staining negative for both Annexin V and PI. Viability of DMSO vehicle control cells represents 0hrs. (b) Cell cycle distribution: At each time-point treated cells were fixed then stained with propidium iodide (PI) before being examined by flow cytometric analysis. The bar chart demonstrates the cell cycle distribution of treated K562 cells as determined by ModFit LT software analysis 48hrs after treatment. Vehicle control is DMSO. Cell cycle distribution of treated cells at 48hrs is representative of earlier time-points. Results are expressed as mean \pm SD and are representative of three independent experiments.

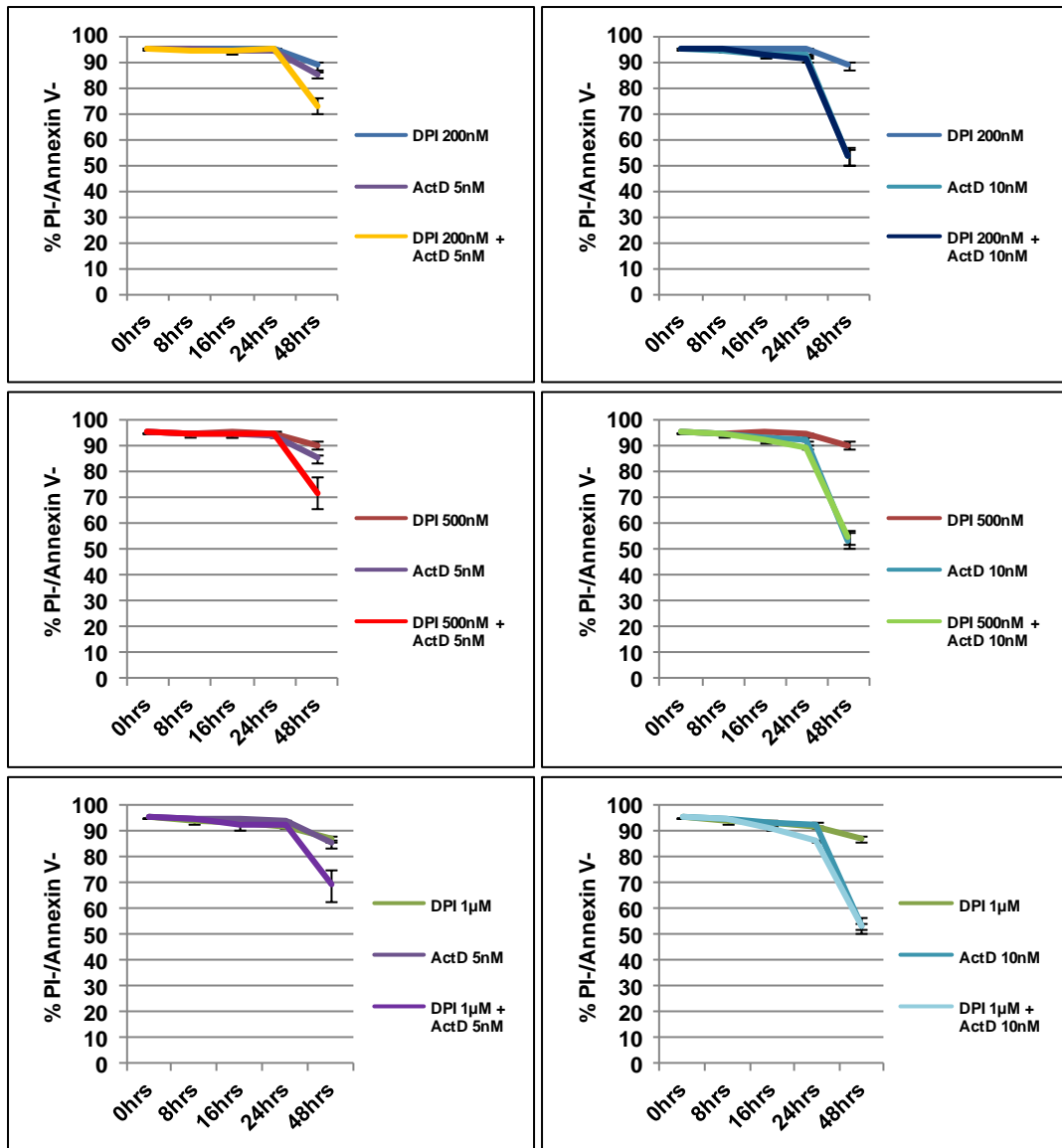
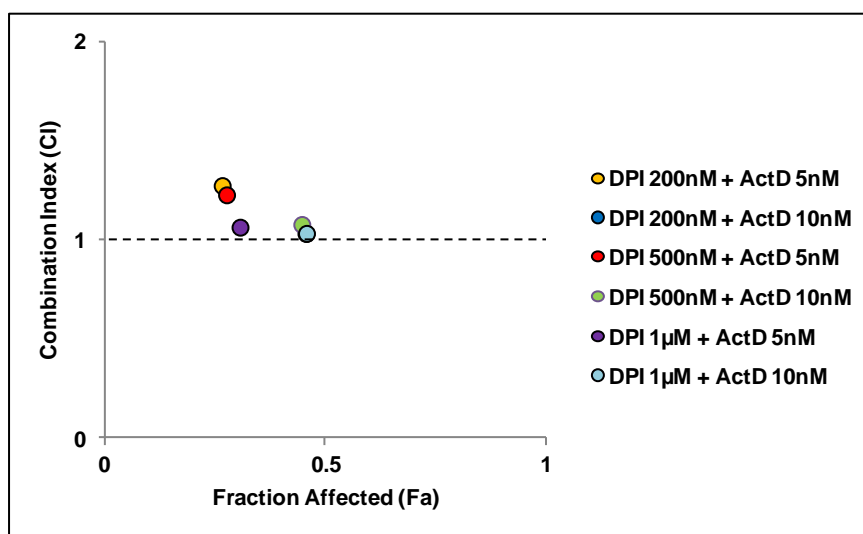


Figure 18a. Combined treatment with both DPI and Acintinomycin D produces an additive effect on cell viability with a minor level of antagonism. K562 cells were simultaneously treated with both DPI and Actinomycin D (ActD) at varying concentration combinations (DPI + ActD respectively: 200nM + 5nM, 200nM + 10nM, 500nM + 5nM, 500nM + 10nM, 1µM + 5nM, 1µM + 10nM) and were examined at the indicated time-points (8hrs, 16hrs, 24hrs and 48hrs). At each time-point treated cells were incubated with Annexin V-FITC and then stained with propidium iodide (PI) immediately before flow cytometric analysis. The line graph demonstrates the percentage of K562 cells staining negative for both Annexin V and PI. Viability of DMSO vehicle control cells represents 0hrs. Results are expressed as mean \pm SD and are representative of three independent experiments.

(i)



(ii)

Drug Combinations	Fa Value	CI Value
DPI 200nM + ActD 5nM	0.2669	1.27724
DPI 200nM + ActD 10nM	0.45675	1.0356
DPI 500nM + ActD 5nM	0.2768	1.23062
DPI 500nM + ActD 10nM	0.44735	1.08088
DPI 1µM + ActD 5nM	0.30735	1.0672
DPI 1µM + ActD 10nM	0.45795	1.03606

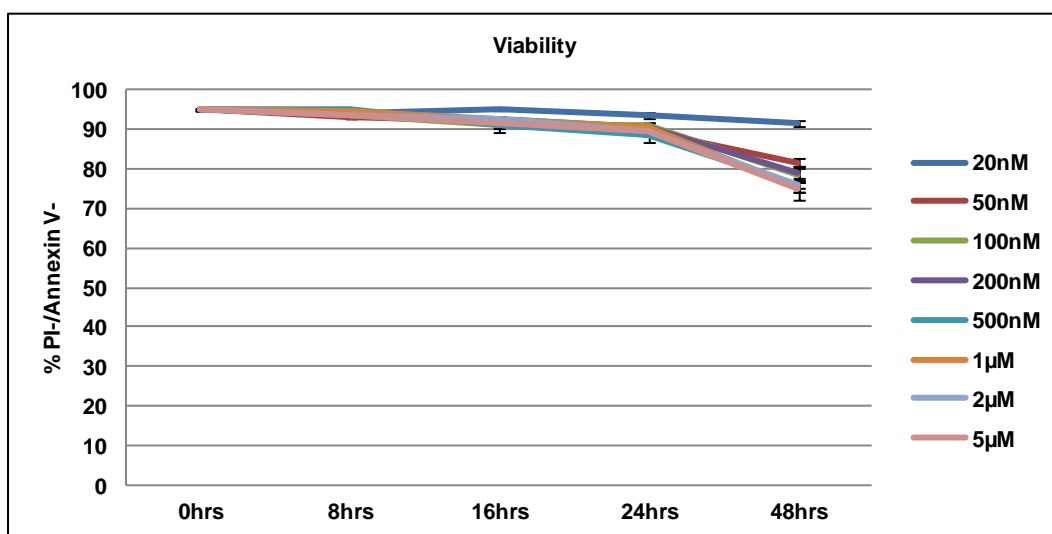
Figure 18b. Combined treatment with both DPI and Acintinomycin D produces an additive effect on cell viability with a minor level of antagonism. K562 cells were simultaneously treated with both DPI and Actinomycin D (ActD) at varying concentration combinations (DPI + ActD respectively: 200nM + 5nM, 200nM + 10nM, 500nM + 5nM, 500nM + 10nM, 1µM + 5nM, 1µM + 10nM) and were examined at the indicated time-points (8hrs, 16hrs, 24hrs and 48hrs). At 48hrs treated K562 cells were incubated with Annexin V-FITC and then stained with propidium iodide (PI) immediately before flow cytometric analysis. Data was analysed using CompuSyn software to determine if the noted changes in K562 cell viability following combined treatment were synergistic ($CI < 1$), additive ($CI = 1$) or antagonistic ($CI > 1$). (i) A F_a -CI plot for all combinations as determined by CompuSyn software analysis at 48hrs. (ii) Table represents F_a and CI values for each combination.

Methotrexate

Methotrexate is a chemical analogue of folic acid which induces the inhibition of dihydrofolate reductase at a high affinity, preventing the synthesis of purines and pyrimidines due to the subsequent depletion of tetrahydrofolates (Abolmaali *et al.*, 2013). Without purines and pyrimidines many metabolic processes are interrupted, most importantly DNA and RNA cannot be synthesised inducing cell cycle arrest and apoptosis of cells.

Treatment of K562 cells with Methotrexate at all concentrations induced some degree of cell death however the level of death observed was significantly lower than with any of the previously studied chemotherapeutics (Figure 19a). Furthermore all concentrations of Methotrexate at or above 100nM induced a substantial increase in the percentage of cells present in G0/G1 accompanied by a significant decrease of cells present in G2/M (Figure 19b). Interesting treatment with 20nM and 50nM increased the percentage of cells present in S phase. Rather significantly all Methotrexate and DPI combination treatments produced a synergistic effect on cell death (Figure 20a and b). With the exception of one of these combinations (DPI 1 μ M + Met 1 μ M 2nM) calculated CI values were the lowest of all the previous combination studies carried out demonstrating a high potential for combined Methotrexate and Nox inhibition in cancer treatment.

(a)



(b)

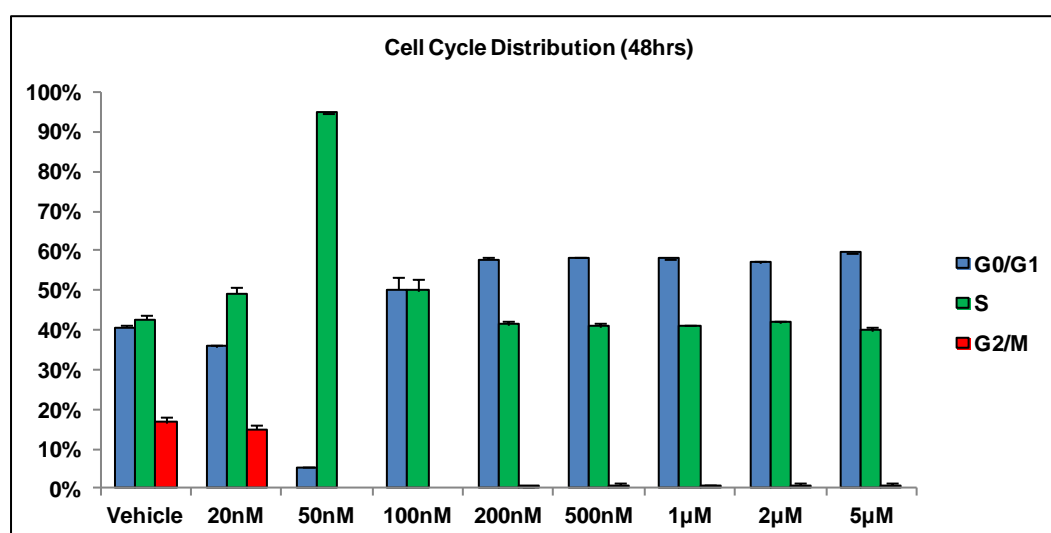


Figure 19. Methotrexate: Determination of optimal concentrations and characterisation of the effects of treatment. K562 cells were treated with increasing concentrations of Methotrexate (20nM, 50nM, 100nM, 200nM, 500nM, 1µM, 2µM, 5µM) and were examined at the indicated time-points (8hrs, 16hrs, 24hrs and 48hrs). (a) Viability: At each time-point treated cells were incubated with Annexin V-FITC and then stained with propidium iodide (PI) immediately before flow cytometric analysis. The line graph demonstrates the percentage of K562 cells staining negative for both Annexin V and PI. Viability of DMSO vehicle control cells represents 0hrs. (b) Cell cycle distribution: At each time-point treated cells were fixed then stained with propidium iodide (PI) before being examined by flow cytometric analysis. The bar chart demonstrates the cell cycle distribution of treated K562 cells as determined by ModFit LT software analysis 48hrs after treatment. Vehicle control is DMSO. Cell cycle distribution of treated cells at 48hrs is representative of earlier time-points. Results are expressed as mean \pm SD and are representative of three independent experiments.

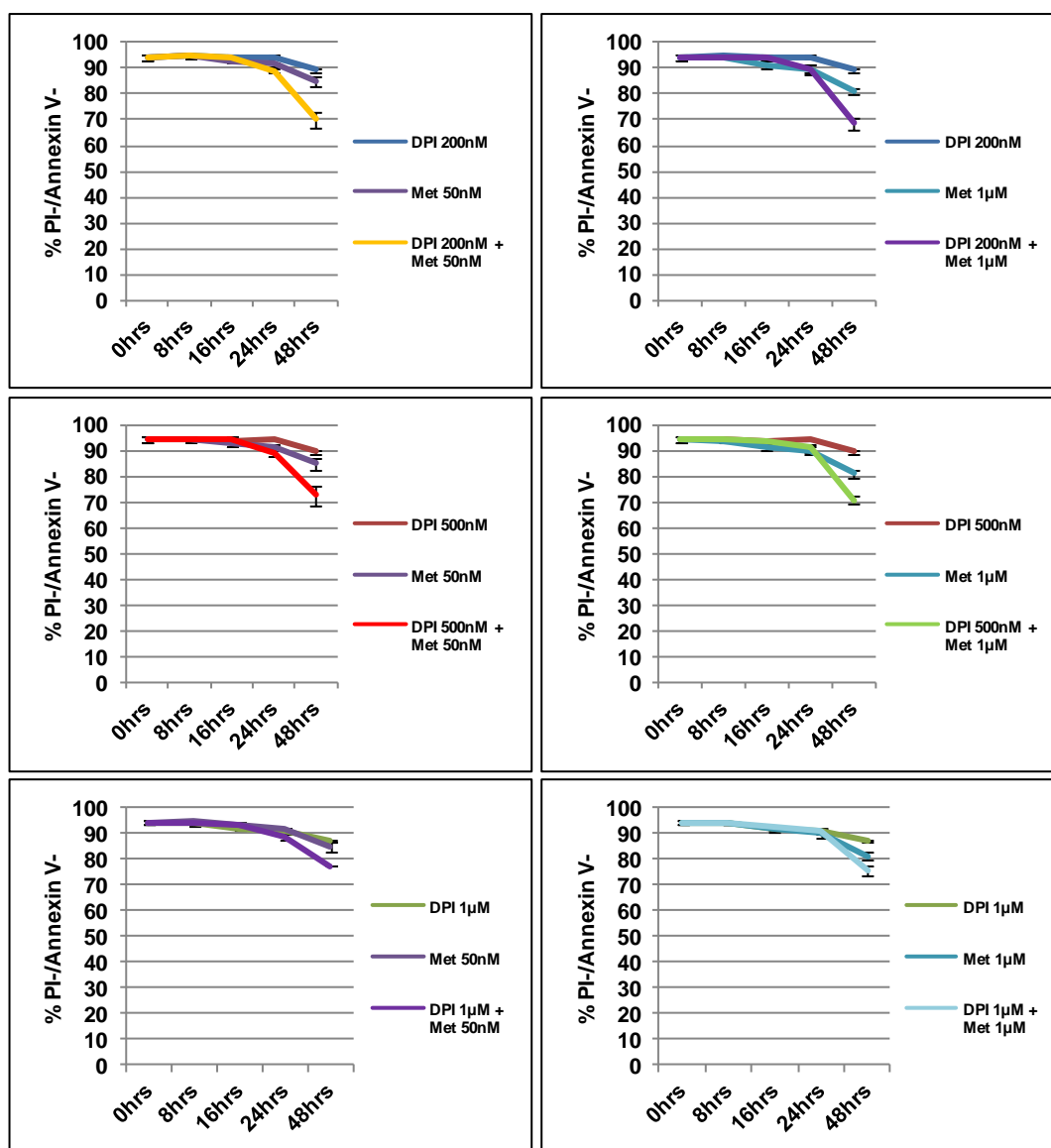
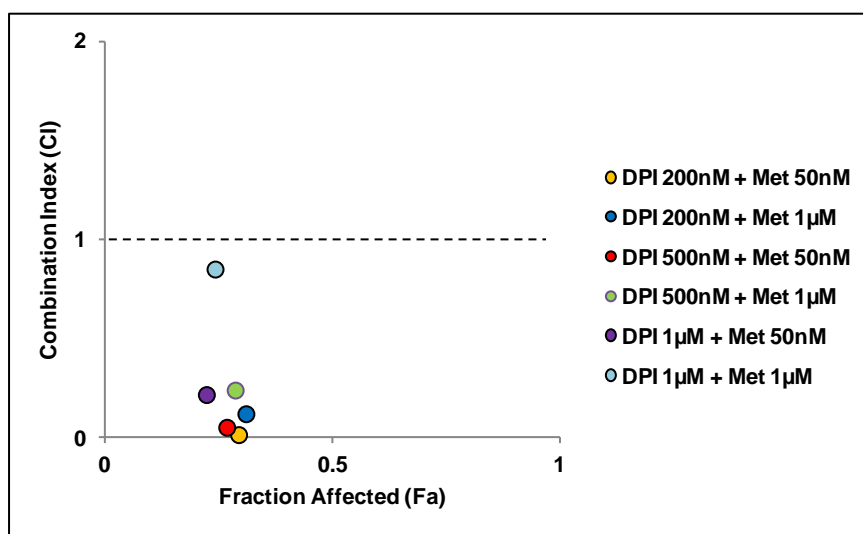


Figure 20a. Combined treatment with both DPI and Methotrexate synergistically decreases cell viability. K562 cells were simultaneously treated with both DPI and Methotrexate (Met) at varying concentration combinations (DPI + Met respectively: 200nM + 50nM, 200nM + 1µM, 500nM + 50nM, 500nM + 1µM, 1µM + 50nM, 1µM + 1µM) and were examined at the indicated time-points (8hrs, 16hrs, 24hrs and 48hrs). At each time-point treated cells were incubated with Annexin V-FITC and then stained with propidium iodide (PI) immediately before flow cytometric analysis. The line graph demonstrates the percentage of K562 cells staining negative for both Annexin V and PI. Viability of DMSO vehicle control cells represents 0hrs. Results are expressed as mean \pm SD and are representative of three independent experiments.

(i)



(ii)

Drug Combinations	Fa Value	CI Value
DPI 200nM + Met 50nM	0.2954	0.01956
DPI 200nM + Met 1µM	0.31145	0.12507
DPI 500nM + Met 50nM	0.26925	0.05672
DPI 500nM + Met 1µM	0.28785	0.24454
DPI 1µM + Met 50nM	0.2244	0.22185
DPI 1µM + Met 1µM	0.2435	0.85559

Figure 20b. Combined treatment with both DPI and Methotrexate synergistically decreases cell viability. K562 cells were simultaneously treated with both DPI and Methotrexate (Met) at varying concentration combinations (DPI + Met respectively: 200nM + 50nM, 200nM + 1µM, 500nM + 50nM, 500nM + 1µM, 1µM + 50nM, 1µM + 1µM) and were examined at the indicated time-points (8hrs, 16hrs, 24hrs and 48hrs). At 48hrs treated K562 cells were incubated with Annexin V-FITC and then stained with propidium iodide (PI) immediately before flow cytometric analysis. Data was analysed using CompuSyn software to determine if the noted changes in K562 cell viability following combined treatment were synergistic (CI < 1), additive (CI = 1) or antagonistic (CI > 1). (i) A F_a -CI plot for all combinations as determined by CompuSyn software analysis at 48hrs. (ii) Table represents F_a and CI values for each combination.

Discussion

Since the development of Imatinib there has been a huge improvement in the treatment of CML. Unfortunately, Imatinib treatment does not completely eradicate the entire leukaemic cell population, leaving residual disease. As a result continued, lifelong treatment is required to avoid the risk of active disease re-establishing. Furthermore, with continual treatment there is a high probability of drug resistance developing. To address these issues several novel TKIs specific for Bcr-Abl have been developed in recent years however they have failed to overcome these underlining issues (Quintás-Cardama *et al.*, 2007; Bixby and Talpaz 2011). Treatments utilising Bcr-Abl inhibition *via* Imatinib in combination with chemotherapeutic agents have been studied as an approach to overcome these obstacles (Gu *et al.*, 2005; Tseng *et al.*, 2005; Giallongo *et al.*, 2011; Bonifacio *et al.*, 2012). Similarly rather than using broad spectrum drugs much research is now focused on the simultaneous targeting of Bcr-Abl in combination with pathways identified as important in CML maintenance and progression (Helgason *et al.*, 2011; O'Hare *et al.*, 2012).

Landry *et al.* (2013) established a link between Bcr-Abl signalling and the generation of Nox-derived ROS, while additional studies demonstrated an importance for these proteins in CML pathogenesis. Furthermore, inhibition of Nox activity significantly increased the effectiveness of Imatinib treatment, identifying Nox proteins as potential therapeutic targets in CML. Unfortunately these studies utilised siRNA to inhibit Nox activity, an approach not currently feasible for patient treatment (Gavrilova and Saltzman, 2012). This study set out to determine if pharmacological inhibition of Nox proteins demonstrated similar therapeutic potential when used in combination with Bcr-Abl inhibitors. As demonstrated, DPI

was used to inhibit Nox protein activity in combination with either Imatinib or Nilotinib (Figure 3 and Figure 7). Rather significantly these studies corresponded with the previous study whereby inhibition of Nox activity *via* p22phox knockdown significantly increased the effectiveness of Bcr-Abl inhibition (Chapter 4, Figure 11). Combined treatment demonstrated a substantial and synergistic increase in cell death through augmentation of apoptosis (Figure 4 and Figure 5). This further emphasised the importance of Nox activity in CML and demonstrated its potential as a therapeutic in CML treatments.

As discussed one of the major obstacles in the advancement of CML treatment is persistence of residual disease despite continual TKI treatment. Interestingly, CML leukaemic stem cells (LSCs), classified by expression of CD34⁺CD38⁻ surface markers, are capable of surviving independent of Bcr-Abl kinase activity and are believed to be the source of residual disease (Hamilton *et al.*, 2011). Interestingly, Nox-derived ROS is known to play important roles in haematopoiesis and hematopoietic growth factor signaling under normal conditions (Sattler *et al.*, 1999; Zhu *et al.*, 2005; Sardina *et al.*, 2011; Hole *et al.*, 2011). Furthermore, Nox protein activity has been identified as a major source of ROS in healthy CD34⁺CD38⁻ haematopoietic stem cells (HSCs) (Piccoli *et al.*, 2007) while also being demonstrated as important in the preservation of the CD34⁺ cell population (Fan *et al.*, 2007). Although these studies were carried out in HSCs they still highlight an important role for Nox activity, suggesting that deregulation of these processes through Nox inhibition could be therapeutically significant in the removal of LSCs and therefore residual disease in CML. Proper assessment of Nox inhibition on CML LSCs would have required examination of CD34⁺CD38⁻ cells obtained from CML patients, which was beyond the scope of this project. However

considering the effectiveness of combined Nox and Bcr-Abl treatment on K562 cells coupled with the established role for Nox proteins in HPCs, there is a strong degree of evidence to suggest the potential of Nox inhibition in eradicating residual disease when combined with Bcr-Abl inhibition.

In addition to residual disease, the development of resistance has become an increasing concern for CML treatment. It is well established that ROS are a key factor in development of genomic instability, which has been repeatedly highlighted for its role in the development of TKI resistance in CML as well as disease progression into Blast phase (CML-BP) (Nowicki *et al.*, 2004; Koptyra *et al.*, 2006; Rassool *et al.*, 2007; Sallmyr *et al.*, 2008; Slupianek *et al.*, 2011; Chakraborty *et al.*, 2012; Nieborowska-Skorska *et al.*, 2012). Furthermore, it is of interest to note that the generation of genomic instability has also been linked to Nox-derived ROS in other cancers (Weyemi *et al.*, 2012a; Weyemi *et al.*, 2012b). Taking this information into account the potential for Nox inhibitors in reducing the development of drug resistance when used in combination with Bcr-Abl TKIs is evident. Considering the effectiveness of DPI in combination with Bcr-Abl inhibition, coupled with the possible roles in reducing residual disease and the development of resistance, this work has identified great potential for the use of Nox inhibitors in the treatment of CML.

Both Imatinib and Nilotinib selectively inhibit Bcr-Abl by interacting with the ATP-binding site of the Abl kinase domain (Schindler *et al.*, 2000; Nagar *et al.*, 2002; Weisberg *et al.*, 2005). Therefore the similar degree of synergy demonstrated by both drugs when used in combination with DPI was to be expected. In contrast to this, the use of another Nox inhibitor, VAS2870, induced contrasting results to the combinations studies which utilised DPI. When used in combination with either

Imatinib or Nilotinib, lower concentrations of VAS2870 were actually shown to antagonise the effects of Bcr-Abl inhibition in K562 cells (Figure 9 and Figure 10). Though combinations with the higher 10 μ M treatments of VAS2870 did induce synergy, this still contradicted with DPI treatment which induced synergy at all concentrations. DPI and VAS2870 are both inhibitors of Nox activity and as a result these contradictory effects were not expected.

Examination of individual DPI and VAS2870 treatments on K562 cells did demonstrate differing results to begin with (Figure 1 and Figure 8). Work in Chapter 3 and 4 characterised the effects of Nox inhibition through knockdown of p22phox. These studies established that removal of p22phox expression decreases ROS levels, which slows the progression of cells from the G1 phase of the cell cycle into S phase while inducing a minor effect on cell death *via* apoptosis. Considering changes in p22phox expression will only influence the activity of Nox proteins 2 and 4 in K562 cells (Nox1 and Nox3 were not detected, Chapter 3, Figure 2), some degree of difference was to be expected between the effects of p22phox knockdown compared to treatment with inhibitors like DPI and VAS2870 which are known to effect the function of all of the Nox protein family members. Interestingly treatment of cells with lower concentrations of DPI had a minimal effect on the level of cell death while inducing a small increase in the percentage of cells present in the G0/G1 phase of the cell cycle thereby complementing p22phox knockdown results (Figure 1). Although lower concentrations were chosen for subsequent combination studies it is important to note that treatment of K562 cells with higher concentrations of DPI actually induced a G2/M phase increase while having a significantly greater effect on cell death (Figure 1). These results corresponded with a previous study by Venkatachalam *et al.* (2008) where G1 phase progression was demonstrated to be

significantly retarded following inhibition of Nox proteins by DPI treatment.

Furthermore extended DPI treatment was also shown to produce an increase of cells present in the G2/M phase.

Treatment of K562 cells with VAS2870 did not demonstrate such comparative results. In contrast to DPI and p22phox knockdown studies, VAS2870 treatment was demonstrated to induce an increase in G2/M phase cells, along with a substantial increase the level of cell death (Figure 8). Furthermore, only one of the three concentrations of VAS2870 (10 μ M) examined demonstrated a decrease in ROS levels for the full duration of treatment. Interestingly, of the concentrations examined 10 μ M was also the only concentration to be synergistic when combined with Bcr-Abl inhibition (Figure 9 and Figure 10). It could be suggested from this that the other concentrations may have been too low to inhibit Nox activity for the duration of treatment. Indeed, ROS levels following treatment with 2 μ M and 5 μ M had returned to basal levels within 2hrs suggesting that Nox proteins were no longer inhibited. However this did not explain why these concentrations of VAS2870 antagonised the effects of Imatinib and Nilotinib. Interestingly treatments with 5 μ M and 10 μ M demonstrated two separate decreases in ROS levels (Figure 8). This second decrease coincided with a rapid increase in the levels of cell death. For the 5 μ M treatment the increase was minimal however 10 μ M treatment induced a substantial increase on cell death. These treatments demonstrated greater levels of cell death than treatment with any concentration of DPI.

Examination of VAS2870 in several studies has lead to it being described as a specific Nox protein inhibitor (Wind *et al.*, 2010; Altenhöfer *et al.*, 2012; Cifuentes-Pagano, *et al.*, 2012; Wingler *et al.*, 2012). Indeed, all these studies give strong evidence for this conclusion however this does not explain the contradictions

noted here when VAS2870 treatment is compared to the effects of DPI or p22phox knockdown. Of these studies which describe VAS2870 as a specific Nox inhibitor none have examined its effects for extended periods of time. Interestingly, a recent study by Sun *et al.* (2012) demonstrated that although an inhibitor of Nox proteins, VAS2870 exerts significant off-target effects, most notably thiol alkylation. This study gave a likely explanation for the effects observed following treatment with higher concentrations and at later time-points. Furthermore, the off target effects of VAS2870 treatment may provide a reason for the antagonism demonstrated by lower concentrations of VAS2870 when used in combination with Bcr-Abl TKIs.

Like VAS2870, DPI is not without its problems as an inhibitor of Nox proteins. As discussed, DPI is a flavoprotein inhibitor extensively used to inhibit Nox activity, interfering with electron transport thereby preventing ROS generation (O'Donnell *et al.*, 1993). Interestingly DPI is a nonspecific inhibitor of many different electron transporters, not only inhibiting all of the NOX isoforms, but also eliciting its effects to a lesser extent on cytochrome P-450 reductase (Prabhakar 2000), nitric oxide synthase (Stuehr *et al.*, 1991), xanthine oxidase (Doussi re and Vignais, 1992) and even mitochondrial complex I (Li and Trush, 1998). Even in light of this DPI is still the most commonly cited compound utilised to inhibit Nox activity (Bedard and Krause, 2007). As previously discussed the mitochondria and Nox proteins are heavily linked to CML disease phenotype, while the other potential targets of DPI are not important sources of ROS under normal physiological conditions (Hole *et al.*, 2011). Furthermore, DPI treatment in K562 cells induced effects very similar to that of targeted and specific inhibition of Nox protein activity through p22phox knockdown which is a further indication of its potential as a Nox inhibitor.

As previously discussed although the activity of Nox proteins is heavily implicated in leukaemia (Kamiguti *et al.*, 2005; Prata *et al.*, 2008; Naughton *et al.*, 2009) it is also known to play key roles in the development of many other cancer types including but not limited to prostate (Brar *et al.*, 2003; Lim *et al.*, 2005; Kumar *et al.*, 2008; Huang *et al.*, 2012a), colon (Fukuyama *et al.*, 2005; Bauer *et al.*, 2012), breast and ovarian (Desouki *et al.*, 2005; Choi *et al.*, 2010), bladder (Shimada *et al.*, 2009; Shimada *et al.*, 2011; Huang *et al.*, 2012b), pancreatic (Vaquero *et al.*, 2004) and thyroid gland cancers (Weyemi *et al.*, 2010) as well as melanoma (Brar *et al.*, 2002; Yamaura *et al.*, 2009) and lymphoma (Lan *et al.*, 2007; Hoffmann *et al.*, 2010). Therefore, the potential of Nox inhibition is not just limited to CML treatment. Although the majority of research today focuses on the development of treatments targeting specific signalling events or processes in the cell, the reality is that treatment of many these cancers still rely on the use of harsh chemotherapeutic drugs. Furthermore many chemotherapeutic treatments also utilise drug combinations to overcome the effects of resistance in addition to increasing effectiveness. As a result it was of interest to examine the effects of Nox inhibition when combined with several broad spectrum chemotherapeutic drugs.

There are five broad types of chemotherapeutics still used today to treat cancers each inducing its cytotoxic effects through a different mechanism. These are alkylating agents (or other similarly reactive compounds which bind DNA and induce crosslinking), anti-metabolites, anti-microtubule agents, Topoisomerase inhibitors and cytotoxic antibiotics. Cisplatin, Methotrexate, Docetaxel, Etoposide and Actinomycin D were respectively chosen to represent each type of chemotherapeutic and provide a broad insight into how their activity may be affected when combined with Nox inhibition. Interestingly each of the chosen

chemotherapeutics has been used to treat many cancers known to be influenced by Nox activity (Siddik, 2003; Montero *et al.*, 2005; Koba and Konopa, 2005; Nitiss 2009; Block and Gorin, 2012; Abolmaali *et al.*, 2013).

Drug combinations are widely used to treat many cancers. Synergy between drugs increases the efficacy of the therapeutic effect, allowing dosages to be decreased maintaining the same efficacy to avoid toxicity while reducing the potential for development of drug resistance. Combined treatment of each of these chemotherapeutics with DPI gave varying results. Four out of the five chemotherapeutics studied demonstrated some degree of synergy with DPI treatment (Figure 12, Figure 14, Figure 16, Figure 18 and Figure 20). Both Docetaxel and Actinomycin D demonstrated additive effects. Interestingly Actinomycin D treatment also demonstrated a small level of antagonism however DPI treatment when used in combination with some concentrations of Cisplatin and Etoposide produced strong antagonistic effects. Conflictingly, as well as being involved in survival signalling, activation of some Nox proteins in response to certain stimuli is known to be involved in the induction of cell death (Bedard and Krause, 2007). This could suggest a reason why such strong antagonistic effects were noted in some treatments. Indeed it was subsequently discovered that the cytotoxicity of Cisplatin was dependent on ROS generation from both the Nox proteins and mitochondria (Kim *et al.*, 2010; Itoh *et al.*, 2011). However this still left the question as to why higher concentrations of these drugs demonstrated synergy when used in combination. Contradictory to these studies it has also been demonstrated that Cisplatin cytotoxicity can be enhanced through inhibition of Nox4 (Chang *et al.*, 2012). This may suggest concentration dependent effects of some of these chemotherapeutics. This coupled with the inhibitory effects of DPI may explain

some of the varied results observed between different concentrations of the same drug.

Out of all the chemotherapeutics examined in combination with DPI treatment, Methotrexate demonstrated the greatest potential. Combinations with Methotrexate induced a level of synergy greater than that observed with either Imatinib or Nilotinib (Figure 20). Indeed Methotrexate has demonstrated its success in the treatment of multiple leukaemia's (Abolmaali *et al.*, 2013) and has even shown success in the treatment of CML in the past (Kanda *et al.*, 1999). One interesting point is that individual treatments with Imatinib, Nilotinib and Methotrexate all induced significant G1 arrests following treatment (Figure 2, Figure 6 and Figure 19). Whether or not this could provide a way of identifying potential combination partners for Nox treatment is uncertain. Regardless this study demonstrated a great potential for Nox inhibition in combination with this anti-metabolite.

While broadly identifying the clinical relevance of simultaneous inhibition of Nox and Bcr-Abl activity, these studies established a significant result in the improvement of this CML treatment. Nevertheless the off target effects of DPI make it a less than ideal drug for the study of Nox protein activity, highlighting the need for the development of more specific and better characterised Nox inhibitors. However considering the similarities demonstrated between DPI treatment and p22phox knockdown, DPI still demonstrates great potential as a Nox inhibitor and considering the results of VAS2870 treatment it is evident that until better Nox inhibitors are developed DPI remains the best available choice. Regardless of these factors these studies still provided the basis for future analysis of Nox inhibition as a potential therapeutic in cancer treatment.

Chapter 6

General Discussion

There is no doubt that the development of Imatinib has been a major triumph for the treatment of CML, continually demonstrating its significance in the clinic by inducing complete haematological response (CHR) as well as cytogenetic response (CCyR) in the vast majority of patients, while lowering the risk and rate of progression into Blast phase (CML-BP) (Druker *et al.*, 2006; Hochhaus *et al.*, 2009; Deininger *et al.*, 2009). What's more, since its clinical implementation many CML patients now can expect to have a life expectancy similar to that of the general population (Gambacorti-Passerini *et al.*, 2011). Unfortunately, even with this high success rate there are still many patients for whom Imatinib treatment is inadequate or produces adverse effects, while resistant to Imatinib treatment through Bcr-Abl-dependent or -independent means has demonstrated a significant problem for treatment (Deininger *et al.*, 2009). A cyclic trend appears to be emerging of new Bcr-Abl tyrosine kinase inhibitors (TKIs) being developed to tackle this problem, only to induce a novel mechanism of resistance themselves, requiring the need to develop more drugs further perpetuating this trend (Quintás-Cardama *et al.*, 2007; Bixby and Talpaz, 2011). At the stem of this problem is the necessity for continual, lifelong treatment with TKIs in order to prevent disease reoccurrence due to residual disease, thereby increasing the potential for this resistance to develop. It is evident that Bcr-Abl TKI treatment alone will only ever conceal or prolong the course of this disease, with the real solution for a complete treatment of CML requiring the removal of residual disease. This has presented a large obstacle for CML treatment, which has mounted much concern, prompting a re-evaluation of therapeutic approach and has demonstrated the need for a greater understanding of this disease in order to development alternative strategies for treatment.

Bcr-Abl expression is one of the key requirements for oncogenesis in CML (McLaughlin *et al.*, 1987; Lugo *et al.*, 1990), achieving oncogenesis in many ways by mimicking the effects of growth factor stimulation in haematopoietic stem and progenitor cells thereby inducing disease phenotype. A number of studies have shown that induced or constitutive expression of Bcr-Abl increases the intracellular levels of Reactive Oxygen Species (ROS) (Sattler *et al.*, 2000; Kim *et al.*, 2005; Naughton *et al.*, 2009; Reddy *et al.*, 2011), which are traditionally seen as the key factors for genomic instability in CML cells, inducing the development of drug resistance as well as influencing disease progression (Nowicki *et al.*, 2004; Koptyra *et al.*, 2006; Rassool *et al.*, 2007; Sallmyr *et al.*, 2008; Nieborowska-Skorska *et al.*, 2012). However, these particular studies have also identified ROS production as a prerequisite for complete signalling activity downstream of Bcr-Abl, identifying them as intracellular signalling molecules, a concept which has now become widely accepted in all cell types (Rhee *et al.*, 2005a; Rhee *et al.*, 2005b; Toledano *et al.*, 2010; Bae *et al.*, 2011).

Naughton *et al.* (2009) demonstrated a link between this ROS production downstream of Bcr-Abl signalling and the professional ROS generators, the NADPH Oxidases (Nox). Considering Bcr-Abl activity in a way mimics growth factor stimulation it is therefore reasonable to expect it to activate Nox proteins, which are known to be heavily influenced by signalling cascades induced downstream of growth factor stimulation (Woolley *et al.*, 2013). What is of significance is that Nox-derived ROS have been demonstrated to be involved in a host of cellular activities in leukaemias, driving disease phenotype by increasing survival, migration, proliferation and even differentiation (Kim *et al.*, 2005; Naughton *et al.*, 2009; Sardina *et al.*, 2010; Hole *et al.*, 2011; Reddy *et al.*, 2011). Although a link between

Bcr-Abl activity and Nox-mediated ROS generation was established by Naughton *et al.* (2009), it was unclear how exactly Bcr-Abl was influencing this process.

Throughout this study the K562 cell line, which constitutively express Bcr-Abl, were used as a CML model. In the first part of this study these cells were used to elucidate a possible novel mechanism of regulation of Nox-dependent ROS production downstream of Bcr-Abl signalling. This work established that specific inhibition of Bcr-Abl activity reduced ROS generation which coincided with the degradation of p22phox, a membrane-bound protein essential for full activity of Nox proteins 1, 2, 3 and 4 (Ambasta *et al.*, 2004; Ueno *et al.*, 2005). Consequently, p22phox was demonstrated to be an important mediator of ROS production downstream of Bcr-Abl signalling. Inhibition of GSK-3 β downstream of both the PI3K/Akt and Raf/MEK/ERK signalling pathways, both of which are activated by Bcr-Abl, was identified to be pivotal for p22phox protein maintenance. These studies thereby established a link between Nox-derived ROS and Bcr-Abl activity through the maintenance of p22phox protein levels (Landry *et al.*, 2013). Interestingly, such control of Nox activity downstream of tyrosine kinase activity is not unique and this method of p22phox degradation and has also been demonstrated on the reintroduction of von Hippel-Lindau tumour suppressor gene (VHL) into VHL-deficient carcinoma cells (Block *et al.*, 2007; Block *et al.*, 2010) and upon inhibition of the FLT3-ITD oncogene in the Acute Myeloid Leukaemia (AML) MV-411 cell line (Woolley *et al.*, 2012).

Further examination in K562 cells demonstrated a significant role for p22phox-mediated ROS production in cell proliferation. Rather significantly enhanced proliferation is a major contributory factor to CML disease phenotype demonstrating the importance of p22phox and Nox proteins in CML pathogenesis.

Numerous studies have also demonstrated such a role for Nox-derived ROS in cell proliferation with some studies drawing a direct link to an importance in p22phox expression and further highlighting the significance of these results in CML (Jeong *et al.*, 2004; Sturrock *et al.*, 2006; Petry *et al.*, 2006; Reddy *et al.*, 2011). Here p22phox-mediated ROS production was shown to influence cell proliferation by having a positive effect on the G1/S transition of the cell cycle, a role for which Nox-derived ROS has been previously highlighted (Venkatachalam *et al.*, 2008). It was suggested that p22phox function mediated this effect by indirectly inhibiting pRb activity through oxidative inactivation of phosphatases known to be important for pRb activation, Protein Phosphatase 1 (PP1) and Protein Phosphatase 2A (PP2A). This was believed to influence Cyclin E proteins levels and therefore cell cycle progression (Rao and Clayton 2002; O’Loghlen *et al.*, 2003; Kolupaeva and Janssens, 2013). Significantly, work by Naughton *et al.* (2009) has also implemented Nox-derived ROS in the inhibition of PP1 α activity downstream of Bcr-Abl signalling.

In addition to having a positive role in cell proliferation, p22phox-mediated Nox-derived ROS was also identified in this study to be important in the overall viability of K562 cells with its removal demonstrating minor increases in the level of apoptotic cell death. Treatments utilising Bcr-Abl inhibition *via* Imatinib in combination with chemotherapeutic agents have been studied as an approach to overcome the known obstacles currently facing CML treatment (Gu *et al.*, 2005; Tseng *et al.*, 2005; Giallongo *et al.*, 2011; Bonifacio *et al.*, 2012). Similarly rather than using broad spectrum drugs much research is now focused on the simultaneous targeting of Bcr-Abl in combination with pathways identified as important in CML maintenance and progression (Helgason *et al.*, 2011; O’Hare *et al.*, 2012). Although

only demonstrating a minor role in the overall survival of these cells this study still identified the importance of p22phox expression in CML pathogenesis. It was evident however that p22phox inhibition alone did not demonstrate a significant enough effect to suggest it as sole treatment for CML. Indeed, combining p22phox removal with Imatinib treatment significantly enhanced the effect of Imatinib treatment. It was concluded from this work that p22phox removal in a way weakens cells, priming Bcr-Abl inhibition to produce a substantially greater effect on cell death demonstrating the clinical potential of targeting Nox proteins in combination with Bcr-Abl inhibition. This potential was further established after DPI was used in combination with Imatinib and Nilotinib, demonstrating a substantial and synergistic increase in cell death through augmentation of apoptosis. Unfortunately, the off target effects of DPI make it a less than ideal compound for therapeutic use, highlighting the need for the development of more specific and better characterised Nox inhibitors. Regardless of this, these studies still provided the basis and reasoning for future analysis of Nox inhibition as a potential therapeutic in CML treatment.

Nox-derived ROS production can lead to increased genomic instability (Weyemi *et al.*, 2012a; Weyemi *et al.*, 2012b), a phenomena which can influence progression into Blast phase (CML-BP) as well as development of TKI resistance (Nowicki *et al.*, 2004; Koptyra *et al.*, 2006; Rassool *et al.*, 2007; Sallmyr *et al.*, 2008; Slupianek *et al.*, 2011; Chakraborty *et al.*, 2012; Nieborowska-Skorska *et al.*, 2012). Therefore, considering the effectiveness of DPI treatment in combination with Bcr-Abl inhibition there is a potential for Nox inhibitors in reducing the development of drug resistance as well as lowering the chance of disease progression

if used in combination. However, as discussed it is evident that in order to truly cure CML, residual disease needs to be removed. Combination treatment is one approach which has received great interest in eradicating residual disease and the risk of reoccurrence, targeting critical pathways in LSCs in order to make these cells Bcr-Abl dependent and therefore more susceptible to Bcr-Abl TKI treatment (Helgason *et al.*, 2011; O'Hare *et al.*, 2012). Although work here demonstrated the potential of combined Nox and TKI treatment in the more mature CD34⁺CD38⁻ K562 cell line, it did not examine the effects of Nox inhibition on LSCs directly. However, for reasons which will now be discussed this study still established the potential of Nox inhibition in enhancing TKI treatment and this work coupled with other studies identifies the possibility of Nox proteins as a target worthy of further examination in respect to the removal of the residual LSC fraction.

LSCs are believed to reside in the bone marrow niche, a factor which is believed to in part confer lack of addiction to Bcr-Abl signalling (Weisberg *et al.*, 2008). This growth factor and cytokine-rich microenvironment is believed to provide extrinsic protection from TKI treatment due to high concentrations of stromal cell-derived factors (Traer *et al.*, 2012; Nair *et al.*, 2012). To date four major signalling pathways all activated by growth factor or cytokine stimulation are believed to be significant contributors to Bcr-Abl independence in LSCs, these are WNT- β -catenin signalling (Zhang *et al.*, 2013), Hedgehog signalling (Zhao *et al.*, 2009), TGF β -FOXO3A-BCL-6 (Naka *et al.*, 2010; Hurtz *et al.*, 2011) and JAK2/STAT (Neviani *et al.*, 2005; Samanta *et al.*, 2009; Hantschel *et al.*, 2012). Indeed, as will be discussed all but one of these pathways, Hedgehog signalling, have demonstrated the requirement for Nox protein activity following stimulation in other systems.

CML LSCs as well as progenitor cells have higher levels of intracellular ROS in comparison to their healthy counterparts (Nieborowska-Skorska *et al.*, 2012). This is interesting as one of the major characteristics of haematopoietic stem cells (HSCs) is quiescence (Doulatov *et al.*, 2012) therefore it would be unexpected for these ROS increases in LSCs to be a result of increased metabolic activity but could rather be due to specific production resulting from increased cytokine and growth factor signalling. Indeed, many haematopoietic growth factors such granulocyte-macrophage colony-stimulation factor (GM-CSF), and interleukin-3 (IL-3), stem cell factor (SCF) and thrombopoietin (TPO) trigger ROS production in human hematopoietic cells and are important in transduction of these growth factor signals (Sattler *et al.*, 1999). Nox-derived ROS are known to play important roles in haematopoiesis and hematopoietic growth factor signaling under normal conditions with growth factors like GM-CSF demonstrated to increase Nox-derived ROS production, vital for contributing to myeloid cell growth (Sattler *et al.*, 1999; Zhu *et al.*, 2005; Sardina *et al.*, 2012; Hole *et al.*, 2011). Furthermore, Nox protein activity has been identified as a major source of ROS in healthy CD34⁺CD38⁻ HSCs (Piccoli *et al.*, 2007) while also being demonstrated as important in the preservation of the CD34⁺ cell population (Fan *et al.*, 2007).

Interestingly, early progenitor cells as a result of Bcr-Abl signalling can be induced to secrete growth factors such as IL-3 and GM-CSF, with this autocrine signalling activating the JAK/STAT pathways which are suggested to play a role in promoting cell-cycle entry of primitive leukemic stem cells and progenitors during the CML-CP (Jiang *et al.*, 1999; Holyoake *et al.*, 2002). Activation of JAK2 signalling as a result of GM-CSF and IL-3 stimulation has been shown to be highly influential in Bcr-Abl TKI resistance in LSCs (Neviani *et al.*, 2005; Samanta *et al.*,

2009; Hantschel *et al.*, 2012; Traer *et al.*, 2012; Nair *et al.*, 2012). Interestingly, Nox4-mediated inhibition of phosphatases has been demonstrated to be required for full activation of the anti-apoptotic JAK2/STAT pathway in pancreatic cells thereby promoting cell survival (Lee *et al.*, 2007). Work in Chapter 3 of this study also demonstrated the importance of IL-3 signalling in the maintenance of p22phox protein levels in the more primitive TonB.210 cells, emphasising the importance of Nox-derived ROS downstream of this cytokine. In addition to JAK/STAT, the WNT- β -catenin signalling has also been implicated in LSCs Bcr-Abl independence (Zhang *et al.*, 2013). Interestingly, Nox1 activation downstream of aberrant RAS activated Raf/MEK/ERK signalling, which is known to occur downstream of Bcr-Abl activity, has also been shown to potentiate cell proliferation by positively influencing the canonical WNT- β -catenin-dependent signalling (Kajla *et al.*, 2012; Rimerman *et al.*, 2000). Finally, TGF β stimulated signalling has been shown to induce the increased expression of Nox4, raising ROS levels required for full activation of downstream signalling (Liu *et al.*, 2010).

These studies reinforce the broad influences of Nox-derived ROS and their significance in growth factor signalling, something which is very well established (Woolley *et al.*, 2013). Considering the importance of Nox proteins in growth factor signalling and the importance of these signalling pathways in LSC TKI resistance, there is potential for Nox protein inhibitors to disrupt these important pathways which confer Bcr-Abl independence. This would make these cells more susceptible to further treatment with Bcr-Abl TKIs and could potentially eradicate the LSC fraction, removing residual disease and the potential for reoccurrence. Proper assessment of the potential of Nox inhibition in CML LSCs will require examination of CD34⁺CD38⁻ cells obtained from CML patients, however from what is known

deregulation of these processes through Nox inhibition could be therapeutically significant in the removal of LSCs and therefore residual disease in CML

Given the plethora of diseases and signalling processes in which Nox-derived ROS are implicated, there has been an ever growing pursuit in recent years for specific inhibitors (Wind *et al.*, 2010; Altenhöfer *et al.*, 2012; Cifuentes-Pagano *et al.*, 2012). Despite this, however, lack of specificity and proper knowledge of mechanisms of action have hindered their use as therapeutics, something which was discussed in Chapter 5. Regardless, this study has highlighted Nox proteins as potential therapeutic targets in the treatment of CML and possibly other neoplasms. Indeed, Nox-derived ROS has been linked to a host biochemical and cellular processes important in the progression and maintenance of many cancers yet it should be emphasised that this area of cancer research is still only in its formative years with much research still required. However, considering the broad influence of these proteins, future studies of Nox-dependent redox signalling could represent the next major advancement in cell and cancer biology.

Bibliography

- Abolmaali, S.S., Tamaddon, A.M., and Dinarvand, R. (2013). A review of therapeutic challenges and achievements of methotrexate delivery systems for treatment of cancer and rheumatoid arthritis. *Cancer Chemother. Pharmacol.* 71, 1115–1130.
- Adams, J.M., Houston, H., Allen, J., Lints, T., and Harvey, R. (1992). The hematopoietically expressed vav proto-oncogene shares homology with the dbl GDP-GTP exchange factor, the bcr gene and a yeast gene (CDC24) involved in cytoskeletal organization. *Oncogene* 7, 611–618.
- Akel, S., Kolialexi, A., Mavrou, A., Metaxotou, C., Loukopoulos, D., and Yataganas, X. (2000). Evaluation at single cell level of residual Philadelphia negative hemopoietic stem cells in chronic phase CML patients. *Cancer Genet. Cytogenet.* 122, 93–100.
- Altenhöfer, S., Kleikers, P.W.M., Radermacher, K. a, Scheurer, P., Rob Hermans, J.J., Schiffers, P., Ho, H., Wingler, K., and Schmidt, H.H.H.W. (2012). The NOX toolbox: validating the role of NADPH oxidases in physiology and disease. *Cell. Mol. Life Sci.* 69, 2327–2343.
- Ambasta, R.K., Kumar, P., Griendling, K.K., Schmidt, H.H.H.W., Busse, R., and Brandes, R.P. (2004). Direct interaction of the novel Nox proteins with p22phox is required for the formation of a functionally active NADPH oxidase. *J. Biol. Chem.* 279, 45935–45941.
- Ameziane-El-Hassani, R., Morand, S., Boucher, J.-L., Frapart, Y.-M., Apostolou, D., Agnandji, D., Gnidehou, S., Ohayon, R., Noël-Hudson, M.-S., Francon, J., et al. (2005). Dual oxidase-2 has an intrinsic Ca²⁺-dependent H₂O₂-generating activity. *J. Biol. Chem.* 280, 30046–30054.
- Arthur, J.R. (2000). The glutathione peroxidases. *Cell. Mol. Life Sci.* 57, 1825–1835.
- Arur, S., Uche, U.E., Rezaul, K., Fong, M., Scranton, V., Cowan, A.E., Mohler, W., and Han, D.K. (2003). Annexin I is an endogenous ligand that mediates apoptotic cell engulfment. *Dev. Cell* 4, 587–598.
- Bae, Y.S., Sung, J.Y., Kim, O.S., Kim, Y.J., Hur, K.C., Kazlauskas, A., and Rhee, S.G. (2000). Platelet-derived growth factor-induced H₂O₂ production requires the activation of phosphatidylinositol 3-kinase. *J. Biol. Chem.* 275, 10527–10531.
- Bae, Y.S., Oh, H., Rhee, S.G., and Yoo, Y. Do (2011). Regulation of reactive oxygen species generation in cell signaling. *Mol. Cells* 32, 491–509.
- Bánfi, B., Molnár, G., Maturana, A., Steger, K., Hegedűs, B., Demaurex, N., and Krause, K.H. (2001). A Ca²⁺-activated NADPH oxidase in testis, spleen, and lymph nodes. *J. Biol. Chem.* 276, 37594–37601.
- Bartram, C.R., de Klein, A., Hagemeijer, A., van Agthoven, T., Geurts van Kessel, A., Bootsma, D., Grosveld, G., Ferguson-Smith, M.A., Davies, T., and Stone, M. (1983). Translocation of c-abl oncogene correlates with the presence of a Philadelphia chromosome in chronic myelocytic leukaemia. *Nature* 306, 277–280.
- Bauer, K.M., Hummon, A.B., and Buechler, S. (2012). Right-side and left-side colon cancer follow different pathways to relapse. *Mol. Carcinog.* 51, 411–421.
- Beckman, K.B., and Ames, B.N. (1998). The free radical theory of aging matures. *Physiol. Rev.* 78, 547–581.
- Bedard, K., and Krause, K. (2007). The NOX Family of ROS-Generating NADPH Oxidases: Physiology and Pathophysiology. *Physiol. Rev.* 87, 245–313.

- Bellodi, C., Lidonnici, M.R., Hamilton, A., Helgason, G.V., Soliera, A.R., Ronchetti, M., Galavotti, S., Young, K.W., Selmi, T., Yacobi, R., *et al.* (2009). Targeting autophagy potentiates tyrosine kinase inhibitor-induced cell death in Philadelphia chromosome-positive cells, including primary CML stem cells. *J. Clin. Invest.* *119*, 1109–1123.
- Ben-Neriah, Y., Daley, G.Q., Mes-Masson, A.M., Witte, O.N., and Baltimore, D. (1986). The chronic myelogenous leukemia-specific P210 protein is the product of the bcr/abl hybrid gene. *Science* *233*, 212–214.
- Berlett, B.S., and Stadtman, E.R. (1997). Protein oxidation in aging, disease, and oxidative stress. *J. Biol. Chem.* *272*, 20313–20316.
- Berndt, N., Dohadwala, M., and Liu, C.W. (1997). Constitutively active protein phosphatase 1alpha causes Rb-dependent G1 arrest in human cancer cells. *Curr. Biol.* *7*, 375–386.
- Berridge, M. V, Herst, P.M., and Tan, A.S. (2005). Tetrazolium dyes as tools in cell biology: new insights into their cellular reduction. *Biotechnol. Annu. Rev.* *11*, 127–152.
- Bienert, G.P., Møller, A.L.B., Kristiansen, K.A., Schulz, A., Møller, I.M., Schjoerring, J.K., and Jahn, T.P. (2007). Specific aquaporins facilitate the diffusion of hydrogen peroxide across membranes. *J. Biol. Chem.* *282*, 1183–1192.
- Biernaux, C., Loos, M., Sels, A., Huez, G., and Stryckmans, P. (1995). Detection of major bcr-abl gene expression at a very low level in blood cells of some healthy individuals. *Blood* *86*, 3118–3122.
- Bixby, D., and Talpaz, M. (2011). Seeking the causes and solutions to imatinib-resistance in chronic myeloid leukemia. *Leuk. Off. J. Leuk. Soc. Am. Leuk. Res. Fund, U.K* *25*, 7–22.
- Bjelakovic, G., Nikolova, D., Gluud, L.L., Simonetti, R.G., and Gluud, C. (2007). Mortality in randomized trials of antioxidant supplements for primary and secondary prevention: systematic review and meta-analysis. *JAMA* *297*, 842–857.
- Block, K., and Gorin, Y. (2012). Aiding and abetting roles of NOX oxidases in cellular transformation. *Nat. Rev. Cancer* *12*, 627–637.
- Block, K., Gorin, Y., Hoover, P., Williams, P., Chelmicki, T., Clark, R. a, Yoneda, T., and Abboud, H.E. (2007). NAD(P)H oxidases regulate HIF-2alpha protein expression. *J. Biol. Chem.* *282*, 8019–8026.
- Block, K., Gorin, Y., New, D.D., Eid, A., Chelmicki, T., Reed, A., Choudhury, G.G., Parekh, D.J., and Abboud, H.E. (2010). The NADPH oxidase subunit p22phox inhibits the function of the tumor suppressor protein tuberlin. *Am. J. Pathol.* *176*, 2447–2455.
- Bokoch, G.M., Diebold, B., Kim, J.-S., and Gianni, D. (2009). Emerging evidence for the importance of phosphorylation in the regulation of NADPH oxidases. *Antioxid. Redox Signal.* *11*, 2429–2441.
- Bonifacio, M., Rigo, A., Guardalben, E., Bergamini, C., Cavalieri, E., Fato, R., Pizzolo, G., Suzuki, H., and Vinante, F. (2012). α -bisabolol is an effective proapoptotic agent against BCR-ABL(+) cells in synergism with Imatinib and Nilotinib. *PLoS One* *7*, e46674.
- Bose, S., Deininger, M., Gora-Tybor, J., Goldman, J.M., and Melo, J. V (1998). The presence of typical and atypical BCR-ABL fusion genes in leukocytes of normal individuals: biologic significance and implications for the assessment of minimal residual disease. *Blood* *92*, 3362–3367.

- Branford, S., Rudzki, Z., Walsh, S., Grigg, A., Arthur, C., Taylor, K., Herrmann, R., Lynch, K.P., and Hughes, T.P. (2002). High frequency of point mutations clustered within the adenosine triphosphate-binding region of BCR/ABL in patients with chronic myeloid leukemia or Ph-positive acute lymphoblastic leukemia who develop imatinib (STI571) resistance. *Blood* 99, 3472–3475.
- Brar, S.S., Corbin, Z., Kennedy, T.P., Hemendinger, R., Thornton, L., Bommarius, B., Arnold, R.S., Whorton, A.R., Sturrock, A.B., Huecksteadt, T.P., *et al.* (2003). NOX5 NAD(P)H oxidase regulates growth and apoptosis in DU 145 prostate cancer cells. *Am. J. Physiol. Cell Physiol.* 285, C353–69.
- Broude, E. V, Swift, M.E., Vivo, C., Chang, B.-D., Davis, B.M., Kalurupalle, S., Blagosklonny, M. V, and Roninson, I.B. (2007). p21(Waf1/Cip1/Sdi1) mediates retinoblastoma protein degradation. *Oncogene* 26, 6954–6958.
- Brown, D.I., and Griendling, K.K. (2009). Nox proteins in signal transduction. *Free Radic. Biol. Med.* 47, 1239–1253.
- Burchert, A., Wang, Y., Cai, D., von Bubnoff, N., Paschka, P., Müller-Brüsselbach, S., Ottmann, O.G., Duyster, J., Hochhaus, A., and Neubauer, A. (2005). Compensatory PI3-kinase/Akt/mTor activation regulates imatinib resistance development. *Leukemia* 19, 1774–1782.
- Cai, H., Li, Z., Davis, M.E., Kanner, W., Harrison, D.G., and Dudley, S.C. (2003). Akt-dependent phosphorylation of serine 1179 and mitogen-activated protein kinase kinase/extracellular signal-regulated kinase 1/2 cooperatively mediate activation of the endothelial nitric-oxide synthase by hydrogen peroxide. *Mol. Pharmacol.* 63, 325–331.
- Calabretta, B., and Perrotti, D. (2004). The biology of CML blast crisis. *Blood* 103, 4010–4022.
- Capdeville, R., Buchdunger, E., Zimmermann, J., and Matter, A. (2002). Glivec (STI571, imatinib), a rationally developed, targeted anticancer drug. *Nat. Rev. Drug Discov.* 1, 493–502.
- Chai, S.K., Nichols, G.L., and Rothman, P. (1997). Constitutive activation of JAKs and STATs in BCR-Abl-expressing cell lines and peripheral blood cells derived from leukemic patients. *J. Immunol.* 159, 4720–4728.
- Chakraborty, S., Stark, J.M., Sun, C.-L., Modi, H., Chen, W., O'Connor, T.R., Forman, S.J., Bhatia, S., and Bhatia, R. (2012). Chronic myelogenous leukemia stem and progenitor cells demonstrate chromosomal instability related to repeated breakage-fusion-bridge cycles mediated by increased nonhomologous end joining. *Blood* 119, 6187–6197.
- Chance, B., Williams, G.R., and Hollunger, G. (1963). Inhibition of electron and energy transfer in mitochondria. I. Effects of Amytal, thiopental, rotenone, progesterone, and methylene glycol. *J. Biol. Chem.* 238, 418–431.
- Chang, F., Steelman, L.S., Lee, J.T., Shelton, J.G., Navolanic, P.M., Blalock, W.L., Franklin, R.A., and McCubrey, J.A. (2003). Signal transduction mediated by the Ras/Raf/MEK/ERK pathway from cytokine receptors to transcription factors: potential targeting for therapeutic intervention. *Leukemia* 17, 1263–1293.
- Chang, G., Chen, L., Lin, H.-M., Lin, Y., and Maranchie, J.K. (2012). Nox4 inhibition enhances the cytotoxicity of cisplatin in human renal cancer cells. *J. Exp. Ther. Oncol.* 10, 9–18.
- Chelikani, P., Fita, I., and Loewen, P.C. (2004). Diversity of structures and properties among catalases. *Cell. Mol. Life Sci.* 61, 192–208.

- Chen, K., Craige, S.E., and Keane, J.F. (2009). Downstream targets and intracellular compartmentalization in Nox signaling. *Antioxid. Redox Signal.* *11*, 2467–2480.
- Cheng, G., and Lambeth, J.D. (2004). NOXO1, regulation of lipid binding, localization, and activation of Nox1 by the Phox homology (PX) domain. *J. Biol. Chem.* *279*, 4737–4742.
- Cheng, G., Diebold, B.A., Hughes, Y., and Lambeth, J.D. (2006). Nox1-dependent reactive oxygen generation is regulated by Rac1. *J. Biol. Chem.* *281*, 17718–17726.
- Choi, C.-H., Lee, B.-H., Ahn, S.-G., and Oh, S.-H. (2012). Proteasome inhibition-induced p38 MAPK/ERK signaling regulates autophagy and apoptosis through the dual phosphorylation of glycogen synthase kinase 3 β . *Biochem. Biophys. Res. Commun.* *418*, 759–764.
- Choi, J.-A., Lee, J.-W., Kim, H., Kim, E.-Y., Seo, J.-M., Ko, J., and Kim, J.-H. (2010). Pro-survival of estrogen receptor-negative breast cancer cells is regulated by a BLT2-reactive oxygen species-linked signaling pathway. *Carcinogenesis* *31*, 543–551.
- Chou, T. C. (2007). Theoretical Basis , Experimental Design , and Computerized Simulation of Synergism and Antagonism in Drug Combination Studies □. *Pharmacol. Rev.* *58*, 621–681.
- Chou, T.C., and Talalay, P. (1984). Quantitative analysis of dose-effect relationships: the combined effects of multiple drugs or enzyme inhibitors. *Adv. Enzyme Regul.* *22*, 27–55.
- Cifuentes-Pagano, E., Csanyi, G., and Pagano, P.J. (2012). NADPH oxidase inhibitors: a decade of discovery from Nox2ds to HTS. *Cell. Mol. Life Sci.* *69*, 2315–2325.
- Circu, M.L., and Aw, T.Y. (2010). Reactive oxygen species, cellular redox systems, and apoptosis. *Free Radic. Biol. Med.* *48*, 749–762.
- Classon, M., and Harlow, E. (2002). The retinoblastoma tumour suppressor in development and cancer. *Nat. Rev. Cancer* *2*, 910–917.
- Clerkin, J.S., Naughton, R., Quiney, C., and Cotter, T.G. (2008). Mechanisms of ROS modulated cell survival during carcinogenesis. *Cancer Lett.* *266*, 30–36.
- Colavitti, R., and Finkel, T. (2005). Reactive oxygen species as mediators of cellular senescence. *IUBMB Life* *57*, 277–281.
- Collins, S., Coleman, H., and Groudine, M. (1987). Expression of bcr and bcr-abl fusion transcripts in normal and leukemic cells. *Mol. Cell. Biol.* *7*, 2870–2876.
- Cooke, M.S., Evans, M.D., Dizdaroglu, M., and Lunec, J. (2003). Oxidative DNA damage: mechanisms, mutation, and disease. *FASEB J.* *17*, 1195–1214.
- Corcoran, A., and Cotter, T.G. (2013). Redox regulation of protein kinases. *FEBS J.* *280*, 1944–1965.
- Cordray, P., Doyle, K., Edes, K., Moos, P.J., and Fitzpatrick, F.A. (2007). Oxidation of 2-Cys-peroxiredoxins by arachidonic acid peroxide metabolites of lipoxygenases and cyclooxygenase-2. *J. Biol. Chem.* *282*, 32623–32629.
- Corso, A., Lazzarino, M., Morra, E., Merante, S., Astori, C., Bernasconi, P., Boni, M., and Bernasconi, C. (1995). Chronic myelogenous leukemia and exposure to ionizing radiation--a retrospective study of 443 patients. *Ann. Hematol.* *70*, 79–82.

- Cortes, J.E., Kantarjian, H.M., Brümmendorf, T.H., Kim, D.-W., Turkina, A.G., Shen, Z.-X., Pasquini, R., Khoury, H.J., Arkin, S., Volkert, A., *et al.* (2011a). Safety and efficacy of bosutinib (SKI-606) in chronic phase Philadelphia chromosome-positive chronic myeloid leukemia patients with resistance or intolerance to imatinib. *Blood* *118*, 4567–4576.
- Cortes J.E., Talpaz M, Kantarjian HM, Smith H, Bixby D, Rafferty U, *et al.* (2011b). A phase 1 study of DCC-2036, a novel oral inhibitor of BCR-ABL kinase, in patients with Philadelphia chromosome positive (Ph+) leukemias including patients with T315I mutation *Blood* (ASH Annual Meeting Abstracts) *118*, 601.
- Cortez, D., Kadlec, L., and Pendergast, A.M. (1995). Structural and signaling requirements for BCR-ABL-mediated transformation and inhibition of apoptosis. *Mol. Cell. Biol.* *15*, 5531–5541.
- Cortez, D., Stoica, G., Pierce, J.H., and Pendergast, A.M. (1996). The BCR-ABL tyrosine kinase inhibits apoptosis by activating a Ras-dependent signaling pathway. *Oncogene* *13*, 2589–2594.
- Crane, J., Mittar, D., Soni, D., McIntyre, C. (2011). Cell Cycle Analysis Using the BD BrdU FITC Assay on the BD FACSVerser™ System. BD Biosciences, http://www.bdbiosciences.com/documents/BD_FACSVerse_CellCycleAnalysis_AppNote.pdf
- Crowley, L.C., Elzinga, B.M., O’Sullivan, G.C., and McKenna, S.L. (2011). Autophagy induction by Bcr-Abl-expressing cells facilitates their recovery from a targeted or nontargeted treatment. *Am. J. Hematol.* *86*, 38–47.
- D’Autréaux, B., and Toledano, M.B. (2007). ROS as signalling molecules: mechanisms that generate specificity in ROS homeostasis. *Nat. Rev. Mol. Cell Biol.* *8*, 813–824.
- Daley, G.Q., and Baltimore, D. (1988). Transformation of an interleukin 3-dependent hematopoietic cell line by the chronic myelogenous leukemia-specific P210bcr/abl protein. *Proc. Natl. Acad. Sci. U. S. A.* *85*, 9312–9316.
- Daley, G.Q., van Etten, R.A., Jackson, P.K., Bernards, A., and Baltimore, D. (1992). Nonmyristoylated Abl proteins transform a factor-dependent hematopoietic cell line. *Mol. Cell. Biol.* *12*, 1864–1871.
- Davies, M.J. (2005). The oxidative environment and protein damage. *Biochim. Biophys. Acta* *1703*, 93–109.
- Deem, T.L., and Cook-Mills, J.M. (2004). Vascular cell adhesion molecule 1 (VCAM-1) activation of endothelial cell matrix metalloproteinases: role of reactive oxygen species. *Blood* *104*, 2385–2393.
- Deininger, M. *et al.* (2009). International Randomized Study of Interferon versus STI571 (IRIS) 8-year follow up: sustained survival and low risk for progression or events in patients with newly diagnosed Chronic Myeloid Leukemia in Chronic Phase (CML-CP) treated with Imatinib. *Blood* (ASH Annual Meeting Abstracts) *114*, 1126
- Deininger, M., Buchdunger, E., and Druker, B.J. (2005). The development of imatinib as a therapeutic agent for chronic myeloid leukemia. *Blood* *105*, 2640–2653.
- Deininger, M.W.N., Goldman, J.M., Melo, J. V, and Dc, W. (2000). The molecular biology of chronic myeloid leukemia. *Blood* *96*, 3343–3356.

- De Deken, X., Wang, D., Many, M.C., Costagliola, S., Libert, F., Vassart, G., Dumont, J.E., and Miot, F. (2000). Cloning of two human thyroid cDNAs encoding new members of the NADPH oxidase family. *J. Biol. Chem.* *275*, 23227–23233.
- Delgado, M.D., Vaqué, J.P., Arozarena, I., López-Illasaca, M.A., Martínez, C., Crespo, P., León, J., Vaque, J.P., Lo, M.A., Martõã, C., *et al.* (2000). H-, K- and N-Ras inhibit myeloid leukemia cell proliferation by a p21WAF1-dependent mechanism. *Oncogene* *19*, 783–790.
- Denu, J.M., and Tanner, K.G. (1998). Specific and reversible inactivation of protein tyrosine phosphatases by hydrogen peroxide: evidence for a sulfenic acid intermediate and implications for redox regulation. *Biochemistry* *37*, 5633–5642.
- Desouki, M.M., Kulawiec, M., Bansal, S., Das, G.M., and Singh, K.K. (2005). Cross talk between mitochondria and superoxide generating NADPH oxidase in breast and ovarian tumors. *Cancer Biol. Ther.* *4*, 1367–1373.
- Dhut, S., Dorey, E.L., Horton, M.A., Ganesan, T.S., and Young, B.D. (1988). Identification of two normal bcr gene products in the cytoplasm. *Oncogene* *3*, 561–566.
- Donato, N.J., Wu, J.Y., Stapley, J., Gallick, G., Lin, H., Arlinghaus, R., and Talpaz, M. (2003). BCR-ABL independence and LYN kinase overexpression in chronic myelogenous leukemia cells selected for resistance to STI571. *Blood* *101*, 690–698.
- Doulatov, S., Notta, F., Laurenti, E., and Dick, J.E. (2012). Hematopoiesis: a human perspective. *Cell Stem Cell* *10*, 120–136.
- Doussière, J., and Vignais, P. V (1992). Diphenylene iodonium as an inhibitor of the NADPH oxidase complex of bovine neutrophils. Factors controlling the inhibitory potency of diphenylene iodonium in a cell-free system of oxidase activation. *Eur. J. Biochem.* *208*, 61–71.
- Drake, J.M., Graham, N.A., Stoyanova, T., Sedghi, A., Goldstein, A.S., Cai, H., Smith, D.A., Zhang, H., Komisopoulou, E., Huang, J., *et al.* (2012). Oncogene-specific activation of tyrosine kinase networks during prostate cancer progression. *Proc. Natl. Acad. Sci. U. S. A.* *109*, 1643–1648.
- Druker, B.J., Tamura, S., Buchdunger, E., Ohno, S., Segal, G.M., Fanning, S., Zimmermann, J., and Lydon, N.B. (1996). Effects of a selective inhibitor of the Abl tyrosine kinase on the growth of Bcr-Abl positive cells. *Nat. Med.* *2*, 561–566.
- Druker, B.J., Guilhot, F., O'Brien, S.G., Gathmann, I., Kantarjian, H., Gattermann, N., Deininger, M.W.N., Silver, R.T., Goldman, J.M., Stone, R.M., *et al.* (2006). Five-year follow-up of patients receiving imatinib for chronic myeloid leukemia. *N. Engl. J. Med.* *355*, 2408–2417.
- Edderkaoui, M., Nitsche, C., Zheng, L., Pandol, S.J., Gukovsky, I., and Gukovskaya, A.S. (2011). NADPH oxidase activation in pancreatic cancer cells is mediated through Akt-dependent up-regulation of p22phox. *J. Biol. Chem.* *286*, 7779–7787.
- Elmore, S. (2007). Apoptosis: A Review of Programmed Cell Death. *35*, 495–516.
- van Engeland, M., Nieland, L.J., Ramaekers, F.C., Schutte, B., and Reutelingsperger, C.P. (1998). Annexin V-affinity assay: a review on an apoptosis detection system based on phosphatidylserine exposure. *Cytometry* *31*, 1–9.

- Engelman, J.A. (2009). Targeting PI3K signalling in cancer: opportunities, challenges and limitations. *Nat. Rev. Cancer* 9, 550–562.
- Esposito, N., Colavita, I., Quintarelli, C., Sica, A.R., Peluso, A.L., Luciano, L., Picardi, M., Del Vecchio, L., Buonomo, T., Hughes, T.P., *et al.* (2011). SHP-1 expression accounts for resistance to imatinib treatment in Philadelphia chromosome-positive cells derived from patients with chronic myeloid leukemia. *Blood* 118, 3634–3644.
- Etoh, T., Inoguchi, T., Kakimoto, M., Sonoda, N., Kobayashi, K., Kuroda, J., Sumimoto, H., and Nawata, H. (2003). Increased expression of NAD(P)H oxidase subunits, NOX4 and p22phox, in the kidney of streptozotocin-induced diabetic rats and its reversibility by interventional insulin treatment. *Diabetologia* 46, 1428–1437.
- Fabbro, D., Ruetz, S., Bodis, S., Pruschy, M., Csermak, K., Man, A., Campochiaro, P., Wood, J., O'Reilly, T., and Meyer, T. (2000). PKC412--a protein kinase inhibitor with a broad therapeutic potential. *Anticancer. Drug Des.* 15, 17–28.
- Faderl, S., Talpaz, M., Estrov, Z., O'Brien, S., Kurzrock, R., and Kantarjian, H.M. (1999). The biology of chronic myeloid leukemia. *N. Engl. J. Med.* 341, 164–172.
- Fan, J., Cai, H., and Tan, W.-S. (2007). Role of the plasma membrane ROS-generating NADPH oxidase in CD34+ progenitor cells preservation by hypoxia. *J. Biotechnol.* 130, 455–462.
- Fischer, R.H., Schauen, M., Spitkovsky, D., and Schubert, J. (2006). Respiratory Chain Deficiency Slows Down Cell-Cycle Progression Via Reduced ROS Generation and is Associated With a Reduction of p21 CIP1 / WAF1. *J. Cell. Physiol.* 209, 103–112.
- Frantz, S., Brandes, R.P., Hu, K., Rammelt, K., Wolf, J., Scheuermann, H., Ertl, G., and Bauersachs, J. (2006). Left ventricular remodeling after myocardial infarction in mice with targeted deletion of the NADPH oxidase subunit gp91PHOX. *Basic Res. Cardiol.* 101, 127–132.
- ten Freyhaus, H., Huntgeburth, M., Wingler, K., Schnitker, J., Bäumer, A.T., Vantler, M., Bekhite, M.M., Wartenberg, M., Sauer, H., and Rosenkranz, S. (2006). Novel Nox inhibitor VAS2870 attenuates PDGF-dependent smooth muscle cell chemotaxis, but not proliferation. *Cardiovasc. Res.* 71, 331–341.
- Fukuyama, M., Rokutan, K., Sano, T., Miyake, H., Shimada, M., and Tashiro, S. (2005). Overexpression of a novel superoxide-producing enzyme, NADPH oxidase 1, in adenoma and well differentiated adenocarcinoma of the human colon. *Cancer Lett.* 221, 97–104.
- Gambacorti-Passerini, C., Antolini, L., Mahon, F.-X., Guilhot, F., Deininger, M., Fava, C., Nagler, A., Della Casa, C.M., Morra, E., Abruzzese, E., *et al.* (2011). Multicenter independent assessment of outcomes in chronic myeloid leukemia patients treated with imatinib. *J. Natl. Cancer Inst.* 103, 553–561.
- Ganguly, S.S., Fiore, L.S., Sims, J.T., Friend, J.W., Srinivasan, D., Thacker, M.A., Cibull, M.L., Wang, C., Novak, M., Kaetzel, D.M., *et al.* (2012). c-Abl and Arg are activated in human primary melanomas, promote melanoma cell invasion via distinct pathways, and drive metastatic progression. *Oncogene* 31, 1804–1816.
- Gao, H.-M., Zhou, H., and Hong, J.-S. (2012). NADPH oxidases: novel therapeutic targets for neurodegenerative diseases. *Trends Pharmacol. Sci.* 33, 295–303.

- Garg, R.J., Kantarjian, H., O'Brien, S., Quintás-Cardama, A., Faderl, S., Estrov, Z., and Cortes, J. (2009). The use of nilotinib or dasatinib after failure to 2 prior tyrosine kinase inhibitors: long-term follow-up. *Blood* 114, 4361–4368.
- Gavrilov, K., and Saltzman, W.M. (2012). Therapeutic siRNA: Principles, challenges, and Strategies. *Yale J. Biol. Med.* 85, 187–200.
- Gerdes, J., Schwab, U., Lemke, H., and Stein, H. (1983). Production of a mouse monoclonal antibody reactive with a human nuclear antigen associated with cell proliferation. *Int. J. Cancer* 31, 13–20.
- Gesbert, F., and Griffin, J.D. (2000). Bcr/Abl activates transcription of the Bcl-X gene through STAT5. *Blood* 96, 2269–2276.
- Giacinti, C., and Giordano, a (2006). RB and cell cycle progression. *Oncogene* 25, 5220–5227.
- Giallongo, C., La Cava, P., Tibullo, D., Parrinello, N., Barbagallo, I., Del Fabro, V., Stagno, F., Conticello, C., Romano, A., Chiarenza, A., *et al.* (2011). Imatinib increases cytotoxicity of melphalan and their combination allows an efficient killing of chronic myeloid leukemia cells. *Eur. J. Haematol.* 86, 216–225.
- Gianni, D., Diaz, B., Taulet, N., Fowler, B., Courtneidge, S.A., and Bokoch, G.M. (2009). Novel p47(phox)-related organizers regulate localized NADPH oxidase 1 (Nox1) activity. *Sci. Signal.* 2, ra54.
- Gianni, D., Taulet, N., DerMardirossian, C., and Bokoch, G.M. (2010). c-Src-mediated phosphorylation of NoxA1 and Tks4 induces the reactive oxygen species (ROS)-dependent formation of functional invadopodia in human colon cancer cells. *Mol. Biol. Cell* 21, 4287–4298.
- Gianni, D., DerMardirossian, C., and Bokoch, G.M. (2011). Direct interaction between Tks proteins and the N-terminal proline-rich region (PRR) of NoxA1 mediates Nox1-dependent ROS generation. *Eur. J. Cell Biol.* 90, 164–171.
- Gioia, R., Leroy, C., Drullion, C., Lagarde, V., Etienne, G., Dulucq, S., Lippert, E., Roche, S., Mahon, F.-X., and Pasquet, J.-M. (2011). Quantitative phosphoproteomics revealed interplay between Syk and Lyn in the resistance to nilotinib in chronic myeloid leukemia cells. *Blood* 118, 2211–2221.
- Goff, S.P., Gilboa, E., Witte, O.N., and Baltimore, D. (1980). Structure of the Abelson murine leukemia virus genome and the homologous cellular gene: studies with cloned viral DNA. *Cell* 22, 777–785.
- Gonzalez, F.J. (2005). Role of cytochromes P450 in chemical toxicity and oxidative stress: studies with CYP2E1. *Mutat. Res.* 569, 101–110.
- Gordon, M.Y., Dowding, C.R., Riley, G.P., Goldman, J.M., and Greaves, M.F. Altered adhesive interactions with marrow stroma of haematopoietic progenitor cells in chronic myeloid leukaemia. *Nature* 328, 342–344.
- Görlach, A., Brandes, R.P., Nguyen, K., Amidi, M., Dehghani, F., and Busse, R. (2000). A gp91phox containing NADPH oxidase selectively expressed in endothelial cells is a major source of oxygen radical generation in the arterial wall. *Circ. Res.* 87, 26–32.
- Griendling, K.K., Minieri, C.A., Ollerenshaw, J.D., and Alexander, R.W. (1994). Angiotensin II stimulates NADH and NADPH oxidase activity in cultured vascular smooth muscle cells. *Circ. Res.* 74, 1141–1148.
- Grimes, C. a, and Jope, R.S. (2001). The multifaceted roles of glycogen synthase kinase 3beta in cellular signaling. *Prog. Neurobiol.* 65, 391–426.
- Groeger, G., Quiney, C., and Cotter, T.G. (2009). Hydrogen peroxide as a cell-survival signaling molecule. *Antioxid. Redox Signal.* 11, 2655–2671.

- Groffen, J., Stephenson, J.R., Heisterkamp, N., de Klein, A., Bartram, C.R., and Grosveld, G. (1984). Philadelphia chromosomal breakpoints are clustered within a limited region, bcr, on chromosome 22. *Cell* 36, 93–99.
- De Groot, R.P., Raaijmakers, J.A., Lammers, J.W., Jove, R., and Koenderman, L. (1999). STAT5 activation by BCR-Abl contributes to transformation of K562 leukemia cells. *Blood* 94, 1108–1112.
- Gu, J.J., Santiago, L., and Mitchell, B.S. (2005). Synergy between imatinib and mycophenolic acid in inducing apoptosis in cell lines expressing Bcr-Abl. *Blood* 105, 3270–3277.
- Häcker, G. (2000). The morphology of apoptosis. *Cell Tissue Res.* 301, 5–17.
- Hantschel, O., Warsch, W., Eckelhart, E., Kaube, I., Grebien, F., Wagner, K.-U., Superti-Furga, G., and Sexl, V. (2012). BCR-ABL uncouples canonical JAK2-STAT5 signaling in chronic myeloid leukemia. *Nat. Chem. Biol.* 8, 285–293.
- Harbour, J.W., and Dean, D.C. (2000). Rb function in cell-cycle regulation and apoptosis. *Nat. Cell Biol.* 2, E65–7.
- Harbour, J.W., Luo, R.X., Santi, A.D., Postigo, A.A., Dean, D.C., Louis, S., S-, P., and Dei Santi, A. (1999). Cdk phosphorylation triggers sequential intramolecular interactions that progressively block Rb functions as cells move through G1. *Cell* 98, 859–869.
- Harrison, R. (2004). Physiological roles of xanthine oxidoreductase. *Drug Metab. Rev.* 36, 363–375.
- Hawkins, E.D., Hommel, M., Turner, M.L., Battye, F.L., Markham, J.F., and Hodgkin, P.D. (2007). Measuring lymphocyte proliferation, survival and differentiation using CFSE time-series data. *Nat. Protoc.* 2, 2057–2067.
- Helgason, G.V., Karvela, M., and Holyoake, T.L. (2011). Kill one bird with two stones: potential efficacy of BCR-ABL and autophagy inhibition in CML. *Blood* 118, 2035–2043.
- Heymes, C., Bendall, J.K., Ratajczak, P., Cave, A.C., Samuel, J.-L., Hasenfuss, G., and Shah, A.M. (2003). Increased myocardial NADPH oxidase activity in human heart failure. *J. Am. Coll. Cardiol.* 41, 2164–2171.
- Hohegger, H., Takeda, S., and Hunt, T. (2008). Cyclin-dependent kinases and cell-cycle transitions: does one fit all? *Nat. Rev. Mol. Cell Biol.* 9, 910–916.
- Hochhaus, A., Kreil, S., Corbin, A.S., La Rosée, P., Müller, M.C., Lahaye, T., Hanfstein, B., Schoch, C., Cross, N.C.P., Berger, U., *et al.* (2002). Molecular and chromosomal mechanisms of resistance to imatinib (STI571) therapy. *Leukemia* 16, 2190–2196.
- Hochhaus, A., O'Brien, S.G., Guilhot, F., Druker, B.J., Branford, S., Foroni, L., Goldman, J.M., Müller, M.C., Radich, J.P., Rudoltz, M., *et al.* (2009). Six-year follow-up of patients receiving imatinib for the first-line treatment of chronic myeloid leukemia. *Leukemia* 23, 1054–1061.
- Hoelbl, A., Schuster, C., Kovacic, B., Zhu, B., Wickre, M., Hoelzl, M.A., Fajmann, S., Grebien, F., Warsch, W., Stengl, G., *et al.* (2010). Stat5 is indispensable for the maintenance of bcr/abl-positive leukaemia. *EMBO Mol. Med.* 2, 98–110.
- Hoffmann, M., Schirmer, M.A., Tzvetkov, M. V, Kreuz, M., Ziepert, M., Wojnowski, L., Kube, D., Pfreundschuh, M., Trümper, L., Loeffler, M., *et al.* (2010). A functional polymorphism in the NAD(P)H oxidase subunit CYBA is related to gene expression, enzyme activity, and outcome in non-Hodgkin lymphoma. *Cancer Res.* 70, 2328–2338.

- Hole, P.S., Darley, R.L. and Tonks, A. (2011). Do reactive oxygen species play a role in myeloid leukemias? *Blood* *117*, 5816–5826.
- Holyoake, T.L., Jiang, X., Drummond, M.W., Eaves, A.C., and Eaves, C.J. (2002). Elucidating critical mechanisms of deregulated stem cell turnover in the chronic phase of chronic myeloid leukemia. *Leukemia* *16*, 549–558.
- Hong, H., Zeng, J.-S., Kreulen, D.L., Kaufman, D.I., and Chen, A.F. (2006). Atorvastatin protects against cerebral infarction via inhibition of NADPH oxidase-derived superoxide in ischemic stroke. *Am. J. Physiol. Heart Circ. Physiol.* *291*, H2210–5.
- Horita, M., Andreu, E.J., Benito, A., Arbona, C., Sanz, C., Benet, I., Prosper, F., and Fernandez-Luna, J.L. (2000). Blockade of the Bcr-Abl kinase activity induces apoptosis of chronic myelogenous leukemia cells by suppressing signal transducer and activator of transcription 5-dependent expression of Bcl-xL. *J. Exp. Med.* *191*, 977–984.
- Hoshi, T., and Heinemann, S. (2001). Regulation of cell function by methionine oxidation and reduction. *J. Physiol.* *531*, 1–11.
- Howlader N, Noone AM, Krapcho M, Garshell J, Neyman N, Altekruse SF, Kosary CL, Yu M, Ruhl J, Tatalovich Z, Cho H, Mariotto A, Lewis DR, Chen HS, Feuer EJ, Cronin KA (eds). SEER Cancer Statistics Review, 1975-2010, National Cancer Institute. Bethesda, MD, http://seer.cancer.gov/csr/1975_2010/, based on November 2012 SEER data submission, posted to the SEER web site, April 2013.
- Huang, W.-C., Li, X., Liu, J., Lin, J., and Chung, L.W.K. (2012a). Activation of androgen receptor, lipogenesis, and oxidative stress converged by SREBP-1 is responsible for regulating growth and progression of prostate cancer cells. *Mol. Cancer Res.* *10*, 133–142.
- Huang, H.-S., Liu, Z.-M., Chen, P.-C., Tseng, H.-Y., and Yeh, B.-W. (2012b). TG-interacting factor-induced superoxide production from NADPH oxidase contributes to the migration/invasion of urothelial carcinoma. *Free Radic. Biol. Med.* *53*, 769–778.
- Huang, W.-S., Metcalf, C.A., Sundaramoorthi, R., Wang, Y., Zou, D., Thomas, R.M., Zhu, X., Cai, L., Wen, D., Liu, S., *et al.* (2010). Discovery of 3-[2-(imidazo[1,2-b]pyridazin-3-yl)ethynyl]-4-methyl-N-{4-[(4-methylpiperazin-1-yl)methyl]-3-(trifluoromethyl)phenyl}benzamide (AP24534), a potent, orally active pan-inhibitor of breakpoint cluster region-abelson (BCR-ABL) kinase including th. *J. Med. Chem.* *53*, 4701–4719.
- Hughes, T., Saglio, G., Branford, S., Soverini, S., Kim, D.-W., Müller, M.C., Martinelli, G., Cortes, J., Beppu, L., Gottardi, E., *et al.* (2009). Impact of baseline BCR-ABL mutations on response to nilotinib in patients with chronic myeloid leukemia in chronic phase. *J. Clin. Oncol.* *27*, 4204–4210.
- Huntly, B.J.P., Shigematsu, H., Deguchi, K., Lee, B.H., Mizuno, S., Duclos, N., Rowan, R., Amaral, S., Curley, D., Williams, I.R., *et al.* (2004). MOZ-TIF2, but not BCR-ABL, confers properties of leukemic stem cells to committed murine hematopoietic progenitors. *Cancer Cell* *6*, 587–596.
- Inanami, O., Johnson, J.L., McAdara, J.K., Benna, J.E., Faust, L.R., Newburger, P.E., and Babior, B.M. (1998). Activation of the leukocyte NADPH oxidase by phorbol ester requires the phosphorylation of p47PHOX on serine 303 or 304. *J. Biol. Chem.* *273*, 9539–9543.

- Isogai, Y., Iizuka, T., and Shiro, Y. (1995). The mechanism of electron donation to molecular oxygen by phagocytic cytochrome b558. *J. Biol. Chem.* *270*, 7853–7857.
- Itoh, T., Terazawa, R., Kojima, K., Nakane, K., Deguchi, T., Ando, M., Tsukamasa, Y., Ito, M., and Nozawa, Y. (2011). Cisplatin induces production of reactive oxygen species via NADPH oxidase activation in human prostate cancer cells. *Free Radic. Res.* *45*, 1033–1039.
- Jackson, S.H., Devadas, S., Kwon, J., Pinto, L.A., and Williams, M.S. (2004). T cells express a phagocyte-type NADPH oxidase that is activated after T cell receptor stimulation. *Nat. Immunol.* *5*, 818–827.
- Jagnandan, D., Church, J.E., Banfi, B., Stuehr, D.J., Marrero, M.B., and Fulton, D.J.R. (2007). Novel mechanism of activation of NADPH oxidase 5. calcium sensitization via phosphorylation. *J. Biol. Chem.* *282*, 6494–6507.
- Janssen-Heininger, Y.M.W., Mossman, B.T., Heintz, N.H., Forman, H.J., Kalyanaraman, B., Finkel, T., Stamler, J.S., Rhee, S.G., and van der Vliet, A. (2008). Redox-based regulation of signal transduction: principles, pitfalls, and promises. *Free Radic. Biol. Med.* *45*, 1–17.
- Jeong, H.Y., Jeong, H.Y., and Kim, C.D. (2004). p22phox-derived superoxide mediates enhanced proliferative capacity of diabetic vascular smooth muscle cells. *Diabetes Res. Clin. Pract.* *64*, 1–10.
- Jiang, X., Lopez, A., Holyoake, T., Eaves, A., and Eaves, C. (1999). Autocrine production and action of IL-3 and granulocyte colony-stimulating factor in chronic myeloid leukemia. *Proc. Natl. Acad. Sci. U. S. A.* *96*, 12804–12809.
- Kajla, S., Mondol, A.S., Nagasawa, A., Zhang, Y., Kato, M., Matsuno, K., Yabe-Nishimura, C., and Kamata, T. (2012). A crucial role for Nox 1 in redox-dependent regulation of Wnt- β -catenin signaling. *FASEB J.* *26*, 2049–2059.
- Kamiguti, A.S., Serrander, L., Lin, K., Harris, R.J., Cawley, J.C., Allsup, D.J., Slupsky, J.R., Krause, K.-H., and Zuzel, M. (2005). Expression and activity of NOX5 in the circulating malignant B cells of hairy cell leukemia. *J. Immunol.* *175*, 8424–8430.
- Kanda, Y., Chiba, S., Honda, H., Hirai, H., and Yazaki, Y. (1999). Long-term third chronic phase of chronic myelogenous leukemia maintained by interferon-alpha and methotrexate. *Leuk. Lymphoma* *33*, 193–197.
- Kantarjian, H.M., Talpaz, M., Dhingra, K., Estey, E., Keating, M.J., Ku, S., Trujillo, J., Huh, Y., Stass, S., and Kurzrock, R. (1991). Significance of the P210 versus P190 molecular abnormalities in adults with Philadelphia chromosome-positive acute leukemia. *Blood* *78*, 2411–2418.
- Khoury, H.J., Cortes, J.E., Kantarjian, H.M., Gambacorti-Passerini, C., Baccarani, M., Kim, D.-W., Zaritsky, A., Countouriotis, A., Besson, N., Leip, E., *et al.* (2012). Bosutinib is active in chronic phase chronic myeloid leukemia after imatinib and dasatinib and/or nilotinib therapy failure. *Blood* *119*, 3403–3412.
- Kim, H.-J., Lee, J.-H., Kim, S.-J., Oh, G.S., Moon, H.-D., Kwon, K.-B., Park, C., Park, B.H., Lee, H.-K., Chung, S.-Y., *et al.* (2010). Roles of NADPH oxidases in cisplatin-induced reactive oxygen species generation and ototoxicity. *J. Neurosci.* *30*, 3933–3946.
- Kim, J.H., Chu, S.C., Gramlich, J.L., Pride, Y.B., Babendreier, E., Chauhan, D., Salgia, R., Podar, K., Griffin, J.D., and Sattler, M. (2005). Activation of the PI3K/mTOR pathway by BCR-ABL contributes to increased production of reactive oxygen species. *Blood* *105*, 1717–1723.

- Kim, Y.-S., Morgan, M.J., Choksi, S., and Liu, Z.-G. (2007). TNF-induced activation of the Nox1 NADPH oxidase and its role in the induction of necrotic cell death. *Mol. Cell* 26, 675–687.
- Koba, M., and Konopa, J. (2005). [Actinomycin D and its mechanisms of action]. *Postepy Hig. Med. Dosw. (Online)* 59, 290–298.
- Kolupaeva, V., and Janssens, V. (2013). PP1 and PP2A phosphatases--cooperating partners in modulating retinoblastoma protein activation. *FEBS J.* 280, 627–643.
- Koptyra, M., Falinski, R., Nowicki, M.O., Stoklosa, T., Majsterek, I., Nieborowska-Skorska, M., Blasiak, J., and Skorski, T. (2006). BCR/ABL kinase induces self-mutagenesis via reactive oxygen species to encode imatinib resistance. *Blood* 108, 319–327.
- Krause, K.-H., Lambeth, D., and Krönke, M. (2012). NOX enzymes as drug targets. *Cell. Mol. Life Sci.* 69, 2279–2282.
- Kris-Etherton, P.M., Lichtenstein, A.H., Howard, B. V, Steinberg, D., and Witztum, J.L. (2004). Antioxidant vitamin supplements and cardiovascular disease. *Circulation* 110, 637–641.
- Kumar, B., Koul, S., Khandrika, L., Meacham, R.B., and Koul, H.K. (2008). Oxidative stress is inherent in prostate cancer cells and is required for aggressive phenotype. *Cancer Res.* 68, 1777–1785.
- Kurzrock, R., Shtalrid, M., Romero, P., Kloetzer, W.S., Talpas, M., Trujillo, J.M., Blick, M., Beran, M., and Gutterman, J.U. (1987). A novel c-abl protein product in Philadelphia-positive acute lymphoblastic leukaemia. *Nature* 325, 631–635.
- Lambeth, J.D., Kawahara, T., and Diebold, B. (2007). Regulation of Nox and Duox enzymatic activity and expression. *Free Radic. Biol. Med.* 43, 319–331.
- Lan, Q., Zheng, T., Shen, M., Zhang, Y., Wang, S.S., Zahm, S.H., Holford, T.R., Leaderer, B., Boyle, P., and Chanock, S. (2007). Genetic polymorphisms in the oxidative stress pathway and susceptibility to non-Hodgkin lymphoma. *Hum. Genet.* 121, 161–168.
- Landry, W.D., Woolley, J.F., and Cotter, T.G. (2013). Imatinib and Nilotinib inhibit Bcr-Abl-induced ROS through targeted degradation of the NADPH oxidase subunit p22phox. *Leuk. Res.* 37, 183–189.
- Lange, S., Heger, J., Euler, G., Wartenberg, M., Piper, H.M., and Sauer, H. (2009). Platelet-derived growth factor BB stimulates vasculogenesis of embryonic stem cell-derived endothelial cells by calcium-mediated generation of reactive oxygen species. *Cardiovasc. Res.* 81, 159–168.
- Laurent, E., McCoy, J.W., Macina, R.A., Liu, W., Cheng, G., Robine, S., Papkoff, J., and Lambeth, J.D. (2008). Nox1 is over-expressed in human colon cancers and correlates with activating mutations in K-Ras. *Int. J. Cancer* 123, 100–107.
- Law, J.C., Ritke, M.K., Yalowich, J.C., Leder, G.H., and Ferrell, R.E. (1993). Mutational inactivation of the p53 gene in the human erythroid leukemic K562 cell line. *Leuk. Res.* 17, 1045–1050.
- Lee, B.C., and Gladyshev, V.N. (2011). The biological significance of methionine sulfoxide stereochemistry. *Free Radic. Biol. Med.* 50, 221–227.
- Lee, J.K., Edderkaoui, M., Truong, P., Ohno, I., Jang, K.-T., Berti, A., Pandol, S.J., and Gukovskaya, A.S. (2007). NADPH oxidase promotes pancreatic cancer cell survival via inhibiting JAK2 dephosphorylation by tyrosine phosphatases. *Gastroenterology* 133, 1637–1648.

- Lee, S.R., Kwon, K.S., Kim, S.R., and Rhee, S.G. (1998). Reversible inactivation of protein-tyrosine phosphatase 1B in A431 cells stimulated with epidermal growth factor. *J. Biol. Chem.* 273, 15366–15372.
- Lee, Y.-M., Kim, B.-J., Chun, Y.-S., So, I., Choi, H., Kim, M.-S., and Park, J.-W. (2006). NOX4 as an oxygen sensor to regulate TASK-1 activity. *Cell. Signal.* 18, 499–507.
- Lepik, D., Jaks, V., Kadaja, L., Värvi, S., and Maimets, T. (2003). Electroporation and carrier DNA cause p53 activation, cell cycle arrest, and apoptosis. *Anal. Biochem.* 318, 52–59.
- Leto, T.L., and Geiszt, M. Role of Nox family NADPH oxidases in host defense. *Antioxid. Redox Signal.* 8, 1549–1561.
- Li, Y., and Trush, M. a (1998). Diphenyleneiodonium, an NAD(P)H oxidase inhibitor, also potently inhibits mitochondrial reactive oxygen species production. *Biochem. Biophys. Res. Commun.* 253, 295–299.
- Li, L., Cheung, S.-H., Evans, E.L., and Shaw, P.E. (2010). Modulation of gene expression and tumor cell growth by redox modification of STAT3. *Cancer Res.* 70, 8222–8232.
- Lim, S.D., Sun, C., Lambeth, J.D., Marshall, F., Amin, M., Chung, L., Petros, J.A., and Arnold, R.S. (2005). Increased Nox1 and hydrogen peroxide in prostate cancer. *Prostate* 62, 200–207.
- Lin, J., Sun, T., Ji, L., Deng, W., Roth, J., Minna, J., and Arlinghaus, R. (2007). Oncogenic activation of c-Abl in non-small cell lung cancer cells lacking FUS1 expression: inhibition of c-Abl by the tumor suppressor gene product Fus1. *Oncogene* 26, 6989–6996.
- Liu, R.-M., Choi, J., Wu, J.-H., Gaston Pravia, K. a, Lewis, K.M., Brand, J.D., Mochel, N.S.R., Krzywanski, D.M., Lambeth, J.D., Hagood, J.S., *et al.* (2010). Oxidative modification of nuclear mitogen-activated protein kinase phosphatase 1 is involved in transforming growth factor beta1-induced expression of plasminogen activator inhibitor 1 in fibroblasts. *J. Biol. Chem.* 285, 16239–16247.
- LLS (2013). The Leukemia and Lymphoma Society, Facts 2013.
- von Löhneysen, K., Noack, D., Hayes, P., Friedman, J.S., and Knaus, U.G. (2012). Constitutive NADPH oxidase 4 activity resides in the composition of the B-loop and the penultimate C terminus. *J. Biol. Chem.* 287, 8737–8745.
- Lozzio, C.B., and Lozzio, B.B. (1975). Human chronic myelogenous leukemia cell-line with positive Philadelphia chromosome. *Blood* 45, 321–334.
- Lugo, T.G., Pendergast, A.M., Muller, A.J., and Witte, O.N. (1990). Tyrosine kinase activity and transformation potency of bcr-abl oncogene products. *Science* 247, 1079–1082.
- Luo, J. (2009). Glycogen synthase kinase 3beta (GSK3beta) in tumorigenesis and cancer chemotherapy. *Cancer Lett.* 273, 194–200.
- Luo, S., and Levine, R.L. (2009). Methionine in proteins defends against oxidative stress. *FASEB J.* 23, 464–472.
- Lyle, A.N., Deshpande, N.N., Taniyama, Y., Seidel-Rogol, B., Pounkova, L., Du, P., Papaharalambus, C., Lassègue, B., and Griendling, K.K. (2009). Poldip2, a novel regulator of Nox4 and cytoskeletal integrity in vascular smooth muscle cells. *Circ. Res.* 105, 249–259.
- Ma, G., Lu, D., Wu, Y., Liu, J., and Arlinghaus, R.B. (1997). Bcr phosphorylated on tyrosine 177 binds Grb2. *Oncogene* 14, 2367–2372.

- Mahon, F.-X., Réa, D., Guilhot, J., Guilhot, F., Huguet, F., Nicolini, F., Legros, L., Charbonnier, A., Guerci, A., Varet, B., *et al.* (2010). Discontinuation of imatinib in patients with chronic myeloid leukaemia who have maintained complete molecular remission for at least 2 years: the prospective, multicentre Stop Imatinib (STIM) trial. *Lancet Oncol.* *11*, 1029–1035.
- Maloney, E., Sweet, I.R., Hockenbery, D.M., Pham, M., Rizzo, N.O., Tateya, S., Handa, P., Schwartz, M.W., and Kim, F. (2009). Activation of NF-kappaB by palmitate in endothelial cells: a key role for NADPH oxidase-derived superoxide in response to TLR4 activation. *Arterioscler. Thromb. Vasc. Biol.* *29*, 1370–1375.
- Malumbres, M., and Barbacid, M. (2009). Cell cycle, CDKs and cancer: a changing paradigm. *Nat. Rev. Cancer* *9*, 153–166.
- Mandal, C.C., Ganapathy, S., Gorin, Y., Mahadev, K., Block, K., Abboud, H.E., Harris, S.E., Ghosh-Choudhury, G., and Ghosh-Choudhury, N. (2011). Reactive oxygen species derived from Nox4 mediate BMP2 gene transcription and osteoblast differentiation. *Biochem. J.* *433*, 393–402.
- Manea, A., Tanase, L.I., Raicu, M., and Simionescu, M. (2010). Transcriptional regulation of NADPH oxidase isoforms, Nox1 and Nox4, by nuclear factor-kappaB in human aortic smooth muscle cells. *Biochem. Biophys. Res. Commun.* *396*, 901–907.
- Maraldi, T., Prata, C., Fiorentini, D., Zambonin, L., Landi, L., and Hakim, G. (2009a). Induction of apoptosis in a human leukemic cell line via reactive oxygen species modulation by antioxidants. *Free Radic. Biol. Med.* *46*, 244–252.
- Maraldi, T., Prata, C., Vieceli Dalla Sega, F., Caliceti, C., Zambonin, L., Fiorentini, D., and Hakim, G. (2009b). NAD(P)H oxidase isoform Nox2 plays a prosurvival role in human leukaemia cells. *Free Radic. Res.* *43*, 1111–1121.
- Maru, Y., and Witte, O.N. (1991). The BCR gene encodes a novel serine/threonine kinase activity within a single exon. *Cell* *67*, 459–468.
- Massagué, J. (2004). G1 cell-cycle control and cancer. *Nature* *432*, 298–306.
- Maxwell, S.A., Kurzrock, R., Parsons, S.J., Talpaz, M., Gallick, G.E., Kloetzer, W.S., Arlinghaus, R.B., Kouttab, N.M., Keating, M.J., and Gutterman, J.U. (1987). Analysis of P210bcr-abl tyrosine protein kinase activity in various subtypes of Philadelphia chromosome-positive cells from chronic myelogenous leukemia patients. *Cancer Res.* *47*, 1731–1739.
- Maytin, M., Siwik, D. a, Ito, M., Xiao, L., Sawyer, D.B., Liao, R., and Colucci, W.S. (2004). Pressure overload-induced myocardial hypertrophy in mice does not require gp91phox. *Circulation* *109*, 1168–1171.
- McCord, J.M., and Fridovich, I. (1988). Superoxide dismutase: the first twenty years (1968-1988). *Free Radic. Biol. Med.* *5*, 363–369.
- McLaughlin, J., Chianese, E., and Witte, O.N. (1987). In vitro transformation of immature hematopoietic cells by the P210 BCR/ABL oncogene product of the Philadelphia chromosome. *Proc. Natl. Acad. Sci. U. S. A.* *84*, 6558–6562.
- McWhirter, J.R., Galasso, D.L., and Wang, J.Y. (1993a). A coiled-coil oligomerization domain of Bcr is essential for the transforming function of Bcr-Abl oncoproteins. *Mol. Cell. Biol.* *13*, 7587–7595.
- McWhirter, J.R., and Wang, J.Y. (1993b). An actin-binding function contributes to transformation by the Bcr-Abl oncoprotein of Philadelphia chromosome-positive human leukemias. *EMBO J.* *12*, 1533–1546.

- Meier, B., Cross, A.R., Hancock, J.T., Kaup, F.J., and Jones, O.T. (1991). Identification of a superoxide-generating NADPH oxidase system in human fibroblasts. *Biochem. J.* 275, 241–245.
- Meischl, C., Krijnen, P.A.J., Sipkens, J.A., Cillessen, S.A.G.M., Muñoz, I.G., Okroj, M., Ramska, M., Muller, A., Visser, C.A., Musters, R.J.P., *et al.* (2006). Ischemia induces nuclear NOX2 expression in cardiomyocytes and subsequently activates apoptosis. *Apoptosis* 11, 913–921.
- Melo, J. V, Gordon, D.E., Cross, N.C., and Goldman, J.M. (1993). The ABL-BCR fusion gene is expressed in chronic myeloid leukemia. *Blood* 81, 158–165.
- Meng, D., Lv, D.-D., and Fang, J. (2008). Insulin-like growth factor-I induces reactive oxygen species production and cell migration through Nox4 and Rac1 in vascular smooth muscle cells. *Cardiovasc. Res.* 80, 299–308.
- Mitsushita, J., Lambeth, J.D., and Kamata, T. (2004). The superoxide-generating oxidase Nox1 is functionally required for Ras oncogene transformation. *Cancer Res.* 64, 3580–3585.
- Mohi, M.G., Boulton, C., Gu, T.-L., Sternberg, D.W., Neuberger, D., Griffin, J.D., Gilliland, D.G., and Neel, B.G. (2004). Combination of rapamycin and protein tyrosine kinase (PTK) inhibitors for the treatment of leukemias caused by oncogenic PTKs. *Proc. Natl. Acad. Sci. U. S. A.* 101, 3130–3135.
- Montero, A., Fossella, F., Hortobagyi, G., and Valero, V. (2005). Docetaxel for treatment of solid tumours: a systematic review of clinical data. *Lancet Oncol.* 6, 229–239.
- Nagar, B., Bornmann, W.G., Pellicena, P., Schindler, T., Veach, D.R., Miller, W.T., Clarkson, B., and Kuriyan, J. (2002). Crystal structures of the kinase domain of c-Abl in complex with the small molecule inhibitors PD173955 and imatinib (STI-571). *Cancer Res.* 62, 4236–4243.
- Nair, R.R., Tolentino, J.H., Argilagos, R.F., Zhang, L., Pinilla-Ibarz, J., and Hazlehurst, L.A. (2012). Potentiation of Nilotinib-mediated cell death in the context of the bone marrow microenvironment requires a promiscuous JAK inhibitor in CML. *Leuk. Res.* 36, 756–763.
- Naka, K., Hoshii, T., Muraguchi, T., Tadokoro, Y., Ooshio, T., Kondo, Y., Nakao, S., Motoyama, N., and Hirao, A. (2010). TGF-beta-FOXO signalling maintains leukaemia-initiating cells in chronic myeloid leukaemia. *Nature* 463, 676–680.
- Nath, K.A., and Norby, S.M. (2000). Reactive oxygen species and acute renal failure. *Am. J. Med.* 109, 665–678.
- Naughton, R., Quiney, C., Turner, S.D., and Cotter, T.G. (2009). Bcr-Abl-mediated redox regulation of the PI3K/AKT pathway. *Leuk. Off. J. Leuk. Soc. Am. Leukemia* 23, 1432–1440.
- Neviani, P., Santhanam, R., Trotta, R., Notari, M., Blaser, B.W., Liu, S., Mao, H., Chang, J.S., Galiotta, A., Uttam, A., *et al.* (2005). The tumor suppressor PP2A is functionally inactivated in blast crisis CML through the inhibitory activity of the BCR/ABL-regulated SET protein. *Cancer Cell* 8, 355–368.
- Nieborowska-Skorska, M., Hoser, G., Kossev, P., Wasik, M.A., and Skorski, T. (2002). Complementary functions of the antiapoptotic protein A1 and serine/threonine kinase pim-1 in the BCR/ABL-mediated leukemogenesis. *Blood* 99, 4531–4539.

- Nieborowska-Skorska, M., Kopinski, P.K., Ray, R., Hoser, G., Ngaba, D., Flis, S., Cramer, K., Reddy, M.M., Koptyra, M., Penserga, T., *et al.* (2012). Rac2-MRC-cIII-generated ROS cause genomic instability in chronic myeloid leukemia stem cells and primitive progenitors. *Blood* *119*, 4253–4263.
- Nitiss, J.L. (2009). Targeting DNA topoisomerase II in cancer chemotherapy. *Nat. Rev. Cancer* *9*, 338–350.
- Nordberg, J., and Arnér, E.S. (2001). Reactive oxygen species, antioxidants, and the mammalian thioredoxin system. *Free Radic. Biol. Med.* *31*, 1287–1312.
- Nowell, P.C., and Hungerford, D.A. (1960). Chromosome studies on normal and leukemic human leukocytes. *J. Natl. Cancer Inst.* *25*, 85–109.
- Nowicki, M.O., Falinski, R., Koptyra, M., Slupianek, A., Stoklosa, T., Gloc, E., Nieborowska-Skorska, M., Blasiak, J., and Skorski, T. (2004). BCR/ABL oncogenic kinase promotes unfaithful repair of the reactive oxygen species-dependent DNA double-strand breaks. *Blood* *104*, 3746–3753.
- O'Donnell, B. V, Tew, D.G., Jones, O.T., and England, P.J. (1993). Studies on the inhibitory mechanism of iodonium compounds with special reference to neutrophil NADPH oxidase. *Biochem. J.* *290* (Pt 1, 41–49.
- O'Hare, T., Shakespeare, W.C., Zhu, X., Eide, C.A., Rivera, V.M., Wang, F., Adrian, L.T., Zhou, T., Huang, W.-S., Xu, Q., *et al.* (2009). AP24534, a pan-BCR-ABL inhibitor for chronic myeloid leukemia, potently inhibits the T315I mutant and overcomes mutation-based resistance. *Cancer Cell* *16*, 401–412.
- O'Hare, T., Zabriskie, M.S., Eiring, A.M., and Deininger, M.W. (2012). Pushing the limits of targeted therapy in chronic myeloid leukaemia. *Nat. Rev. Cancer* *12*, 513–526.
- O'Loughlen, a, Pérez-Morgado, M. I., Salinas, M., Martín, M., O'Loughlen, A., and Martín, M.E. (2003). Reversible inhibition of the protein phosphatase 1 by hydrogen peroxide. Potential regulation of eIF2 α phosphorylation in differentiated PC12 cells. *Arch. Biochem. Biophys.* *417*, 194–202.
- Ogawa, S., Hirano, N., Sato, N., Takahashi, T., Hangaishi, a, Tanaka, K., Kurokawa, M., Tanaka, T., Mitani, K., and Yazaki, Y. (1994). Homozygous loss of the cyclin-dependent kinase 4-inhibitor (p16) gene in human leukemias. *Blood* *84*, 2431–2435.
- Ohtsubo, M., Theodoras, A.M., Schumacher, J., Roberts, J.M., Ohtsubo, M., Theodoras, A.M., Schumacher, J., Roberts, J.M., and Pagano, M. (1995). Human cyclin E, a nuclear protein essential for the G1-to-S phase transition. *Mol. Cell. Biol.* *15*, 2612–2624.
- Otsuki, T., Clark, H.M., Wellmann, A., Jaffe, E.S., and Raffeld, M. (1995). Involvement of CDKN2 (p16INK4A /MTS1) and p15INK4B/MTS2 in Human Leukemias and Lymphomas. *Cancer Res.* *55*, 1436–1440.
- Pandey, D., and Fulton, D.J.R. (2011). Molecular regulation of NADPH oxidase 5 via the MAPK pathway. *Am. J. Physiol. Heart Circ. Physiol.* *300*, H1336–44.
- Pane, F., Frigeri, F., Sindona, M., Luciano, L., Ferrara, F., Cimino, R., Meloni, G., Saglio, G., Salvatore, F., and Rotoli, B. (1996). Neutrophilic-chronic myeloid leukemia: a distinct disease with a specific molecular marker (BCR/ABL with C3/A2 junction). *Blood* *88*, 2410–2414.
- Park, H.S., Lee, S.H., Park, D., Lee, J.S., Ryu, S.H., Lee, W.J., Rhee, S.G., and Bae, Y.S. (2004). Sequential activation of phosphatidylinositol 3-kinase, beta Pix, Rac1, and Nox1 in growth factor-induced production of H₂O₂. *Mol. Cell. Biol.* *24*, 4384–4394.

- Pastore, A., Piemonte, F., Locatelli, M., Lo Russo, A., Gaeta, L.M., Tozzi, G., and Federici, G. (2001). Determination of blood total, reduced, and oxidized glutathione in pediatric subjects. *Clin. Chem.* *47*, 1467–1469.
- Pendergast, A.M., Muller, A.J., Havlik, M.H., Maru, Y., and Witte, O.N. (1991). BCR sequences essential for transformation by the BCR-ABL oncogene bind to the ABL SH2 regulatory domain in a non-phosphotyrosine-dependent manner. *Cell* *66*, 161–171.
- Pendergast, A.M., Quilliam, L.A., Cripe, L.D., Bassing, C.H., Dai, Z., Li, N., Batzer, A., Rabun, K.M., Der, C.J., and Schlessinger, J. (1993). BCR-ABL-induced oncogenesis is mediated by direct interaction with the SH2 domain of the GRB-2 adaptor protein. *Cell* *75*, 175–185.
- Perrotti, D., Jamieson, C., Goldman, J., and Skorski, T. (2010). Chronic myeloid leukemia: mechanisms of blastic transformation. *J. Clin. Invest.* *120*, 2254–2264.
- Peshavariya, H., Dusting, G.J., Jiang, F., Halmos, L.R., Sobey, C.G., Drummond, G.R., and Selemidis, S. (2009). NADPH oxidase isoform selective regulation of endothelial cell proliferation and survival. *Naunyn. Schmiedebergs. Arch. Pharmacol.* *380*, 193–204.
- Peters, D.G., Hoover, R.R., Gerlach, M.J., Koh, E.Y., Zhang, H., Choe, K., Kirschmeier, P., Bishop, W.R., and Daley, G.Q. (2001). Activity of the farnesyl protein transferase inhibitor SCH66336 against BCR/ABL-induced murine leukemia and primary cells from patients with chronic myeloid leukemia. *Blood* *97*, 1404–1412.
- Petry, A., Djordjevic, T., Weitnauer, M., Kietzmann, T., Hess, J., and Görlach, A. (2006). NOX2 and NOX4 mediate proliferative response in endothelial cells. *Antioxid. Redox Signal.* *8*, 1473–1484.
- Pfarr, N., Korsch, E., Kaspers, S., Herbst, A., Stach, A., Zimmer, C., and Pohlenz, J. (2006). Congenital hypothyroidism caused by new mutations in the thyroid oxidase 2 (THOX2) gene. *Clin. Endocrinol. (Oxf)*. *65*, 810–815.
- Piccoli, C., D'Aprile, A., Ripoli, M., Scrima, R., Lecce, L., Boffoli, D., Tabilio, A., and Capitanio, N. (2007). Bone-marrow derived hematopoietic stem/progenitor cells express multiple isoforms of NADPH oxidase and produce constitutively reactive oxygen species. *Biochem. Biophys. Res. Commun.* *353*, 965–972.
- Piemonte, F., Pastore, A., Tozzi, G., Tagliacozzi, D., Santorelli, F.M., Carrozzo, R., Casali, C., Damiano, M., Federici, G., and Bertini, E. (2001). Glutathione in blood of patients with Friedreich's ataxia. *Eur. J. Clin. Invest.* *31*, 1007–1011.
- Pluk, H., Dorey, K., and Superti-Furga, G. (2002). Autoinhibition of c-Abl. *Cell* *108*, 247–259.
- Posthuma, E.F., Falkenburg, J.H., Apperley, J.F., Gratwohl, A., Roosnek, E., Hertenstein, B., Schipper, R.F., Schreuder, G.M., D'Amaro, J., Oudshoorn, M., *et al.* (1999). HLA-B8 and HLA-A3 coexpressed with HLA-B8 are associated with a reduced risk of the development of chronic myeloid leukemia. The Chronic Leukemia Working Party of the EBMT. *Blood* *93*, 3863–3865.
- Prabhakar, N.R. (2000). Oxygen sensing by the carotid body chemoreceptors. *J. Appl. Physiol.* *88*, 2287–2295.

- Prata, C., Maraldi, T., Fiorentini, D., Zambonin, L., Hakim, G., and Landi, L. (2008). Nox-generated ROS modulate glucose uptake in a leukaemic cell line. *Free Radic. Res.* *42*, 405–414.
- Puttini, M., Coluccia, A.M.L., Boschelli, F., Cleris, L., Marchesi, E., Donella-Deana, A., Ahmed, S., Redaelli, S., Piazza, R., Magistrini, V., *et al.* (2006). In vitro and in vivo activity of SKI-606, a novel Src-Abl inhibitor, against imatinib-resistant Bcr-Abl+ neoplastic cells. *Cancer Res.* *66*, 11314–11322.
- Pylayeva-Gupta, Y., Grabocka, E., and Bar-Sagi, D. (2011). RAS oncogenes: weaving a tumorigenic web. *Nat. Rev. Cancer* *11*, 761–774.
- Quah, B.J.C., Warren, H.S., and Parish, C.R. (2007). Monitoring lymphocyte proliferation in vitro and in vivo with the intracellular fluorescent dye carboxyfluorescein diacetate succinimidyl ester. *Nat. Protoc.* *2*, 2049–2056.
- Quintás-Cardama, A., Kantarjian, H., and Cortes, J. (2007). Flying under the radar: the new wave of BCR-ABL inhibitors. *Nat. Rev. Drug Discov.* *6*, 834–848.
- Rassool, F. V., Gaymes, T.J., Omidvar, N., Brady, N., Beurlet, S., Pla, M., Reboul, M., Lea, N., Chomienne, C., Thomas, N.S.B., *et al.* (2007). Reactive oxygen species, DNA damage, and error-prone repair: a model for genomic instability with progression in myeloid leukemia? *Cancer Res.* *67*, 8762–8771.
- Redaelli, S., Piazza, R., Rostagno, R., Magistrini, V., Perini, P., Marega, M., Gambacorti-Passerini, C., and Boschelli, F. (2009). Activity of bosutinib, dasatinib, and nilotinib against 18 imatinib-resistant BCR/ABL mutants. *J. Clin. Oncol.* *27*, 469–471.
- Reddy, M.M., Fernandes, M.S., Salgia, R., Levine, R.L., Griffin, J.D., and Sattler, M. (2011). NADPH oxidases regulate cell growth and migration in myeloid cells transformed by oncogenic tyrosine kinases. *Leukemia* *25*, 281–289.
- Reinehr, R., Becker, S., Eberle, A., Grether-Beck, S., and Häussinger, D. (2005). Involvement of NADPH oxidase isoforms and Src family kinases in CD95-dependent hepatocyte apoptosis. *J. Biol. Chem.* *280*, 27179–27194.
- Rey, F.E., Li, X.-C., Carretero, O.A., Garvin, J.L., and Pagano, P.J. (2002). Perivascular superoxide anion contributes to impairment of endothelium-dependent relaxation: role of gp91(phox). *Circulation* *106*, 2497–2502.
- Rhee, S.G., and Woo, H.A. (2011). Multiple functions of peroxiredoxins: peroxidases, sensors and regulators of the intracellular messenger H₂O₂, and protein chaperones. *Antioxid. Redox Signal.* *15*, 781–794.
- Rhee, S.G., Chae, H.Z., and Kim, K. (2005a). Peroxiredoxins: a historical overview and speculative preview of novel mechanisms and emerging concepts in cell signaling. *Free Radic. Biol. Med.* *38*, 1543–1552.
- Rhee, S.G., Kang, S.W., Jeong, W., Chang, T.-S., Yang, K.-S., and Woo, H.A. (2005b). Intracellular messenger function of hydrogen peroxide and its regulation by peroxiredoxins. *Curr. Opin. Cell Biol.* *17*, 183–189.
- Rhee, S.G., Woo, H.A., Kil, I.S., and Bae, S.H. (2012). Peroxiredoxin functions as a peroxidase and a regulator and sensor of local peroxides. *J. Biol. Chem.* *287*, 4403–4410.
- Richards, S.M., and Clark, E.A. (2009). BCR-induced superoxide negatively regulates B-cell proliferation and T-cell-independent type 2 Ab responses. *Eur. J. Immunol.* *39*, 3395–3403.
- Rimerman, R.A., Gellert-Randleman, A., and Diehl, J.A. (2000). Wnt1 and MEK1 cooperate to promote cyclin D1 accumulation and cellular transformation. *J. Biol. Chem.* *275*, 14736–14742.

- Rousselot, P., Huguët, F., Rea, D., Legros, L., Cayuela, J.M., Maarek, O., Blanchet, O., Marit, G., Gluckman, E., Reiffers, J., *et al.* (2007). Imatinib mesylate discontinuation in patients with chronic myelogenous leukemia in complete molecular remission for more than 2 years. *Blood* 109, 58–60.
- Rousselot, P. *et al.* (2011). Discontinuation of dasatinib or nilotinib in chronic myeloid leukemia (CML) patients (pts) with stable undetectable Bcr-Abl transcripts: results from the French CML group (FILMC). *Blood (ASH Annual Meeting Abstracts)* 118, 277.
- Rowley, J.D. (1973). Letter: A new consistent chromosomal abnormality in chronic myelogenous leukaemia identified by quinacrine fluorescence and Giemsa staining. *Nature* 243, 290–293.
- Sallmyr, A., Fan, J., and Rassool, F.V. (2008). Genomic instability in myeloid malignancies: increased reactive oxygen species (ROS), DNA double strand breaks (DSBs) and error-prone repair. *Cancer Lett.* 270, 1–9.
- Salomoni, P., Condorelli, F., Sweeney, S.M., and Calabretta, B. (2000). Versatility of BCR/ABL-expressing leukemic cells in circumventing proapoptotic BAD effects. *Blood* 96, 676–684.
- Samanta, A.K., Chakraborty, S.N., Wang, Y., Kantarjian, H., Sun, X., Hood, J., Perrotti, D., and Arlinghaus, R.B. (2009). Jak2 inhibition deactivates Lyn kinase through the SET-PP2A-SHP1 pathway, causing apoptosis in drug-resistant cells from chronic myelogenous leukemia patients. *Oncogene* 28, 1669–1681.
- Santos, C.X.C., Tanaka, L.Y., Wosniak, J., and Laurindo, F.R.M. (2009). Mechanisms and implications of reactive oxygen species generation during the unfolded protein response: roles of endoplasmic reticulum oxidoreductases, mitochondrial electron transport, and NADPH oxidase. *Antioxid. Redox Signal.* 11, 2409–2427.
- Sardina, J.L., López-Ruano, G., Sánchez-Abarca, L.I., Pérez-Simón, J. a, Gaztelumendi, a, Trigueros, C., Llanillo, M., Sánchez-Yagüe, J., and Hernández-Hernández, a (2010). p22phox-dependent NADPH oxidase activity is required for megakaryocytic differentiation. *Cell Death Differ.* 17, 1842–1854.
- Sardina, J.L., López-Ruano, G., Sánchez-Sánchez, B., Llanillo, M., and Hernández-Hernández, A. (2012). Reactive oxygen species: are they important for haematopoiesis? *Crit. Rev. Oncol. Hematol.* 81, 257–274.
- Sattler, M., Salgia, R., Okuda, K., Uemura, N., Durstin, M.A., Pisick, E., Xu, G., Li, J.L., Prasad, K. V, and Griffin, J.D. (1996). The proto-oncogene product p120CBL and the adaptor proteins CRKL and c-CRK link c-ABL, p190BCR/ABL and p210BCR/ABL to the phosphatidylinositol-3' kinase pathway. *Oncogene* 12, 839–846.
- Sattler, M., Winkler, T., Verma, S., Byrne, C.H., Shrikhande, G., Salgia, R., and Griffin, J.D. (1999). Hematopoietic growth factors signal through the formation of reactive oxygen species. *Blood* 93, 2928–2935.
- Sattler, M., Verma, S., Shrikhande, G., Byrne, C.H., Pride, Y.B., Winkler, T., Greenfield, E. a, Salgia, R., and Griffin, J.D. (2000). The BCR/ABL tyrosine kinase induces production of reactive oxygen species in hematopoietic cells. *J. Biol. Chem.* 275, 24273–24278.

- Sattler, M., Mohi, M.G., Pride, Y.B., Quinnan, L.R., Malouf, N.A., Podar, K., Gesbert, F., Iwasaki, H., Li, S., Van Etten, R.A., *et al.* (2002). Critical role for Gab2 in transformation by BCR/ABL. *Cancer Cell* 1, 479–492.
- Savage, D.G., Szydlo, R.M., and Goldman, J.M. (1997). Clinical features at diagnosis in 430 patients with chronic myeloid leukaemia seen at a referral centre over a 16-year period. *Br. J. Haematol.* 96, 111–116.
- Sawyers, C.L., McLaughlin, J., and Witte, O.N. (1995). Genetic requirement for Ras in the transformation of fibroblasts and hematopoietic cells by the Bcr-Abl oncogene. *J. Exp. Med.* 181, 307–313.
- Schauen, M., Spitkovsky, D., Schubert, J., Fischer, J.H., Hayashi, J., and Wiesner, R.J. (2006). Respiratory chain deficiency slows down cell-cycle progression via reduced ROS generation and is associated with a reduction of p21CIP1/WAF1. *J. Cell. Physiol.* 209, 103–112.
- Scherz-Shouval, R., and Elazar, Z. (2011). Regulation of autophagy by ROS: physiology and pathology. *Trends Biochem. Sci.* 36, 30–38.
- Schindler, C., Levy, D.E., and Decker, T. (2007). JAK-STAT signaling: from interferons to cytokines. *J. Biol. Chem.* 282, 20059–20063.
- Schindler, T., Bornmann, W., Pellicena, P., Miller, W.T., Clarkson, B., and Kuriyan, J. (2000). Structural mechanism for STI-571 inhibition of abelson tyrosine kinase. *Science* 289, 1938–1942.
- Schrader, M., and Fahimi, H.D. (2004). Mammalian peroxisomes and reactive oxygen species. *Histochem. Cell Biol.* 122, 383–393.
- Serrander, L., Cartier, L., Bedard, K., Banfi, B., Lardy, B., Plastre, O., Sienkiewicz, A., Fórró, L., Schlegel, W., and Krause, K.-H. (2007a). NOX4 activity is determined by mRNA levels and reveals a unique pattern of ROS generation. *Biochem. J.* 406, 105–114.
- Serrander, L., Jaquet, V., Bedard, K., Plastre, O., Hartley, O., Arnaudeau, S., Demarex, N., Schlegel, W., and Krause, K.-H. (2007b). NOX5 is expressed at the plasma membrane and generates superoxide in response to protein kinase C activation. *Biochimie* 89, 1159–1167.
- Serrano, F., Kolluri, N.S., Wientjes, F.B., Card, J.P., and Klann, E. (2003). NADPH oxidase immunoreactivity in the mouse brain. *Brain Res.* 988, 193–198.
- Shah, N.P., Nicoll, J.M., Nagar, B., Gorre, M.E., Paquette, R.L., Kuriyan, J., and Sawyers, C.L. (2002). Multiple BCR-ABL kinase domain mutations confer polyclonal resistance to the tyrosine kinase inhibitor imatinib (STI571) in chronic phase and blast crisis chronic myeloid leukemia. *Cancer Cell* 2, 117–125.
- Shah, N.P., Tran, C., Lee, F.Y., Chen, P., Norris, D., and Sawyers, C.L. (2004). Overriding imatinib resistance with a novel ABL kinase inhibitor. *Science* 305, 399–401.
- Shimada, K., Nakamura, M., Anai, S., De Velasco, M., Tanaka, M., Tsujikawa, K., Uji, Y., and Konishi, N. (2009). A novel human AlkB homologue, ALKBH8, contributes to human bladder cancer progression. *Cancer Res.* 69, 3157–3164.
- Shimada, K., Fujii, T., Anai, S., Fujimoto, K., and Konishi, N. (2011). ROS generation via NOX4 and its utility in the cytological diagnosis of urothelial carcinoma of the urinary bladder. *BMC Urol.* 11, 22.
- Shtivelman, E., Lifshitz, B., Gale, R.P., and Canaani, E. (1985). Fused transcript of abl and bcr genes in chronic myelogenous leukaemia. *Nature* 315, 550–554.

- Siddik, Z.H. (2003). Cisplatin: mode of cytotoxic action and molecular basis of resistance. *Oncogene* 22, 7265–7279.
- Sillaber, C., Gesbert, F., Frank, D.A., Sattler, M., and Griffin, J.D. (2000). STAT5 activation contributes to growth and viability in Bcr/Abl-transformed cells. *Blood* 95, 2118–2125.
- Silver, R.T., Woolf, S.H., Hehlmann, R., Appelbaum, F.R., Anderson, J., Bennett, C., Goldman, J.M., Guilhot, F., Kantarjian, H.M., Lichtin, A.E., *et al.* (1999). An evidence-based analysis of the effect of busulfan, hydroxyurea, interferon, and allogeneic bone marrow transplantation in treating the chronic phase of chronic myeloid leukemia: developed for the American Society of Hematology. *Blood* 94, 1517–1536.
- Simon, H.U., Haj-Yehia, A., and Levi-Schaffer, F. (2000). Role of reactive oxygen species (ROS) in apoptosis induction. *Apoptosis* 5, 415–418.
- Sirard, C., Laneuville, P., and Dick, J.E. (1994). Expression of bcr-abl abrogates factor-dependent growth of human hematopoietic M07E cells by an autocrine mechanism. *Blood* 83, 1575–1585.
- Skorski, T., Kanakaraj, P., Nieborowska-Skorska, M., Ratajczak, M.Z., Wen, S.C., Zon, G., Gewirtz, A.M., Perussia, B., and Calabretta, B. (1995). Phosphatidylinositol-3 kinase activity is regulated by BCR/ABL and is required for the growth of Philadelphia chromosome-positive cells. *Blood* 86, 726–736.
- Skorski, T., Bellacosa, A., Nieborowska-Skorska, M., Majewski, M., Martinez, R., Choi, J.K., Trotta, R., Wlodarski, P., Perrotti, D., Chan, T.O., *et al.* (1997). Transformation of hematopoietic cells by BCR/ABL requires activation of a PI-3k/Akt-dependent pathway. *EMBO J.* 16, 6151–6161.
- Slupianek, A., Poplawski, T., Jozwiakowski, S.K., Cramer, K., Pytel, D., Stoczynska, E., Nowicki, M.O., Blasiak, J., and Skorski, T. (2011). BCR/ABL stimulates WRN to promote survival and genomic instability. *Cancer Res.* 71, 842–851.
- Smith, K.M., Yacobi, R., and Van Etten, R.A. (2003). Autoinhibition of Bcr-Abl through its SH3 domain. *Mol. Cell* 12, 27–37.
- Sobell, H.M. (1985). Actinomycin and DNA transcription. *Proc. Natl. Acad. Sci. U. S. A.* 82, 5328–5331.
- Srinivasan, D., and Plattner, R. (2006). Activation of Abl tyrosine kinases promotes invasion of aggressive breast cancer cells. *Cancer Res.* 66, 5648–5655.
- Stelman, L.S., Pohnert, S.C., Shelton, J.G., Franklin, R. a, Bertrand, F.E., and McCubrey, J. a (2004). JAK/STAT, Raf/MEK/ERK, PI3K/Akt and BCR-ABL in cell cycle progression and leukemogenesis. *Leuk. Off. J. Leuk. Soc. Am. Leuk. Res. Fund, U.K* 18, 189–218.
- Stielow, C., Catar, R. a, Muller, G., Wingler, K., Scheurer, P., Schmidt, H.H.H.W., and Morawietz, H. (2006). Novel Nox inhibitor of oxLDL-induced reactive oxygen species formation in human endothelial cells. *Biochem. Biophys. Res. Commun.* 344, 200–205.
- Stuehr, D.J., Fasehun, O.A., Kwon, N.S., Gross, S.S., Gonzalez, J.A., Levi, R., and Nathan, C.F. (1991). Inhibition of macrophage and endothelial cell nitric oxide synthase by diphenylethylidonium and its analogs. *FASEB J.* 5, 98–103.

- Sturrock, A., Cahill, B., Norman, K., Huecksteadt, T.P., Hill, K., Sanders, K., Karwande, S. V, Stringham, J.C., Bull, D.A., Gleich, M., *et al.* (2006). Transforming growth factor-beta1 induces Nox4 NAD(P)H oxidase and reactive oxygen species-dependent proliferation in human pulmonary artery smooth muscle cells. *Am. J. Physiol. Lung Cell. Mol. Physiol.* *290*, 661–673.
- Sun, Q.-A., Hess, D.T., Wang, B., Miyagi, M., and Stamler, J.S. (2012). Off-target thiol alkylation by the NADPH oxidase inhibitor 3-benzyl-7-(2-benzoxazolyl)thio-1,2,3-triazolo[4,5-d]pyrimidine (VAS2870). *Free Radic. Biol. Med.* *52*, 1897–1902.
- Sundaresan, M., Yu, Z.X., Ferrans, V.J., Irani, K., and Finkel, T. (1995). Requirement for generation of H₂O₂ for platelet-derived growth factor signal transduction. *Science* *270*, 296–299.
- Suryanarayan, K., Hunger, S.P., Kohler, S., Carroll, A.J., Crist, W., Link, M.P., and Cleary, M.L. (1991). Consistent involvement of the bcr gene by 9;22 breakpoints in pediatric acute leukemias. *Blood* *77*, 324–330.
- Takahashi, N., Miura, I., Saitoh, K., and Miura, A.B. (1998). Lineage involvement of stem cells bearing the philadelphia chromosome in chronic myeloid leukemia in the chronic phase as shown by a combination of fluorescence-activated cell sorting and fluorescence in situ hybridization. *Blood* *92*, 4758–4763.
- Tanaka, K., Takechi, M., Hong, J., Shigeta, C., Oguma, N., Kamada, N., Takimoto, Y., Kuramoto, A., Dohy, H., and Kyo, T. (1989). 9;22 translocation and bcr rearrangements in chronic myelocytic leukemia patients among atomic bomb survivors. *J. Radiat. Res.* *30*, 352–358.
- Tanis, K.Q., Veach, D., Duewel, H.S., Bornmann, W.G., and Koleske, A.J. (2003). Two distinct phosphorylation pathways have additive effects on Abl family kinase activation. *Mol. Cell. Biol.* *23*, 3884–3896.
- Tegtmeier F, Walter U, Schinzel R, Wingler K, Scheurer P, Schmidt H (2005) Compounds containing a N-heteroaryl moiety linked to fused ring moieties for the inhibition of NAD(P)H oxidases and platelet activation. European Patent 1 598 354 A1
- Terada, L.S. (2006). Specificity in reactive oxidant signaling: think globally, act locally. *J. Cell Biol.* *174*, 615–623.
- Toledano, M.B., Planson, A.-G., and Delaunay-Moisan, A. (2010). Reining in H₂O₂ for safe signaling. *Cell* *140*, 454–456.
- Tonks, N.K. (2005). Redox redux: revisiting PTPs and the control of cell signaling. *Cell* *121*, 667–670.
- Torres, M. (2003). Mitogen-activated protein kinase pathways in redox signaling. *Front. Biosci.* *8*, d369–91.
- Trachootham, D., Lu, W., Ogasawara, M. a, Nilsa, R.-D.V., and Huang, P. (2008). Redox regulation of cell survival. *Antioxid. Redox Signal.* *10*, 1343–1374.
- Traer, E., MacKenzie, R., Snead, J., Agarwal, A., Eiring, A.M., O’Hare, T., Druker, B.J., and Deininger, M.W. (2012). Blockade of JAK2-mediated extrinsic survival signals restores sensitivity of CML cells to ABL inhibitors. *Leukemia* *26*, 1140–1143.
- Trotta, R., Vignudelli, T., Candini, O., Intine, R. V, Pecorari, L., Guerzoni, C., Santilli, G., Byrom, M.W., Goldoni, S., Ford, L.P., *et al.* (2003). BCR/ABL activates mdm2 mRNA translation via the La antigen. *Cancer Cell* *3*, 145–160.

- Tseng, P.-H., Lin, H.-P., Zhu, J., Chen, K.-F., Hade, E.M., Young, D.C., Byrd, J.C., Grever, M., Johnson, K., Druker, B.J., *et al.* (2005). Synergistic interactions between imatinib mesylate and the novel phosphoinositide-dependent kinase-1 inhibitor OSU-03012 in overcoming imatinib mesylate resistance. *Blood* *105*, 4021–4027.
- Turrens, J.F. (2003). Mitochondrial formation of reactive oxygen species. *J. Physiol.* *552*, 335–344.
- Ueno, N., Takeya, R., Miyano, K., Kikuchi, H., and Sumimoto, H. (2005). The NADPH oxidase Nox3 constitutively produces superoxide in a p22phox-dependent manner: its regulation by oxidase organizers and activators. *J. Biol. Chem.* *280*, 23328–23339.
- Ushio-Fukai, M. (2006). Redox signaling in angiogenesis: role of NADPH oxidase. *Cardiovasc. Res.* *71*, 226–235.
- Ushio-Fukai, M. (2009). Forum Review: Article Compartmentalization of Redox Signaling Through NADPH Oxidase–Derived ROS. *Antioxid. Redox Signal.* *11*, 1289–1299.
- Usui, S., Oveson, B.C., Lee, S.Y., Jo, Y.-J., Yoshida, T., Miki, A., Miki, K., Iwase, T., Lu, L., and Campochiaro, P.A. (2009). NADPH oxidase plays a central role in cone cell death in retinitis pigmentosa. *J. Neurochem.* *110*, 1028–1037.
- Van Etten, R.A., Jackson, P., and Baltimore, D. (1989). The mouse type IV c-abl gene product is a nuclear protein, and activation of transforming ability is associated with cytoplasmic localization. *Cell* *58*, 669–678.
- Van Etten, R.A., Jackson, P.K., Baltimore, D., Sanders, M.C., Matsudaira, P.T., and Janney, P.A. (1994). The COOH terminus of the c-Abl tyrosine kinase contains distinct F- and G-actin binding domains with bundling activity. *J. Cell Biol.* *124*, 325–340.
- Vanhaesebroeck, B., Stephens, L., and Hawkins, P. (2012). PI3K signalling: the path to discovery and understanding. *Nat. Rev. Mol. Cell Biol.* *13*, 195–203.
- Vaquero, E.C., Edderkaoui, M., Pandol, S.J., Gukovsky, I., and Gukovskaya, A.S. (2004). Reactive oxygen species produced by NAD(P)H oxidase inhibit apoptosis in pancreatic cancer cells. *J. Biol. Chem.* *279*, 34643–34654.
- Venkatachalam, P., de Toledo, S.M., Pandey, B.N., Tephly, L. a, Carter, a B., Little, J.B., Spitz, D.R., and Azzam, E.I. (2008). Regulation of normal cell cycle progression by flavin-containing oxidases. *Oncogene* *27*, 20–31.
- Verbon, E.H., Post, J.A., and Boonstra, J. (2012). The influence of reactive oxygen species on cell cycle progression in mammalian cells. *Gene* *511*, 1–6.
- Vivekananthan, D.P., Penn, M.S., Sapp, S.K., Hsu, A., and Topol, E.J. (2003). Use of antioxidant vitamins for the prevention of cardiovascular disease: meta-analysis of randomised trials. *Lancet* *361*, 2017–2023.
- Vonlanthen, S., Heighway, J., Tschan, M.P., Borner, M.M., Altermatt, H.J., Kappeler, a, Tobler, a, Fey, M.F., Thatcher, N., Yarbrough, W.G., *et al.* (1998). Expression of p16INK4a/p16alpha and p19ARF/p16beta is frequently altered in non-small cell lung cancer and correlates with p53 overexpression. *Oncogene* *17*, 2779–2785.
- Vousden, K.H., and Lu, X. (2002). Live or let die: the cell's response to p53. *Nat. Rev. Cancer* *2*, 594–604.

- Wang, Y., Cai, D., Brendel, C., Barrett, C., Erben, P., Manley, P.W., Hochhaus, A., Neubauer, A., and Burchert, A. (2007). Adaptive secretion of granulocyte-macrophage colony-stimulating factor (GM-CSF) mediates imatinib and nilotinib resistance in BCR/ABL+ progenitors via JAK-2/STAT-5 pathway activation. *Blood* *109*, 2147–2155.
- Warsch, W., Kollmann, K., Eckelhart, E., Fajmann, S., Cerny-Reiterer, S., Hölbl, A., Gleixner, K. V, Dworzak, M., Mayerhofer, M., Hoermann, G., *et al.* (2011). High STAT5 levels mediate imatinib resistance and indicate disease progression in chronic myeloid leukemia. *Blood* *117*, 3409–3420.
- Weinberg, F., and Chandel, N.S. (2009). Reactive oxygen species-dependent signaling regulates cancer. *Cell. Mol. Life Sci.* *66*, 3663–3673.
- Weisberg, E., Manley, P.W., Breitenstein, W., Brügger, J., Cowan-Jacob, S.W., Ray, A., Huntly, B., Fabbro, D., Fendrich, G., Hall-Meyers, E., *et al.* (2005). Characterization of AMN107, a selective inhibitor of native and mutant Bcr-Abl. *Cancer Cell* *7*, 129–141.
- Weisberg, E., Wright, R.D., McMillin, D.W., Mitsiades, C., Ray, A., Barrett, R., Adamia, S., Stone, R., Galinsky, I., Kung, A.L., *et al.* (2008). Stromal-mediated protection of tyrosine kinase inhibitor-treated BCR-ABL-expressing leukemia cells. *Mol. Cancer Ther.* *7*, 1121–1129.
- Weyemi, U., Caillou, B., Talbot, M., Ameziane-El-Hassani, R., Lacroix, L., Lagente-Chevallier, O., Al Ghuzlan, A., Roos, D., Bidart, J.-M., Virion, A., *et al.* (2010). Intracellular expression of reactive oxygen species-generating NADPH oxidase NOX4 in normal and cancer thyroid tissues. *Endocr. Relat. Cancer* *17*, 27–37.
- Weyemi, U., and Dupuy, C. (2012a). The emerging role of ROS-generating NADPH oxidase NOX4 in DNA-damage responses. *Mutat. Res.* *751*, 77–81.
- Weyemi, U., Lagente-Chevallier, O., Boufraquech, M., Prenois, F., Courtin, F., Caillou, B., Talbot, M., Dardalhon, M., Al Ghuzlan, a, Bidart, J.-M., *et al.* (2012b). ROS-generating NADPH oxidase NOX4 is a critical mediator in oncogenic H-Ras-induced DNA damage and subsequent senescence. *Oncogene* *31*, 1117–1129.
- Wilson, G., Frost, L., Goodeve, A., Vandenberghe, E., Peake, I., and Reilly, J. (1997). BCR-ABL transcript with an e19a2 (c3a2) junction in classical chronic myeloid leukemia. *Blood* *89*, 3064.
- Wind, S., Beuerlein, K., Eucker, T., Müller, H., Scheurer, P., Armitage, M.E., Ho, H., Schmidt, H.H.H.W., and Wingler, K. (2010). Comparative pharmacology of chemically distinct NADPH oxidase inhibitors. *Br. J. Pharmacol.* *161*, 885–898.
- Wingler, K., Altenhoefer, S. a, Kleikers, P.W.M., Radermacher, K. a, Kleinschnitz, C., and Schmidt, H.H.H.W. (2012). VAS2870 is a pan-NADPH oxidase inhibitor. *Cell. Mol. Life Sci.* *69*, 3159–3160.
- Wood, Z.A., Poole, L.B., and Karplus, P.A. (2003). Peroxiredoxin evolution and the regulation of hydrogen peroxide signaling. *Science* *300*, 650–653.
- Woolley, J.F., Naughton, R., Stanicka, J., Gough, D.R., Bhatt, L., Dickinson, B.C., Chang, C.J., and Cotter, T.G. (2012). H₂O₂ production downstream of FLT3 is mediated by p22phox in the endoplasmic reticulum and is required for STAT5 signalling. *PLoS One* *7*, e34050.
- Woolley, J.F., Corcoran, A., Groeger, G., Landry, W.D., and Cotter, T.G. (2013). Redox-regulated growth factor survival signaling. *Antioxid. Redox Signal.* *19*, 1815–1827.

- Wu, W.-S. (2006). The signaling mechanism of ROS in tumor progression. *Cancer Metastasis Rev.* 25, 695–705.
- Xiao, Q., Luo, Z., Pepe, A.E., Margariti, A., Zeng, L., and Xu, Q. (2009). Embryonic stem cell differentiation into smooth muscle cells is mediated by Nox4-produced H₂O₂. *Am. J. Physiol. Cell Physiol.* 296, C711–23.
- Xu, C., Kim, N.-G., and Gumbiner, B.M. (2009). Regulation of protein stability by GSK3 mediated phosphorylation. *Cell Cycle* 8, 4032–4039.
- Yamaura, M., Mitsushita, J., Furuta, S., Kiniwa, Y., Ashida, A., Goto, Y., Shang, W.H., Kubodera, M., Kato, M., Takata, M., *et al.* (2009). NADPH oxidase 4 contributes to transformation phenotype of melanoma cells by regulating G2-M cell cycle progression. *Cancer Res.* 69, 2647–2654.
- Yang, S., Madyastha, P., Bingel, S., Ries, W., and Key, L. (2001). A new superoxide-generating oxidase in murine osteoclasts. *J. Biol. Chem.* 276, 5452–5458.
- Ye, D., Wolff, N., Li, L., Zhang, S., and Ilaria, R.L. (2006). STAT5 signaling is required for the efficient induction and maintenance of CML in mice. *Blood* 107, 4917–4925.
- Yokoyama, H., Ikehara, Y., Kodera, Y., Ikehara, S., Yatabe, Y., Mochizuki, Y., Koike, M., Fujiwara, M., Nakao, A., Tatematsu, M., *et al.* (2006). Molecular basis for sensitivity and acquired resistance to gefitinib in HER2-overexpressing human gastric cancer cell lines derived from liver metastasis. *Br. J. Cancer* 95, 1504–1513.
- Zhang, B., Li, M., McDonald, T., Holyoake, T.L., Moon, R.T., Campana, D., Shultz, L., and Bhatia, R. (2013). Microenvironmental protection of CML stem and progenitor cells from tyrosine kinase inhibitors through N-cadherin and Wnt- β -catenin signaling. *Blood* 121, 1824–1838.
- Zhao, C., Chen, A., Jamieson, C.H., Fereshteh, M., Abrahamsson, A., Blum, J., Kwon, H.Y., Kim, J., Chute, J.P., Rizzieri, D., *et al.* (2009). Hedgehog signalling is essential for maintenance of cancer stem cells in myeloid leukaemia. *Nature* 458, 776–779.
- Zhou, T., Commodore, L., Huang, W.-S., Wang, Y., Thomas, M., Keats, J., Xu, Q., Rivera, V.M., Shakespeare, W.C., Clackson, T., *et al.* (2011). Structural mechanism of the Pan-BCR-ABL inhibitor ponatinib (AP24534): lessons for overcoming kinase inhibitor resistance. *Chem. Biol. Drug Des.* 77, 1–11.
- Zhu, Q.-S., Xia, L., Mills, G.B., Lowell, C. a, Touw, I.P., and Corey, S.J. (2006). G-CSF induced reactive oxygen species involves Lyn-PI3-kinase-Akt and contributes to myeloid cell growth. *Blood* 107, 1847–1856.

Appendix 1

**Inhibition of protein-tyrosine phosphatase 1B
(PTP1B) mediates ubiquitination and degradation of
Bcr-Abl protein.**

Alvira, D., Naughton, R., Bhatt, L., Tedesco, S., Landry,
W.D., Cotter, T.G.

J. Biol. Chem., 2011; 286, 32313–23.

Appendix 2

Redox-regulated growth factor survival signaling.

Woolley, J.F., Corcoran, A., Groeger, G., Landry, W.D.,
Cotter, T.G.

Antioxid. Redox. Signal., 2013; 19, 1815-27.

